THE DEVELOPMENT OF AN IN-VIVO METHOD FOR ASSESSING THE ANTITHROMBOTIC PROPERTIES OF PHARMACEUTICAL COMPOUNDS.

by

RICHARD WILLIAM HARTLEY

A Doctoral Thesis

Submitted in partial fulfilment of the requirements
for the award of

Doctor of Philosophy of the Loughborough University of Technology

1989

CONTENTS

ABSTRACT

THE DEVELOPMENT OF AN IN-VIVO METHOD FOR ASSESSING THE ANTITHROMBOTIC PROPERTIES OF PHARMACEUTICAL COMPOUNDS.

R.W. HARTLEY.

The formation of a thrombus stems from the malfunction of a normal physiological function referred to as haemostasis and the activity of blood platelets; such thrombi give rise to debilitating and often fatal strokes. Consequently much effort is associated with the search for pharmacological compounds capable of their prevention or dispersion. Most of the primary screens associated with such work rely on in-vitro tests and, in separating the blood from it's vasculature, the influence and results associated with several naturally occuring moderators may be lost. There therefore exists the incentive to develop more representative in-vivo screening methods.

Following an introduction to the underlying physiology and pharmacology and a review of established screening methods, this thesis proceeds to describe the development of a novel technique suitable for such in-vivo studies. It's inception is shown to be a consequence of an amalgamation of ultrasonic methods associated with the clinical detection of occlusions and laser Doppler velocimetry. Both topics are individually surveyed and then brought together through a concept whereby the efficacy of compounds might be evaluated in animal models by measuring the velocity of blood in the fluid jet formed distal to an induced thrombus.The main underlying assumption is that the jet velocity will reflect the degree of encroachment of the thrombus into the vasculature.

In accord with the evolved measurement rationale there then follows a description of a specific laser Doppler velocimeter and some associated experiments, designed to qualitatively appraise the validity of the underlying assumptions. The ensuing results in turn give rise to the design of a laser Doppler microscope, an analyser for extracting the required velocity information from the Doppler shift spectrum and an additional series of experiments. Central to this latter stage of validation is the use of a thrombus analogue in a narrow bored glass flow tube. Finally, some preliminary in-vivo experiments and results are presented.

ACKNOWLEDGEMENTS

It is a pleasure to record the appreciation I feel due to the many people who in some way have been instumental in the production of this thesis.That the work could be undertaken in the first place was largely due to the efforts of my supervisor,John Lloyd.It's completion must in part be credited to his timely and apposite interventions and for this I am indeed very grateful.

It is through more than a sense of duty that I acknowledge the time and facilities allowed me by the senior management of Glaxo Group Research Limited. In particular I thank Pat Humphrey,Vic Jacobson and Jim Gall, all of whom have held the fate of my thesis in their hands at some time during it's preparation. I also thank Dr. Roy Brittain, Director of Biological Research, for his continued support and good will.

Dr. Mike Drew and his staff in Cardiovascular Pharmacology were, as far as circumstances could allow, most tolerant and accomodating when the time came for pharmacological experimentation. In addition to Mike my thanks also especially go to Dr. Ian Watts whose advise and assistance helped to clear the way through a degree of incipient hesitation.

Without the full co-operation of the members of the Bioengineering Unit the work would undoubtedly have foundered. For practical help,

support and the free time their commitment helped to create,my thanks go to each and every one. I gladly acknowledge the part played by the lunch time discussion I had with my colleague John Wheable: it eventually led to the 'Magsep' model.

That I could type and edit my own thesis was largely made possible through the use of 'Wordwise' running on a BBC microcomputer: my thanks go to Mrs Marlene Svensson for introducing me to it.

Finally my sincere thanks and appreciation for the help and support I've been fortunate enough to receive from my family. I'm aware that I've monopolized the home computer, slunk off to the study and roared for quiet on so many occasions during the past 6 years. A special thanks to my wife Pat, for support,encouragement and many valuable discussions.

PREFACE

This thesis describes the development of a new in-vivo method for assessing the antithrombotic properties of pharmacological compounds. In so doing it is necessary to describe the background to the problem, the current range of methodologies and the underlying concepts associated with the new method. This in turn gives rise to descriptions of work associated with several different disciplines; anatomy, physiology, pharmacology, biochemistry, fluid dynamics, optics and electronics being amongst the prime ones. Hence one of the characteristics of this thesis is that it is multidisciplinary. Another is that it is orientated to design, experiment and practice: it describes the events leading through the design to the construction and evaluation of an innovative item of instrumentation. The purpose of this preface is to put the project and its component disciplines into one readily assimilated context before embarking on the more discrete format of the main text.

Thrombi form inside blood vessels and, if the degree of ensuing occlusion is sufficient, may give rise to oxygen starvation in critical tissues. For example, if a thrombus occurs in the region of the brain the general condition known as a stoke results. Such strokes often lead to debilitating partial paralysis or even death. The formation of a thrombus stems from the malfunction of the normal haemostatic process and such malfunctions may be induced by any one, or even a combination, of a variety of factors. Particularly at risk are those with

unsatisfactory diets and/or lifestyles and people recovering from major surgery. Much effort is now associated with the search for pharmacologically active compounds which are cabable of preventing or dispersing thrombi.

Most of the primary screens currently associated with the search for compounds with the required profile of action rely on in-vitro tests. That is, blood is drawn from an animal or volunteer and the necessary procedures carried out in a sample tube or cuvette. However, there is now evidence to suggest that such screens may not be entirely representative: in separating the blood from the vasculature the influence of several naturally occuring moderators may be lost. Such moderators are to be found in the cellular components of the vasculature wall. There therefore exists the incentive to develop in-vivo screening methods.

Such screens may focus on either the growth of the final product, the thrombus, or the status of component precursors, platelet activity for example. As previously stated, in-vitro screens have tended to be the de facto method of pharmacological screening and aspects of platelet activity have been an integral part of many of them. There has however existed a parallel interest in thrombus formation and that has been in their clinical detection in patients - an inherently in-vivo situation. In recent years the method of choice has been via the use of ultrasonic Doppler shift techniques. Although getting a basic blood flow signal by such means is now relatively easy, extracting sufficient information upon which to base a diagnosis has proved more difficult. Never the less

many such techniques do now exist and one of them, flow disturbance analysis, does in principle lend itself to transposing to the laboratory sceening environment. Such a transposition becomes all the more attractive if the technique could be used with small animals, the rat for example. Whereas ultrasonic Doppler techniques do not readily lend themselves to the required degree of miniaturisation, an analogous technique known as laser Doppler velocimetry would appear to do so.

Thus the concept develops whereby the efficacy of compounds might be evaluated in animal models by using laser Doppler techniques to measure blood flow disturbances in the vicinity of an induced thrombus. The main underlying assumption is that the degree of disturbance will reflect the degree of encroachment of the thrombus into the vasculature. This in turn should reflect the efficacy of any introduced compounds. The particular manifestation of blood flow disturbance chosen for examination within the context of this thesis is the velocity of the fluid jet, formed as a result of the imposed thrombotic restriction.

There are three basic laser Doppler velocimeter configurations but many different implementations. Thus a relatively simple implementation of a dual beam device was assembled during the experimental phase of study and used to appraise the validity of those concepts expressed in the previous paragraph. The presence of a thrombus was modelled by a small glass 'pip' pressed into the bore of a capillary flow tube and, although lacking in many respects, gave results sufficiently encouraging to justify further work. In particular, the shape of the associated Doppler shift spectra suggested the design of a circuit for extracting

velocity information from the frequency signal and operating restrictions encountered with the prototype velocimeter gave rise to the design of a laser Doppler microscope. Before embarking on the second design phase the largely empirical findings associated with the initial phase were substantiated as far as possible by a retrospective assessment of any known supporting theory.

Initially the experiments undertaken with the new equipment closely followed those performed at the prototype stage and simply served to validate the underlying design concepts. Soon, however, a new and improved thrombus analogue was introduced and, through it, a new series of experiments undertaken. The new analogue involved the use of iron oxide loaded charcoal granules: they could be introduced into a flow circuit and attracted by a magnet at a specific point of the glass flow tube to form a partial occlusion. The advantage of this model was that it allowed occlusion dynamics to be followed and didn't give rise to optical distortions in the flow tube.

Following the apparent success with the new system it became possible to justify using the equipment with an animal model. The choice of such a model was not staightforward and an additional complication was the dependence upon contributions from personnel qualified to carry out the necessary experiments within the bounds of Home Office legislation. Eventully the superficial branch of the rat femoral vein was chosen as a suitable preparation. Initially the functional aspects of the laser Doppler equipment were validated in the newly introduced in-vivo environment by appraising derived flow measurements against

known dose response curves for isoprenaline.

It then became possible to sensibly enter the final phase of development, in which the growth of an induced in-vivo thrombus was to be monitored. It was decided that such thrombi should be created by passing an electric current across the desired target site. The results from the experiments were all favourable and amply vindicated all parts of the work undertaken within the terms of reference of this thesis and research study. Further validation of the technique must now depend upon it's level of acceptance and use by those qualified in the relevant disciplines.

CHAPTER 1

THE CIRCULATORY SYSTEM, HAEMOSTASIS AND THROMBUS FORMATION

1.1. Introduction

"The movement of the blood is constantly in a circle, and is brought about by the beat of the heart." When William Harvey reached this conclusion in 1628 the proof he offered clearly demonstrated that the same blood which leaves the heart through the arteries returns to it along the veins. His reasoning was based on a consideration of the function of the valves of the veins (these had been described by Fabricius in 1603), on experiment, calculation and logical argument about the structure of the heart. He had managed to create a chain of reason and evidence in which only one link awaited visual confirmation. This eventually came in 1661 when the introduction of the microscope enabled Malpighi to observe capillaries in the lung of the frog. Capillaries are tiny vessels which Harvey had surmised should exist as connections between the smallest arteries, now called arterioles, and the smallest veins or venules.

The circulatory or vascular system thus consists of a closed network of blood vessels through which the blood is unidirectionally forced by the heart. Foremost amongst its functions is that of transporting to the body tissues those materials such as oxygen and nutriments which are necessary for their growth, sustenance and activity: associated with this it must also provide the means whereby

waste metabolic products are removed from tissues and conveyed to the lungs and kidneys for elimination from the body. The circulatory system also provides the route whereby disease is attacked and tissue injury repaired. Possibly less obvious roles served by the system include that of regulating body temperature,water balance and the transport of hormones for system regulation.

1.2.The Cardiovascular System

The heart is a rhythmically contracting muscular pump. It has two upper chambers called atria and two lower chambers called ventricles. Each of these pairs of chambers is separated by a thin septum and a fibrous ring separates the atria from the ventricles. During a cardiac cycle blood first of all enters the right atrium and then by atrial contraction is made to pass to the right ventricle for discharge to the lungs. The atria have to expend only small amounts of work in transferring their contents to the ventricles; the ventricles do most of the work of the heart. Consequently the walls of the atria are thin in relation to those of the ventricles. Valves ensure the direction of blood flow.

Oxygenated blood returns from the lungs via the left atrium to the left ventricle and from here it is discharged by ventricular contraction through the arteries to the body generally. The arteries, capillaries and veins associated with the lungs form the pulmonary circulation and those associated with the rest of the body form the systemic circulation.Figure 1.1 shows a schematic diagram of the mammalian

circulatory system.

The cardiac cycle described above is initiated by electrical events within specialised cells associated with the heart muscle.The cycle is then propagated by a depolarisation chain reaction which involves groups of adjacent cells. Because the body fluids are good conductors,fluctuations in potential which represent the algebraic sum of these depolarisation potentials can be recorded from the surface of the body. Such a recording is known as an electrocardiogram (E.C.G.). Specific points on the E.C.G. can be identified with specific events in the cardiac cycle. This is illustrated in figure 1.2.

Both the large arteries seen leaving the heart, the pulmonary artery to the lungs and the aorta to the systemic circulation, form branches. These branches themselves divide and, by repeated branching, ever smaller and more numerous arteries are formed. The smallest branches, the arterioles, end in plexuses of vessels of very small diameter. These are the capillaries, required by Harvey and found by Malpighi. Capillary networks, whose meshes vary in size and form in different regions of the body, are found in all tissues except cartilage, epidermis and the cornea of the eye.

As blood flows along the capillaries some of it's fluid passes through their very thin walls.This acts to replenish the interstitial fluid, which occupies the tissue spaces and is the medium of metabolic exchange.Returning fluid re-enters the capillary network further along. The capillaries are themselves then drained by the veins. Finally the

veins unite with one another to form progressively larger trunks and the largest of these, the vena cava, returns the blood to the atria for recirculation. An artery-capillary-vein network is illustrated in Figure 1.3a.

Functionally the vascular system might well be likened to a system of pipes and conduits. It is, however, important to realise that in reality the blood vessels are made up from cells and are therefore themselves living tissue. Furthermore, the composition of the tissue changes with location.For example,when the heart contracts,blood is suddenly forced into the aorta and it's primary large branches.So these vessels, in addition to a basic endothelium content, have a large amount of elastic tissue in their walls and are considerably distended with each systole. This distension serves to protect the smaller vessels beyond from sudden strain and, additionally, the elastic recoil of the distended wall during diastole serves to drive the blood on and so promote a steadier stream of blood.

In medium and small size arteries there is a predominance of spindle shaped plain muscle cells and their presence helps to regulate the supply of arterial blood to various organs in accordance with their state of activity.The degree of contraction of these muscles is under involuntary nervous control and so, should a given area need more blood, they are made to relax and the vessel lumen increases. Should less blood be required the muscle cells are made to contract and the lumen is correspondingly diminished.

In veins the blood flows at a lower velocity than in arteries and at a considerably lower pressure. Accordingly, their lumena are larger and their walls thinner than those of their associated arteries. Structurally they are similar to arteries but in general they are poorer in muscular and elastic tissue and richer in white fibrous tissue. Transverse sections of an artery and a vein are illustrated in figure 1.3b.

1.3. The Composition of the Blood

Eighty per cent of blood is water. Despite the fact that chemical substances and cellular elements are constantly entering and leaving the bloodstream its general composition is relatively uniform in the higher order animals. This results from a number of regulatory mechanisms acting in conjunction with a rapid circulation. Any potentially large variations in blood composition which may be initiated by tissue metabolic processes are reduced by virtue of the large volume of blood flowing through the organs concerned.

The blood flowing round the circulation consists of a pale yellow fluid, the plasma, in which the red cells, white cells and platelets are suspended. The specific gravity of whole blood ranges from 1.055 to 1.065 while that of plasma varies between 1.028 and 1.032. The viscosity of blood is about 2.5 times that of water but may vary in accordance with changes in the temperature and degree of hydration of the body.

1.4. Plasma and Plasma Proteins.

Plasma, the fluid suspension medium of the blood, readily separates off to the top if a column of blood is allowed to stand and clotting is prevented. Water makes up about 91% of its volume, plasma protein makes up another 7% and the remainder is made up of inorganic salts and substances being transported from one part of the body to another.

Plasma proteins exert an osmotic pressure of around 25 mm Hg., this is instrumental in influencing the exchange of fluid between blood and tissue. In addition to this they combine with many different substances to form complexes which are then capable of being carried out by the blood to appropriate sites and released.

There are four main types of plasma protein, prothrombin, fibrinogen, globulin and albumin. Prothrombin is the precursor of thrombin, this is a protein-splitting enzyme and is responsible for breaking fibrinogen down into smaller units which then 'polymerise' into fibrin. Fibrin is insoluble and forms wound-healing clots: this is discussed in more detail later. The viscosity of plasma is largely due to fibrinogen.

The globulins are classified as α, β and γ. They are produced mainly in the liver and have a wide range of molecular weights, varying from 90,000 to 1,300,000. Each fraction is associated with different binding tasks, globulin for example binds with antibodies. The albumins are the most abundant of the plasma proteins and they have molecular

weights of the order of 68,000. At normal concentrations plasma albumin is responsible for around 80% of the total osmotic pressure of the plasma proteins.

1.5.Red Blood Cells (Erythrocytes)

Red cells are biconcave discs with diameter of the order of 8.8um and a maximum thickness of about 2.2um. They have no nuclei and their structure is such that they can take up an elongated shape in small capillaries - their normal shape is subsequently regained on moving into larger blood vessels.

The main function of the red cells is to carry haemoglobin, a compound of ferrous iron containing the pigment haem combined with protein. Haemoglobin combines loosely with oxygen and is effectively the molecular vehicle for its transport round the circulation to the tissues. If the haemoglobin were to be carried directly by plasma,without the intermediate action of the red cells,blood viscosity would be of such a high value that the circulation of blood would be extremely difficult. Furthermore haemoglobin is rapidly removed from plasma, whereas the life of a red cell is around 120 days.

There are normally about 5×10^{6} red cells mm^{-3} of blood and they account for about 45% blood volume. Since the total volume of blood in the body is of the order of 5L there are about 25×10^{12} red cells in the circulation. New red cells are made in the bone marrow and about 2×10^{11} have to be produced each day to replace the losses incurred by

their finite lifetime.

1.6 White Blood Cells (Leucocytes)

Five different types of white cell may be observed through the microscope. They are divided firstly into granulocytes, which have granules in their cytoplasm, and lymphocytes and monocytes which do not, (cytoplasm is the name given to the general protoplasmic contents of a cell and excludes its nucleus). The granulocytes are then further subdivided into neutrophils, eosinophils and basophils, according to the affinity of their granules. In the granulocyte series the cell diameter varies from 8 to 12um, with the lymphocytes the cell diameter range is 7 to 15um, while the monocytes have diameters varying between 16 and 22um. The granulocyte series accounts for about 70% of the white cells in the blood of an adult, lymphocytes account for a further 25% and monocytes for the remaining 5%.

In total there are far fewer white cells than there are red cells, the ratio being in the order of 1 : 600. There are therefore in the order of 8,000 white cells per cubic centimetre of blood. The life time of a white cell is typically only a few days.

1.7 The Platelets (Thrombocytes)

Blood platelets were without recognition in the early days of haematological microscopy, simply because they are smaller than either red or white cells and consequently easily overlooked. The circulating

mammalian platelet is an annuclear body and appears as a smooth colourless disc, with a diameter of 2 - 3um and a thickness of 0.5um. Donne provided the first description of platelets in 1842 but little importance was attached to them at that time. Even by 1906 Buckmaster was arguing that they were technical artifacts and only present in blood samples if the blood had been taken with insufficient care.

There are in the order of 2.5×10^5 platelets per cubic millimetre of blood. Their role in the body is concerned with the preservation of vascular integrity, specifically the arrest of bleeding. At the site of a wound in a blood vessel platelets will clump together to form aggregates and,in a small capillary,an aggregate may be able to plug the wound. In a larger vessel, however, a more powerful system is necessary. This system involves the formation of fibrin based blood clots and is referred to as haemostasis.

1.8.Haemostasis

The function of the normal haemostatic mechanism is to prevent blood loss from intact vessels and to stop excessive bleeding from severed ones. Structural integrity and the presence of normal platelets are known prerequisites for the prevention of blood loss from intact vessels: other aspects of the process are not fully understood.

Arrest of bleeding following trauma is known to be controlled by three complex and interrelated factors. Involved are the reaction of the blood vessel itself, the formation of a platelet plug and the

coagulation of the blood.

A blood vessel reacts physically to injury by constricting in the vicinity of the wound. This is a transient response, lasting less than one minute. The mechanism of this constriction is uncertain but it is thought to invlove local mechano receptors and/or substances released during the initial stages of the ensuing platelet plug and blood coagulation process. The purpose of the response is to slow down blood flow and thereby allow other ensuing processes a chance to operate.

The second stage of the haemostasis process is the formation of an unstable platelet plug on the damaged area of the endothelium. Normally platelets do not adhere to an intact endothelium; a natural anticoagulant called prostacyclin is produced by the endothelial cells and prevents the process. However, when endothelium is injured the underlying collagen is exposed and platelets are able to adhere quite rapidly to it. Under the influence of adenosin diphosphate (ADP),which is released by the damaged tissue, the platelets also start to adhere to each other.

The platelet plug so formed is only directly able to stop bleeding in cases involving minimal damage to small capillary vessels. In larger vessels the blood pressure is too great and the plug is expelled when the vessel spasm relaxes. To be totally effective it is necessary for the platelet plug to be reinforced and rendered stable. This happens when the third stage of haemostasis, coagulation, takes place.

Blood coagulates (clots) when the soluble plasma protein fibrinogen changes into insoluble strands of fibrin. Fibrin forms a network of long strands which entrap blood cells and, because the strands are sticky, the clot so formed will adhere to the surrounding tissues. At first the clot is soft and jelly like but after about ten minutes it starts to contract down and will harden within about two hours if exposed to air. A clot further plugs the bleeding and, by attaching to the torn tissue and contracting, pulls the tear together.

A blood clot represents the successful completion of a biochemical chain reaction. It is a process which requires the presence of many component parts; precursor substances in the blood are activated and in turn activate other conversions. Although complex,each successive stage has the advantage of representing a cascading of system gain. The effect is such that when the fibrinogen is converted to fibrin it happens almost instantaneously: this means that the fibrin is formed sufficiently quickly for it not to be flushed away by further bleeding.

There are in fact two routes by which the fibrin conversion is effected. Either by activation of a relatively slow intrinsic pathway or by activation of the more rapid extrinsic pathway. The intrinsic pathway is activated by contact of a blood factor with collagen or skin and the extrinsic pathway is activated by tissue thromboplastin,derived from damaged endothelial cells and extra vascular tissue. Both systems are activated when blood passes out of the vasculature and both are necessary for normal haemostasis.

A full description of the coagulation process, essentially biochemical in content, would be out of place in this thesis. The process is inherently complex, fourteen interacting factors are involved, and its description does not lend itself to simplification. That coagulation, hence full haemostasis, is inexorably linked with platelet activity is shown schematically in figure 1.4.

1.9.Thrombosis

Under normal conditions platelets are carried along in the circulating blood separately from each other and do not adhere to the endothelium.However, pathological damage to the endothelium alone, without necessarily damage to the rest of the vessel, can precipitate the formation of a probably quite unwanted haemostatic plug. This plug, unlike the extravascular one associated with the normal haemostatic process, now exists as an intravascular clot.

A clot formed abnormally in any blood vessel is termed a thrombus and the clinical condition is known as thrombosis. If such a clot is friable or occurrs in a site where the blood flow past it is able to break off parts of it, the detached and freely circulating fragments are called emboli.

Thrombi which form in high flow systems are mainly composed of platelet aggregates held together by strands of fibrin and are known as platelet thrombi. Thrombi which form in areas of complete stasis are composed of red cells with a large amount of interspersed fibrin and are

known as coagulation thrombi. Thrombi which form in regions of slow to moderate flow are composed of a mixture of red cells, platelets and fibrin: they are known as mixed platelet fibrin thrombi.

There are four major sites of thrombus formation. These are the veins, arteries, microcirculation and heart.Although similarities exist, pathogenesis and structure of the thrombi at these sites give rise to a number of important differences. Venous thrombi are usually formed in regions of slow flow,such as the apex of a valve cusp pocket.Initially they are formed as small mixed platelet fibrin thrombi and grow out of the valve pocket in the direction of blood flow. As the growing thrombus starts to occlude the lumen, flow is slowed and the thrombus propagates both proximally and distally: mainly in the latter direction. When the lumen is totally occluded blood flow ceases and further propagation occurrs in the form of a red coagulation thrombus. When a vessel tributory is reached the propagating thrombus is exposed to flowing blood and extends into the lumen as a mixed platelet fibrin thrombus. This second lumen becomes progressively occluded, blood flow reduced and the scene set for the coagulation thrombus cycle to start all over again.

Arterial thrombi tend to occur in regions of disturbed flow. Such regions occur at bifurcations or where there is narrowing and irregularity. Because arteries represent regions of rapid flow, arterial thrombi tend to remain mural and not totally occlusive. Fresh arterial platelet thrombi may embolise or grow to form successive layers. Such growths can become incorporated into the vessel wall and produce

atherosclerotic plaque. These plaques increase the disturbance in blood flow and this in turn encourages the further development of mural thrombi. A condition of positive feedback therefore develops with a hardening of the arteries as the net result.

Thrombosis of the micro circulation can be caused by activation of blood coagulation, by endothelial damage or by disseminated platelet aggregation. Most microcirculatory thrombi are of the mixed type, containing fibrin and platelets.

Thrombosis of the heart may be thought of as being either intrinsic or extrinsic. In intrinsic cases the thrombus is associated with parts of the heart's pumping chambers, viz, the endocardium, myocardium and valves. These cardiac thrombi vary in size and consist of fibrin enmeshed in ventricular tissue. This can give rise to a mural thrombus or become a detached emboli which then enters the systemic or pulmonary circulation.

In extrinsic cases the thrombus develops in the coronary artery supplying the heart muscle. Platelet and fibrin deposits gradually narrow the lumen. Initially there will be ischemic pain on exertion, due to an inadequate supply of oxygen to the heart muscle. This condition is commonly known as angina. Ultimately the obstruction may become complete, the ventricle muscle is totally deprived of oxygen and a coronary thrombosis is diagnosed. Often the condition is fatal.

In addition to the 'spontaneous' formations already described there

are several medical procedures which carry the risk of thrombus generation as a side effect. Surgery, implantation of prosthetic heart valves, organ transplant or platelet contact with renal dialysis membranes can all give rise to pathological clotting and thrombosis.

The property of platelets to aggregate has previously been described as being a common and essential feature of both the haemostatic and thrombotic process. Methods of studying aggregation tendancy are therefore of great interest in the context of thrombus formation and prevention; they are reviewed in the following chapter.

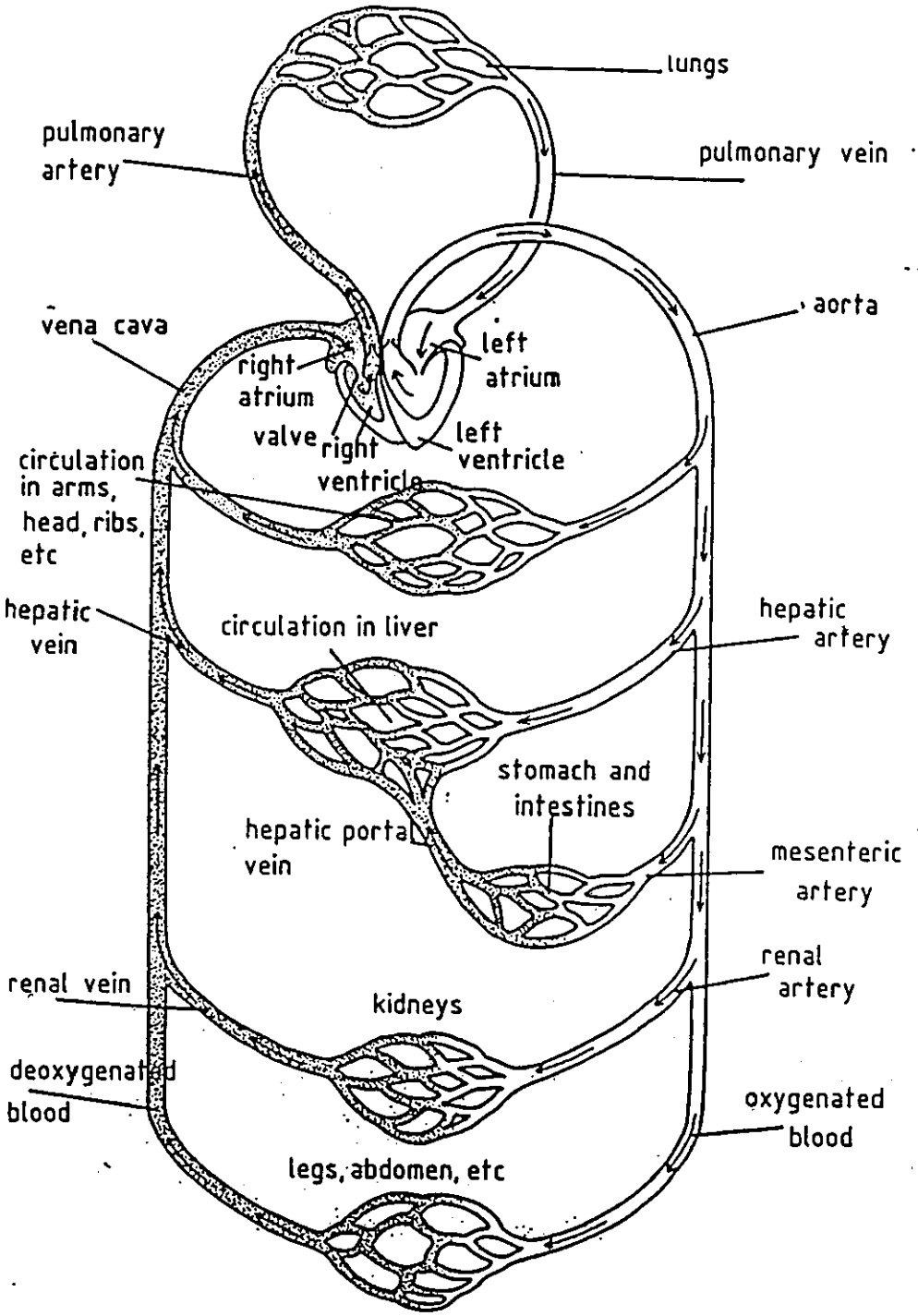

Figure 1.1: Schematic diagram of the mammalian circulatory system.

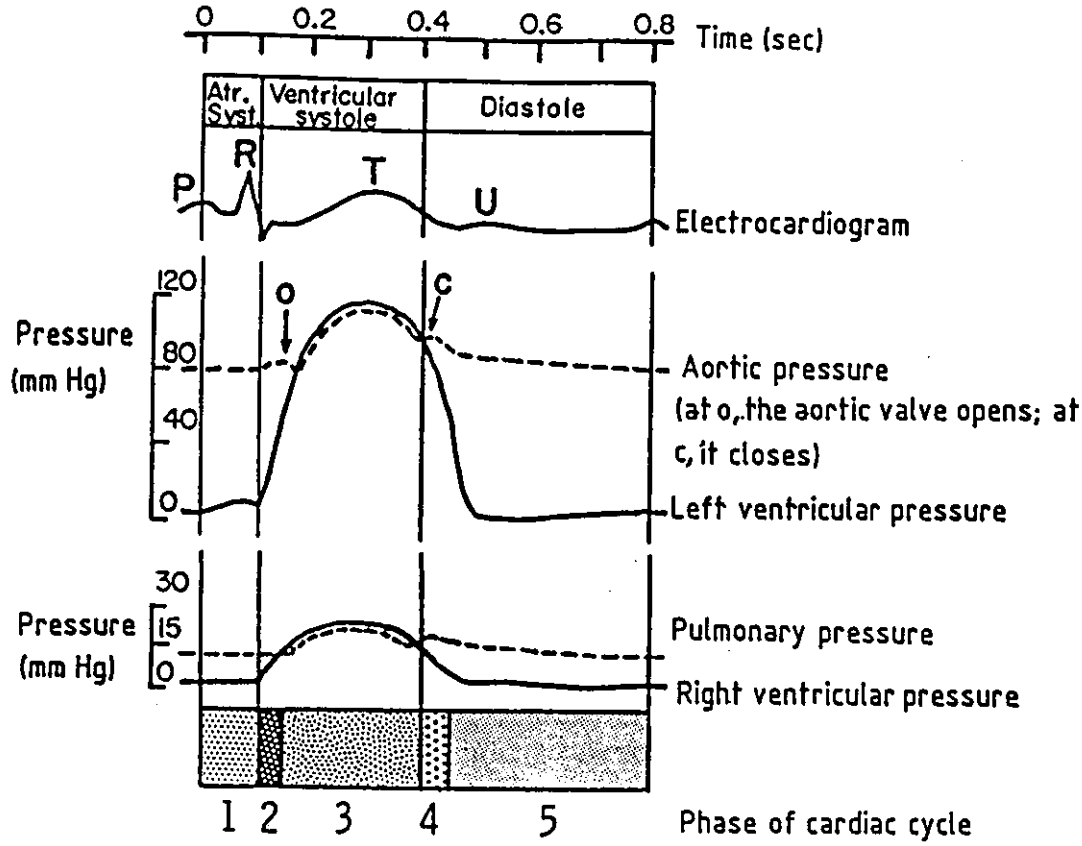

Figure 1.2 Events of the cardiac cycle at a heart rate of 75 beats per minute.The phases of the cardiac cycle identified by the numbers at the bottom are: 1,atrial systole; 2,isometric ventricular contraction; 3,ventricular ejection; 4,isometric ventricular relaxation; 5,venticular filling.

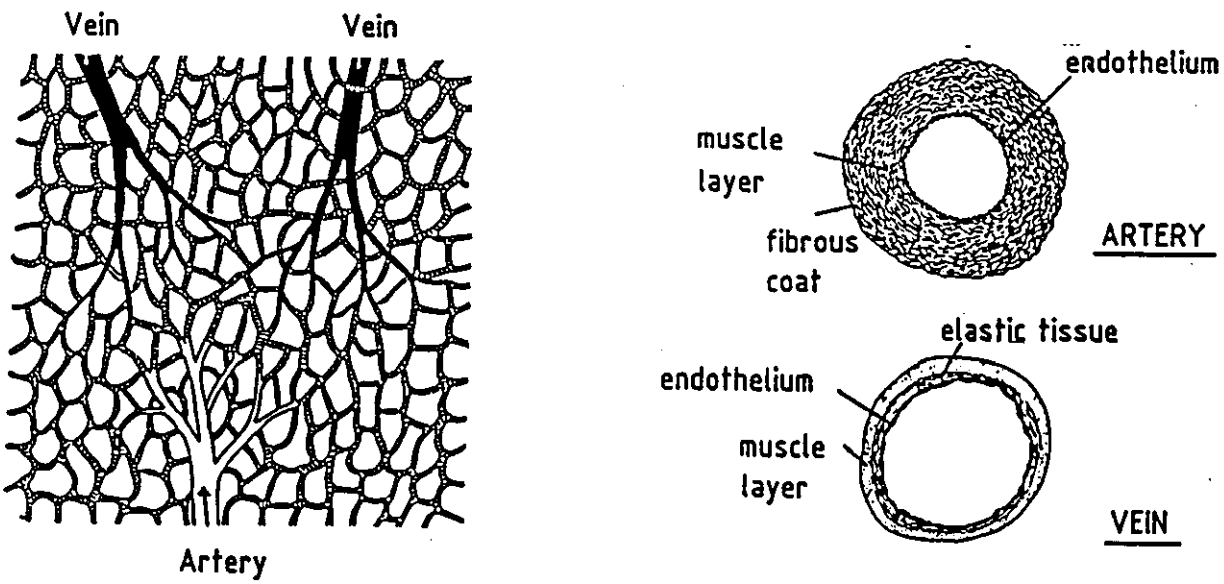

(a) Artery-Capillary-Vein network (b)Transverse section of artery and vein

Figure 1.3 The ciculatory system shown in two levels of detail.

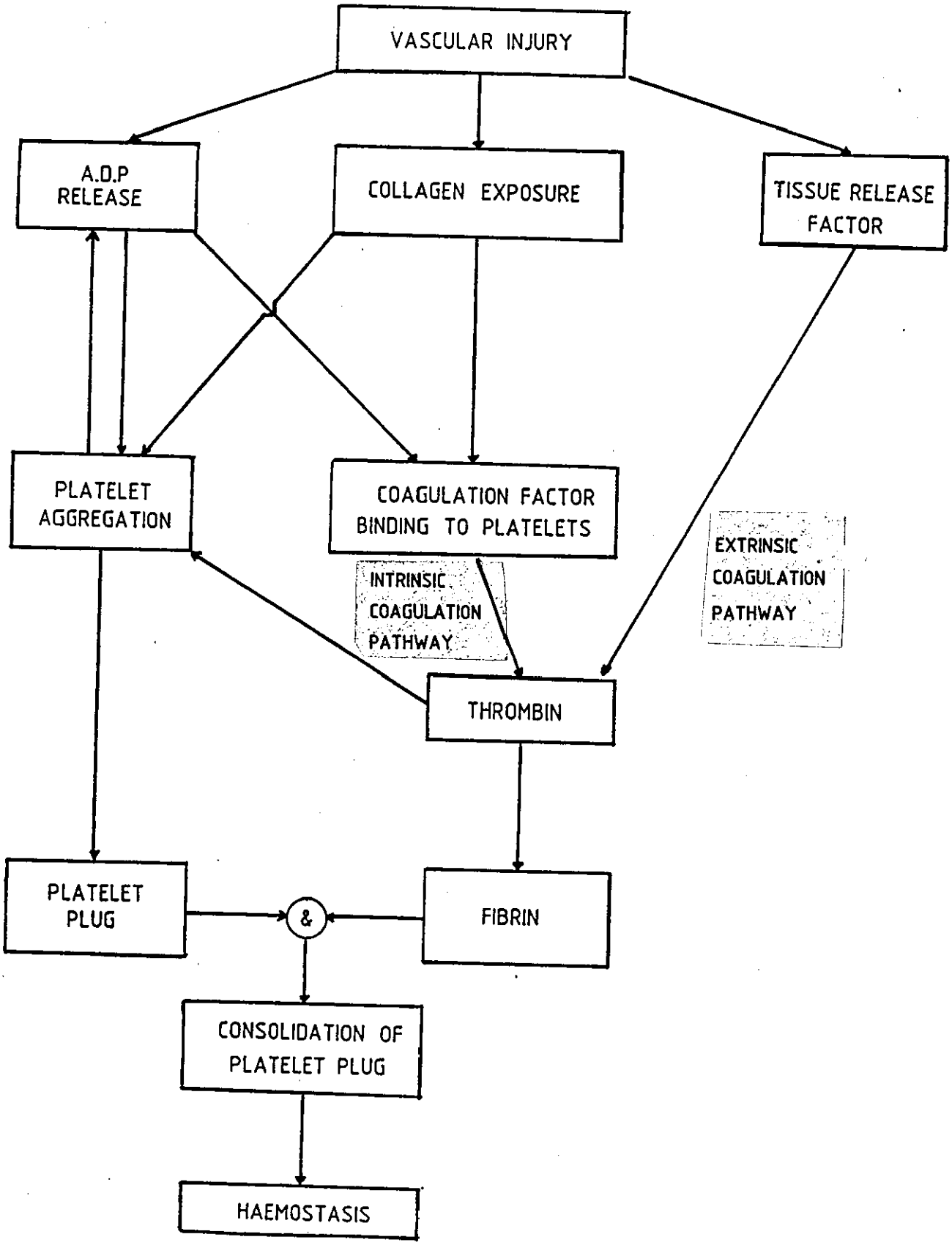

Figure 1.4: Schematic representation of the interrelationship between vascular injury, platelet activity and haemostasis.

CHAPTER 2

AGGREGOMETRY - METHODS FOR MEASURING PLATELET AGGREGATION ACTIVITY

2.1. Introduction

The extensive research being carried out into platelet behaviour has given rise to a plethora of techniques and associated equipment. Some utilise equipment developed specifically for platelet studies and some make use of equipment initially developed for more general purpose particle sizing applications.

All but a few make use of equipment which utilises either the optical or electronic properties of blood and it's cellular components. The tracer labelling of platelets by radioisotopes is a notable exception. Virtually all the techniques are in-vitro: they rely on blood samples being drawn and the experiments then conducted in sample tubes or cuvettes.The significance of this lies in the fact that platelet behaviour is moderated by biochemical environment.Consequently platelet behaviour in the sample tube may not always represent platelet behaviour in the body.

2.2 Microscopy

One method of studying aggregation on a quantitative basis is to do so visually with the aid of a microscope,often one of the phase contrast

variety.Objects such as blood cells provide little contrast with their environs but,because their presence is associated with changes in refractive index,they may be detected by phase changes in the transmitted beam.The technique was invented by the Dutch physicist Zernike in 1934.

Although phase microscopy has in the past enabled minimally experienced technicians to count platelets accurately and enabled scientists to make objective appraisals of aggregation activity, the technique is now usually considered to be too time consuming and tedious for routine use. This is particularly the case when financial considerations are such that the newer, semi-automated techniques can be realistically regarded as more favourable alternatives. Even so,if used by a skilled operator for short periods of time (to minimise errors caused by eye strain), it may be regarded as the quality assurance method of choice.Consequently new instrumentation methods are often verified by reference to it. (Brecher et al 1953. Bull et al 1965. Day et al 1980. Lumley and Humphrey 1981).

2.3. The Born Aggregometer

A great stimulus was given to the study of platelets in 1962 when Born described his turbidometric device for quantitating blood - platelet aggregation. Although changes in the optical density of a suspension of aggregating platelets had been reported by Jurgens and Braunsteiner (1950), it was Born and co-workers (Born 1962a,1962b; Born and Cross 1964; Born and Hume 1967) who developed a quantitative

instrument and supporting theory.

The principle of the aggregometer is simple. Blood plasma containing platelets (platelet rich plasma - PRP) is prepared from blood, citrated to prevent initial clotting, and a small aliquot pipetted into a glass cuvette. The cuvette is equipped with a stirrer and is heated to 37°C. A light beam shines through the cuvette and the intensity of it's emerging, unscattered fraction is detected with a photo electric cell. When aggregating agents such as Collagen or ADP are added to the cuvette an increase in transmitted light is observed,one which is proportional to the aggregation response. A schematic diagram of a Born type aggregometer is shown in Fig.2.1a.

The explanation for increased light passage lies in the distribution of platelets.Whereas when the aggregates are formed the light that hits them will be completely absorbed,an increasing volume within the cuvette will concurrently be becoming platelet free, due to the diminishing number of individual particles left. Comprehensive formulae linking intensity changes to different aspects of aggregation dynamics have been developed by Cronberg (1970).

The inherent sensitivity of the aggregometer is demonstrated by its ability to pick up and display the so called shape change phenomenae. This is a precursor to aggregation and is associated with platelets changing from a disc shape into an irregularly shaped sphere. The irregularities are in fact protruding pseudo-podia. It is through the pseudo podia that the platelets initially come into contact with each

other and proceed to aggregation. The shape change is believed to be isovolumic. (Born 1970). A typical optical density output trace from an aggregometer, showing shape change and aggregation, is shown in figure 2.1b.

Apart from the fact that it is an in-vitro technique, an additional limitation of the Born aggregometer is that it only functions with translucent cell suspensions such as PRP.In particular, it will not work with whole blood. This could be important in view of recent findings that leucocytes can generate the potent anti-aggregating agent prostacyclin and that platelets are, therefore, likely to behave differently in blood and in PRP. Another problem is that the preparation of PRP from blood may take 15-30 minutes and so labile naturally occuring modulators of aggregation may decay substantially during sample preparation.

2.4.Eriometry and Aggregometry

The term eriometry refers to the study of Fraunhofer diffraction patterns to obtain information on the size of small objects. Credit for first using the technique goes to Young who used it to measure the thickness of wool fibres and compare the sizes of blood cells (Young 1813). His investigations in fact attracted little attention at the time and the method may be said to have been rediscovered by Pijper (Pijper 1918). Improvements to the technique, particularly the introduction of a monochromatic light source, were later made by Ponder (Cox and Ponder 1941).

Many facets of science and technology require information about particle size distributions. Eriometry offers some particularly unique opportunities for remote or non invasive measurements. The technique has now been applied in fields as diverse as crystal growth measurements and fuel injector design. In addition to a basic demand, the advent of the laser as a cheap coherent light source and the availability of cheap but versatile micro computers have both contributed to a present day revival in eriometry.

The conditions for Fraunhofer far-field diffraction can normally be met at a relatively small distance by forming the diffraction pattern at the focal plane of a converging lens. Since the Fraunhofer diffraction pattern formed by an object is the Fourier Transform of the object, the converging lens which facilitates the formation of the Fraunhofer diffraction pattern is often referred to as the Fourier Transformation lens. This lens will focus any light diffracted at a particular angle to the same point in the diffraction plane, regardless of the position of the scattering object.The diffraction pattern is therefore unaffected by particle movement.

If the object under study is a sphere, the Fraunhofer diffraction pattern will be the Airy disc pattern. Taking into account the effect of the transform lens, the intensity of the disc at a radius r may be written as:

$$I(r) = I(o) \left[\frac{2J_1(\pi D r / \lambda Z)}{\pi D r / \lambda Z} \right]^2$$

where:

$I(r)$ = intensity at radius r

$I(o)$ = intensity at r = 0

D = particle diameter

r = radius in diffraction plane

λ = wavelength of illuminating radiation

Z = focal length of Transform lens

J_1 = Bessel function of the first kind and of order zero.

If instead of a single particle there are N, arranged at random over the extent of the incident beam, then the array theorem (Talbot,1966) shows that the diffracted intensity is N times the intensity from the one particle.

If the particles are not spheres the resulting diffraction pattern will still display circular symmetry provided there are a large number of randomly orientated particles.That is,all angles in the plane of the sample must be equally represented. There are practical limitations to this: the number of particles must obviously be finite and irregular shapes may well have a preferred orientation while moving in a fluid stream. Deviations from the ideal often results in the diffraction pattern having a grainy appearance.

When an essentially mono sized population of particles of reasonably regular shape is under study,the diffraction pattern is fairly simple and the data analysis straight forward.If the population

of particles is polydisperse the diffraction pattern increases in complexity and the data analysis becomes correspondingly more difficult. The approach adopted by Felton (1979) is to assume a form of the size distribution, calculate a corresponding theoretical light energy distribution and then, finally, iteratively adjust the weightings of the parameters in that distribution to achieve a best fit with the detected distribution from the sample. Kaye (1980) has critisised the best fit method on the grounds that gross errors may occur if the distribution is monodisperse or bimodal.

The system developed by Felton measures the focal plane energy distribution pattern by means of a detector composed of 30 concentric, semi circular, photo-sensitive rings. The signal from the detector is transmitted to a mini/micro computer for processing. See Fig.2.2. A similar detector head configuration has been described by Mullaney et al (1976).

The system described by Felton now forms the basis of a range of instruments produced by Malvern Instruments Ltd. Some preliminary studies conducted by Lumley (1984) suggest that one model, the 2200/3300 Particle Sizer, could be of great use in platelet aggregation studies.However,the instrument's standard sample cell must be replaced by one which provides a constant temperature of $37^{o}C$,a method of stirring and be made of a material which does not encourage platelet adhesion; ideally it should have a volume of about 5 ml.

The Malvern Particle Sizer has been tested with platelet rich

plasma and with blood diluted with saline in the ratio 1:10. Although it is an in-vitro technique and of limited resolution,it does have the advantage that platelet aggregation can be followed in the sample cell, within the limitations of the processing speed of the computer. Thus the kinetics of aggregation, the formation of doublets and triplets etc, can be investigated.See figure 2.3.Studies such as these would augment the work already carried out by, for example, Ayyub and Bikhazi (1978).

The wide dynamic range is a further advantage of diffraction based techniques.Aggregating platelets rapidly reach volumes which exceed the measurement aperture of some electrical sensing zone measurement based counting techniques (see section 2.7); diffraction based instruments are sensitive only to the area of the face presented by the particle aggregate.

2.5.Luminescence and Aggregation

The exogenous addition of an aggregating agent to platelet rich plasma results in the primary phase of aggregation. A release reaction then follows when the platelets secrete adenosin diphosphate (ADP) and adenosin triphosphate (ATD). This was shown schematically in Fig 1.4. and it may be remembered that within Chapter 1 the released ADP was ascribed as being responsible for stimulating the second phase of the aggregation chain. Recently instrumentation has been developed which gives information about aggregation by measuring the ATP fraction of the release secretion. The technique relies on an ATP sensitive chemo - luminescence reaction.

The characteristic green glow of the firefly is produced when the adenyl salt of luciferin undergoes oxidation. The reaction may be summarised by the following simplified equations:

$$\text{ATP} + \text{Luciferin} \underset{\text{Luciferase}}{\rightleftharpoons} \text{Adenyl Luciferin}$$

$$\text{Adenyl Luciferin} + O_2 \longrightarrow \text{Adenyl Oxyluciferin} + CO_2 + \text{light}$$

The emitted light has a wavelength maximum of 562nm and the number of photons emitted, hence intensity, is essentially equal to the number of reacting molecules.

So, in principle, an aggregating agent may be added to platelet rich plasma mixed with a luciferin - luciferase reagent and the light,which is proportional to the ATP index of platelet activity, measured with a photo multiplier circuit. In practice the reaction is sensitive to such variables as pH, temperature, luciferase and ATP concentrations. A pH of 7.75 and a temperature of 25°C are prescribed as being optimal and, additionally, a linear relationship of light emission to ATP concentration only exists below 10^{-6} M. The luciferase concentration is important because concentrations that are either too high or too low will cause decay of the emitted light.

By phosphorylation of ADP to ATP the luminescence technique can also be applied to measuring the ADP levels associated with platelet release and aggregation. ADP and ATP levels that accompany platelet

aggregation have a clinical significance in their own right. The information obtained from chemo-luminescence studies therefore tends to be used to complement information obtained from other aggregometers, rather than as an alternative to it. Chemo-luminescence is inherantly an in-vitro technique and relies on measurements in plasma, it is therefore open to the same general critisisms as the Born optical aggregometer.

2.6. The Electronic Aggregometer.

The design of this instrument stemmed from an observation by Cardinal and Flower (1980) that the electrical resistance of platelet-rich plasma increased during a collagen induced aggregation. Electron microscopy indicates that the following events are responsible for the above observation.

During the initial contact with blood the electrodes become coated with platelets.If no aggregating agents are added, then no further interactions occur between the platelets and the electrodes. However, in the presence of aggregating agents,platelets form aggregates with the monolayer already coating the electrodes and there follows a gradual build up. This further covers the electrodes and impairs conduction between them.

Physically the cuvette stage for the instrument developed from the above principle is similar to that developed for the Born Aggregometer. The cuvette is maintained at 37^{o}C by a heated block and the contents are stirred with a flea magnet. However, the electronic aggregometer

requires no optical transmission path and so the heating block can be solid. Instead, an electrode assembly is mounted in a cap that fits over the top of the cuvette.

Cardinal and Flower report that the most consistent results were usually obtained at a stirring rate of 400 - 600 r.p.m. and that small teflon coated magnets tended to give more reproducible stirring than wire 'fleas'. While attaching importance to the temperature stability of the cuvette ($\pm$ 0.1%), the authors ascribe greater importance to the quality and reproducibility of the stirring system. Stirring of inconsistent speed produces an erratic trace that is unsuitable for quantitative work.

The configuration of the electrode assembly also is of importance.Cardinal and Flower report the optimum design to be two 0.25mm diameter platinum wires,15mm long and separated by a gap of 1mm. The position that the electrodes occupy in the cell is also important; the best results being obtained when each electrode is located midway between the centre of the cell and the rim.Both electrodes are then facing the stirred blood. From the theoretical viewpoint finer electrodes are superior to thick ones since they require less of the total platelet population of the cuvette to form the initial monolayer. They will, therefore, be more completely covered (hence show a greater impendance change) by smaller numbers of platelets. A schematic diagram of the cuvette and electrodes is shown in Fig.2.4a.

An oscillator must be used to provide the potential difference

across the electrodes because DC will inevitably produce polarisation. Cardinal and Flower report that after considerable experimentation a sine wave of 15 Khz with a peak amplitude of 100mV was chosen. The potential difference across the blood sample is then amplified, demodulated and fed to a chart recorder. A block diagram of the circuit is shown in Fig.2.4b.

The electronic aggregometer has several distinct advantages over the Born type turbidometric device. Probably the main advantage is that it can measure platelet aggregation in whole blood, as well as in platelet rich plasma. This enables a more realistic measuring environment to be obtained. Also of importance is the fact that there is no sample preparation time required before blood is transferred to the measuring cuvette. Thus, allowing for an equilibrium time of about 2 minutes while the platelets coat the electrodes with an initial mono layer, aggregation responses may be obtained very rapidly.There is therefore less opportunity for the concentration of labile mediators such as prostacyclin to decline during the experimental period.

Aggregation responses obtained are very similar to those found with the Born aggregometer and this, coupled with electron microscope studies of platelet build up on the electrodes, suggests that the device represents a valid and improved way of examining aggregation in drawn off samples. However, it is an in-vitro technique and, additionally, sensitive to small changes in operating conditions. Constant stirring speed in particular is of prime importance. A typical aggregation response obtained with the instrument is shown in Fig.2.4c; shape change

information is largely absent.

2.7.Platelet Counting by the Electrical Sensing Zone Method.

When blood cells which have been suspended in an otherwise particle free electrolyte are passed through a small aperture in which a current path had been established,impedance changes proportional to the volumes of the individual cells are introduced.The low conductivity cells alter the electrical resistance of the orifice by displacing a tiny amount of higher conductivity electrolyte. Therefore such a system can count individual cells and provide size distribution information:this discovery was made by W H Coulter in 1953.

Second generation electrical sensing zone instruments have now been introduced and provide greatly improved resolution. The key improvement lies in the use of hydrodynamic focusing; a particle free sheath fluid is used to constrain the particle to be measured to the centre of the measuring orifice. This is important because there is a tendency for the non-uniform current density at different locations within a cylindrical hole of restricted length to make the impedance pulse height dependent on the path that an individual particle takes through the orifice.(Grover 1969, Spielman and Goren 1968) Circuits to detect and edit off axis pulses have been developed (Katchel 1973) but do not deliver the precision of a focused system. As an added bonus hydrodynamic focusing virtually eliminates clogging of the orifice.

In order to achieve a wide dynamic range of particle sizing it is

also necessary to eliminate artifact pulses.The main source of these pulses is large particles recirculating in the fluid eddy currents formed by the jet of fluid emerging from the orifice. These ghost pulses have a wide size distribution but are about one-tenth the height of a true transit pulse and will therefore tend to obscure smaller particles. Editing techniques might be applied to discriminate these pulses but the use of a second sheath to eliminate recirculation is quite effective (Thom 1972). The system as described therefore requires the controlled fluid flow rate of three distinct fluid elements: the particle-containing sample and each of the two particle free sheaths. The flow rate of each will vary with air pressure applied to its containing vessel, with the liquid pressure of the fluid height in each vessel and with the fluid resistance of each path.

Utilizing the principles described above, special purpose whole blood platelet analysers have been developed. One such is the Clay Adams Ultra Flow 100, described by Haynes and Shoor (1978) and Haynes (1980). Fluid control in the instrument utilizes small-bore tubing as fluid resistors in a configuration analogous to an electronic Wheatstone bridge. This gives independant control of fluid flow in each pathway, relative freedom from sensitivity to fluid levels and all driven by a single non critical air pressure. A simplified diagram of the particle detection head of the Ultra Flow 100 is shown in figure 2.5a and the effects of the backsheath are shown in figure 2.5b.

Following suitable amplification the output of the detector head must be passed into circuitry capable of translating impedance changes

into particle size data. The circuit is made up of variable aperture window discriminator logic elements. For an instrument designed primarily for use in a clinical environment there is a tendancy for the aperture to be preset. In a research environment there is a possibility that user variable aperture levels might give greater flexibility of operation.

In the Ultra Flow 100 logic there are effectively two counting channels, one discriminating for platelets and the other for red blood cells (RBC).Initially the RBC count of a sample must be accurately predetermined and dialed into the instrument.An accurate platelet count is then displayed once 1/100 of the dialed R.B.C. count has been registered, a process taking about 13 - 19 secs. Ratio systems increase the precision of counting by cancelling out coincidence counting errors and by providing freedom from sample dilution errors. The output from the instrument relates to numbers of single platelets, aggregation activity is witnessed by a fall in this population (Lumley and Humphrey 1981). Instruments such as the Baker Diagnostic 810 series, similar in sensing head design but utilizing the philosophy of variable input apertures and multi channel analyser outputs, potentially allow platelet aggregation growths to be followed, rather than deduced.

The impedance measurement method of quantifying platelet activity has several advantages to offer. The first is that aggregation is studied in whole, albeit dilute, blood;this situation more closely resembles conditions in vivo. The fact that it is not necessary to prepare PRP samples also means that labile substances are less likely to

disappear during the interval between sampling and analyzing. However,it is an in-vitro technique and must therefore still impose a measure of uncertainty on any results achieved.

2.8. Radioisotopic Tracer Methods

Isotope labelled platelets have been used over many years for monitoring platelet kinetics in-vivo: upto recently the most commonly used isotope has been Chromium-51 (Cohen et al, 1961). Currently Indium -111 is gaining in popularity because Chromium -51 now tends to be seen as having too long a half life,a low gamma emission, high in-vivo elution and inefficient platelet labelling capability. Indium -111 on the other hand has a 2.8 day half life and gamma photon energies of 173 KeV (84%) and 247 KeV (96%). When platelets are labelled using a lipid soluble complex of the isotope there is an uptake of up to 90% and no impairment of platelet behaviour. Consequently Indium -111 labelling now forms the basis of several discretely different deposition techniques.

Gryglewski et al (1978) reported a procedure based on the determination of the increase in weight of a rabbit tendon when that tendon was superfused with blood; the tendon is rich in collagen and readily promotes platelet deposition under normal circumstances. Badimon et al (1982) have modified and improved the procedure by estimating the amount of Indium -111 labelled platelets deposited on the surface of the tendon.Using a gamma counter,results are expressed as counts per minute per gramme of tendon, corrected for the radionuclide decay. Badimon et

al conclude that the tracer technique is an improvement on the weight gain method because of its specificity, lower variability and higher sensitivity.

McCabe (1982) has developed a procedure whereby Indium labelled platelets are caused to be deposited on selected areas of guinea pig carotid artery. Methods of traumatising blood vessels to cause controlled and localised platelet aggregation are reviewed in a later chapter of this thesis but for the present it may be sufficient to note that in the methodology developed by McCabe the blood vessel was subjected to a localised burning by the application of a current of 2mA for 60 seconds. Labelled platelets are then injected into the guinea pig and, over a period of 1 hour, form aggregates at the treated area. The animal is then killed, the artery removed and placed in a gamma counter. A piece of undamaged contralateral artery may also be removed and analysed for labelled platelet deposition: this acts as a control.

Baumgartner (1973) described a system which allowed the exposure of natural vascular surfaces to blood under controlled fluid dynamic conditions. The technique is now generally referred to as a Baumgartner chamber.In its original form it was designed to allow a visual and quantitive morphological examination of platelet build up.However, the basic chamber may also be used in Indium labelling experiments.

In principle, everted vessel segments which have been denuded of endothelium are drawn onto a rod which is then placed in a tube so that an annulus of blood can be circulated along it's length.The segments, up

to six in number, present collagen rich surfaces to the circulating platelets. Referring to Fig.2.6,the blood enters the wide tube, is distributed around the body by the pointed end of the rod, streams along the rod forming an annulus and then leaves the tube through four holes at the base of the rod. In experiments conducted by Turitto and Baumgartner (1979) great attention was paid to the haemodynamic design of the chamber, in order to quantify the influence of such variables as wall shear rate.

For antithrombogenic assessment studies, where knowledge about platelet morphology may not be at a high premium, a deposition index may well suffice. It is under these conditions that Indium labelled platelets may be introduced into the blood perfusing the Baumgartner chamber. Visual inspection is then replaced by gamma photon counting. The chamber retains its role of providing a controlled haemodynamic environment.

Radio isotopic tracer techniques have undoubtedly made great contributions to the study of platelet interactions in flowing blood. They have the potential of being virtually non invasive and can yield quantitative data. However, the isotope must be prepared within narrow limits of time, the platelets must be labelled with the isotope (see Fig 2.7) and a gamma counter is required. The labelling involves several time consuming steps, the gamma counter may or may not be a general facility within a department.

Work started largely by Oster et al (1985) does in fact now promise to improve some of the time aspects of the radio labelling technique.Cultivated platelet specific monoclonal antibodies that have been labelled with Indium-111 may be injected into the blood stream and will then bind directly onto the platelets:no separation stage is required.Presently the emphasis of the work is upon the clinical detection of thrombi by gamma camera techniques but,in principal,it might be converted to a quantitative method by direct scintillation counting.

2.9. Platelet Counting in-vivo.

For the reasons already indicated in the previous sections, platelet aggregation studies should ideally be carried out in pharmacologically normal conditions. Arguably this involves the use of in-vivo models.

An in-vivo determination of Indium labelled platelet deposition may also be carried out with the aid of a gamma camera (Fuster et al 1979).Studies of this kind do not yield the quantitative information associated with,for example, the work by Baumgartner.Rather,they are used in conjunction with experimental animals to assess the likely extent of endothelial damage following such procedures as bypass graft surgery.

Hornstra (1970) published the first quantitative method of measuring platelet aggregation in-vivo. In this method an aortic loop is

created which allows heparinized blood to be passed through a filter in an extra-corporeal circuit. Aggregating agents then cause the platelets to partially obstruct the filter. The degree to which obstruction occurs is revealed by measuring the pressure difference across the filter; this in turn reveals the potency of the aggregating agent. The technique has some advantages but also several serious disadvantages - collagen cannot be studied, heparin is required and creation of the aortic loop is difficult.

Smith and Freuler (1973) have developed a continous counting technique which allows an improved in-vivo study to be conducted. Their technique makes use of a Technicon auto-counter,an optically based particle counting device.The overall layout is shown in Fig.2.8a.

Blood is removed from the carotid artery of the animal model,but in order to avoid the injection of a systemic anticoagulant,a double cannula is used.This allows 3.8% trisodium citrate to be introduced into the sampled blood, in the manner shown in Fig.2.8b.The citrated blood is withdrawn at the rate of 0.1 ml min^{-1} by a pump and then passed into a manifold where dilution and destruction of the red blood cells takes place. This selective destruction (lysing) of the red blood cells is by means of a 1% ammonium oxalate/.002% saponin solution. The remaining cells are then counted by the Autocounter.

A schematic diagram of the Autocounter is shown in Fig.2.8c.With particles in the flow cell there are two ways in which light from the source may reach the receiving photomultiplier: either by direct

transmission or by indirect, scattered,transmission. In the Autocounter a darkfield disc prevents direct transmission. Thus only scattered light, with an intensity proportional to particle count, is collected by the objective lens and brought to a focus at the detector. A chart recorder makes a permanent record of the counts.

In the context under discussion all nonlysed particles, of platelet size and larger, are counted. The leucocyte count (determined independantly) is subtracted from the total count to give the platelet count. When a thrombogenic agent is injected into the experimental animal there will be a reduction in the number of recorded circulating platelets, due to a percentage of the population becoming involved in intravascular aggregation and adhesion.

The method allows continuous platelet counting in-vivo, the surgery required is minimal and both the thrombotic response and the drug effect are reproducibly quantitated. Free platelet aggregates in the arterial circulation may give rise to problems of interpretation under some conditions.

2.10. Discussion.

No one aggregometry method can be considered as the method of choice. Rather, each one must be regarded as making a unique but complementary contribution to the understanding of platelet aggregation and allied phenomona. However, it is clear that for both pharmacological and logistic reasons, a minimal disturbance to the haematological

environment is to be sought after in antithrombotic drug research.The in-vivo method developed by Smith and Freuler (1973) and several of the radioisotopic labelling techniques come close to the ideal.

The main disadvantage of the Smith and Freuler technique is that the measurements are not made at the site of thrombus formation.In the research laboratory environment the main disadvantages associated with the radioisotopic techniques are,as yet,the preparation of the labelled platelets and the use of expensive gamma counting equipment. It was as a result of these considerations that the decision came about to look for an alternative method of assessing the anti thrombotic activity of drugs.

Taking one of the best existing techniques as a starting point, one notices that the radio labelling techniques are assessing platelet activity by the amount of radio labelled material collecting at a traumatized point. This is an extension of either weighing the deposition or a visual inspection of it.Either way,platelet activity is being measured by the end product,thrombus formation.

The present line of investigation then developed further following the conjecture that much the same information might be acquired by investigating the effect of a growing thrombus on the flow of blood in a vessel.The line of reasoning went that the development of a suitable in-vivo measure of blood flow should lead to an in-vivo measure of thrombus formation,with all attendant advantages over in-vitro methods of sceening for antithrombotic drugs.The advantages over radio labelling

should be found in the lack of sample preparation and the cost and convenience of the associated instrumentation.

From the outset it was known that ultrasonic Doppler techniques were used extensively in the clinical diagnosis of established thrombus occlusions.They were,therefore,an obvious starting point for the proposed development studies.Accordingly,ultrasonic Doppler flow principles and their application to occlusion measurements are discussed in the next chapter.

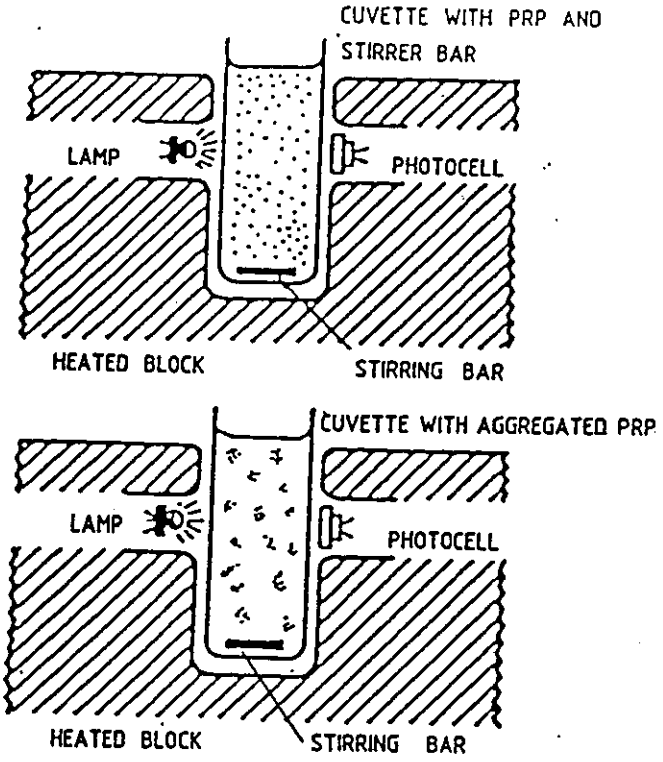

Figure 2.1a: Schematic diagram showing the operation of the 'Born' turbidometric aggregometer. In a cuvette full of stirred unaggregated platelets most of the light is scattered but when the platelets aggregate there is an increase in the transmitted light, since the aggregated platelets occupy a smaller effective volume.

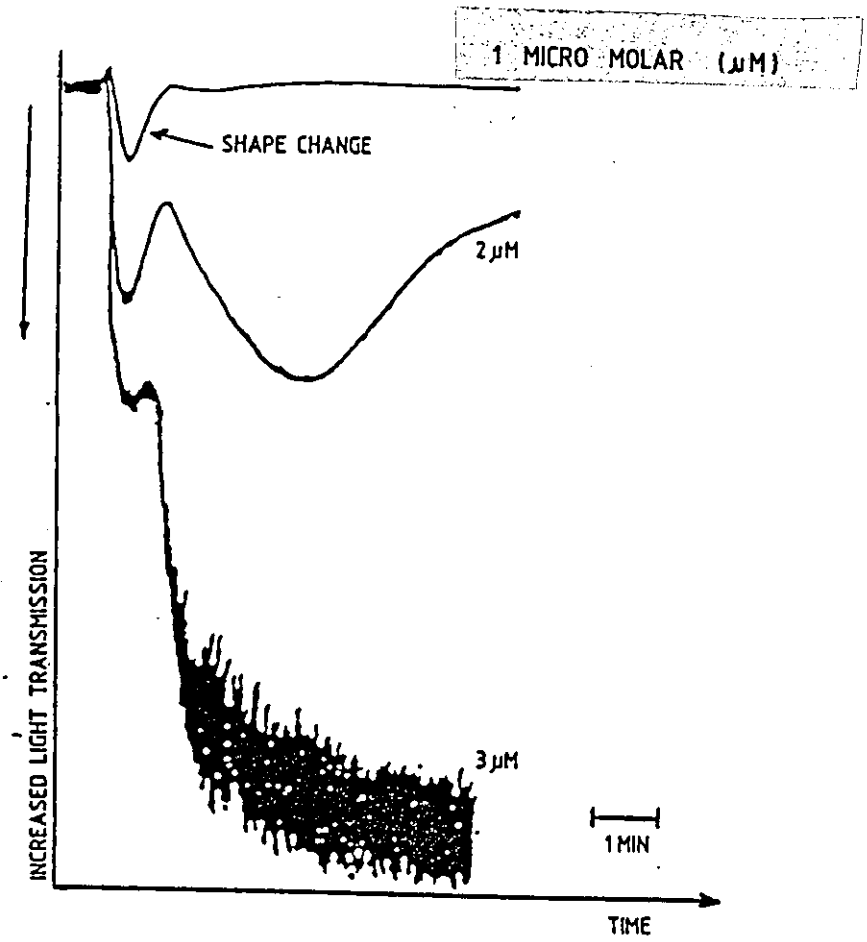

Figure 2.1b: Optical transmission changes induced by the effect of three different concentrations of ADP on platelet rich plasma.

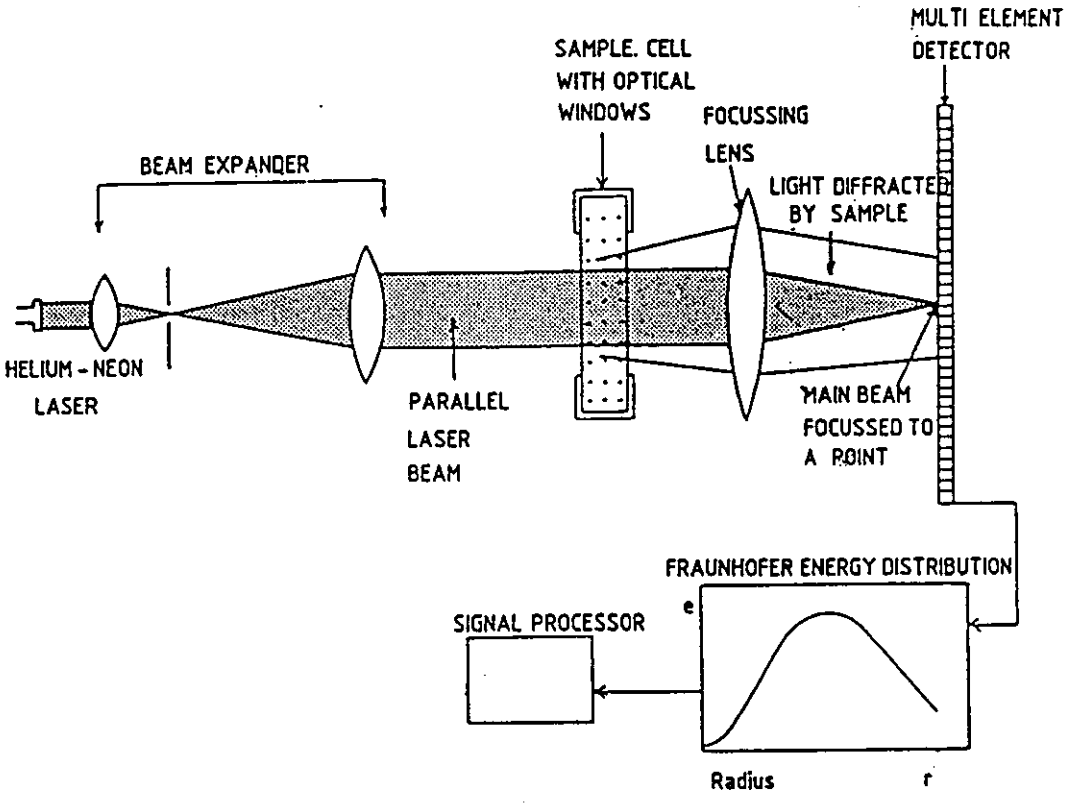

Figure 2.2. Diffraction based particle sizer,of the type developed by Felton(1979).

CONTROL .SHL

MALVERN 2200/3300 PARTICLE SIZER

MALVERN INSTRUMENTS LTD,SPRING LANE,MALVERN,ENGLAND.

PRINTING PARAMETERS

RUN NO.	TIME	MODEL	X BAR	H	LOG ERROR
8	10-36-50	LOG-NRM	2.83	1.66	4.81

PRINTING RESULTS FROM DATA BLOCK 1

SAMPLE CONCENTRATION = 0.0007% BY VOLUME OBSCURATION = 0.11

SIZE BAND UPPER	SIZE BAND LOWER	CUMULATIVE WT BELOW	WEIGHT IN BAND	CUMULATIVE % WT ABOVE
32	31	100.0	0.0	0.0
31	30	100.0	0.0	0.0
30	29	100.0	0.0	0.0
29	28	100.0	0.0	0.0
28	27	100.0	0.0	0.0
27	26	100.0	0.0	0.0
26	25	100.0	0.0	0.0
25	24	100.0	0.0	0.0
24	23	100.0	0.0	0.0
23	22	100.0	0.0	0.0
22	21	100.0	0.0	0.0
21	20	100.0	0.0	0.0
20	19	100.0	0.0	0.0
19	18	100.0	0.0	0.0
18	17	100.0	0.0	0.0
17	16	100.0	0.0	0.0
16	15	99.9	0.0	0.0
15	14	99.9	0.0	0.1
14	13	99.9	0.1	0.1
13	12	99.8	0.1	0.1
12	11	99.6	0.2	0.2
11	10	99.3	0.3	0.4
10	9	98.8	0.5	0.7
9	8	97.9	0.9	1.2
8	7	96.2	1.7	2.1
7	6	93.0	3.2	3.8
6	5	86.8	6.2	7.0
5	4	75.1	11.7	13.2
4	3	54.5	20.6	24.9
3	2	24.7	29.8	45.0
2	1	2.0	22.6	75.3
1	0	0.0	2.0	98.0

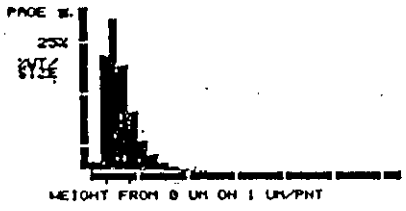

(a)

ADP AGR 1UM

MALVERN 2200/3300 PARTICLE SIZER

MALVERN INSTRUMENTS LTD,SPRING LANE,MALVERN,ENGLAND.

PRINTING PARAMETERS

RUN NO.	TIME	MODEL	X BAR	H	LOG ERRO
11	11-09-20	LOG-NRM	3.48	2.01	4.73

PRINTING RESULTS FROM DATA BLOCK 1

SAMPLE CONCENTRATION = 0.0007% BY VOLUME OBSCURATION = 0.11

SIZE BAND UPPER	SIZE BAND LOWER	CUMULATIVE WT BELOW	WEIGHT IN BAND	CUMULATIVE % WT ABOVE
32	31	[illegible]	[illegible]	[illegible]
31	30	99.9	0.0	0.1
30	29	99.9	0.0	0.1
29	28	99.9	0.0	0.1
28	27	99.8	0.0	0.1
27	26	99.8	0.0	0.2
26	25	99.8	0.0	0.2
25	24	99.7	0.0	0.2
24	23	99.7	0.1	0.3
23	22	99.6	0.1	0.3
22	21	99.5	0.1	0.4
21	20	99.4	0.1	0.5
20	19	99.3	0.1	0.6
19	18	99.1	0.2	0.7
18	17	98.9	0.2	0.9
17	16	98.6	0.3	1.1
16	15	98.2	0.4	1.4
15	14	97.7	0.5	1.8
14	13	97.1	0.6	2.3
13	12	96.2	0.9	2.9
12	11	95.1	1.1	3.8
11	10	93.5	1.6	4.9
10	9	91.4	2.1	6.5
9	8	88.4	3.0	8.6
8	7	84.2	4.2	11.6
7	6	78.3	5.9	15.8
6	5	69.9	8.4	21.7
5	4	57.9	11.9	30.1
4	3	41.6	16.4	42.1
3	2	21.3	20.2	58.4
2	1	3.7	17.7	78.7
1	0	0.0	3.7	96.3

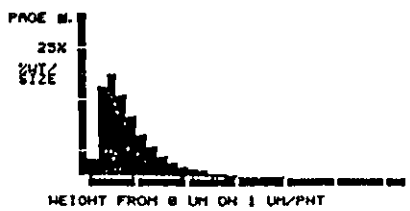

(b)

ADP AGR 3UM

MALVERN 2200/3300 PARTICLE SIZER

MALVERN INSTRUMENTS LTD,SPRING LANE,MALVERN,ENGLAND.

PRINTING PARAMETERS

RUN NO.	TIME	MODEL	X BAR	H	LOG ERR
10	10-53-40	LOG-NRM	8.37	2.30	8.6

PRINTING RESULTS FROM DATA BLOCK 1

SAMPLE CONCENTRATION = 0.0009% BY VOLUME OBSCURATION = 0.10

SIZE BAND UPPER	SIZE BAND LOWER	CUMULATIVE WT BELOW	WEIGHT IN BAND	CUMULATIVE % WT ABOVE
32	31	98.2	0.2	1.6
31	30	98.0	0.2	1.8
30	29	97.8	0.2	2.0
29	28	97.6	0.2	2.2
28	27	97.4	0.3	2.4
27	26	97.1	0.3	2.6
26	25	96.7	0.3	2.9
25	24	96.4	0.4	3.3
24	23	95.9	0.4	3.6
23	22	95.4	0.5	4.1
22	21	94.9	0.6	4.6
21	20	94.2	0.6	5.1
20	19	93.5	0.7	5.8
19	18	92.6	0.9	6.5
18	17	91.6	1.0	7.4
17	16	90.5	1.2	8.4
16	15	89.1	1.4	9.5
15	14	87.5	1.6	10.9
14	13	85.5	1.9	12.5
13	12	83.2	2.3	14.5
12	11	80.5	2.7	16.8
11	10	77.2	3.3	19.5
10	9	73.2	4.0	22.8
9	8	68.3	4.8	26.8
8	7	62.5	5.9	31.7
7	6	55.3	7.2	37.5
6	5	46.6	8.7	44.7
5	4	36.2	10.4	[illegible]
4	3	24.3	11.9	[illegible]
3	2	11.0	12.4	[illegible]
2	1	2.2	8.6	[illegible]
1	0	0.0	2.2	97.8

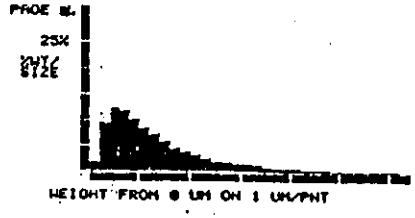

(c)

Figure 2.3. Sample print out from a Malvern 2200/3300 Particle Sizer for three platelet responses. (a) is a control, (b) the response to 1 micro molar ADP, (c) the response to 3 micro molar ADP. The examples have been chosen to illustrate the use of an instrument,they do not represent any particular experiment.

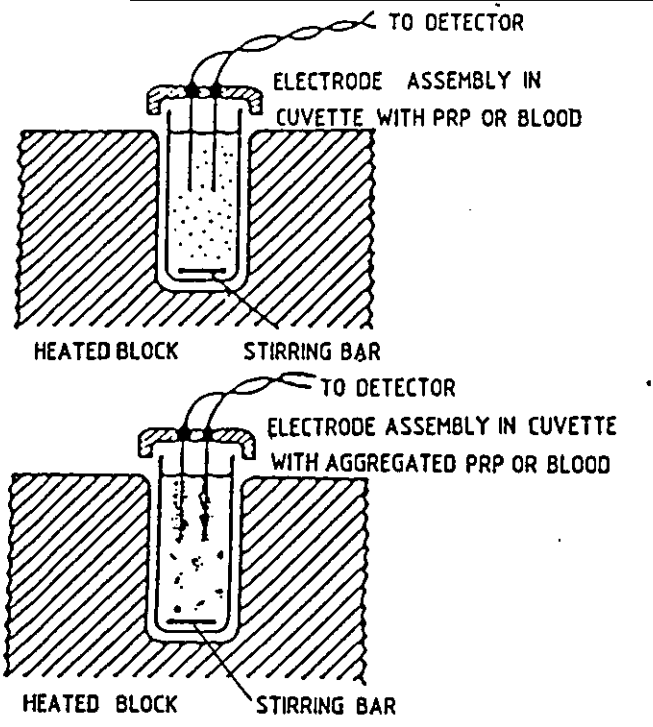

Figure 2.4a.Schematic diagram showing the electronic aggregometer.The electrodes become coated with a primary layer of platelets,this is built up during aggregation and there is an increase in the cell's impedance.

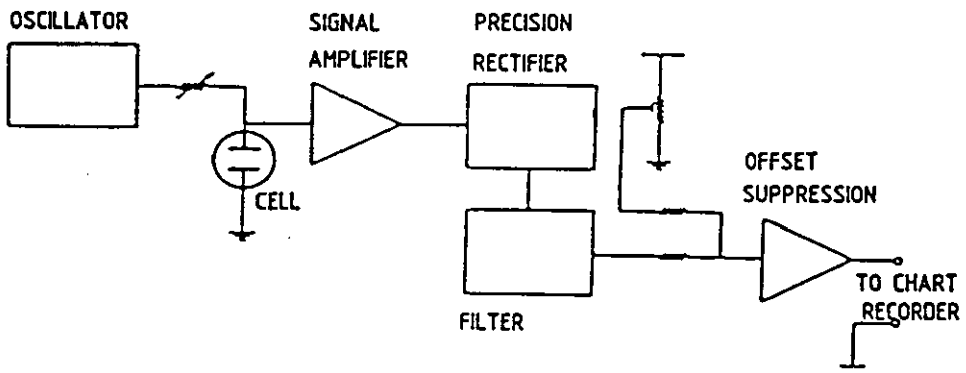

Figure 2.4b. A block diagram of the circuit elements employed in the electronic aggregometer.

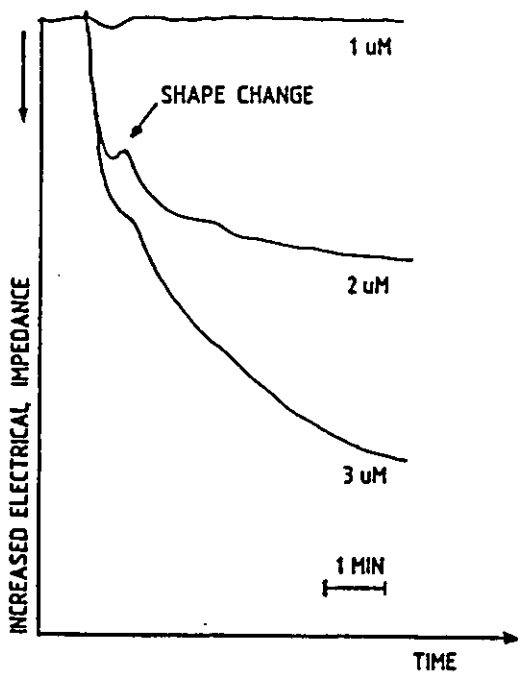

Figure 2.4c. Impedance changes induced by three different concentrations of ADP on platelet rich plasma.Note the decrease in response to shape change.

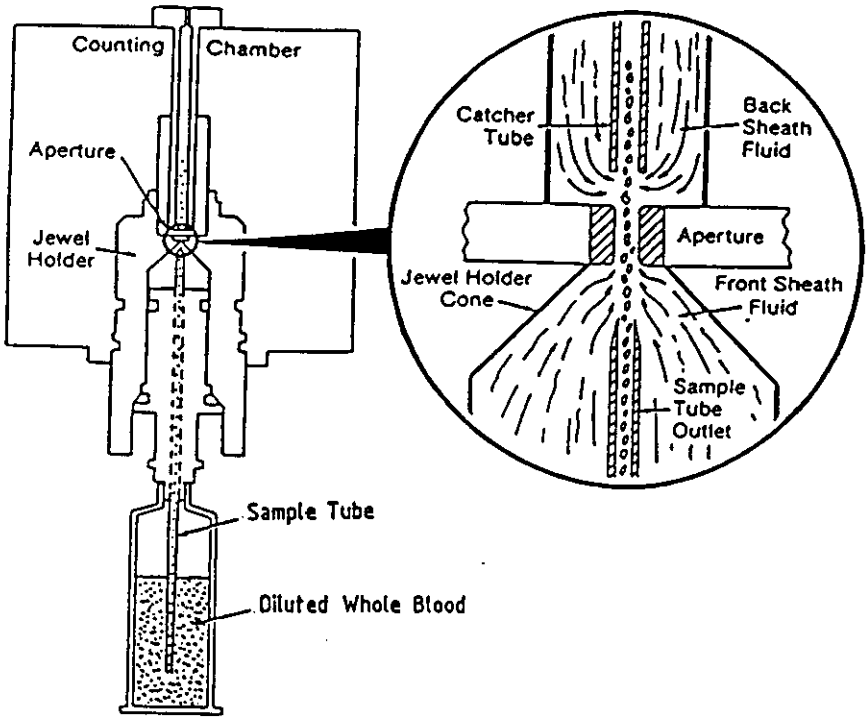

Figure 2.5a. The focused aperture and the counting chamber of the Ultra Flow 100.

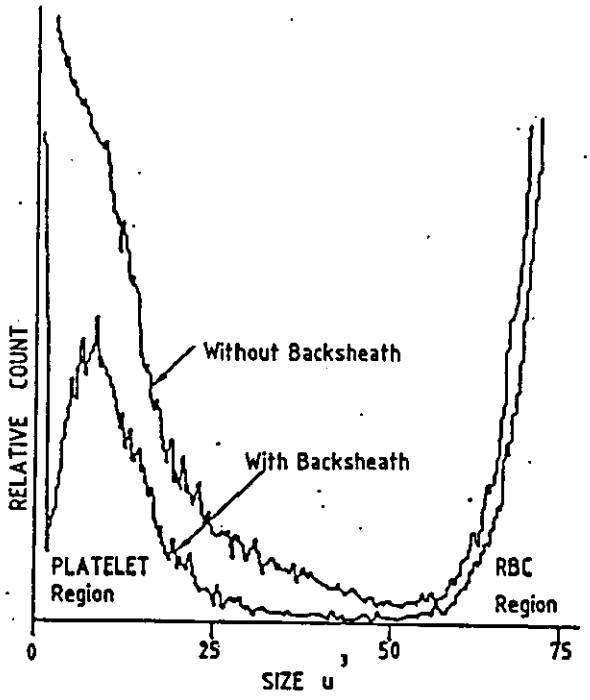

Figure 2.5b. Curves with and without back sheath show it's effect in eliminating ghost pulses.(after Haynes,1980).

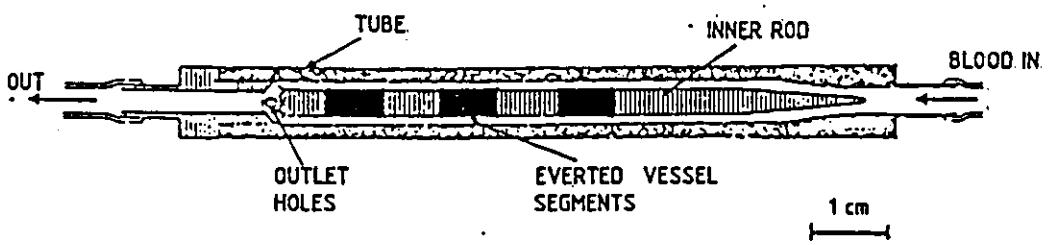

Figure 2.6. Diagram of a Baumgartner chamber.

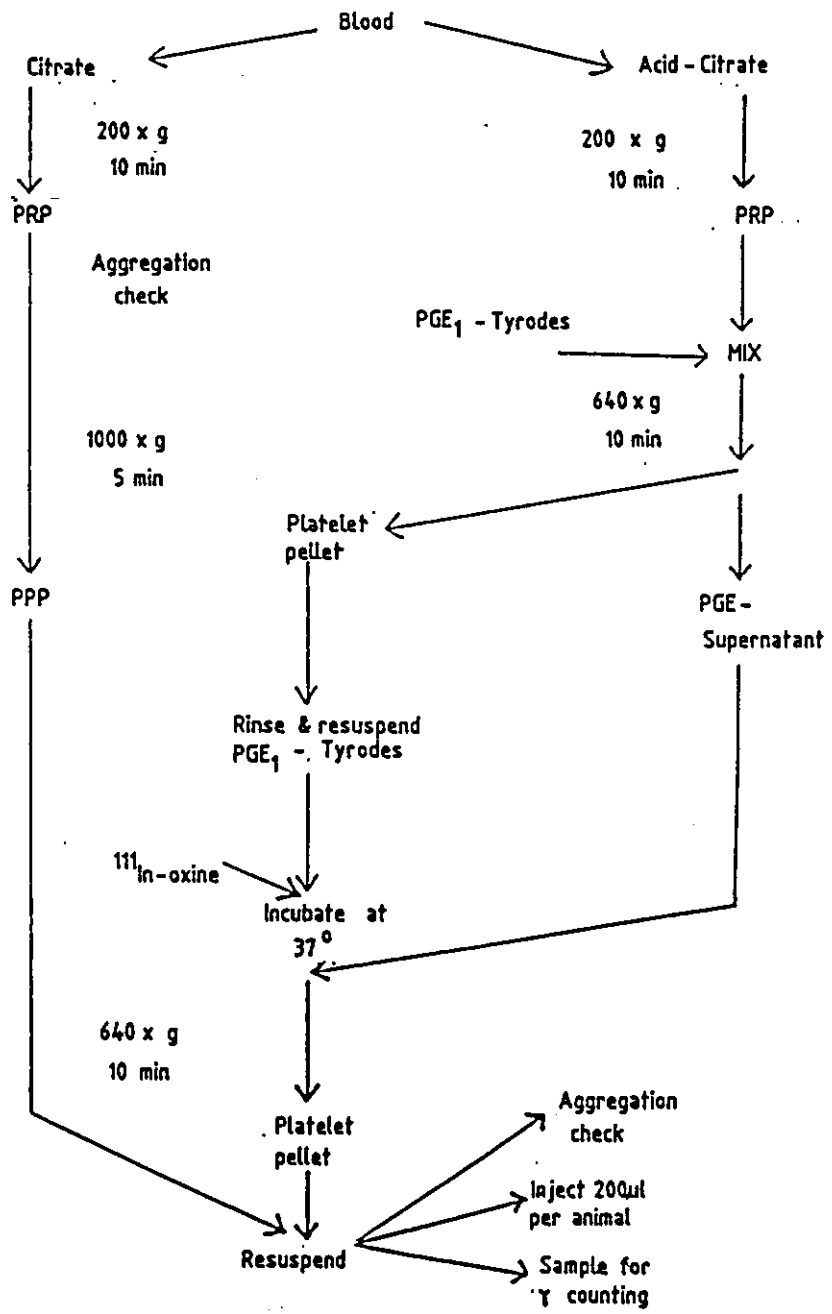

Figure 2.7. Schematic representation of the steps involved in labelling platelets with Indium -111. The letter "g" is indicative of centrifuging.

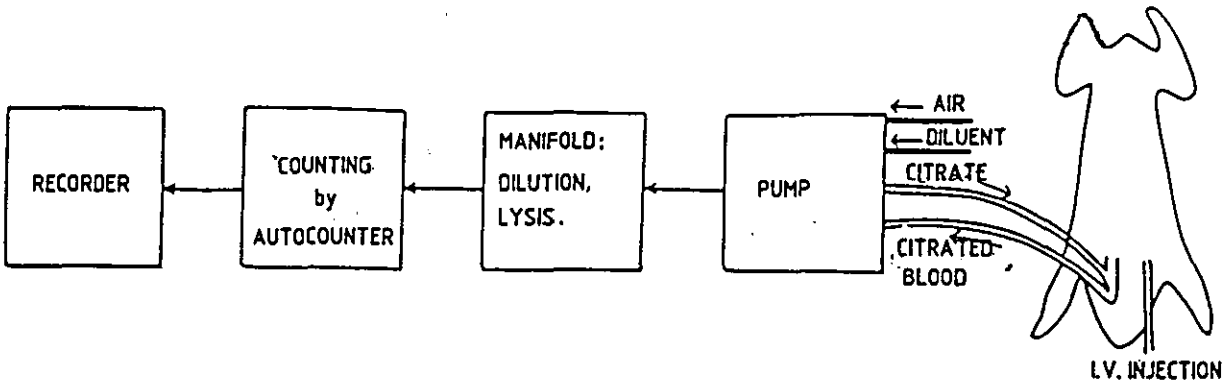

Figure 2.8a. Schematic diagram of continuous platelet counting.

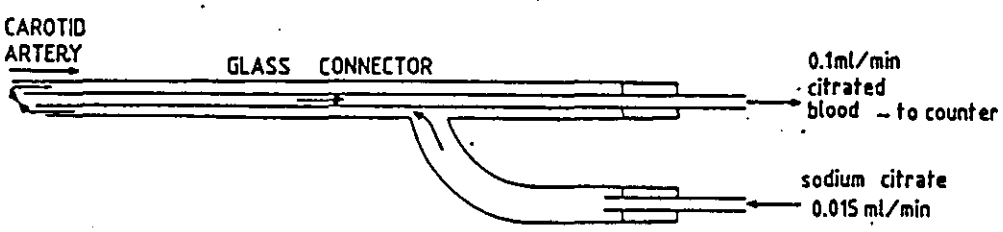

Figure 2.8b. Double cannula for the removal of citrated blood.Trisodium citrate is pumped through the side arm of a "Y" shaped connecter to the tip of the outer cannula (outer diameter 2mm) where it is mixed with arterial blood.Citrated blood is then removed through the inner tube (outer diameter 1 mm).

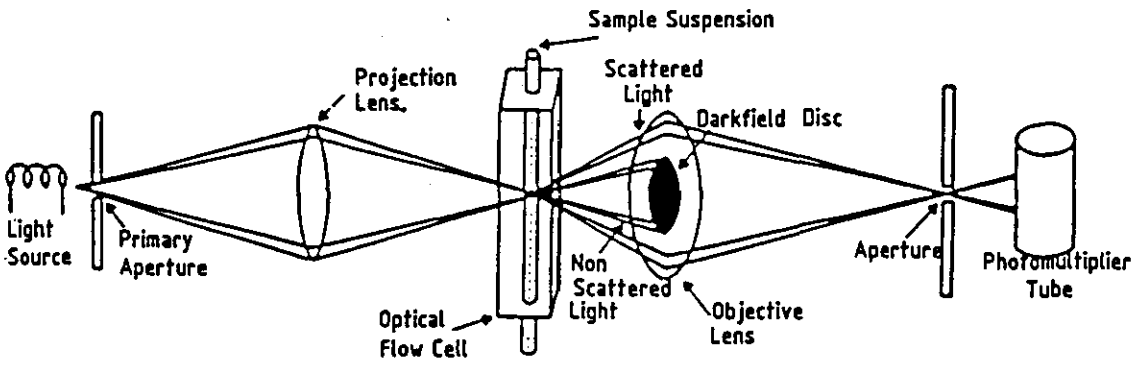

Figure 2.8c. Schematic diagram of the Technicon Autocounter showing how the darkfield optical system detects particles in the optical flow cell.

CHAPTER 3

ULTRASONIC BLOOD FLOW MEASUREMENTS

3.1. Introduction

Innumerable methods have been proposed, and used, for the measurement of blood flow. Some measure the volume of blood flowing and others measure the velocity. Many,the electromagnetic flowmeter for example,rely on inherently invasive techniques and involve the direct attachment of a probe on to the vessel under examination.Ultra sonic Doppler flow measurements constitute a notable exeption and, because it is non invasive, the methodology is used extensively in clinical studies,including those designed to detect the presence of a thrombotic occlusion or stenosis. Consequently it represents the method of choice when first exploring the rationale developed in the previous chapter.

3.2. The Ultrasonic Doppler Flowmeter

The term 'ultrasonic' is used to describe non-ionising pressure waves in the frequency range 20 KHz to 1 GHz; in clinical practice frequencies in the range 1 - 15 MHz are employed. Since longitudinal waves are involved, energy flows without an accompanying net movement in an interposed biological medium and any particles contained therein merely oscillate about their mean position.

When a wave source moves relative to an observer a frequency shift can be noted. The relative movement may be caused by actual movement of the source, receiver, propagating medium or intervening reflector or scatterer. The shifts are generally called 'Doppler' after the Austrian physicist C.J. Doppler, who predicted the effect in 1842.

If all the relative motion is along the same axis the received frequency f_r is given by the equation

$$f_r = \left(\frac{C - V_r}{C - V_s}\right).f$$

Where C is the propagation velocity, V_r is the receiver velocity, V_s is the source velocity and f is the transmitted frequency. The Doppler shift frequency, $f_D = f_r - f$, is therefore given by

$$f_D = \left(\frac{C - V_r}{C - V_s}\right) - 1$$

If V_r and V_s are both zero and the wave travels from the source to the receiver by reflection from an interface having a vector component of velocity V_i, along the direction of an ultrasonic beam axis away from the source, then

$$f_D = -\left(\frac{2\ V_i}{C + V_i}\right) . f$$

If $C >> V_i$, and this is always the case in physiological systems, the equation can be written simply

$$V_i = - f_D \frac{C}{2f}$$

The absolute velocity of the reflector along the direction flow is given by the equation:

$$V_i = -f_D \frac{C}{2f \cos \varphi}$$

where φ is the angle between the direction of movement and the ultrasonic beam axis. Where the various velocities do not all act along the same direction, f_D must be calculated using the appropriate velocity vectors.

The simplest Doppler device is the continuous-wave flowmeter, used by Satomura (1957) in the first successful attempt to monitor blood velocity non-invasively. A beam of ultrasound is directed onto the flowing blood and the frequency changes produced in the backscattered radiation are monitored by mixing the transmitted beam and the reflected beam to produce a beat signal. The cellular component concentrations within blood mean that the red cells are the predominant source of Doppler shifted signals.

The most common type of ultrasonic probe uses two separate piezo electric transducer crystals, one acting as the transmitter and the other as the receiver. An acoustic insulator is used to decouple the transducers from each other and from the probe housing. Although the formulae given previously indicate that the maximum Doppler frequency will be obtained when $\varphi = 0^\circ$, i.e. when the ultrasonic beam is directed parallel to the direction of flow, this is clearly impractical in many circumstances.Equally,in theory,no Doppler shift signal should be detected when the transducer is held at right angles to the blood

vessel. However in practice blood cells do not travel strictly in parallel lines and, furthermore, the ultrasonic beam always diverges. As a result, a significant Doppler output can always be obtained. Angles of 30° - 40° represent a satisfactory practical compromise.

In the basic Doppler instrument it is not possible to observe whether the shift in frequency is up or down. The simple non-directional Doppler instrument does find many applications in tests such as detection of deep vein thrombosis or the detection of the foetal heart beat: for such tests an audible beat frequency tone is often an adequate signal for diagnosis. However, for many clinical purposes it can be extremely useful to know the direction of flow. In the simplest situation flow may well be in only one direction at any given moment, so that it is only necessary to determine whether flow is in the forward or reverse direction. In other situations there may be a complex flow profile and flow components may exist in both directions.

Many of the 'true' directional Doppler instruments now use single sideband demodulation, a form of demodulation originally developed for radio receivers. In the Doppler context this entails the transmitter crystal being energised by a signal E cos wt and the signal from the receiving crystal being split into two paths, one in which it is multiplied by transmitted signal E cos wt and the other in which it is multiplied by a 90° phase shifted version of the transmitted signal. After low pass filtering the two quadrature multiplied outputs are again multiplied, this time with quadrature outputs from a second oscillator; sine is multiplied with sine and cos with cos. Finally the outputs from

the second pair of multipliers are summed.Frequencies above a resultant resting level, W_s ,then represent forward flow and frequencies below W_s represent reverse flow.

In principle the Doppler signal contains all the information needed to describe what proportion of the blood in the vessel is moving with a particular velocity and direction. Since the blood velocity is contained in the frequency content of the Doppler signal,it follows that the obvious form of analysis for extracting the flow information must be frequency analysis. Ideally it should be done in real time so that there is some operator feedback to the examination being performed.

With the advent of the microprocessor and its associated technology it has become possible for an implementation of the fast Fourier transform to be used as a cost effective basis for frequency analysis.It is an important technique with wide spread applications;the underlying principle is given in Appendix A.It's application specifically to ultrasonic Doppler measurements has been described by such authors as Kubak et al (1974).

3.3 Analysis of Doppler Shift Signals

As previously indicated,non-invasive Doppler shift based systems have become important in the routine screening of patients for occlusive vascular disease.Their use is greatly enhanced by the application of mathematical techniques to the extraction of diagnostic information from the associated waveforms.

Two main methods have evolved,waveshape analysis and flow disturbance analysis.The former started with the qualitative observations by Strandness et al.(1967) and Yao et al.(1970) that the velocity waveforms recorded distal to an arterial stenosis are dampened.Gosling et al.(1969) are attributed with being the first to realise the potential of such observations for quantitative analysis.Since that date impulse analysis (Morris et al.,1975), the Laplace transform method (Skidmore,1979), the Z transform (Brown et al.,1978) and principal component analysis (Martin et al.,1980) have all been applied to quantifying the shape of the deformed pulse.A pulse is a fundamental requirement of the general methodology;it is not therefore applicable to steady state flow of the type found in veins. Flow disturbance anaysis on the other hand is applicable to pulsatile or steady flow.

3.4 Flow Disturbance Analysis

In any fluid system laminar flow is only preserved up to a certain velocity.Once that value is exceeded the motion becomes turbulent and constantly changing eddies of small dimensions are superimposed on the flow.In 1833 Reynolds demonstrated that there are in fact two critical velocities associated with turbulence. There is a lower one at which laminar flow is unstable and turbulence possible and a higher one, above which turbulence is inevitable.

The lower velocity value depends only on the fluid density, ρ grammes per cc, the viscosity η and the radius of the tube, r . Thus:

$$U_c = \frac{K\eta}{\rho r}$$

where K is about 1150 and is called the Reynolds number.If K is less than about 1150 the flow will be laminar and if it is greater than that value the flow will probably be turbulent. Therefore, in general:

1. The higher the fluid velocity, u, the greater the tendency for turbulence.

2. The lower the viscosity, the greater the tendency for turbulence.

3.The larger the pipe diameter, the greater the tendency for turbulence.

The lower critical velocity value is well defined but the upper critical value is not. In extremely quiescent conditions laminar flow has been observed with Reynolds numbers as high as 10,000. This however is extreme and in most conditions laminar flow will not exist if the Reynolds number is above 2,000. Thus for Reynolds numbers between 1150 and 2,000 a region of uncertainty exists and the flow may be either laminar or turbulent, depending upon the presence or absence of turbulence promoters such as roughness, sharp corners and vibration.

For a long time after the work by Reynolds, despite obvious interest, discussions concerning the onset of turbulence in blood vessels were largely speculative. The position was only changed when the technique of hot film constant temperature anemometry became available and was applied to the problem by such workers as Ling et al (1968) and Seed and Wood (1970). Subsequently workers such as Nerem et al (1972, 1974) and Giddens et al (1976) have been able to report upon

disturbances identified distal to experimentally produced stenoses and occuring prior to the development of any observable pressure gradient.Because hot wire anemometry is associated with a direct invasion of the blood stream, ultrasonic blood flow meters now tend to be the method of choice when making flow disturbance measurements.

The mean velocity of blood in the aorta during the injection of blood from the heart is in the order 0.2 metres per second and the associated Reynolds number is about half the critical value for turbulence.However,the critical velocity value will be exceeded during part of the injection cycle. Additionally, during excercise, when the cardiac output may be four to five times greater than when the subject is at rest, turbulence may exist for a proportionally longer part of the injection period. In normal physiological states there will be no other part of the circulation outside of the heart exhibiting turbulence. In pathological states, particularly those associated with a stenosis, the conditions may be somewhat different.

As a stenosis develops the nature of the flow in its vicinity is altered. The degree of alteration is strongly influenced by the severity of the stenosis and for moderate to severe cases highly disturbed regions of turbulent flow commonly occur distally.

The turbulence is of interest for two reasons: the first being that it may be used as a clinical diagnosis aid, the second being that evidence now exists suggesting there to be a degree of positive feedback between the development of the stenosis and the turbulence it produces.

In the case of atherosclerosis in particular, it has been suggested that a localised change in pressure or shearing stress may trigger certain biological mechanisms whereby the endothelial cells lining the vessel wall proliferate with a subsequent narrowing of the lumen (Robard 1966). In the case of thrombus formation it is suggested that the existence of high shear regions may cause damage to red cells and endothelial cells (Fry 1968) and possible platelet - fibrin interactions (Fox and Hugo 1966). Thus in addition to clinical studies on the detection and interpretation of turbulence,its physiological significance also has been extensively studied in the laboratory. See Devanathan and Parvathamma (1983).

3.5 A Flow Disturbance Study

One particularly comprehensive flow disturbance study has been reported by Thiele et al (1983).They describe a study aimed at determining to what extent the flow disturbances, measured with hot film anemometers by Nerem and by Giddens, could be identified with ultra sonic instrumentation. They also report upon attempts to quantify the disturbances relative to the degree of stenosis.

In experiments involving mongrel dogs the descending thoracic aorta was exposed and a portion encircled with a 3 mm wide teflon tape. The tape was connected to a caliper type device so that incremental changes in diameter could be produced. Distances corresponding to one vessel diameter upstream (proximal) and one, two and three diameters downstream (distal) were identified and marked by a suture. This is shown

schematically in Figure 3.1.

The sensing apparatus consisted of a pair of 20 MHz pulsed Doppler probes,mounted in acrylic holders to ensure a constant angle of incidence of 60° to the aorta. By range gating techniques the sampling depth could be adjusted from 1 mm to a maximum depth of 11 mm; from diameter measurements it was therefore possible to ensure that centre stream velocities were being recorded.The recordings obtained at the measurement sites were analysed with a fast Fourier transform type spectrum analyser interfaced to a mini computer.

At the conclusion of the velocity data acquisition the series of stenoses was recreated and two catheters,attached to pressure transducers at their far ends,were inserted into the blood vessels.One was inserted proximal to the stenosis and the other distal.Using this method the pressure relationships over the range of stenoses could be evaluated.

The experiments therefore made the following information available for interpretation.

1. The relationship between mean peak velocity, percent diameter reduction, and pressure gradient across the stenosis.

2. The averaged spectra from selected points during the pulse wave.

3. A five line spectral contour plot over the sampling period, consisting of the mode and the 2dB and 8dB lines above and below the mode (most common) frequency.

4. The mode frequency from all the averaged spectra.

5. Spectral widths,obtained by measuring the width between the 8 dB points over the whole period of sampling.

3.6 The Velocity and Spectral Width Results.

The centre stream velocity could be calculated from a hard copy output display of peak frequency. In fact it was computed by determining the mean peak frequency of three consecutive pulse cycles. Values were obtained for both the proximal site and a site two diameters distal to the stenosis, for each degree of stenosis. A typical relationship between velocity change and pressure gradient is depicted in Fig.3.2.

In all the dogs studied the mean peak velocity, measured at the 2 diameters distal point,increased dramatically prior to the development of the pressure gradient across that stenosis. In addition,variations from resting values were also observed one diameter proximal to the stenosis. While these latter changes were not as marked as those seen downstream of the stenosis, a reduction in peak velocity was a constant feature with all the animals studied.

Spectral width is a measure of the instantaneous frequency content at varying points in time in the pulse cycle: it is proportional to the velocities of red cells within the area being sampled. A narrow spectral width is indicative of uniform red cell velocity and laminar flow, increases in spectral width are suggestive of variations of velocity and early flow disturbance. Thus quantitative spectral width analysis, as a measure of turbulance, might be expected to be of interest when one is

trying to quantify stenosis magnitude.Therefore,in experiments designed to yield qualitative information about the extent of propagation,velocity spectra were obtained from the centre stream sampling sites at one,two and three diameters downstream of the stenoses.

A summary of the specral width results is shown in table 3.1 (see page 66). The values of spectral width in time represent the mean plus and minus one standard deviation obtained from six animal experiments. The maximum increases in spectral width are seen to have been observed at the two diameter location and were first detectable with a 15% diameter reducing stenosis. Significant changes in spectral width also occurred at the one diameter site and the parameter showed least change at the three diameter site.

As spectral width increased with increasing degree of stenosis,so the time after the onset of systole at which these changes were first detected decreased. Thus at the two diameter location with a 15% stenosis the increase in spectral width occurred at 244 - 79 ms, with a 60% stenosis the change was detected at 79 - 73 ms. Similar trends were observed at the one and three diameter locations.

3.7 Fluid Jets - an explanation for the results

Although not specifically described as such by Thiele et al.,the spatially short lived velocity increase found round and about two vessel diameters distal to an occlusion has many of the characteristics of a

fluid jet.Such jets occur when there has been an enforced alteration to a fluid's velocity profile. In the case of laminar flow of a Newtonian fluid,flowing through a straight circular tube,the velocity profile is parabolic and the stream lines are straight and parallel. If however a converging-diverging section is added the veolcity profile will change and there will be a subsequent change in other attendant flow characteristics.Alternatively,in more macroscopic terms,the velocity profile will reflect the velocity change associated with passing the same bulk of fluid through a locally reduced tube diameter.Fluid momentum effects are responsible for its detectable distal presence. In blood flow studies a stenosis represents the converging-diverging section.

In addition to the formation of a fluid jet,a stage is reached when stream line divergence may give rise to areas of flow separation. When the stream lines are diverging the mean velocity decreases in the direction of flow and there is an increase in pressure due to the Bernoulli effect. This increased pressure, when combined with the pressure drop due to viscous friction, may be large enough to cause an adverse pressure gradient to develop, ie.,the resultant pressure may be increasing in the direction of flow.Because of viscous effects a thin layer of fluid adjacent to the vessel wall is moved forward by the fluid above it but,simultaneously,it will be retarded by the wall friction and the adverse pressure gradient. If the adverse pressure gradient becomes sufficiently large it will cause slowly moving particles of fluid near the wall to reverse their direction of flow and a separation region will develop. For low Reynolds numbers the separation region is well defined

and there is no mixing. However, as the Reynolds number is increased and the separation region grows larger, turbulant eddies will develop and some will move downstream.

Forrester and Young (1970) were probably the first to develop a mathematical model for flow through a mild stenosis and determine velocity profiles from the resultant equations.The model is described in appendix B but it is,however,limited to the consideration of steady axisymmetric flow of a Newtonian fluid. These conditions are unlikely to be found in a biological system but, never the less, the results from the model are qualitatively correct. The model has also served as a valuable basis from which others have evolved. Most have been concerned with the development of turbulence;in the context of vessel pathology a jet possesses less apparent clinical causal significance than fully developed turbulence and so has received less attention.

Since Forrester and Young's original work there have been many attempts at refinement, mainly assuming less ideal conditions as the basis for the model and thereby extending its versatility. Thus authors such as Young and Tsai (1973) and Padmanabhan (1980) have extended the model to deal with unsteady flow, Padmanabhan and Devanathan (1981) have made allowances for vessel elasticity and then, later, Devanathan and Parvathamma (1983) have treated the blood as a micropolar fluid. Qualitatively the results are all in agreement with the original work, differences occur in the magnitude of such parameters as vessel wall shear force and in positions of points of flow separation.

3.8 Discussion

In the context of thrombus development, ultrasonic Doppler blood flow measurements are of great value, both clinically in the diagnosis of occlusion sites and experimentally in determining causal factors. However,the resolution and probe size associated with the basic technique are such that it does not readily lend itself to small animal investigations.

The use of small animals such as the rat or rabbit is likely to be preferred,at least during the early stages,in the search for drugs with antithrombotic activity.This preference is also likely to be expessed in other pharmacological screens. Economic, logistic and emotive factors would all be prime considerations in animal selection. In the context of the rationale now being developed for the in-vivo method,the time over which a thrombus might be expected to grow to have a significant effect on the blood flow would also suggest the use of small animal vasculature.

By using light instead of sound,the scale of Doppler blood flow measurments can be reduced. The alternative but related technique is known as laser Doppler velocimetry (LDV). So, in principle, flow disturbance behaviour of the type described by Thiele et al.(1983) should still be detectable in those small animals where even quite major vessels may have diameters of only 1 mm or less. It may then be postulated that, should this prove to be the case, such disturbances might be used to quantify the growth of an induced in-vivo thrombus and

thereby reflect the efficacy of any antithrombotic drug to which it,the thrombus,may be exposed.

It is to be anticipated that the use of the afore mentioned LDV technique will be limited to experimental situations;it will not compete with it's ultrasonic counterpart in the clinical investigation of thrombi.Laser Doppler velocimetry is examined in the next chapter.

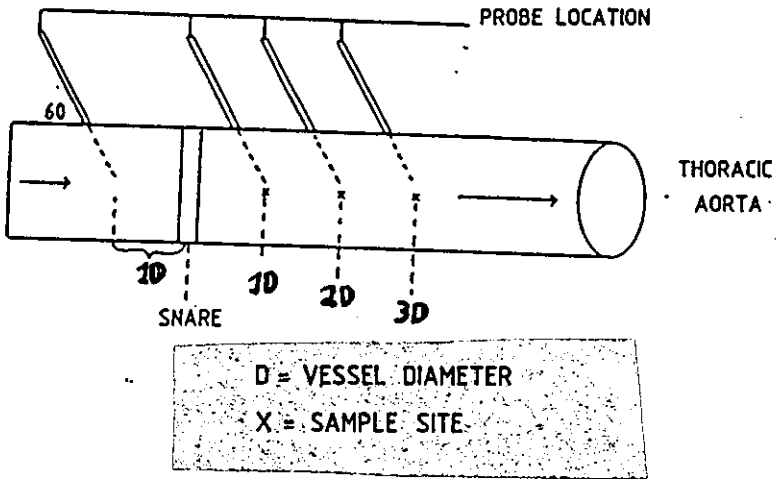

Figure 3.1 Schematic representation of the sites in the dog thoracic aorta from which recordings were obtained by Thiele et al (1983).

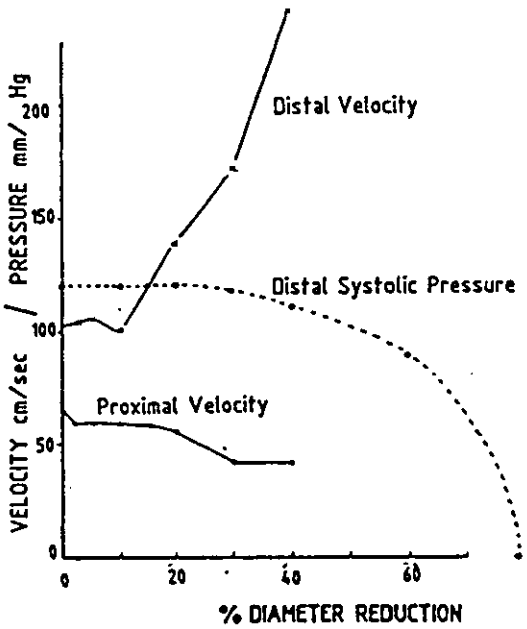

Figure 3.2 Relationship between calculated percent diameter reduction,centrestream velocity,and pressure gradient across the stenosis.In this experiment,a gradient developed at a 40% diameter reduction.The distal velocity was calculated from the site two diameters downstream of the stenosis.

Distance downstream	1 Diameter		2 Diameters		3 Diameters	
%Stenosis	Peak spectral width	Onset (ms)	Peak spectral width	Onset	Peak spectral width	Onset
0	3·9 ± 1·8	294 ± 55	3·3 ± 1·7	332 ± 87	3·3 ± 1·2	339 ± 95
2·5	2·9 ± 1·0	305 ± 92	3·0 ± 1·6	330 ± 80	2·3 ± 0·8	359 ± 102
5	3·1 ± 0·7	315 ± 83	3·6 ± 1·7	299 ± 90	2·4 ± 0·9	353 ± 103
10	3·7 ± 1·1	271 ± 57	3·7 ± 1·3	276 ± 79	2·9 ± 1·6	321 ± 114
15	4·5 ± 1·8	260 ± 94	5·9 ± 2·4	244 ± 78	4·6 ± 2·3	279 ± 92
20	6·9 ± 0·8	204 ± 18	6·9 ± 1·3	208 ± 53	4·8 ± 2·2	271 ± 99
30	8·8 ± 1·9	168 ± 22	8·0 ± 2·2	182 ± 28	7·1 ± 2·0	202 ± 30
40			9·1 ± 1·8	154 ± 25		
60			9·0 ± 0·8	79 ± 73		

TABLE 3.1

Peak spectral width (KHz) and onset of spectral broadening (ms after R wave) with degree of stenosis (% diameter reduction and distance distal to the stenosis).All figures represent the mean +/- standard deviation of six experiments.

CHAPTER 4

LASER DOPPLER VELOCIMETRY

4.1. Introduction

The technique of using the Doppler shift of laser light to determine velocities was first demonstrated by Yeh and Cummins (1964); they observed the frequency shift of light scattered from particles carried in a water flow (the presence of particles in the flow is a fundamental requirement). There are now a number of variations of the technique, broadly described as laser Doppler velocimetry and abbreviated to 'LDV' or laser Doppler anemometry and commonly abbreviated to 'LDA'. The term 'velocimetry' is used here in preference to 'anemometry' since the latter suggests a restriction to air or gas flow.

Since the particle velocities encountered are usually very small compared with the velocity of light, the corresponding Doppler shifts are also very small.The only method suitable for measuring very small relative phase or frequency shifts uses the heterodyning ('beating') of two frequencies.Ultrasonic Doppler shift blood flow meters, discussed in the previous chapter,are based on the same principle.

Analytically there is no real distinction between optical heterodyning and the possibly more general principles of interferometry.However,the latter term is usually applied to systems

using specular reflection from optically prepared surfaces, rather than those using randomly scattered light. In the application to optical velocity measurements, Doppler shifted scattered light is heterodyned either with unshifted light obtained directly from the original source or with light which has been scattered through a different angle and therefore has a different shift frequency associated with it.

4.2. Derivation of the Doppler Shift on Scattering

Consider light of frequency ν radiated by a source S and scattered by a moving object P, the scattered light being observed at Q. The angles that the objects direction of motion make with PS and PQ are denoted by ϕ_1 and ϕ_2 and the velocity of that motion is v.

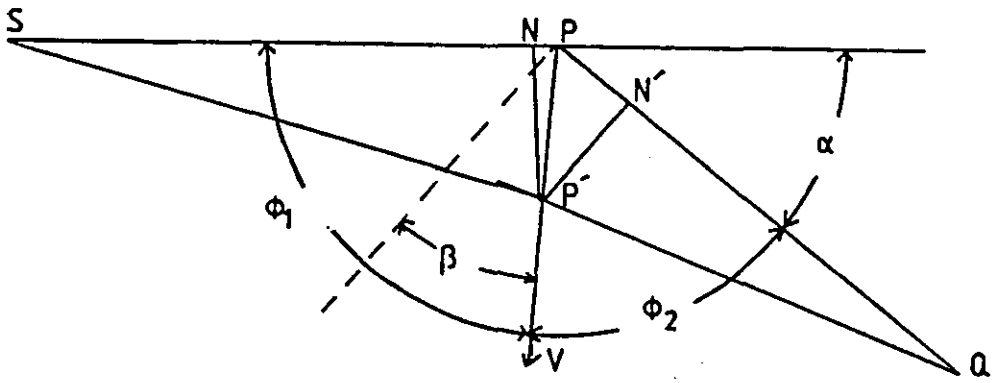

If n is the number of wavelengths or cycles along the light path from source to observer, then the change in the number of cycles arriving at the observer as a result of the objects movement is equal to that number removed from the path SP→ PQ. Hence

$$\Delta\nu = -\frac{dn}{dt}$$

Suppose that P moves to P′ in an infinitesimal interval of time, δt. The distance moved will be $v\delta t$. The reduction in the number of cycles in the optical path is

$$-\delta n = \frac{PN}{\lambda} + \frac{PN'}{\lambda'}$$

where P'N and P'N' are drawn perpendicularly to SP and PQ respectively. λ and λ' are the wavelength before and after scattering and PP' is assumed infinitesimally small.

By substitution:

$$-\delta n = \frac{v\delta t \cos\Phi_1}{\lambda} + \frac{v\delta t \cos\Phi_2}{\lambda'}$$

Since:

$$v\lambda = v'\lambda' = c$$

then:

$$\Delta v = v' - v = \frac{v.v \cos\Phi_1}{c} + \frac{v.v\cos\Phi_2}{c}$$

thus:

$$\frac{v'}{v} = \frac{1 + (v/c)\cos\Phi_1}{1 - (v/c)\cos\Phi_2}$$

Assuming Rayleigh scattering such that λ and λ' are indistinguishable and that the object velocity is small compared with the velocity of light, the frequency shift may be re-written:

$$\Delta v = v' - v = \frac{v.v}{c}(\cos\Phi_1 + \cos\Phi_2)$$

By applying a trigonometrical identity:

$$\Delta v = \frac{2vv}{c} \cdot \frac{\cos\Phi_1+\Phi_2}{2} \cdot \frac{\cos\Phi_1-\Phi_2}{2}$$

Now from the diagram it will also be seen that

$$\alpha = \pi - (\Phi_1 + \Phi_2)$$

where α is the angle of scattering. Therefore:

$$\sin \frac{\alpha}{2} = \frac{\cos (\phi_1 + \phi_2)}{2}$$

It is now relevant to introduce β, the angle between the velocity vector V and PB, the bisector of the angle between PS and PQ. PB is the direction of the scattering vector and as such represents the momentum changes of the radiation on scattering.

Thus

$$\beta = \frac{\phi_1 - \phi_2}{2}$$

By substitution:

$$\frac{\Delta \nu}{\nu} = \frac{2v}{c} \cos \beta . \sin \frac{\alpha}{2}$$

It may therefore be seen that the Doppler shift depends on the sine of half the angle of scattering and on $v.\cos\beta$, the component of v resolved in the direction of the scattering vector.

The equation may also be written in terms of the wavelength:

$$\Delta \nu = \frac{2v}{\lambda} \cos \beta . \sin \frac{\alpha}{2}$$

This tends to be the most used form of the Doppler shift equation.

4.3 Configurations

Virtually every new application of the LDV technique appears to be associated with a new optical configuration. However, all the geometries employed in these designs can be identified as belonging to one of three

basic categories. They employ either a reference beam configuration, a dual beam configuration or the two scattered beam configurations. The principal features of each is shown in Fig.4.1.

In the reference beam mode,where use is made of local oscillator heterodyning, the laser beam is split into a relatively intense incident beam and a relatively weak reference beam. The reference beam is directed onto a detector surface where it beats with light that has been scattered from the strong beam by particles moving with the flow. The frequency of the scattered light has been altered by the Doppler effect and the interference with the reference beam provides a frequency difference which is directly proportional to the particle velocity. This is the archetypal configuration, employed in the pioneer work of Yeh and Cummins, and subsequently used by many other authors.A simple variation on this basic configuration yields the 'external reference' sub classification.

The dual beam system uses two intersecting light beams of equal intensity and presents a problem analogous to one of taxonomy. Its function may be analysed in terms of conventional LDV parlance or it may be described as a fringe system. Thus either the signal may be considered as arising from the coherent mixing of Doppler shifted light which has been scattered through different angles or it may be considered, as by Rudd (1969), that the two incident beams create interference fringes and there is an intensity modulation of the scattered light as it passes through them.

In fact Drain (1972) has shown that the two approaches give equivalent results and that both types of phenomena contribute simultaneously to the signal. The detection aperture and the particle concentration largely dictate which mechanism predominates. With a small detector aperture and when a large number of particles are involved the coherent LDV mechanism predominates. With a large aperture and a small number of particles the non coherent fringe modulation predominates.

The third optical arrangement,the dual scattered beam or differential Doppler device,is due to Durst and Whitelaw (1971). A single focused laser beam is directed into the flow and light scattered by a particle in two directions is collected symmetrically about the system axis. When the scattered beams are combined the relative phase of their wavefronts depends on the distance of the particles from each light collecting aperture. Hence, as the particle moves across the beam the scattered light beams interfere constructively and destructively, leading to a light intensity at the photodetector which fluctuates at the Doppler frequency. The operation is in many ways analogous to a fringe modulation system with the role of the transmitter and receiver being reversed.

Little use has been made of the dual scatter technique, possibly because of alignment difficulties. There is however the potential advantage that more than one component of velocity can be measured simultaneously, by receiving scattered light from a number of directions.

There exists no essential distinction between forward and backward scattering optical arrangements. The three geometries discussed have all been in a forward scatter configuration:they could equally well be employed in the backward scatter mode.Light collection in the forward direction is preferred when ever possible since light scattering is almost always greatest in that direction,often by two or three orders of magnitude. However, at times a back scattering configuration may be unavoidable because the available optical access to the experiment is limited to one side only. This is frequently the case with biological preparations.

Many of the biological studies that make use of laser Doppler methods require small measuring volumes; the coherence associated with a laser beam makes the associated focussing relatively easy. A basic LDV system with additional focussing optics is often referred to as a laser Doppler microscope; many have been built around conventional microscope stages.

4.4. Directional Ambiguity

For reasons exactly analogous to those associated with its ultra sonic counterpart, a fundamental problem in laser Doppler velocimetry is the discrimination of the direction of velocity. The Doppler beat frequency is the difference of two frequencies but in the basic form it is not possible to tell which one is the higher. Thus a change in the sign of a velocity produces no difference in frequency.

In some applications the directional flow is known and is always the same. However, when dealing with regions of recirculating or pulsatile flow, there is quite likely to be reversal. Fortunately several methods for direction discrimination can be incorporated into laser Doppler system designs; they include two-phase detection, phase modulation and frequency shifting. The latter method is now the most commonly used, because it requires no major modifications to the optics and because it allows velocity fluctuations to be followed smoothly through zero. It's principle of action is as follows.

Referring to Fig.4.2, we suppose that the frequency of the incident laser light is V_o and the Doppler shift frequency is f_D. The frequency of the scattered light is then either $(V_o + f_D)$ or $(V_o - f_D)$, depending upon the direction of the velocity. Beating with light of the original frequency, V_o, produces a signal of frequency f_D in either case. However, if the frequency of the reference beam is increased by f_s, as shown, the corresponding beat frequencies are $(f_s + f_D)$ and $(f_s - f_D)$. Thus directional discrimination becomes possible. To avoid ambiguity the frequency shift must be greater than the maximum Doppler shift frequency.

Rotating diffraction gratings, rotating half wave plates and electro optic techniques have all been used to induce reference beam frequency shifts. Electro optics, in particular in the form of the Bragg cell, offer many advantages in terms of dynamic range and so has become the method of choice for many investigations.Bragg cell frequency shifting relies on acoustic wave induced refractive index changes, this

mode of action is shown schematically in figure 4.3. The way in which the Bragg cell may be used to impart a frequency shift to a laser beam is shown in figure 4.4.

4.5 Some L.D.V. Systems for Biological Applications

As stated previously,virtually every new application of the LDV technique gives rise to a new implementation of one of the three basic configurations.This section contains information regarding five main references which,between them,contain the principal design features of a biologically orientated sub classification.Almost exclusively,for reasons of accessibility,this sub classification is associated with back scatter detection.

One of the first laser Doppler microscopes was described by Mishina and Asakura (1972). Its application to the measurement of flow velocities in venules and capillaries was later described by Mishina, Ushizaka and Asakura (1976). The instrument, a dual beam device, is made up of two main parts. One is a beam splitter which produces two parallel beams and the other is an imaging system which collects the scattered light with a high spatial resolution.

The beam splitter is shown in figure 4.5a and is seen to be made up of a Koester prism and three subsidiary mirror units. The mirrors can be adjusted to allow for any error within the main prism. The two beams emerging from the splitter unit cross at the focal plane of a converging lens and are then focussed onto the probing area by a microscope

objective.

Figures 4.5b and c show how the basic beam splitter may be incorporated into, respectively, a forward scatter device and a back scatter device. In the forward scatter configuration the optical axes of the beam splitter section and the microscope part are arbitrarily chosen to be equal or different. This means that the axes of the incident and scattered beams are freely differentiated from each other: incident beams can therefore be prevented from reaching the detector directly. This prevents saturation of the detector and enhances the overall signal to noise ratio of the Doppler beat signals. The signal to noise ratio is also improved by a slit, placed in the image plane of the probing area and in front of the detector. By suitable adjustment of the slit width only light emanating from the probing area reaches the detector. The beam splitter cube placed within the optical configuration is an integral part of an observation system, used to assist in the setting up procedure of the sample object.

The resolution of the forward scatter configuration was such that Mishina et al (1976) were able to plot the flow across a 70 um diameter venule in the capillary network of a frog's foot.

In the backscatter configuration the two beams from the beam splitter section are sent, via a beam splitter cube, into a microscope objective and onto the probing area. The separation angle of the incident beams is limited by the entrance aperture of the objective. In theory this should place a limiting restriction on the number of beat

waves that can be observed, in practice the limit is imposed by focussing restrictions. The direct pathway for the backscattered light is back through the objective, through the beam splitter and into the detector. That basic path is in fact modified by beam splitters and other associated components to facilitate object illumination and viewing.

Riva et al (1972) demonstrated the feasibility of using laser Doppler velocimetry to measure blood flow in retinal vessels. Alterations of blood flow in the retinal vascular system, whether associated with specific ocular diseases or with systemic diseases such as diabetes, may lead to a serious impairment of visual function.Laser Doppler velocimetry is the only known noninvasive technique able to provide quantitative measurements of retinal blood flow.

The laser Doppler velocimeter developed by Riva for clinical studies is shown schematically in Fig.4.6a. The basic optical component is a standard fundus camera which has been modified with laser input optics, an internal fixation target and an optical fibre for collection of the scattered light.

The linearly polarised beam of a HeNe laser impinges on the subject's eye after being reflected by a small mirror mounted in front of the ophthalmoscopic lens of the camera. The eye focuses the beam to a spot approximately 200 um in diameter onto the retina and the beam position is adjusted so that it illuminates an individual retinal

vessel.In order to maintain the position of the beam on the vessel the subject fixates a target that is imaged in a plane conjugate with the retina.The target is in fact the exit aperture of a small illuminated fibre optic.Prior to being aimed into the eye, the intensity of the beam is attenuated with a rotatable polarizer to a level well below the maximum permissible for continuous irradiance of 0.1 W/cm^2 (Sliney and Freasier, 1973).

The portion of the light scattered back by red blood cells within the vessel and accepted by the entrance pupil of the fundus camera is collected by another optical fibre, mounted in a scanning ocular. The entrance aperture of this fibre is also located in an image plane conjugate with the retina, the position of the fibre in that plane is adjusted to coincide with the illuminated portion of the vessel. In addition to the light backscattered by the cells there is also a contribution from the vessel wall. The light scattered from the wall is unshifted in frequency and thus acts as the reference beam in the heterodyne detection process. The light collected by this second fibre, both shifted and reference, is relayed to a detector.

Using this equipment Feke and Riva (1978) successfully produced spectra from retinal vessels and arteries. Spectra obtained from arteries show cut off characteristics that vary markedly as measurements are made throughout the cardiac cycle; this is due to the pulse linked velocity fluctuations of the red blood cells. Examples of such arterial recordings are shown in figure 4.6b.

Born, Melling and Whitelaw (1978) took the basic concept of the device developed by Mishina et al and modified its implementation to suit studies involving blood flow in the mouse mesentery: The new system is shown schematically in Fig.4.7. A half silvered mirror, M1, and a fully silvered mirror, M2, are first used to split the output from a 5mW laser into two parallel beams. These two beams then pass through holes in the mirror M3 and are focused by lens L1 (of focal length 100 mm) and objective lens L2 into the test section.

Scattered light from the system under study is collected back through the objective and lens L1 and, after reflection from the mirror M3, is focused through lens L3 (of focal length 200mm) on to the photomultiplier aperture. Lenses L1, L3,the beam splitter and mirror were designed as a single unit which could be moved relative to the objective lens, in order to match the separation of the beams to the aperture of the objective. The optical viewing system, consisting of an inverted microscope underneath the specimen stage, is essentially independent of the laser velocimeter.

The mouse under study was held on a perspex plate fixed to the microscope stage and the mesentery stretched over a transparent support. The support was surrounded by a shallow trough which allowed the preparation to be bathed with oxygenated Krebs solution. A blood vessel was selected by illuminating the preparation from overhead, examining the mesentery through the inverted microscope and manipulating the stage to bring the chosen vessel into the centre of the field of view. Minor adjustments to the stage position were then made to centralize the laser

measuring volume on the diameter of the vessel.

Three relatively simple laser Doppler microscope systems, suitable for measurements of blood flow in narrow vessels, have been described by Cochrane and Earnshaw (1978). The three designs are shown in figure 4.8. They correspond to differential Doppler, internal reference beam and external reference beam modes, respectively.All are forward scatter instruments and built around standard microscope systems.

In the differential Doppler arrangement the laser beam is split by a cube beam splitter into two parallel beams. These are reflected by a 45/45 beam splitting pellicle and passed symmetrically about the optical axis of the focusing lens L1. The lens, in fact the substage condenser lens with the top element removed, brings the two beams to a common focus. The position of the focus is vertically adjusted using the microscope substage control to make it coincide with the flow in the test section.Light scattered by particles moving with the flow is collected by the microscope objective and focussed by the optical system on to the photomultiplier.The movable mirror in the viewing column of the microscope swings in to enable the test section to be viewed directly. Field illumination for the viewing is provided by white light passing through the specimen from below.

In the internal reference beam model the optical components are virtually the same as those used in the differential Doppler system. However, one of the light beams passes axially through the microscope optics but the other passes off axis. Again the beams are arranged to

intersect within the test region. In this design, however, light scattered from the off axis beam mixes at the detector with the axial reference beam to produce the characteristic beat frequency. To enable the beat term to predominate over other terms in the signal, the intensity of the reference beam is adjusted relative to that of the scattered light by the use of a neutral density filter.

In the external reference beam model only one beam enters the flow region and it's scattered light is mixed with a reference beam that has been directed in such a manner as to avoid its own scattering and absorption. The mirror M must be carefully adjusted so that wavefronts of the reference beam align with those of the scattered light. The mirror must be rigidly mounted to prevent vibration from modulating the beat signal. The alignment of the components of this microscope is more difficult than in the other two configurations.

The authors suggest that the differential Doppler and internal reference designs, where in both cases the reference beam is itself directly influenced by the sample, are best suited to situations where the density of scatterers in the flowing sample is low. For blood, a dense and complex scattering medium, they conclude that the external reference beam design yields an improved signal upto higher concentrations. However, the improvement is only temporary, as progressively more dense suspensions are used the scattered spectrum becomes complicated by the appearance of double and multiple scattering terms and the suppression of single scattering by absorption.

Johnson (1982,1983) has developed a highly sophisticated laser Doppler microscope for investigating the flow of sugar in the sieve tubes of plants. The instrument is a single beam device and is built around a Vickers Instrument M74 metalurgical microscope. See figure 4.9.

The output from a 5 mW plane polarised HeNe laser is directed down onto the specimen by a tiltable half silvered mirror and focused to the required measured volume dimension by a Zeiss 'Antiflex' objective lens. The fact that the half silvered lens is tiltable is doubly significant. It allows particle motion parallel to the objective lens to be studied and it can assist in defining the true scattering volume.

If, in a single beam microscope, the laser light emerges and returns parallel to the axis of the objective lens, it must be at right angles to the flow. There will be only a small component of motion along the beam and so the scattered light will have only a small Doppler shift. There are in fact two ways round this problem. The first, described by Earnshaw and Steer (1979) is to incline the specimen on the microscope stage: this is only possible if the objective lens has an adequate working distance. An alternative method, and the one developed by Johnson, involves aiming the laser beam so that it emerges at an angle to the lens axis. The angle can be adjusted by altering the tilt of the mirror. However, if the microscope is to be used for measuring flow it is necessary to know the angle between the direction of flow and an imaginary line bisecting the angle between the incident and detected light.

Generally, if a beam enters a specimen obliquely, it and the returning scattered light will be refracted through various angles by the various changes of refractive index they encounter at the surface of the specimen and inside it. A special case exists if the microscope is set up to collect light backscattered at 180^{o} to the incident beam. The angles of incidence and detection are then the same as their bisector.Additionally,if the laser beam were to be projected into the specimen along the axis of the objective lens it would cause light to be scattered from a volume whose shape depends on the diameter of the beam at various depths in the specimen: the beam diameter will increase above and below the waist where it is focused. A detector viewing the specimen along the same axis will detect light from the full length of the beam and moving particles, anywhere in the beam, will cause the detected intensity to vary. The intensity of the light scattered from an individual particle will depend on the variation of intensity of the beam across its diameter and on its divergence. Particles above and below the point of focus will therefore contribute a range of Doppler frequencies to the detected signal. By arranging for the beam to leave the objective lens at an angle to its axis, the length of the beam from which light is to be detected may be defined by a movable aperture in the image plane of the microscope.Details of the scattering geometry are shown in figure 4.10. To achieve the collection of the back scattered light at the required angle an aperture is positioned in the projected back focal plane of the objective lens at a known distance from its axis. A Bertrand lens performs the required projection.

The Zeiss 'Antiflex' objective lens system is utilised because it

contains a rotatable quarter wave plate and polaroid analyser; it is used to separate heterodyne and homodyne components in the returning back scattered light. The heterodyne component arises from moving particles beating with a reference beam scattered or reflected from stationary parts of the microscope. The homodyne component arises from the light scattered from moving particles beating with light scattered from other moving particles. The 'Antiflex' lens is of the oil-immersion type and dictates that the specimen be under a coverslip.

Thus back-scattered light returns from the specimen into the lens, passes through the half silvered mirror and on towards a photomultiplier tube. The angle of scattered light seen by the detector is selected by means of the movable aperture previously described. The aperture and specimen diffraction pattern may be viewed through a retractable telescope.

The specimen and the position of the laser beam in it may be viewed or photographed by using a hinged mirror to divert the light path from the specimen towards an auxiliary eyepiece.A microscope lamp and condenser lens below the specimen stage provide the necessary illumination.

4.6 Fibre Optic Laser Doppler Velocimetry

Because they may be used as small diameter flexible light guides,the use of fibre optics in laser Doppler velocimetry promises increased versatility of the technique and novel optical designs.Several

fibre based LDV systems have been described,all use one of three types of fibre.They are:

i) Step-index multimode fibre: This may be regarded as the archetypal fibre and guides light rays by total reflection at the core-cladding interface.These fibres have typical core diameters of 100 um and numerical aperture values from 0.2 to 0.5.The larger the numerical aperture value and the larger the angle of the cone of incident radiation,the larger the total number of guided propagation modes. This leads to dispersion within the cable and hence carrier pulse broadening. Low bandwidth is the most significant disadvantage of step-index fibres.

ii) Graded - index fibres: These fibres represent a compromise in coupling efficiency in order to reach higher bandwidths: it is achieved by giving the core a non-uniform refractive index profile. This profile causes the light to travel on wavelike tracks because the longer pathlength of an outer ray is compensated for by the higher speed of light in the outer core region.

In general the higher the bandwidth of the graded index fibre, the more difficult it is to achieve a wide wavelength range. The fibres tend to be standardised to a 50 um core diameter and a 125 um cladding diameter.Numerical aperture values are typically 0.2

At this point it is worth noting another interesting application of radial gradient optical technology. This is the development by a Japanese company of Selfoc GRIN rods. A rod 1 or 2 mm in diameter is

made with a radial gradient of refractive index (hence GRIN); the rays of light entering such a rod become curved as they oscillate from one side to the other in a sinusoidal manner. A succession of images may then be formed wherever the curved rays cross each other. These images are successively inverted, then erect, then inverted etc., at a longitudinal separation of several millimeters. Accordingly,if the rod is cut to the correct length and its ends are polished, it will act like a lens, forming an erect or inverted image as required.

iii) Monomode fibres: These fibres have the highest performance in bandwidth. At its simplest their construction is the same as that of the step-index kind, except that the core diameter is so small that only one mode can propagate. Typically they have 5 - 12 um core and 125 um cladding diameters.The small core diameter leads to difficulties in achieving good fibre / source coupling efficiency.

Tanaka and Benedek (1975) were probably the first to describe the in vivo measurement of blood flow using a fibre optic catheter and optical mixing spectroscopy. Their catheter was a 0.5 mm fibre, introduced directly through the vessel wall and into the blood stream. Although not mentioned specifically the year, diameter and drawings all indicate that the fibre was of the step index variety.

Their experimental set up is shown in figure 4.11a. Initially polarised laser light is divided by BS,a half silvered mirror type beam splitter. Half the light passes through the beam splitter and is trapped by the trap T, the other half goes into the lens L1 and is focussed onto

the entrance of the fibre. This light passes through the fibre and emerges at its far end. The exit face is in fact cut and polished at an angle of 30^{o} so that the majority of the light is reflected out through the side wall of the fibre, passes into the blood stream and is scattered by the flowing erythrocytes. The 30^{o} cut to the fibre exit face is used to avoid getting flow information back from regions of turbulence. This rationale is illustrated in figure 4.11b. A portion of the backscattered light comes back to the exit face, some is reflected back but the remainder travels back through the fibre and out through the original entrance. In addition to the backscattered light there is a contribution arising from light which did not pass from the fibre into the blood stream but was scattered elastically from the exit face, and now remains to act as the reference frequency for the Doppler shift demodulation. Both the reference and the backscattered light lose their polarisation in passing through the optical fibre.

The light now re-emerging at the original entrance face of the fibre is then made parallel by lens L1. Scattered light that comes back into the fibre with a large angle,from the direction of the unshifted backscatter,emerges from the original launching entrance at a large angle from the axis. It can therefore be excluded by a slit, S.

The mixed beam then passes through a polariser and lens, L2,into the photomultiplier tube detector. The polariser is used to exclude that light which has been reflected back directly from the lens L1 and the fibre entrance. This light would otherwise also enter the PMT and produce a high noise level. The directly reflected light retains its

polarisation and so can be blocked by a crossed polariser; the signal and reference light becomes randomly polarised by passing through the fibre optic and so 50% of it is able to pass through to the PMT.

The photocurrent output of the detector is proportional to the Doppler shift signal and is analysed using an 18 channel digital autocorrelator. The correlator is gated by a pulse derived from the experimental animals's electrocardiogram. It is gated in such a way that the correlator operates only for certain sampling times Δt (40 ms), which can be located at an arbitary point on the cardiac cycle. See figure 4.11c.

At the end of their paper Tanaka and Benedek report upon results obtained from in vivo measurements of blood flow speed in a femoral vein of a rabbit. In a 2mm diameter vein they recorded a non pulsatile flow velocity of 2.1 cm/sec. This was substantially in agreement with direct measurements obtained by cutting the vein and accumulating the blood over a period of time. The authors were therefore able to conclude that their apparatus provided a quick, simple and accurate means of measuring average blood flow velocity, particularly in small diameter vessels.

Dyott (1978) also has described a fibre optic Doppler velocimeter, the fibre is of the multimode graded index variety and the beam splitting is performed by a holed mirror. The basic configuration of the instrument is shown in figure 4.12.

Polarised laser light passes through a 1mm hole in a front silvered

mirror which is placed at 45° to the beam axis.The light is then focussed onto the end of the optical fibre and thus travels down to the tip.A small fraction is reflected back along the fibre to form a reference beam, the rest radiates with a narrow cone of angles from the tip. Johnson (1984) has pointed out that the small fraction reflected directly back from the tip primarily owes its existence to the difference in refractive index between the fibre core and that of the surrounding medium.The amount of reflection may therefore be used to measure the refractive index of a specimen.

Any particles close to the fibre tip will scatter light back towards it, enter the fibre and so travel back towards the original launching end. Both the scattered light and the light reflected from the fibre tip are directed by the inclined mirror through a polarisation analyser and lens into a photodiode detector. The polarisation analyser prevents the detection of those spurious reflections which would otherwise give rise to signal noise. The detection process is then heterodyne, with the scattered light acting as the frequency modulated signal and the reflected light as a local oscillator.

The configuration described may be seen as offering relatively high collection efficiency and good spatial resolution. The holed mirror reflects about 90% of the light emerging back from the fibre and 50% of this, because its polarisation has become scrambled, is passed by the polariser. Therefore the collection efficiency for the detection stage is 45%. The optical fibre used in the system has an outer diameter of 125 um and a core diameter of 50 um, it presents a numerical aperture

equal to 0.15 in air. In water the fibre collects scattered light over a cone of angles upto 6.45° .

Johnson (1984) reports the use of fibre lengths of up to 2m with the above system . He found the limit to be set by the acoustic properties of the fibre. Random vibrations in the fibre impart a low frequency modulation to the returned light; this is because the multimode propagation paths are sensitive to any flexing of the fibre.

Nishihara et al (1982) have described a high resolution laser Doppler velocimeter system that makes use of a fibre optic some 150 m long and 150 um diameter. The system uses a catheter tip type measuring probe and is capable of measuring pulsatile blood flows. A multimode graded index fibre with a 50 um core diameter is used; it represents a compromise between coupling and heterodyne efficiencies.The length of fibre used allows the laser and associated optics to be housed in a separate room, some 100 m away from the animal laboratory and the measuring tip.

The whole velocimeter system is shown schematically in figure 4.13a. A linearly polarised laser beam is divided by a prismatic beam splitter, half of the light passes through a polarisation beam splitter, is focused onto the entrance of the optical fibre and passes to the fibre tip. The other half of the divided beam is used as a frequency shifted reference beam.

With the aid of the catheter holder, shown in figure 4.13b, the

fibre tip is inserted into the blood vessel at an angle ϕ. The backscattered, Doppler shifted, light is partially collected by the same tip and transmitted back to the entrance.

The Doppler shifted light that emerges from the original entrance has a shift frequency given by

$$\Delta f = 2 n v \cos \Phi / \lambda$$

where v is the blood flow velocity

n is the refractive index of the blood

ϕ is the angle between the fibre axis and the blood flow

λ is the laser radiation wavelength in free space.

The frequency shift when $\lambda = 633$ nm and $\phi = 60^{\circ}$ is therefore in the order of 2 MHz if the blood velocity is 1 m/sec.

The frequency shifted reference beam, produced by a Bragg cell driven at frequency f_1 (40 MHz), enables forward and reverse blood flow to be distinguished. If f_0 is the original laser frequency, the shifted reference beam becomes $f_0 - f_1$ and this is mixed in the detection stage with the Doppler shifted signal of frequency $f_0 + \Delta f$. An avalanche photodiode is employed in the detector stage,for the low power level (< 1 u W) received in blood flow measurements it has better signal to noise ratio characteristics than a photomultiplier. The photocurrent from the detector then passes to a spectrum analyser.

The spectrum of the photocurrent is shown schematically in figure 4.13c. The sign of Δf (positive or negative) depends on the direction of

the blood flow (forward or reverse). Δf is positive for $0° < \Phi < 90°$ and is negative for $90° < \Phi < 180°$; accordingly the signal spectrum appears to the right of the shifter frequency, f_t , for foward blood flow and to the left for reverse flow.

To evaluate the accuracy of the blood flow velocity measurements, several steady and known velocities were produced by means of blood filled circular grooves on a rotating turntable. Figure 4.13d shows examples of the Doppler signals obtained.

The spectra A,B and C were obtained, respectively, when the fibre tip was placed close to the surface of the blood flow, just into the blood flow, and deeply into the blood flow. In case A the signal shows a narrow distribution since the flow is not disturbed. In case B the spectrum is very much broader, this is attributed to the flow disturbance caused by inserting the fibre into the blood.In case C the spectrum shows a small subpeak in the vicinity of f_{cut} of spectrum B. The subpeak appears because of the Doppler signal scattered from the turntable itself. This is taken to indicate that the value of f_{cut} gives the correct velocity of blood flow.

As an in-vivo application of the method the authors report results obtained from dog femoral arteries and from dog coronary arteries. Both show that pulsatile blood velocity measurements can be made and that the results are in good agreement with those obtained from electromagnetic flowmeter type instruments.

The continuous recording of tissue blood flow, as opposed to discrete vessel flow, is clinically useful in a number of disciplines including dermatology, plastic surgery and anaesthesiology: the possibility of applying laser Doppler techniques was first pointed out by Stern (1975);a fibre optic approach to the method has now been developed by Nilsson (1980,1984).

In one of the earlier systems developed by Nilsson, light from a 2mW He-Ne laser was guided to the tissue by a 1.5mm diameter plastic optical fibre and another used to pick up backscattered radiation and guide it to a solid state detector. However,noise attributable to laser beam mode interference was of such a magnitude that low flow recordings were virtually impossible.In order to overcome this problem a differential detector system was designed.

The back scattered light from the adjacent scattering areas of the tissue is gathered by a pair of fibres and guided to two separate photodetectors.The beat signals produced in the detectors are then high pass filtered,amplified and normalised in an identical way in both channels.Both channels are then fed into a difference amplifier and common components such as mode noise from the laser are suppressed. The beat signal produced by the random fashion in which the red cells pass through the two scattering areas can be considered as independent realisations of the same stochastic process. Consequently the overall blood flow related output signal is not suppressed in the difference process.

Extensive and encouraging studies of the instrument have been carried out under the direct auspices of Nilsson and co-workers.Additionally,the flow meter is now commercially available (Perimed Periflux PF II laser Doppler flow meter) and has been enthusiastically received by independent groups.See Cochrane et al (1986) for example.

4.7 Laser Doppler Velocimetry and Semiconductor Laser Diodes

Laser diodes are essentially Light Emitting Diodes (LED's) but with several structural and operational differences; both are manufactured from a block of semiconductor material containing a p-n junction. As with other semiconducting devices, current is carried by free electrons and holes within the crystal lattice. When the diode is forward biased carriers are injected from the p- and n- type layers into a recombination region,where they recombine and emit a photon in the process.A resonant cavity,formed by cleaved crystal planes, and high drive current stimulated recombinations give rise to light amplification.Self sustaining lasing action occurs when enough carriers are injected to provide the electronic gain needed to overcome the cavity's internal losses.

The output beam emitted from a laser diode is both highly divergent and elliptical in cross section. Beam divergence typically runs between 40 and 60 degrees; divergences up to 90 degrees are not unusual. Beam divergence in the direction perpendicular to the active layer is typically two to six times the divergence in the plane parallel to the

layer.Failure to correct the out-of-roundness of the beam is sometimes unimportant,but when the beam is collimated the far-field beam divergence can be different in each direction.

It is only within the past few years that the cost of semiconductor laser diodes has fallen to a level where they now represent a cost effective alternative to low power HeNe devices. The fall in cost stems largely from developments within the telecommunications industry and the additional demand generated by various forms of optical storage device.

One of the few laser diode LDV devices developed specifically for blood studies is the blood flow monitor probe described by de Mul et al (1984). Described as a mini laser source by the authors, a Philips 498 CQL laser diode is used to provide 5 mW of radiation at a wavelength of 840 nm. Detection is by means of two Philips BPX40 photodiodes.This particular laser diode was selected mainly because of its relatively high coherence length and low cost. The photodiodes were chosen on account of their favourable spectral matching.

The flow monitor is shown schematically in figure 4.14. The laser diode is held in an aluminium jacket (for cooling purposes) and the two photodiodes positioned aside from the output beam. A perspex cover affords some physical protection for the probe end and, presumably, provides a degree of reflection that contributes towards the heterodyning reference beam. The authors do actually say that scattering by the blood vessel wall is used as a randomised reference beam and that

the Doppler shift frequency spectrum is therefore smeared out to provide only an averaged value of red cell velocity.

The two photodiode output signals are amplified and then subtracted from each other to suppress D.C. components in the signal. The resulting signal is then fed into a real time spectrum analyser. The differential detector configuration is similar to that used in the fibre optic flowmeter by Nilsson et al (1980).

4.8 Discussion

In the context of quantifying thrombus development by the effects on blood flow in small vessels, LDV techniques do, with some reservations, appear to offer a viable alternative to ultra sonic Doppler shift measurements. There are certainly some advantages in terms of scale and accessibility, the latter because the method is effectively contact free.However, it is also apparent that problems associated with multiple scattering, photon diffusion and general uncertainty about laser beam penetration depth,can add up to create a substantial measure of doubt about the interpretation of laser Doppler blood flow measurements. This would tend to suggest that some reported LDV measurements might be presupposing a level of accuracy that in reality is not being attained.

Possibly, therefore, any thrombus growth index based on detailed haemodynamic information might well turn out to be overly sophisticated and even misleading.So, whereas measurements of something as relatively

detailed as occlusion associated turbulence might appear problematical,the measurement of something as relatively gross as mean jet velocity would appear to be realistic. Accordingly, a system was designed and built to test out the basic concepts. It,and some preliminary results,are described in the next chapter.

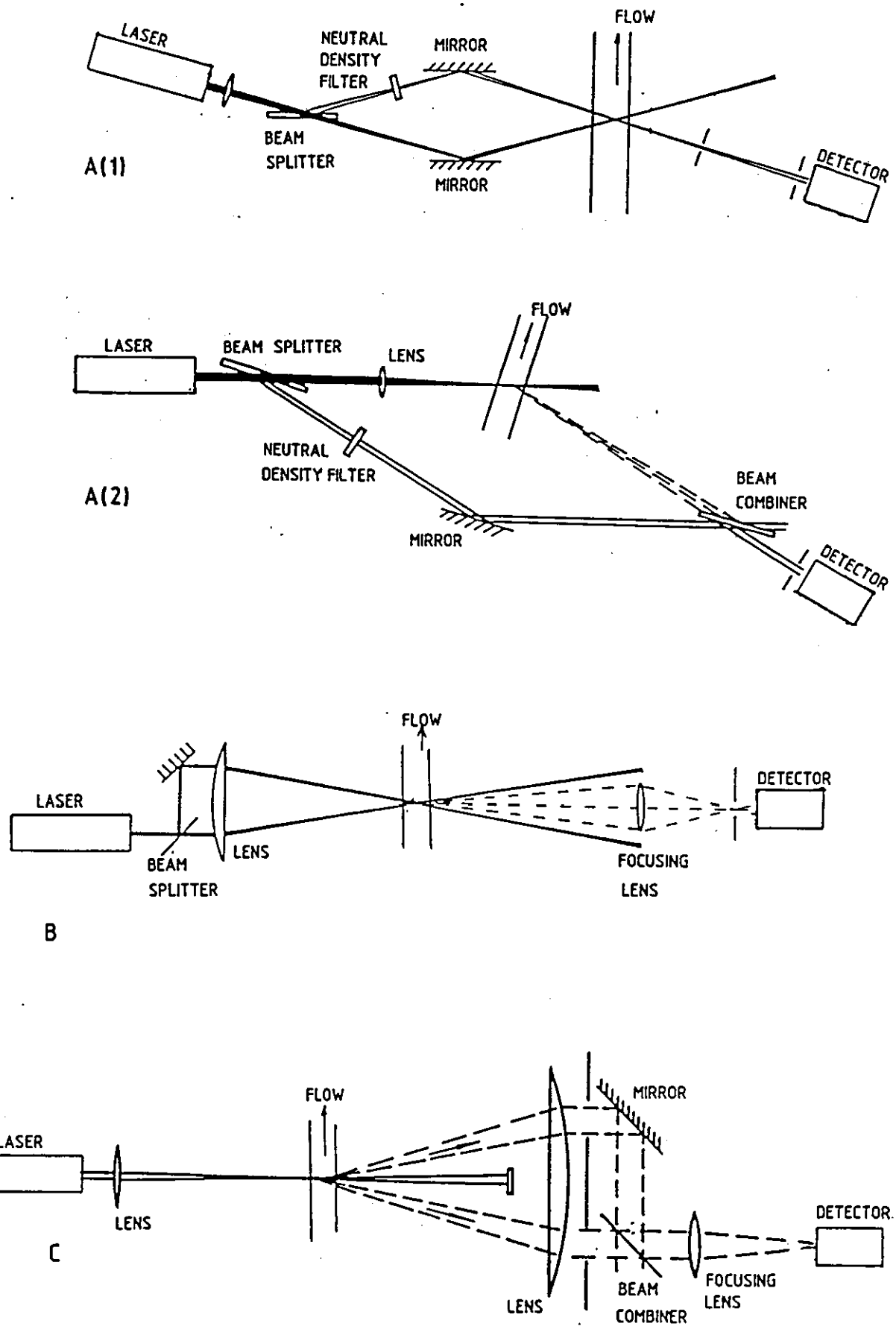

Figure 4.1: Basic optical arrangements for laser Doppler velocimetry: A(1) reference beam type, A(2) is fundamentally the same but makes use of an external reference beam. B, dual beam configuration. C, dual scatter configuration.

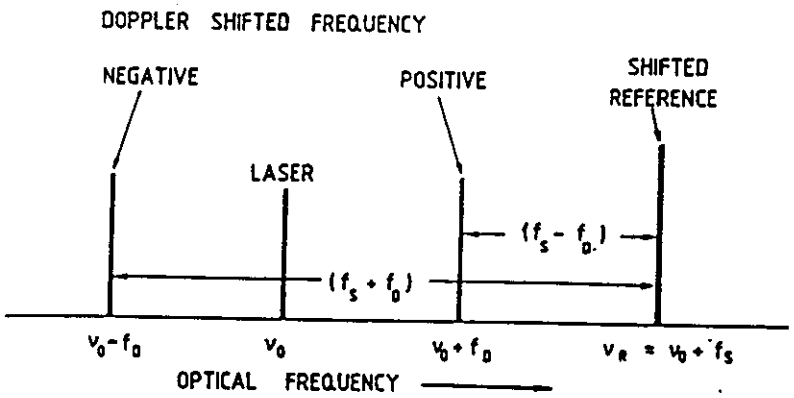

Figure 4.2: Diagram illustrating the beating of a Doppler shifted light with a frequency shifted reference beam.

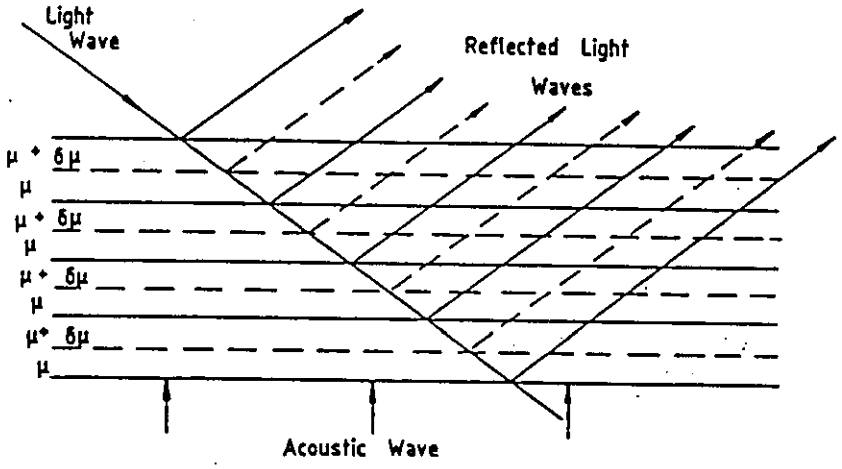

Figure 4.3: Bragg reflection by an acoustic wave.

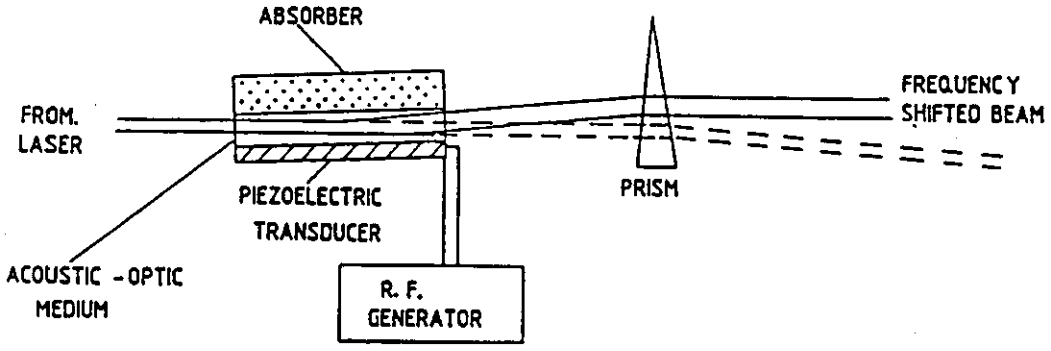

Figure 4.4: Shifting the frequency of a light beam by the use of an acousto-optic cell.

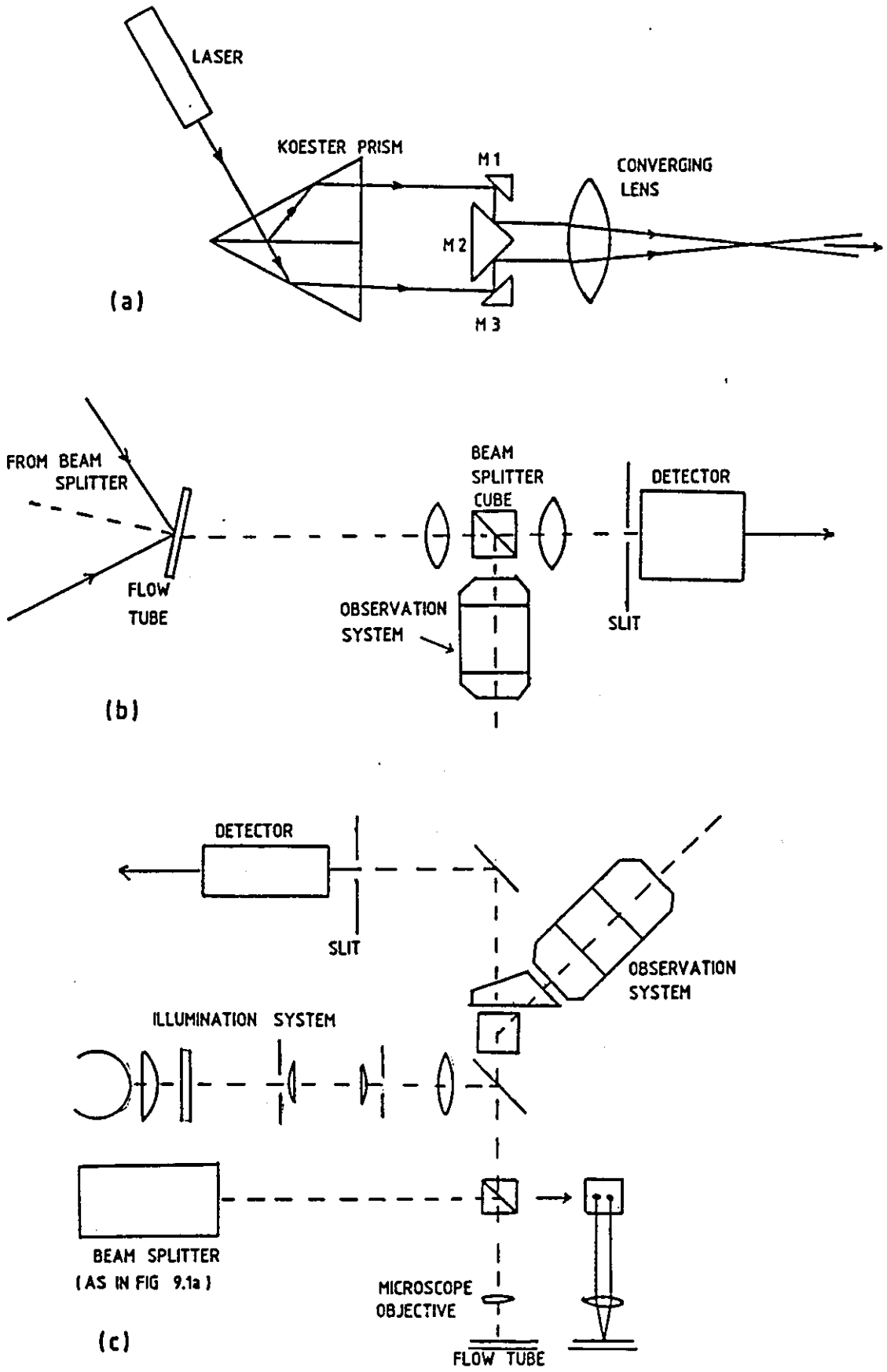

Figure 4.5: The double beam microscope described by Mishina and Asakura in 1972. (a) The basic beam splitter. (b) A forward scatter configuration. (c) A backscatter configuration

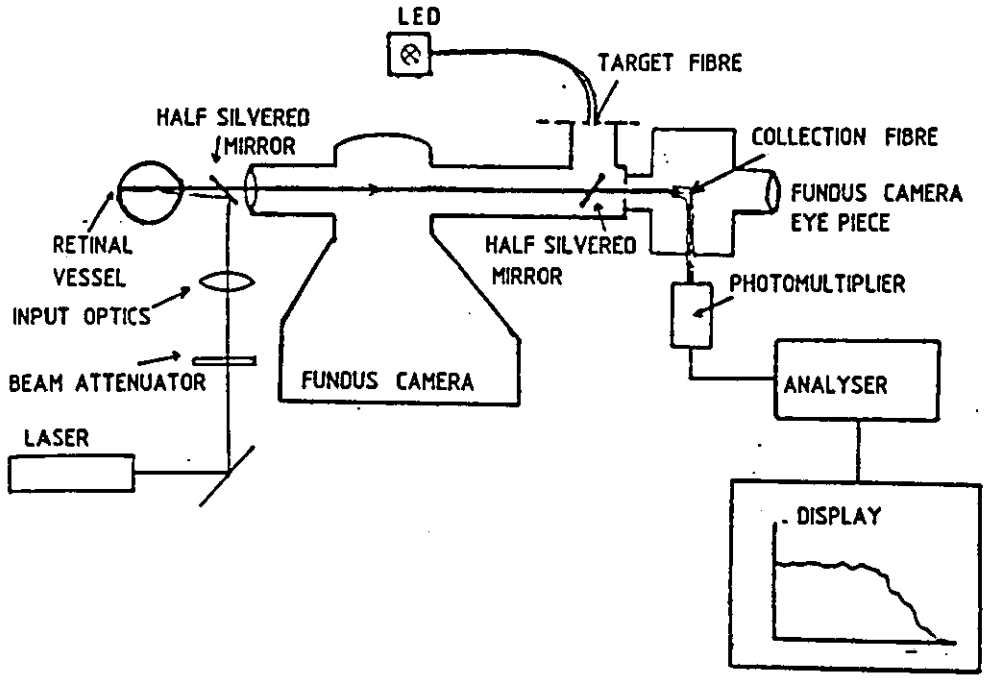

Figure 4.6a: The retinal blood flow measuring system developed by Riva et al (1972).

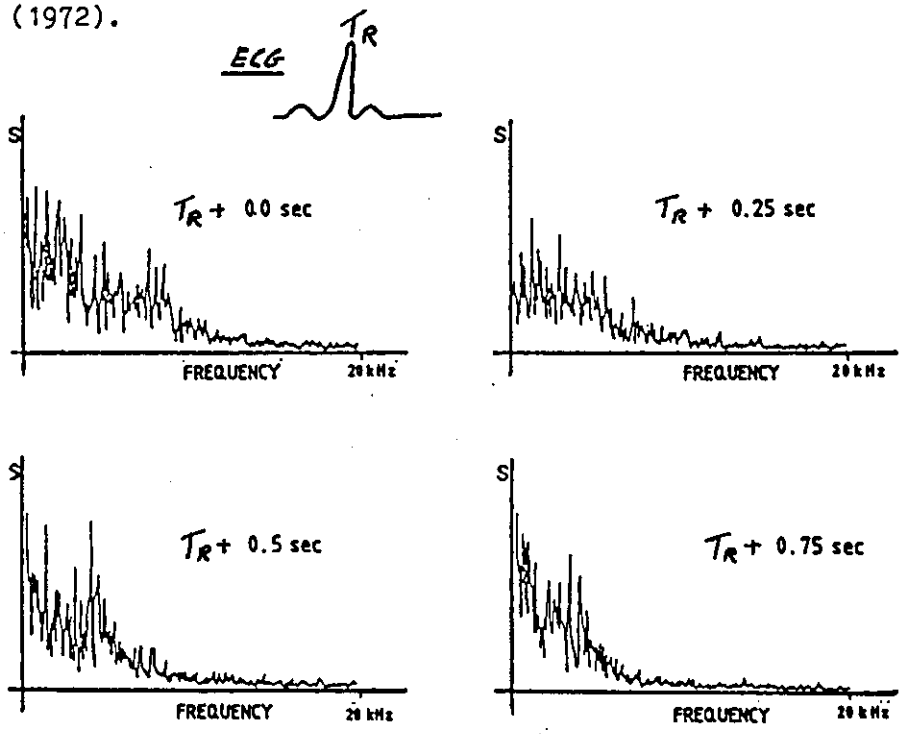

Figure 4.6b: Spectra obtained from a human retinal artery during four portions of the cardiac cycle,the relative positions are indicated.

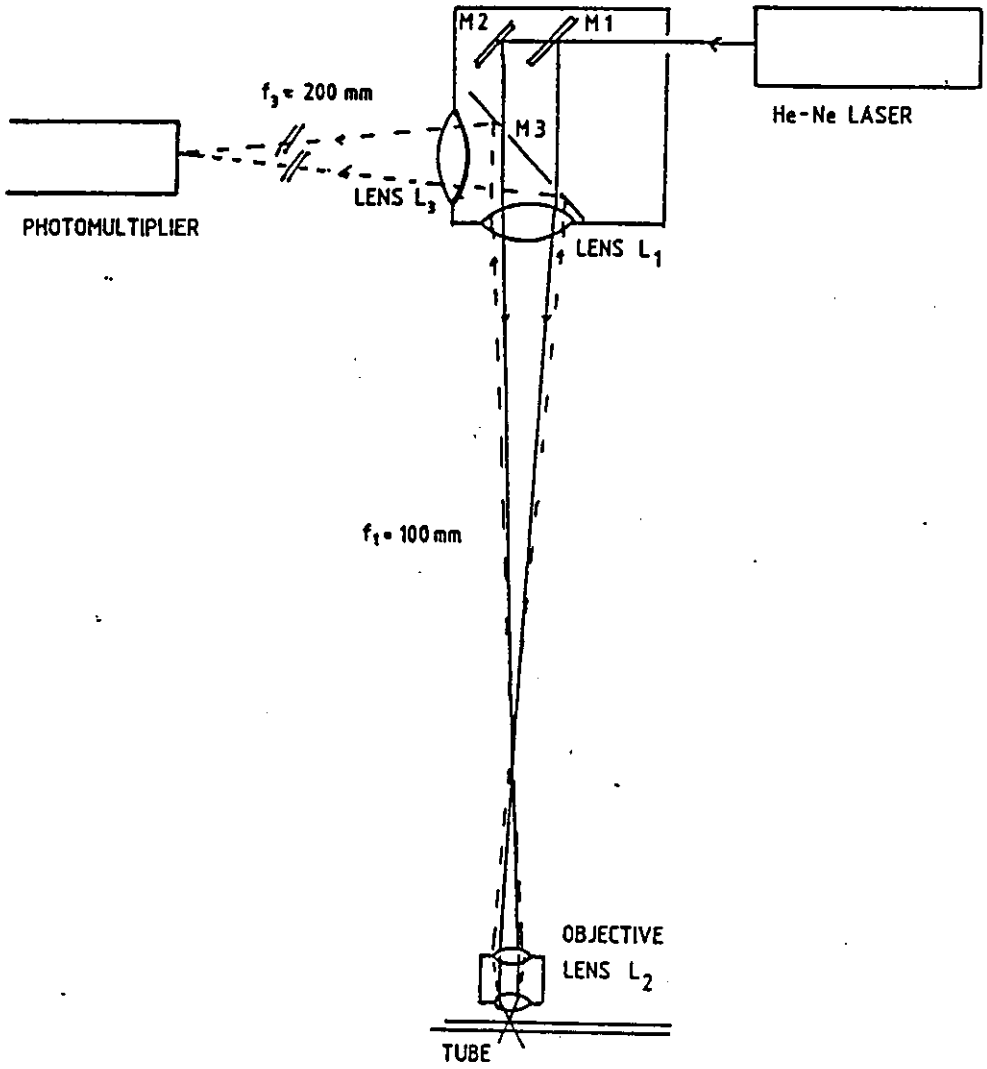

Figure 4.7: The laser Doppler microscope developed by Born,Melling and Whitelaw (1978). The authors were a little pessimistic about the use of the technique in blood flow studies.

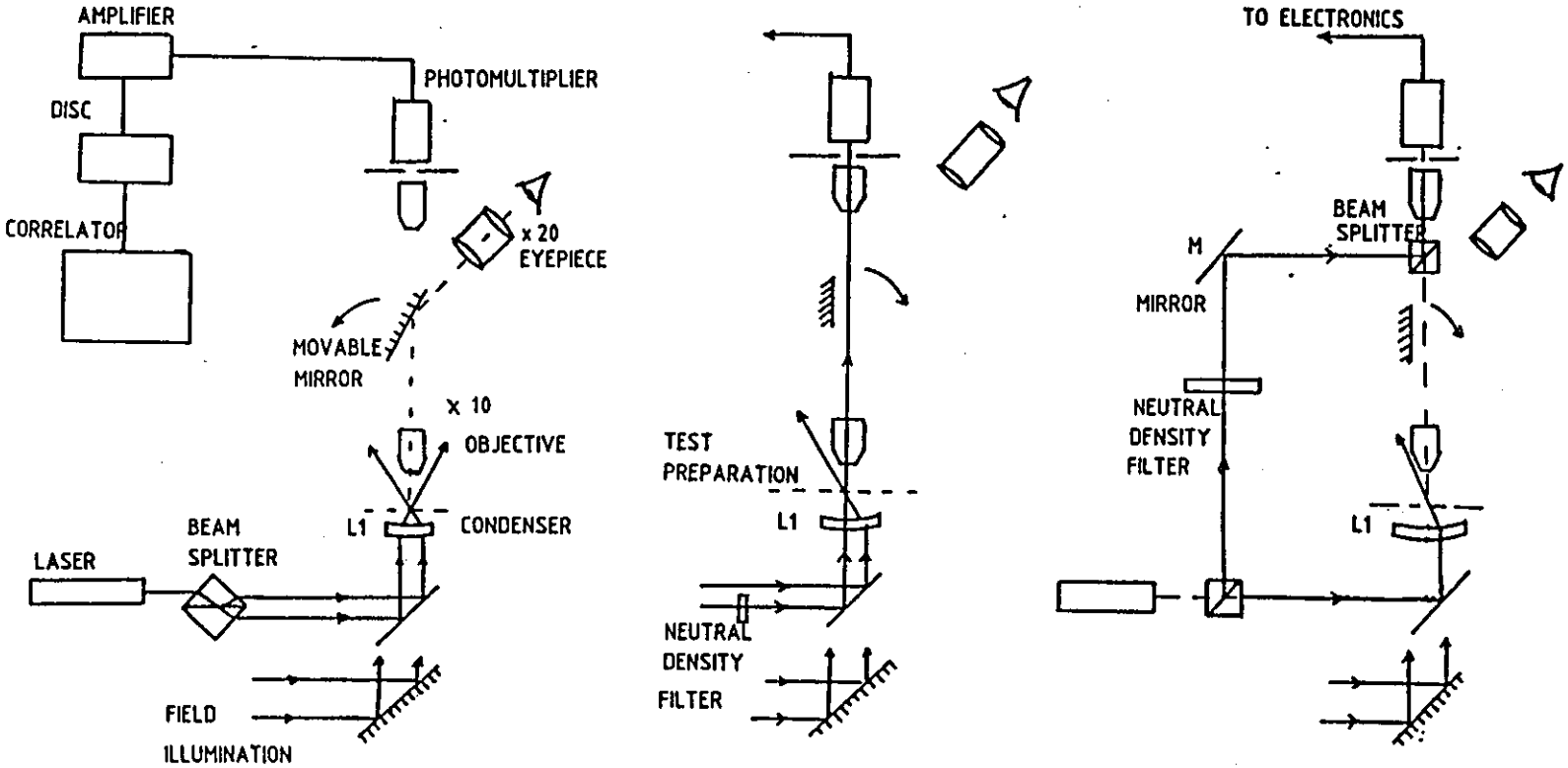

Figure 4.8: Three laser Doppler microscope systems developed by Cochrane and Earnshaw. (a) differential Doppler.(b) internal reference beam.(c) external reference beam.

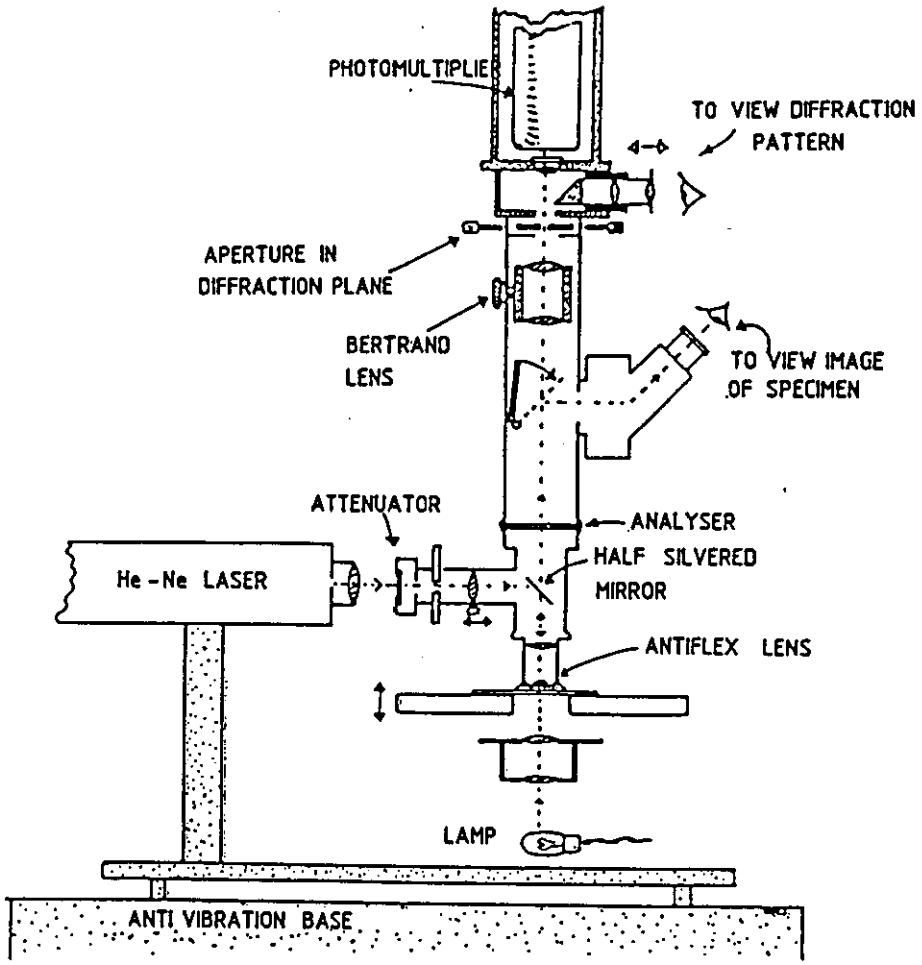

Figure 4.9: The laser Doppler microscope developed by Johnson (1982,1983).

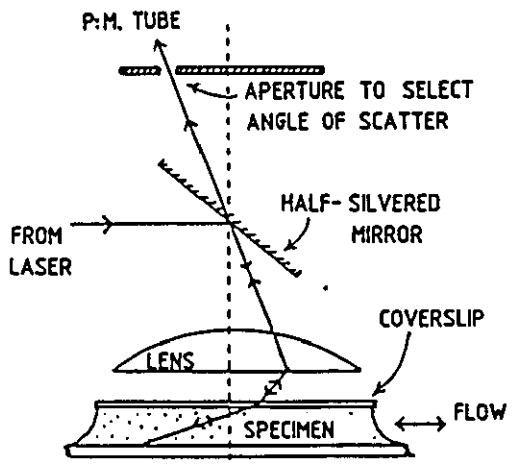

Figure 4.10: The scattering geometry employed by Johnson to achieve non-perpendicular shift vector measurements.

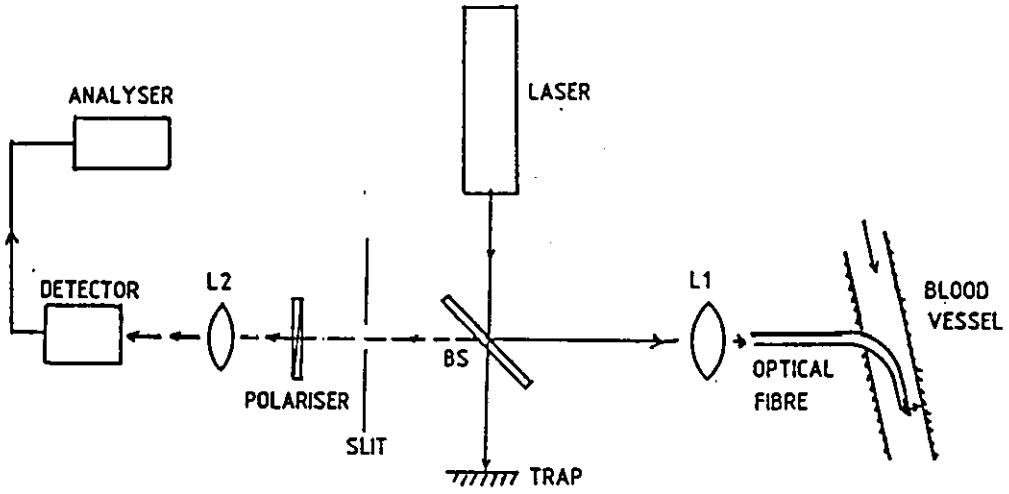

Figure 4.11a: The fibre optic laser Doppler velocimeter designed by Tanaka and Benedek (1975)

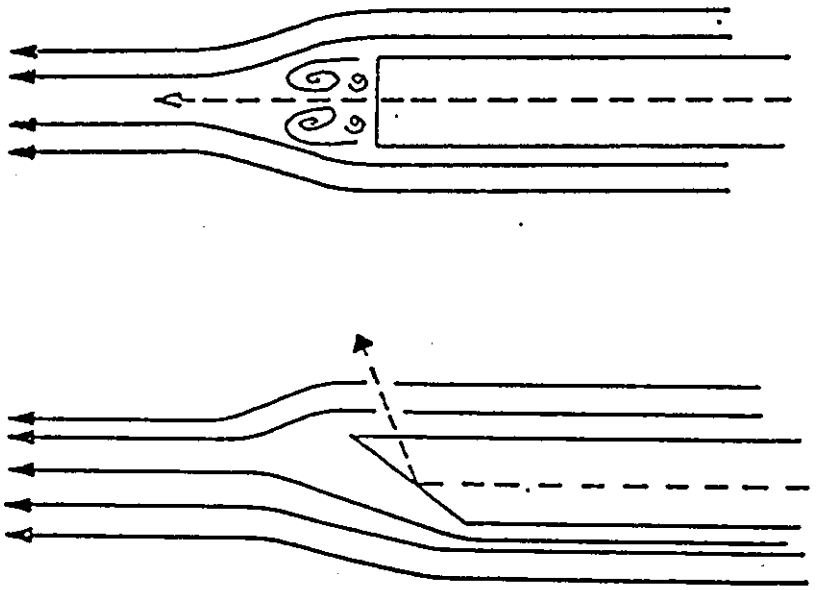

Figure 4.11b: Showing how a 30° cut to the fibre face can be used to avoid making the measurements in regions of fibre induced turbulence.

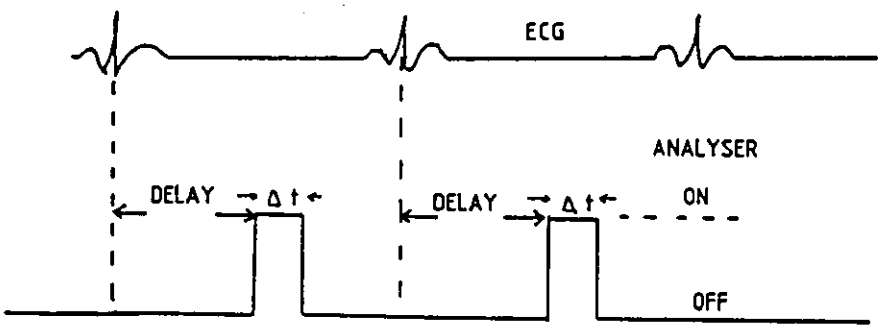

Figure 4.11c: Showing how the analyser was triggered after specific points of the ECG. A similar technique was used by Riva to obtain the spectra shown in figure 9.2b.

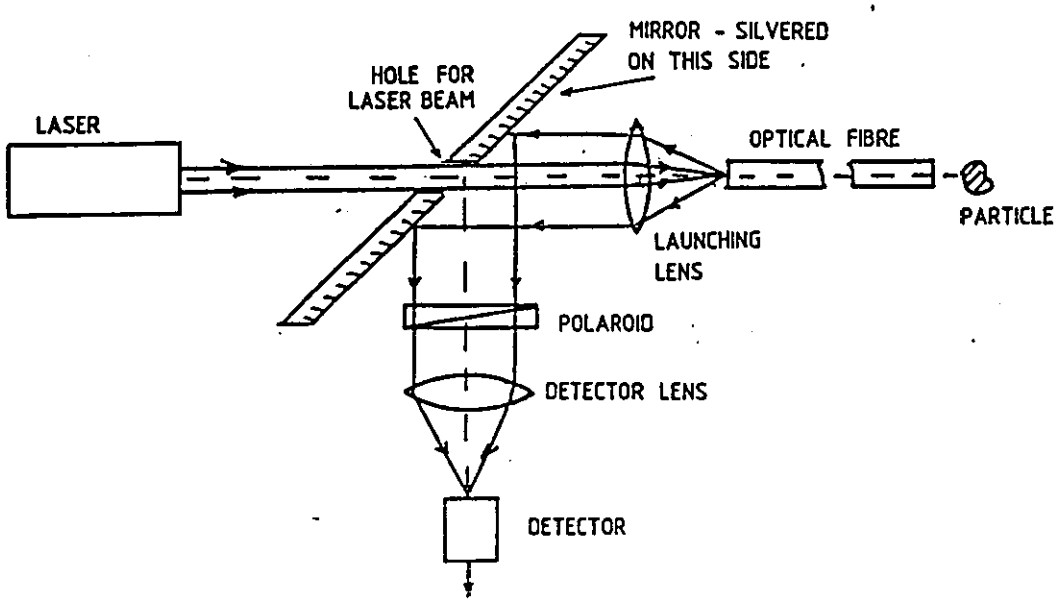

Figure 4.12: The fibre optic velocimeter developed by Dyott (1978).

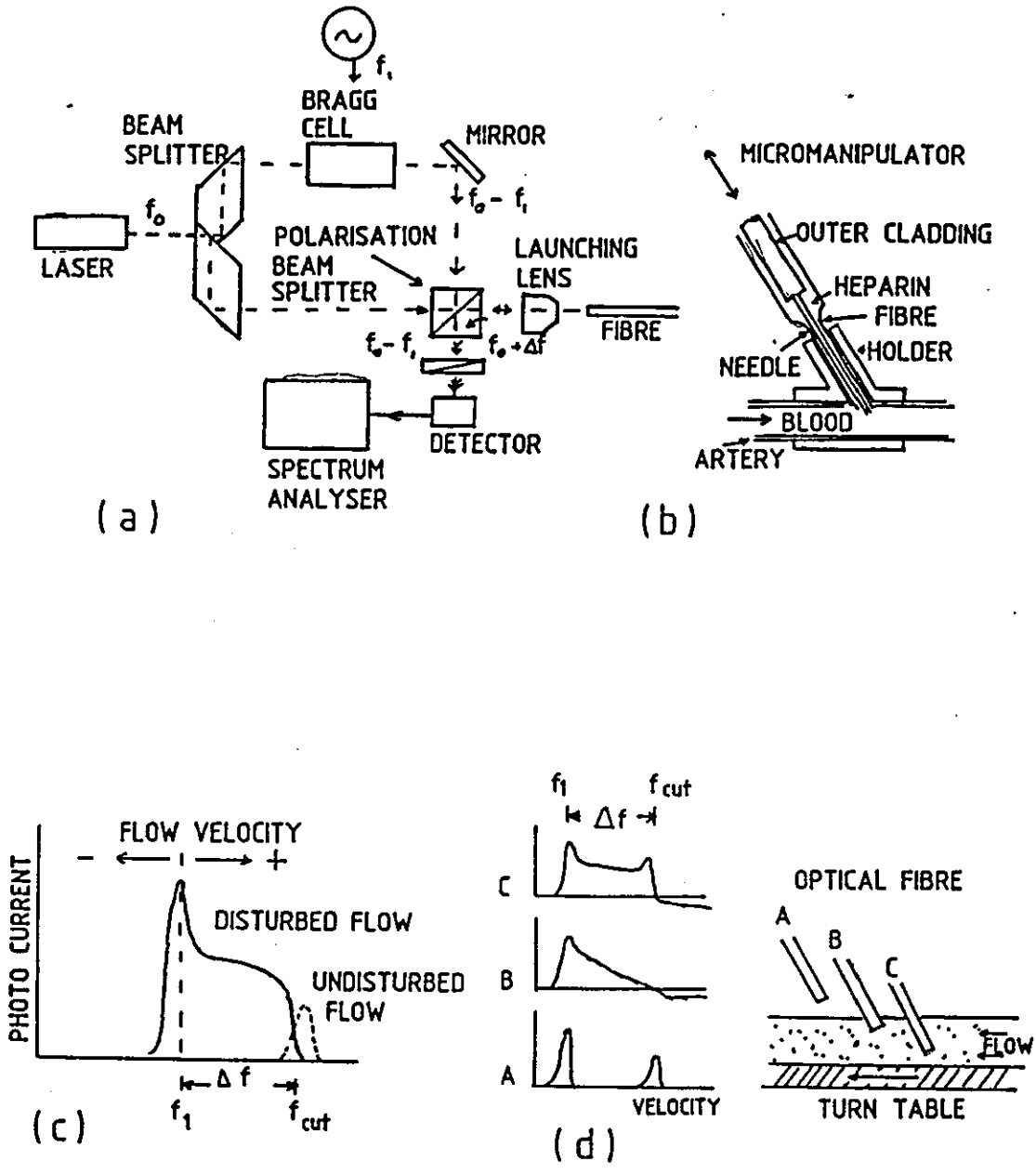

Figure 4.13: (a) Optical configuration of the fibre optic laser Doppler velocimeter designed by Nishihara et al (1982). (b) Detail of the catheter holder used for inserting the fibre into the blood stream. (c) Schematic diagram of the photocurrent spectrum, showing the separation of forward and reverse flow. (d) Method of calibration and associated spectra.

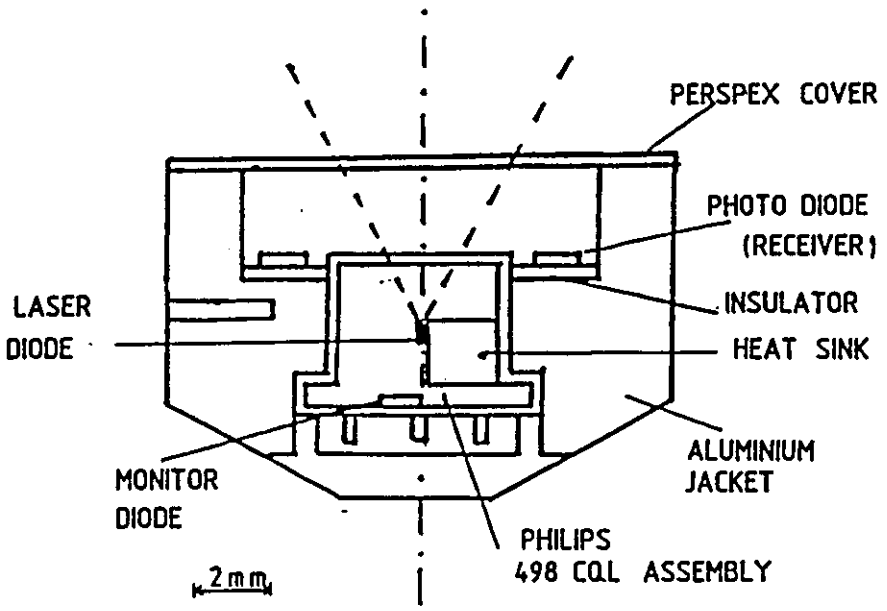

Figure 4.14: The flow monitor described by de Mul et al (1984).

CHAPTER 5

A PROTOTYPE LASER DOPPLER VELOCIMETER AND SOME PRELIMINARY RESULTS

5.1 Introduction

Having arrived at the rationale described in the previous chapters, the next stage in the proceedings was the construction of a laser Doppler velocimter for evaluation purposes.The chosen configuration was a dual beam system, designed around the use of a laser diode as the source of coherent radiation.

Although used in some of the pioneering studies of this type of blood flow measurement (Mishina et al,1976.Born et al,1978), it is now recognised that the dual beam system has fundamental limitations (Cochrane and Earnshaw,1978). Using the fringe model of Doppler frequency generation (Rudd,1969), one can understand that high particle densities and refraction at vessel/fluid interfaces must have adverse affects on signal quality. Never the-less, the system does retain it's original reputation of being simple to implement and align. This is the reason why, despite known criticism, it was chosen at the present juncture.As things transpired much useful work could be performed and an early measure of confidence was established in the proposed experimental rationale.

5.2 The Dual Beam System

The design of the velocimeter is shown in figure 5.1. That it is

compact and robust is partly due to the choice of a laser diode as the source of coherent radiation. The particular diode used is the Hitachi HL7801E, radiating at 780nm with an output power of approximately 3mW. This laser diode, although having the option via a built in monitor photodiode to run at a constant optical output power,is run in the constant current mode.Any alteration in a laser diode's injection current produces both intensity and frequency modulation of the output (Dandridge and Goldberg, 1982).

In order to simplify the overall system design a rather pragmatic view was taken of the laser diode optical arrangement. As described in chapter 4, the output beam from a laser diode is divergent, elliptical and may also be astigmatic. Therefore, to obtain maximum output efficiency, non-spherical optics should be used (Kuntz, 1984). However, in the work under discussion here, adequate output characteristics were achieved using a simple x20 microscope objective lens, L1. Fuhr (1985) has presented a comparison of the efficiency with which various microscope objectives and custom lenses collimate laser diode beams. The microscope objective may be expected to have a coupling efficiency of about 45%, compared with 92% for a custom designed lens system.

In addition to the requirements for efficient propagation,under some circumstances it may be necessary to prevent optical feedback from glass surfaces to the laser cavity: such feedback can seriously degrade the line width of the laser output (Miles et al, 1980). Optical feedback isolators are available commercially but in the context under discussion, because there was in fact no obvious evidence of line width

broadening,only minimal isolation was introduced - in the form of a half wave retarder.

Refering again to figure 5.1, the collimated beam emerging from the laser diode and associated optical components first passes into a beam splitter. This unit is made up of a beam splitter cube and a front silvered mirror which has been bonded to the adjustable face plate of a kinematic mount. The beam splitter cube, mounted with one of it's faces normal to the incident beam, allows approximately 45% to pass straight through and, by internal reflection at its interface, diverts another 45% through 90°. A beam splitter cube was chose in preferance to a half silvered mirror because its lack of refraction induced beam displacement simplifies overall system alignment.

The undiverted beam travels 35mm before it also is reflected through 90° by the front silvered mirror:it is now parallel to the beam diverted by the beam splitter cube. That the two beams are parallel is ensured by fine adjustment of the mirror mount; they will be separated by 35mm.

The two parallel beams are brought to a common focal point by the convex lens, L2. This focal point will be the position from which the Doppler signals are received. The lens has a diameter of 50mm, a focal length of 120 mm and the beams enter at two horizontally opposing positions symmetrically placed 17.5 mm from the central optical axis. The centre of the lens is drilled through with a 25 mm hole: this is to accommodate a short focal length collecting lens,L3.The collecting lens

is plano convex and aspheric. It has a diameter of 25 mm,a focal length of 20 mm and is mounted with the convex surface towards the sample holder.An aspheric lens was chosen as the collecting element because of it's favourable focal length to diameter ratio.It is held in place by isocryanate adhesive.

Several test sample configurations have been used with this laser Doppler system, the diagram shows a fine tubular flow cell. For ease of traversing,the cell would normally be mounted on a micromanipulator stage. The point of interest in the flow cell would be positioned at the focal point of the lens L2 and the backscattered Doppler shifted light collected by lens L3.The laser diode radiates at a wavelength which is just beyond normal human vision.Consequently target alignment is primarily by result but may be aided by the use of an infrared viewing screen.(Fiberlab,type S 1908)

Thus the backscattered light from the moving sample is collected and then, ultimately, brought to a focus at the surface of a photodetector.Before detection it is in fact passed through an interference filter, an aperture and a polaroid analyser before reaching the detector. The interference filter is centred at 780 nm with a bandwidth of 30 nm and is used to prevent ambient light from reaching the detector and causing noise or saturation. The aperture is a 200u hole in the centre of a disc and enhances the signal to noise ratio of the system by providing a degree of spatial filtering against components originating from non aligned scattering centres: the hole size was determined empirically. The polaroid analyser was included as a means of

filtering out any unscattered components in the incoming light. Such components could be expected to arise from specular reflectance at vessel walls and, if sufficiently intense, could saturate the detector.

The detector used is the Mullard BPX65, a planar silicon PIN photodiode. It was chosen on account of its high frequency response and high sensitivity at the laser diode wavelength. It is connected by a short length of coaxial cable to a local amplifier stage, the output of which goes to the rest of the signal processing equipment

5.3. Signal Processing For System Evaluation

The signal processing equipment is shown schematically in figure 5.2.As previously mentioned, the BPX 65 photodiode detector of the LDV is first of all connected to a local amplifier stage. This stage provides current to voltage conversion and good noise immunity, because of its low output impedence. The local amplifier output is fed into a Barr and Stroud EF5 variable filter so that a variety of bandpass characteristics may be applied to the signal, the filter amplifier also allows upto 40dB of gain to be introduced. The output from the filter is split three ways and goes into:

1. An audio monitor.
2. A Hewlett Packard 3582A spectrum analyser.
3. A Gould OS4000 digital storage oscilloscope.

The audio monitor is a simple 3 watt audio amplifier and loud

speaker: it gives excellent qualitative information about signal quality and thereby provides a tuning signal with which to optimize optical alignment when setting up the velocimeter. Johnson (1982) has reported upon the value of an audio monitor when used in conjunction with his laser Doppler microscope.

The HP 3582A spectrum analyser is a dual channel device. By combining advanced digital filtering techniques with a microcomputer execution of the Fast Fourier Transform it is able to offer real time frequency analysis in the range .02Hz to 25.5 KHz. In addition to frequency domain and phase measurements the instrument is able to make measurements involving system transfer and coherence functions. In order to reduce the uncertainty of the estimate of random spectral components an RMS averaging mode allows the power average of 4 to 256 successive spectra to be made,an external trigger input allows the data acquisition and averaging to be time locked to a specific part of a waveform. In the context under discussion, the Doppler shift frequency spectrum may therefore be built up from a well defined part of a pulsatile flow cycle.(cf, for example,Tanaka and Benedek,1975 or Riva et al,1972). In addition to being available on a built-in display screen, the spectra produced by the analyser are available in analogue form for outputting to an X-Y plotter and in digital form for further processing by an IEEE bus linked computer.

The position at which the spectral analysis is performed on a waveform is adjusted by introducing a variable delay between an associated synchronising pulse and the spectrum analyser's trigger

input. Many pulse generators have such an input/output delay facility, the one used here is an Advanced Instruments type PG58.

The Gould OS400 two channel digital storage oscilloscope is used primarily as a monitor for checking incoming signal levels and for setting up the spectrum analyser's triggering points. Information held in store is available as an optional analogue output, therefore a 'hard copy' of a captured signal may also be produced on an X-Y plotter.

The signal processing equipment described so far was assembled together for system evaluation purposes. Later on in this thesis it will be described how, as a result of the information obtained from those evaluation studies, it became possible to implement a design for special purpose signal processing instrumentation. From the outset it was recognised that special purpose instrumentation might eventually offer advantages in terms of cost saving, extended operating range and ease of interpretation.

5.4. Initial System Test Procedure

To ascertain that there were no fundamental design problems, an initial functional check was performed on the laser Doppler velocimeter and associated signal processing equipment. The requisite particle movement was modelled by vibrating a sheet of crocus paper; this is a very fine abrasive material used in the surface preparation of a variety of engineering materials. It is made up of a reasonably homogeneous monolayer of an oxide of iron bonded to a paper backing material, the

oxide particle size is in the order of 50um. Only back scatter configured LDV systems may be tested with such a material.

A small moving coil electro-mechanical vibration generator (Ling Dynamic Systems Ltd) was used as the means of moving the crocus paper. In principle a rotating plate attached to the shaft of a variable speed motor would have been a viable alternative but the vibration generator had been used is a previous project and so was immediately available. It also had the added advantage of being able to accept a variety of displacement inducing waveforms.

Therefore,by attaching the crocus paper to the vibration generator,a variety of velocity and acceleration profiles may be imposed on a monolayer of 50 um particles. The orientation of the crocus paper and vibration generator combination is such that the particle displacement is in the same horizontal plane, but at right angles to, the principal axis for the measuring optics.

The power function generator used for driving the vibration generator was a Feedback Instrument type PFG605. It provides sine, square or sawtooth output waveforms within the frequency range .0001 Hz to 1 KHz. An auxillary output socket provides a fixed voltage square wave which may be used to trigger the pulse delay generator, which in turn triggers the spectrum analyser. This allows the production of moving particle associated Doppler shift spectra from well defined parts of their driving waveform.

Because this part of the work is so obviously peripheral to the main study, it is proposed to present only that data which is considered sufficient to establish equipment credibility and to support any observations which might be made. Therefore,apart from stating that the dual beam LDV worked well enough to satisfy initial expectations, the following observations are considered worthy of note.

1: Unless 'cleaned up' by filtering it is not easy to detect the Doppler Signal on the oscilloscope screen. The raw signal does however produce a low pass limited spectrum and bursts associated with individual particle movement can be detected by ear with the aid of the audio monitor. With suitable high pass filtering classical Doppler bursts can be observed on the oscilloscope screen. The effects of 500 Hz high pass filtering on the signal from the double beam velocimeter are shown qualitatively in figure 5.3. The associated frequency/power spectra all result from operating the F.F.T. spectrum analyser in an 8 fold synchronised averaging mode.

By high pass filtering one is removing low frequency noise from the signal; that noise originates from several sources. There is a mains frequency component, a mechanical vibration component and what is effectively a cross talk component from adjacent particles within the measuring volume. The magnitude of the individual components will depend on such factors as mechanical design, opto-electronic sensitivity and measuring volume size.

At this stage it may be anticipated that such susceptibility to low

frequency noise as there is in this implementation will not prove to be a limiting fault in the context of the intended blood flow studies; the required Doppler frequencies lie well above the spectrum of the majority of the noise components. Hence, at this evaluation stage, little attempt was made to improve upon signal to noise ratios.

2: The linearity of a particular system can be checked by changing the amplitude of the input signal to the vibration generator. In principle a frequency change at the input could also be used to produce a linked velocity change of the crocus paper particles. However, this latter procedure was not employed because of uncertainty about the electro-mechanical transfer function associated with the vibration generator.For the same reason, it would have been difficult to determine absolute velocity measurements without extra measuring equipment. Hence linearity was only checked against the amplitude of the driving waveform. Figure 5.4 shows some results associated with the double beam device; in the interest of resolution the dynamic range has been intentionally restricted. By operating at a higher input frequency Doppler shift frequencies up to the spectrum analyser's 25.5 KHz maximum were at times induced.

3: The waveform following properties of a particular velocimeter system can be demonstrated by putting a sinusoidal waveform into the vibration generator. By making use of the trigger pulse delay generator, sample points can be selected along any part of the curve and a velocity correspondence ascertained.

Figure 5.5 shows the results from such a sinusoidal drive waveform,the frequency was chosen to be of the same order of magnitude as a blood pulse. The Doppler shift frequency has been plotted against the cosine of the input waveform because this, as the first derivative of the input, is proportional to velocity. In addition to the limitations imposed by the particular velocimeter design and the crocus paper model, the waveforms associated with figure 5.5 show evidence of additional spectrum broadening. This is caused by the finite FFT sampling time. (100 ms for the 2.5 KHz range) and the change in velocity during that interval. Apparent clipping of the sinusoidal input waveform is a display artifact caused by limitation in the digital storage oscilloscope's resolution and subsequent write out.

5.5.Preliminary Flow Experiments

Professionally, morally and logistically it is highly desirable that a new instrument, destined for use on animal preparations, be first tested and evaluated by simulation. This is in addition to any preliminary functional tests of the type described in the previous section.The present section therefore describes results from experiments where the conditions were intended to be analogous to those encountered in a small vein. Consequently flow rates are small, in the order of a few centimetres per second,and there is no pulsatility. A thin walled glass micropipette tube (Camlab) with an internal diameter of 1 mm was used as the flow vessel.

The relatively narrow bore of the tubes combined with the relatively high viscosity of blood precludes the practical use of a constant head gravity fed system for providing the fluid flow. Thus some form of pumping is necessary and peristaltic pumps, on account of their intrinsic fluid barrier, tend to be the de facto way of pumping blood. Some pulsatility is inevitable but the degree can be minimised by maximising the number of pump rollers and using some form of hydraulic accumulator. In the system now being described, a Watson-Marlow type MHRE flow inducer was used.

Fluid from a 20 ml capacity reservoir is fed into a short length of silicon rubber peristaltic pump tubing and from there,via an accumulator and a 5 metre length of 1.0 mm I.D. polythene tubing,is pumped into the glass flow vessel.A short length of polythene tubing then forms the recirculation link back to the reservoir.The accumulator is made up from a thin silastic rubber fountain pen bladder and is 'T'-ed into the flow line just after the peristaltic element.The apparently excessively long length of polythene feeder tubing also contributes to the pulse damping,it is wound into a coil for ease of accommodation.

The flow vessel is placed in a mat black holder and it,in turn,is attached to the x-y-z translational stage of a micromanipulator (Prior). 'Target' alignment is therefore achieved by moving the vessel, rather than the velocimeter.

Initially a latex suspension was used as the particle-bearing test

fluid. However, the fluid dynamic properties were sufficiently different from those of blood for the LDV spectra to be shifted quite markedly in frequency. Consequently, in all the experiments about to be described,blood (from dogs) is the fluid used. Coagulation is prevented by collecting the blood in pots treated with EDTA (a potassium salt of Ethylene - Diamine Tetra-Acetic acid). Typically 10 ml of blood was used during any one experimental session; it was readily available from in vivo experiments being conducted elsewhere.

The steady state nature of the flow associated with this part of the evaluation work obviates the need for any synchronisation of the spectrum analyser, indeed there is nothing to synchronise it to. The F.F.T. analysis is therefore initiated manually.

5.6. Steady Flow in a Test Section -The Results

The first thing one notices when assessing the LDV spectra associated with blood flow is that buried not too deeply in noise there is an underlying form. This becomes more apparent if one uses the multi sweep root mean square (R.M.S.) averaging facility of the HP3582A F.F.T. spectrum analyser. The R.M.S. average mode combines a new spectrum with a partial result on a point by point basis. Following the Nth averaging operation,the amplitude at any discrete frequency point,f, is given by:

$$A_f = \sqrt{\frac{1}{N} \sum_{i=1}^{N} A_i^2}$$

Thus Figure 5.6 shows the R.M.S. spectra associated with N =1,2,4,8,16 and 32 sweeps. The blood is flowing with a constant velocity of 1.5 cm/sec and the sweeps are asynchronous. By the time N=16 the majority of the noise has been smoothed out and one is left with a relatively clean signal spectrum. By eye, the spectrum has taken on something of the appearance of a logarithmic decay. This is in general qualitative agreement with the findings of such authors as Bonner and Nossal (1981).

Figure 5.7 shows LDV spectra from blood flowing at a range of different velocities during one particular experiment.As would be anticipated,the spectra show a tendancy towards higher cut-off frequencies as the flow rate increases.The dotted line accompanying each linear spectral plot is a 2dB/division logarithmic plot, an alternative output from the FFT analyser. This plot has a dynamic range of 16dB but can be offset in nine increments up to a total of 80 dB to position the display about a particular part of the amplitude/frequency curve. A straight line, fitted by eye through a particular logarithmic output, serves to further enhance the earlier impressions regarding the character of the LDV blood flow curves.

Within the limits of the experimental conditions described so far,the slope of the afore mentioned straight line can be seen to move in a manner showing an approximately inversely linear relationship with increasing flow. This is further illustrated in figure 5.8,where the reciprocal of the slope is plotted against flow.

The non zero LDV signal for zero blood flow is attributable to random red cell motion - the discrepancy disappears if the contents of the flow tube are frozen by spraying the outside of the tube with a Dichlorodifuoromethane freezing aerosol. The upper limit of the graph is set by restrictions imposed by the pumping of blood through a relatively narrow bore tube.

One practical way in which more blood can be pumped through the flow tube involves diluting the blood with normal saline and thereby decreasing its viscosity.Experiments along these lines reveal new facets of LDV and its application to blood flow measurements.

If the dilution ratio is 1:1, the basic logarithmic decay curve is maintained but the signal is slightly reduced in intensity.Based on the slope of the log line concept,the velocity of the fluid is seen to increase.This trend,in both signal intensity and line slope,continues with further dilution of the blood and is illustrated in figure 5.9.

5.7 Pulsatile Flow Experiments

That the LDV system is capable of following a pulsatile flow can,in principle,be demonstrated by removing two out of three of the peristaltic pumps' rollers.However,the simple one roller flow inducer thus created has virtually no non-return valve action associated with it;the spontaneous back flow is often as large as the driven forward flow.As an initial way of overcoming this limitation a separate non-return valve was incorporated into the flow line. Unfortunately the

construction of the valve was such that its efficiency became impaired by deposits forming on the working faces. An alternative arrangement was found in the form of an elevated reservoir as the feed for the pulsatile flow inducer. A relatively small head height was found to be sufficient to prevent back flow and gave rise to only a small superimposed steady state flow.The situation is in fact a fair representation of arterial flow, only in a large vessel such as the aorta does the flow drop down to zero. In most other vessels there is a finite resting level, associated with the diastolic pulse pressure.

With the creation of a pulsatile signal came the necessity for synchronising the spectrum analyser to various, but specific, parts of the flow waveform. This was achieved by placing a small reflective strip at one point on the periphery of the rotating roller carrier.A simple opto-reflective sensor mounted on a convenient part of the pump body then produced a reference pulse everytime the reflective strip passed it. The output from the sensor was used to trigger the pulse delay generator,which in turn triggered the spectrum analyser. The delay was set so that the final trigger pulse coincided with the required part of the flow waveform, as monitored by an in-line electromagnetic flow probe and associated electronics.

Figure 5.10 shows the frequency spectra associated with three different portions of the pulsatile flow signal. The results are encouraging but do demonstrate the presentation limitations associated with sequential processing and display.

It is worth noting that the FFT averager is still being operated in the RMS mode because although a synchronising signal is now available there is still little coherence in the individual components of the LDV signal.

5.8 System Resolution

Centre stream readings have been assumed in the blood flow experiments described so far, by dint of the intercept position of the two LDV beams. Investigations show that, with the particular system implementation under discussion, the assumption is difficult to prove or disprove. The spectra show little change as one scans through the Z axis of the flow tube. This low Z axis resolution may be attributed to two main factors:

1.Photon diffusion,multiple scattering and refraction all contribute to make the location of a point volume somewhat conjectural when dealing with blood.

2.Although the system is working primarily in the double beam mode there is,concurrently,a degree of external reference beam operation.This is demonstrated by blanking off one beam and observing an attenuated (approximately 10db down) persisting LDV signal.This external beam mode occurs as a result of scattering and weak reflection of the input beams at the glass tube surfaces. Consequently its position in the Z axis is not amenable to alteration and its contribution remains substantially fixed.

5.9. Steady Flow in a Locally Restricted Test Section.

Prior to the final test in the present series it was necessary to make a test vessel which would simulate the flow characteristics of a small vein with a thrombus in it.By this time it was felt that the changing velocity content of a pulsatile flow signal probably made it unsuitable for jet related velocity increase detection,at least during the evaluation phase of the method and instrumentation.

Initially the glass tubes used hitherto were replaced by thin walled narrow bore plastic cannula tubing and a pinch screw applied to compress part of the wall into the bore. Within limitations this worked but the physical movement which accompanied the pinch screw action made some target re-alignment inevitable. In addition, the tubing often became punctured after only three or four adjustments of the pinch screw.

The 1 mm I.D. glass flow tube was then returned to and an indentation pressed down into the bore.Without diverting time into making a complicated jig it was difficult to control the profile and volume of the ensuing intra-luminal obstruction.This gave rise to problems when it became necessary to replace a tube following a breakage; reproducibility of results was poor.However,as shown in figure 5.11, results could be obtained from any one particular scan along the length of a tube that were indicative of the presence and detection of a jet related velocity increase.It will be noted that:

1) A log plot of the Doppler shift frequency has been used.This was found to be a less conjectural indicator than it's linear counterpart.

2) The heavy attenuation of the spectrum at the centre of the indentation (d= 0),is probably an artifact.In heating up the glass to create the indentation some distortion is inevitable,this gives rise to a relative displacement of the velocimeter beams and erroneous readings.

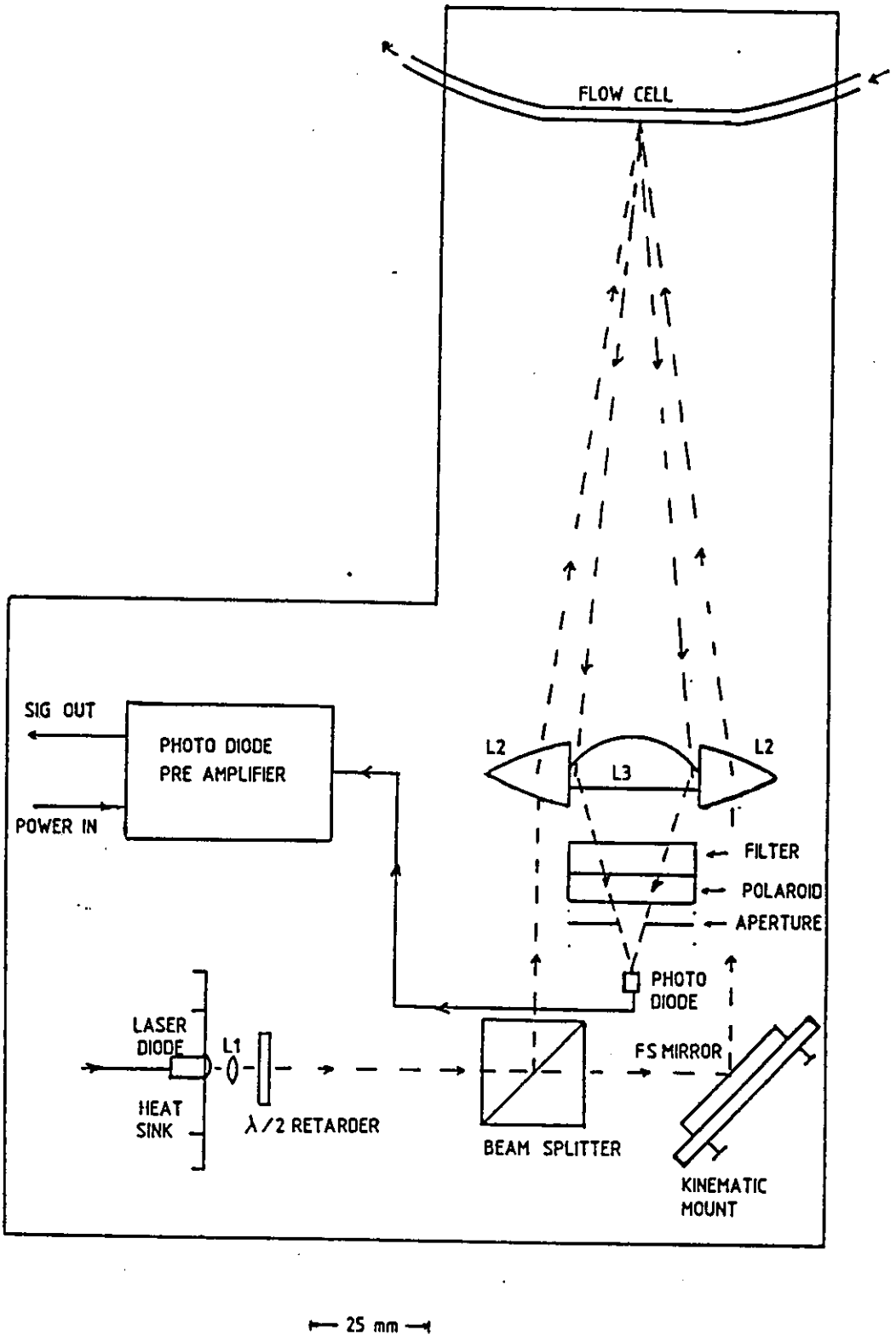

Figure 5.1: Schematic diagram of the dual beam laser Doppler velocimeter.The majority of the proposed experimental rationale was validated by it's use.

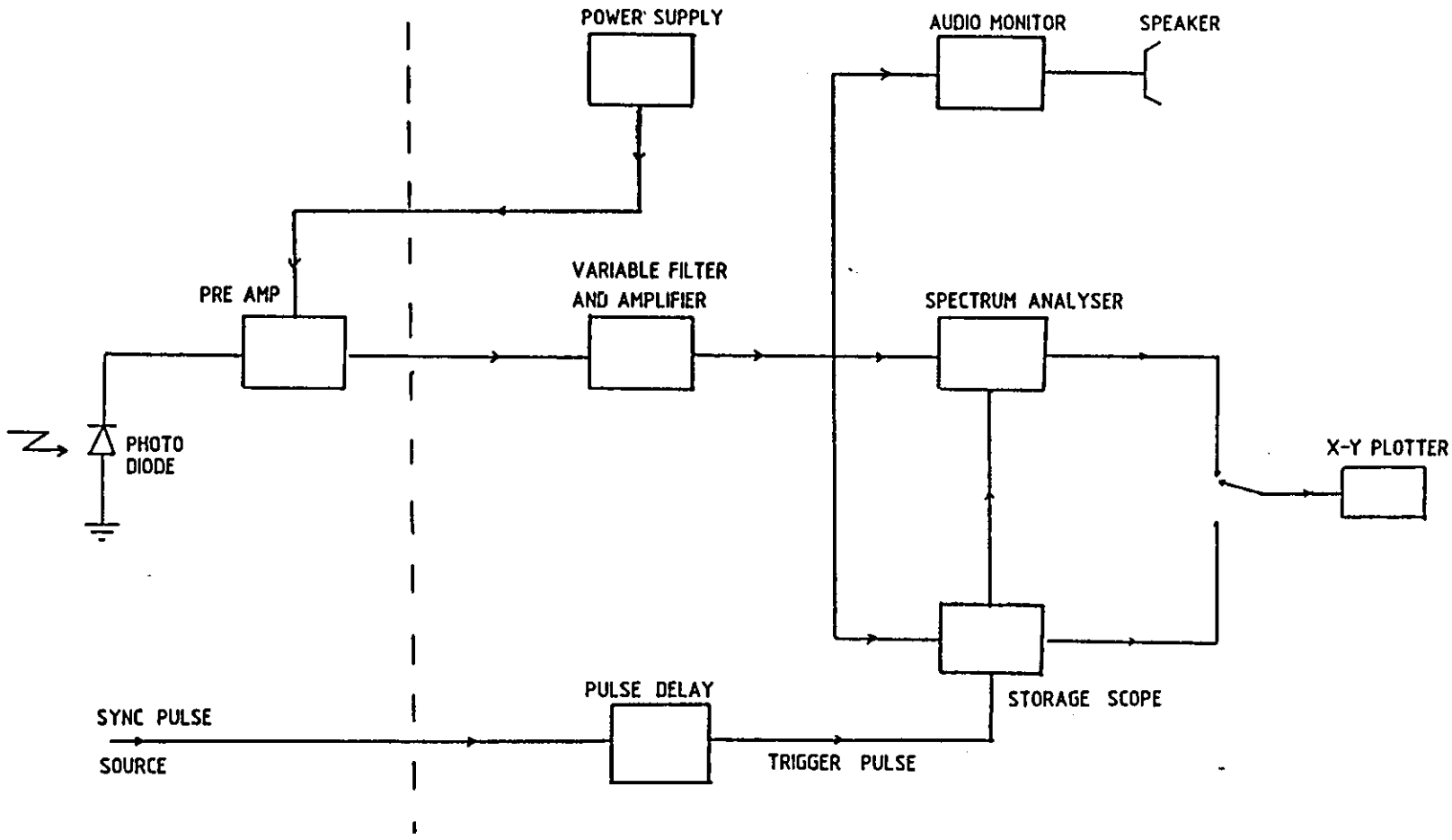

Figure 5.2: Schematic diagram of the signal processing equipment.Components to the left of the dotted line are incorporated within the velocimeter construction.

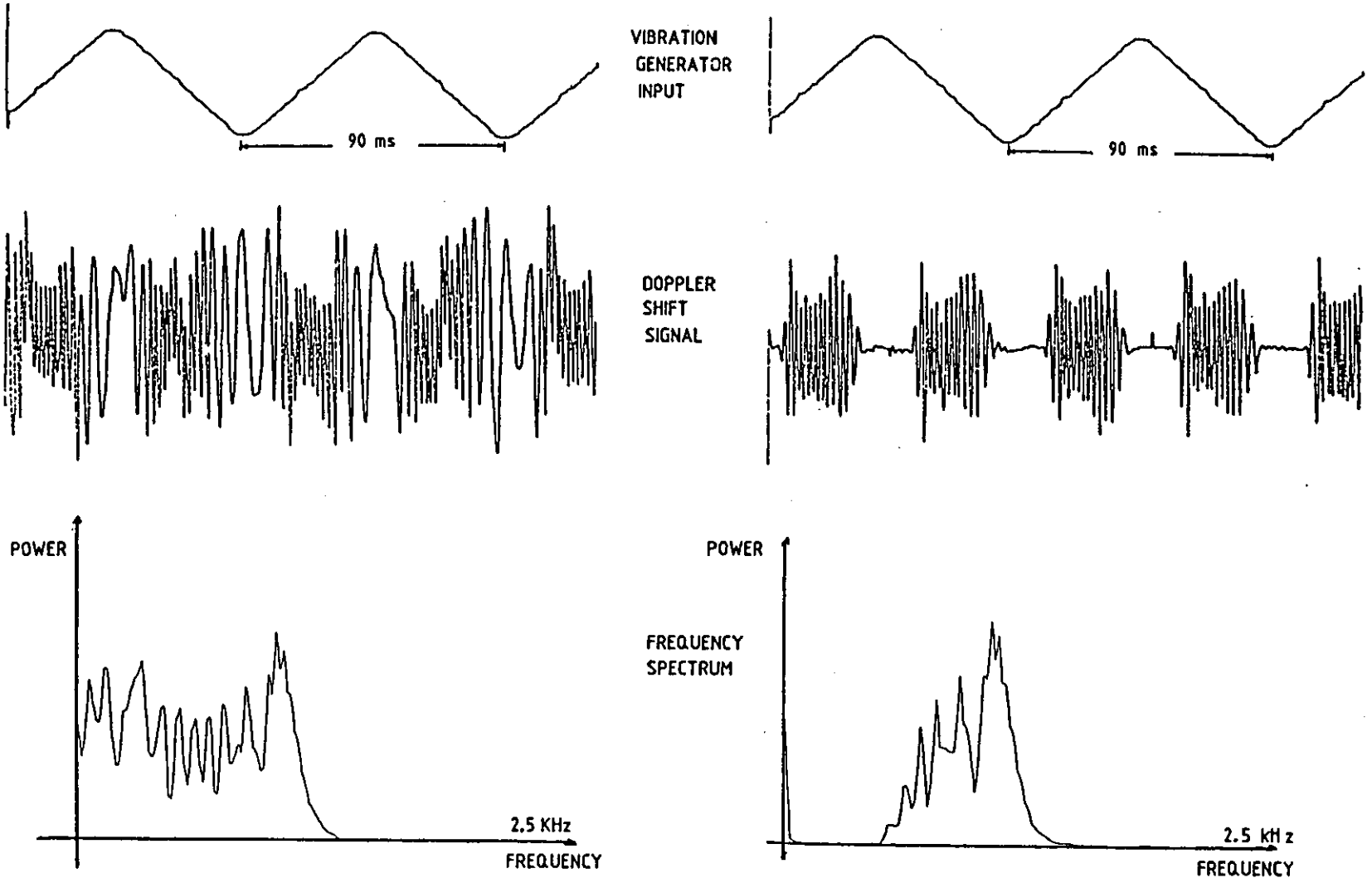

Figure 5.3: Examples of the Doppler shift signal and the frequency spectra associated with the dual beam velocimeter,made with the aid of the vibrating crocus paper test rig.The signal and spectrum to the right show the effect of 500 Hz high pass filtering.

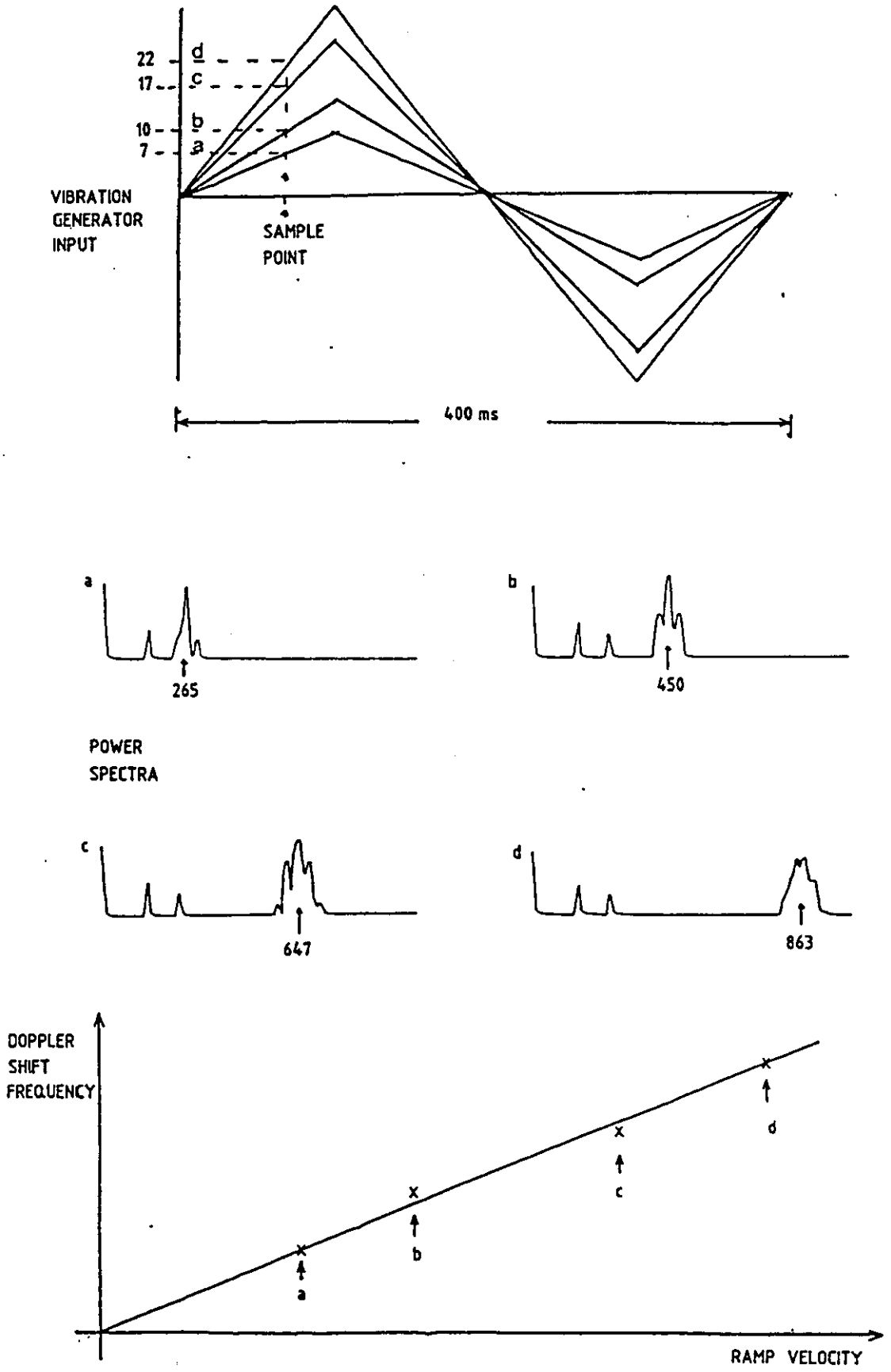

Figure 5.4: Examples of spectra obtained to establish the basic linearity of the double beam velocimeter.

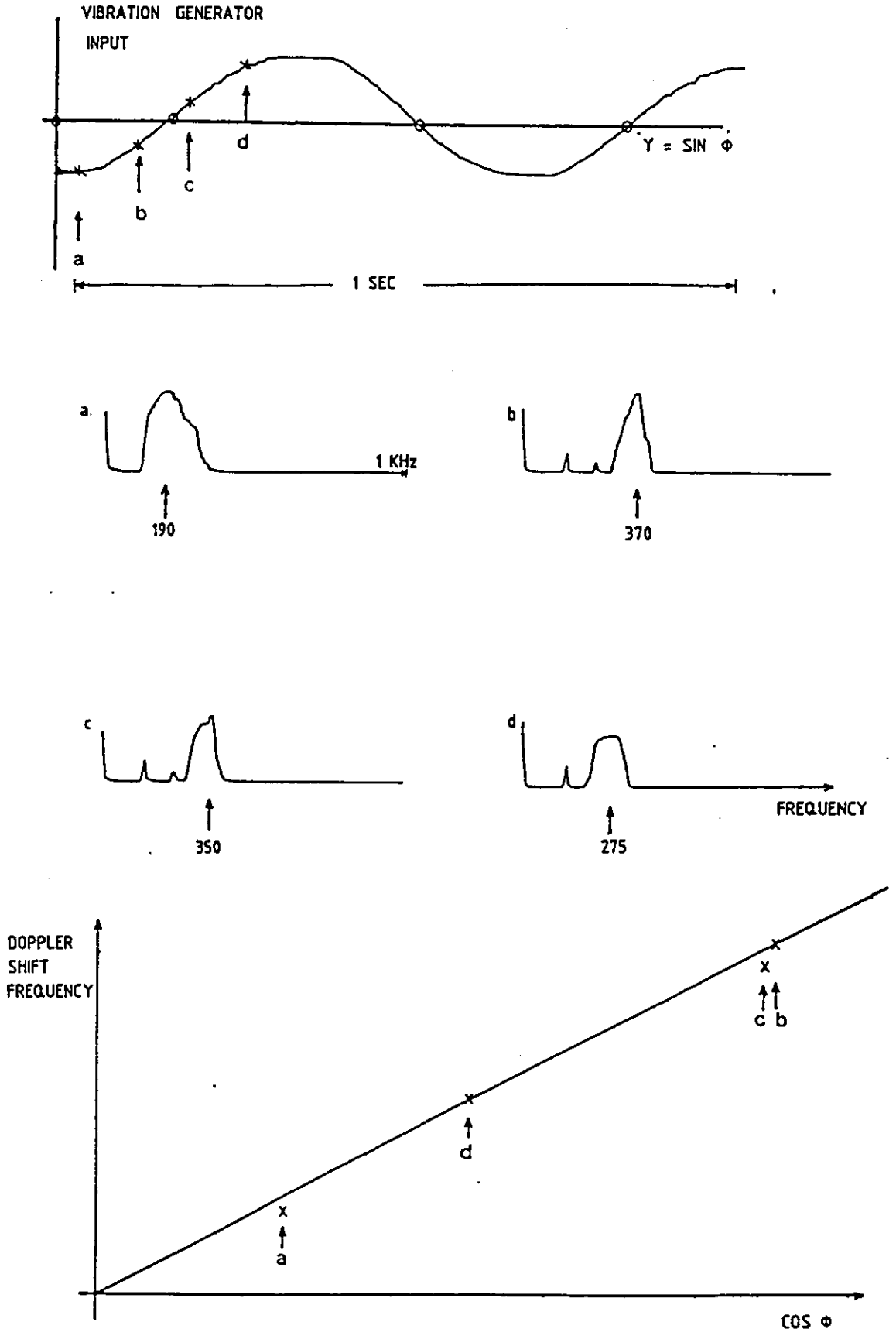

Figure 5.5: Examples of spectra obtained to establish the waveform following properties of the double beam velocimeter.Doppler shift frequency is shown plotted against the first derivative of the driving waveform.Despite signal synchronisation there is evidence of spectrum broadening - caused by the 100 ms. samping time associated with the FFT.

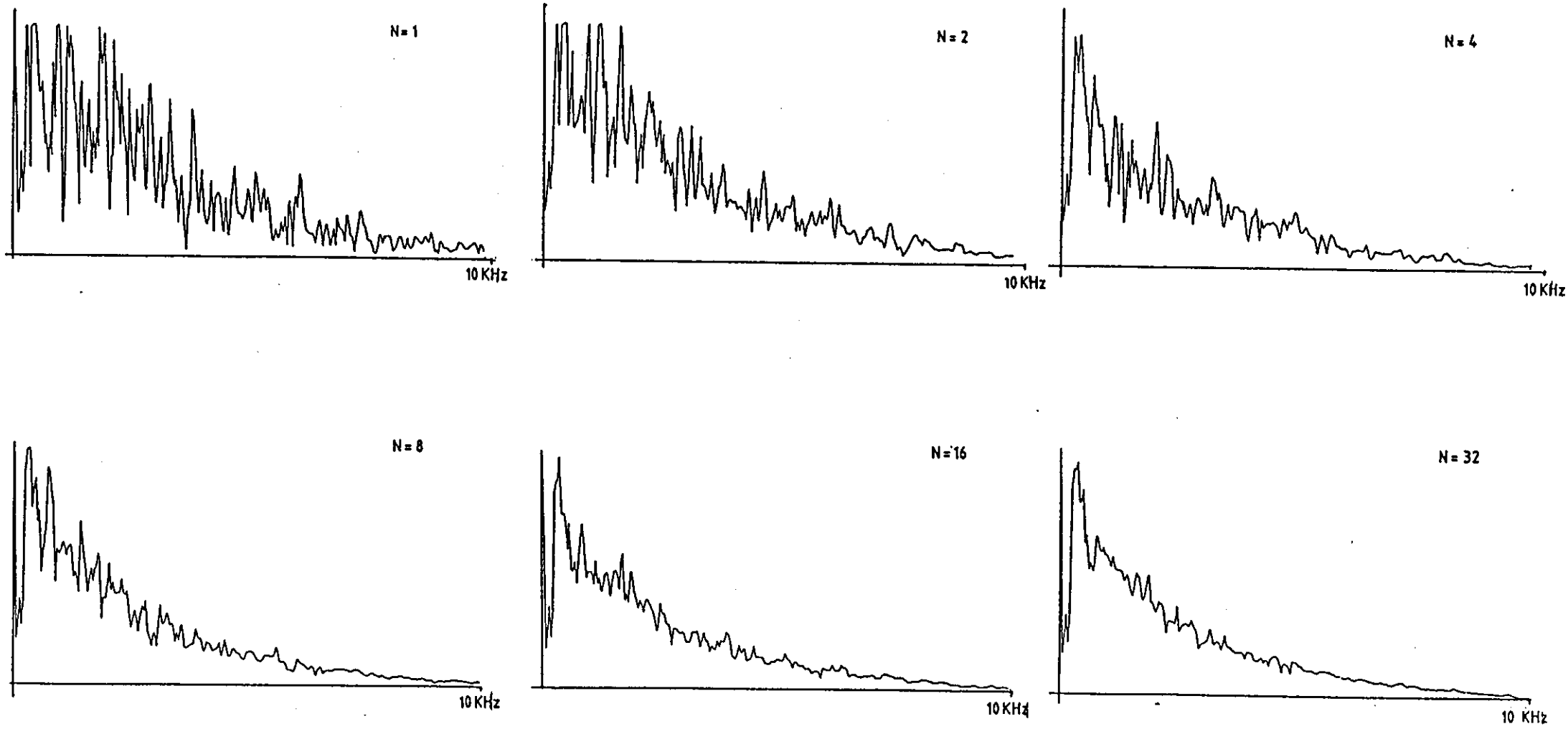

Figure 5.6: Showing the effects of multiple RMS averaging sweeps on the Doppler frequency spectra of flowing blood.

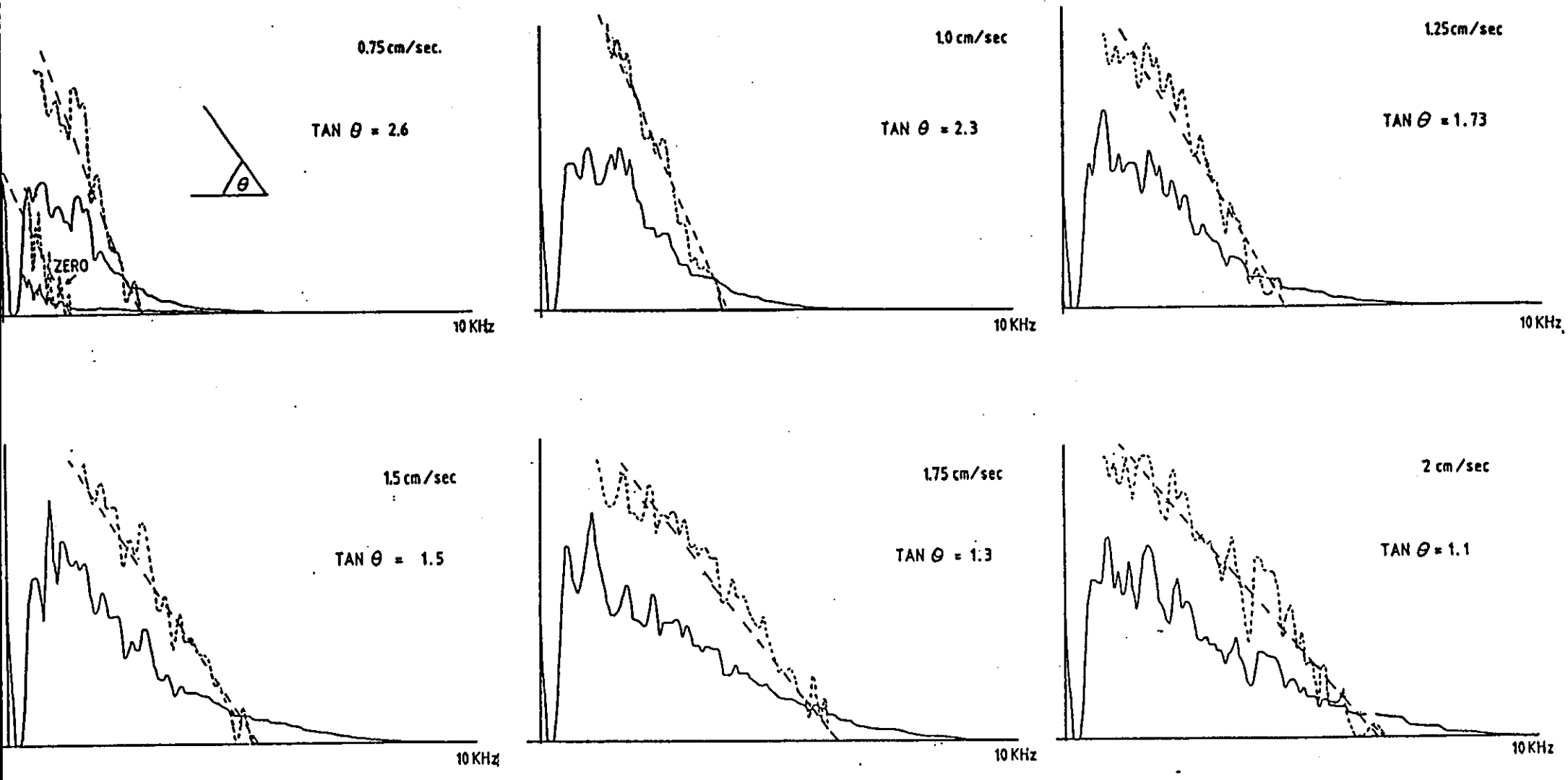

Figure 5.7: The LDV spectra from blood flowing at a range of different velocities. The unbroken line is the linear plot, the dotted line a log plot and the broken line is a straight line fitted by eye through the log plot.

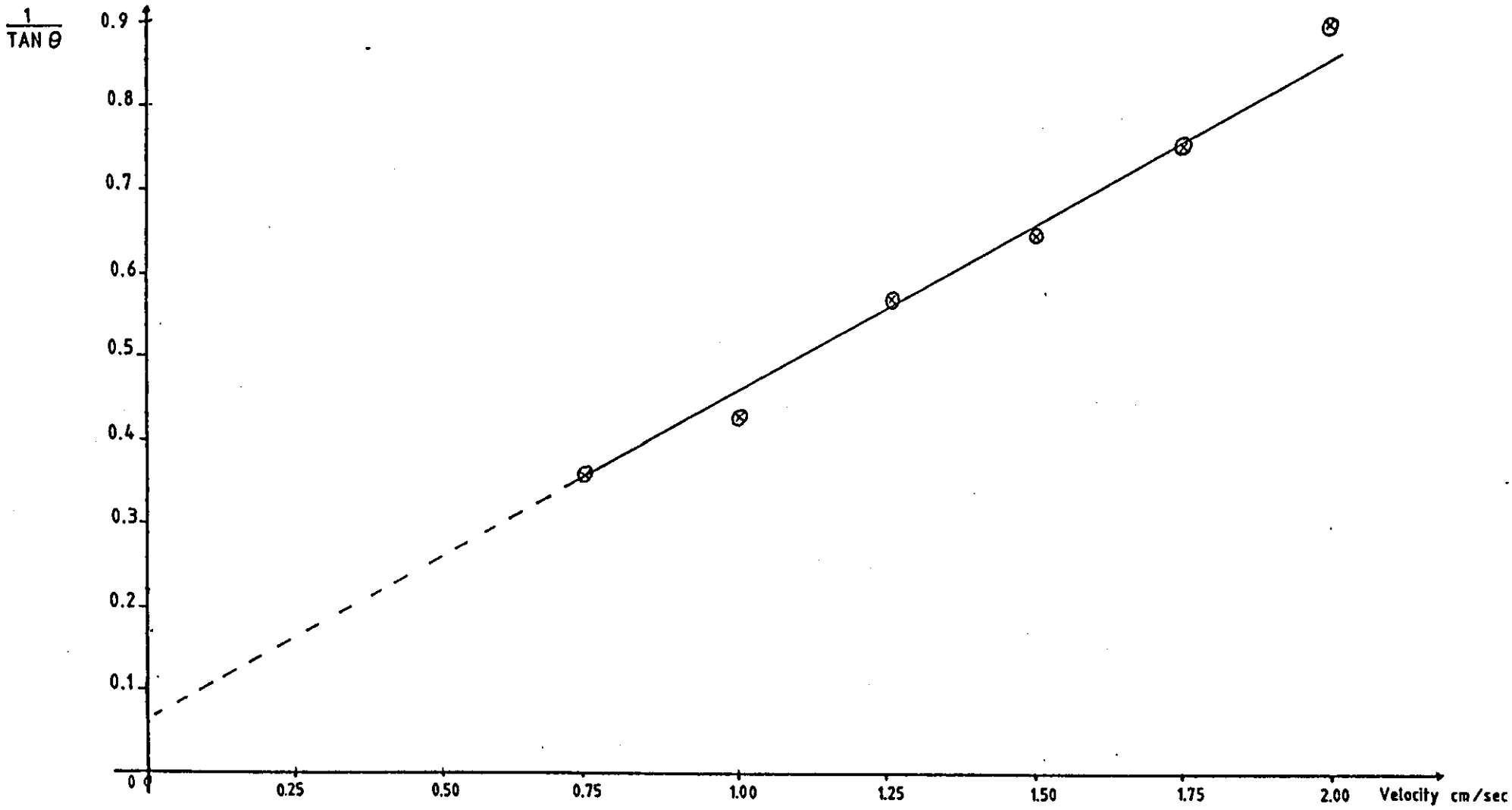

Figure 5.8: Showing how the reciprocals of the slopes of the log plots associated with figure 5.7 correlate with velocity.

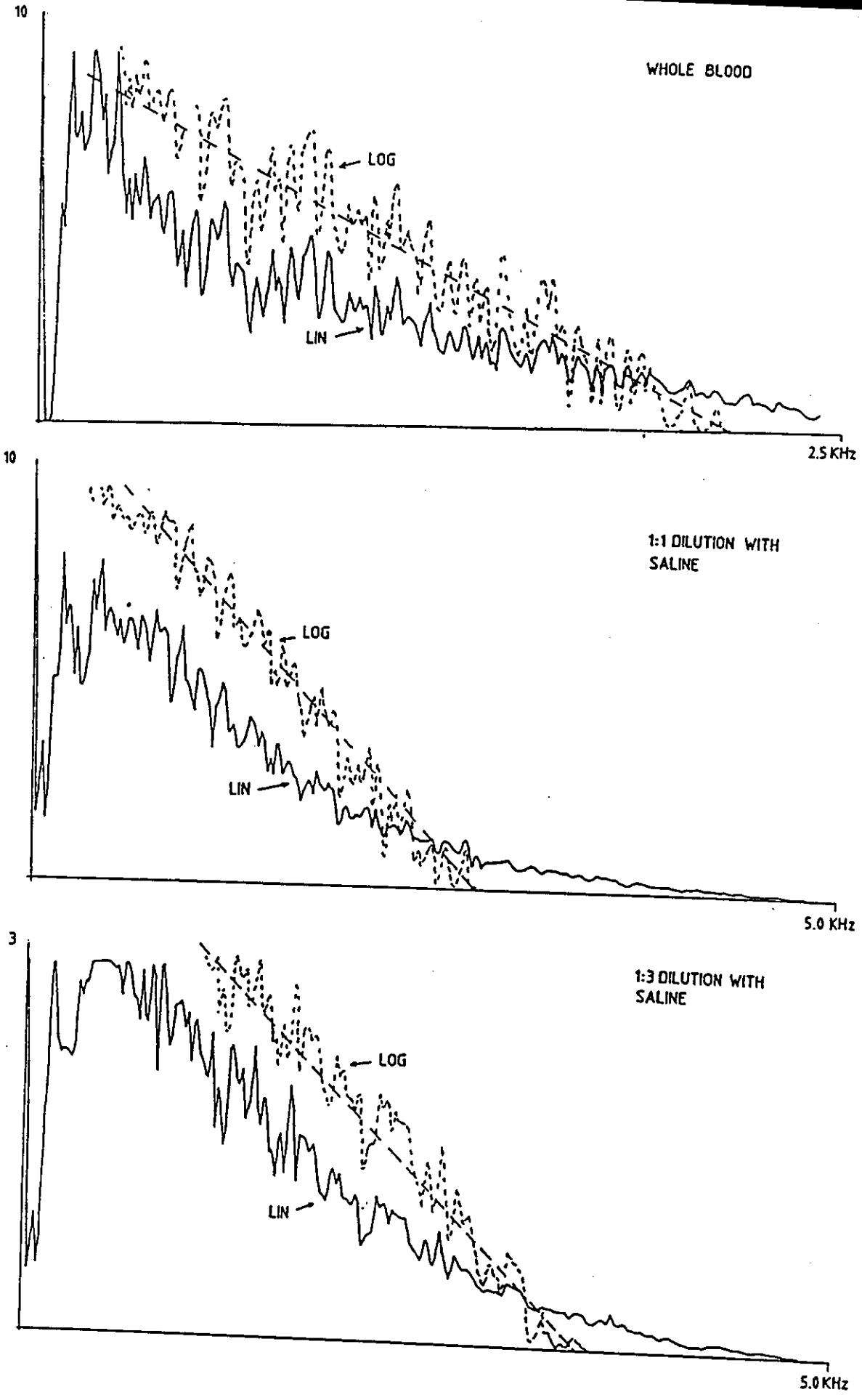

Figure 5.9: Showing the effects of diluting the blood with saline. As might be anticipated, with the decrease in viscosity the mean velocity increases and, with the decrease in red cell population density, the signal amplitude falls. Note the changes in frequency and amplitude scales made necessary by the dilution.

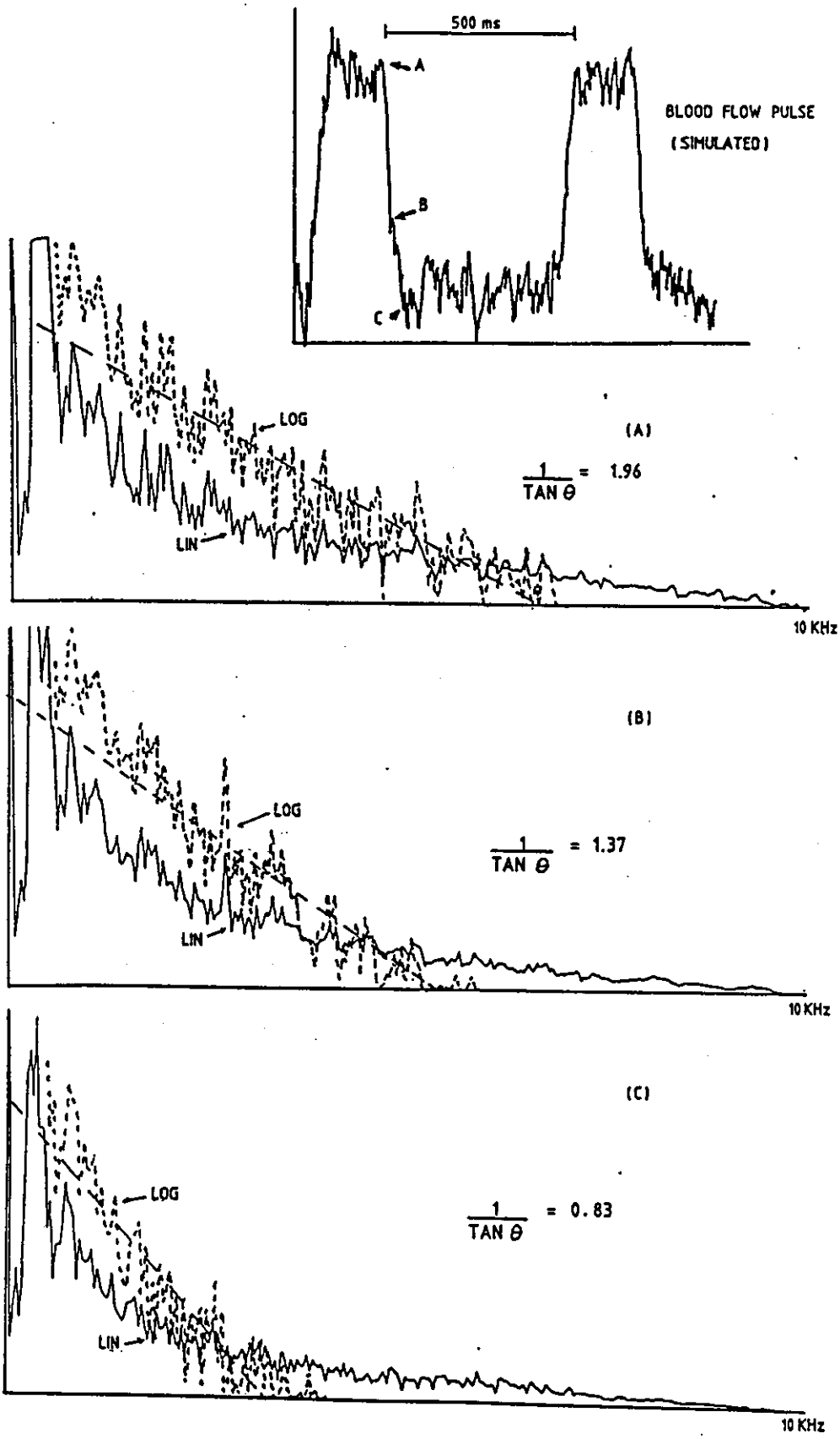

Figure 5.10: Showing how the reciprocal log slope criterion can be used to follow the velocity changes associated with a simulated blood flow pulse.The figure also demonstrates the limitations imposed by following an amplitude vs time signal with a frequency transform analyser.

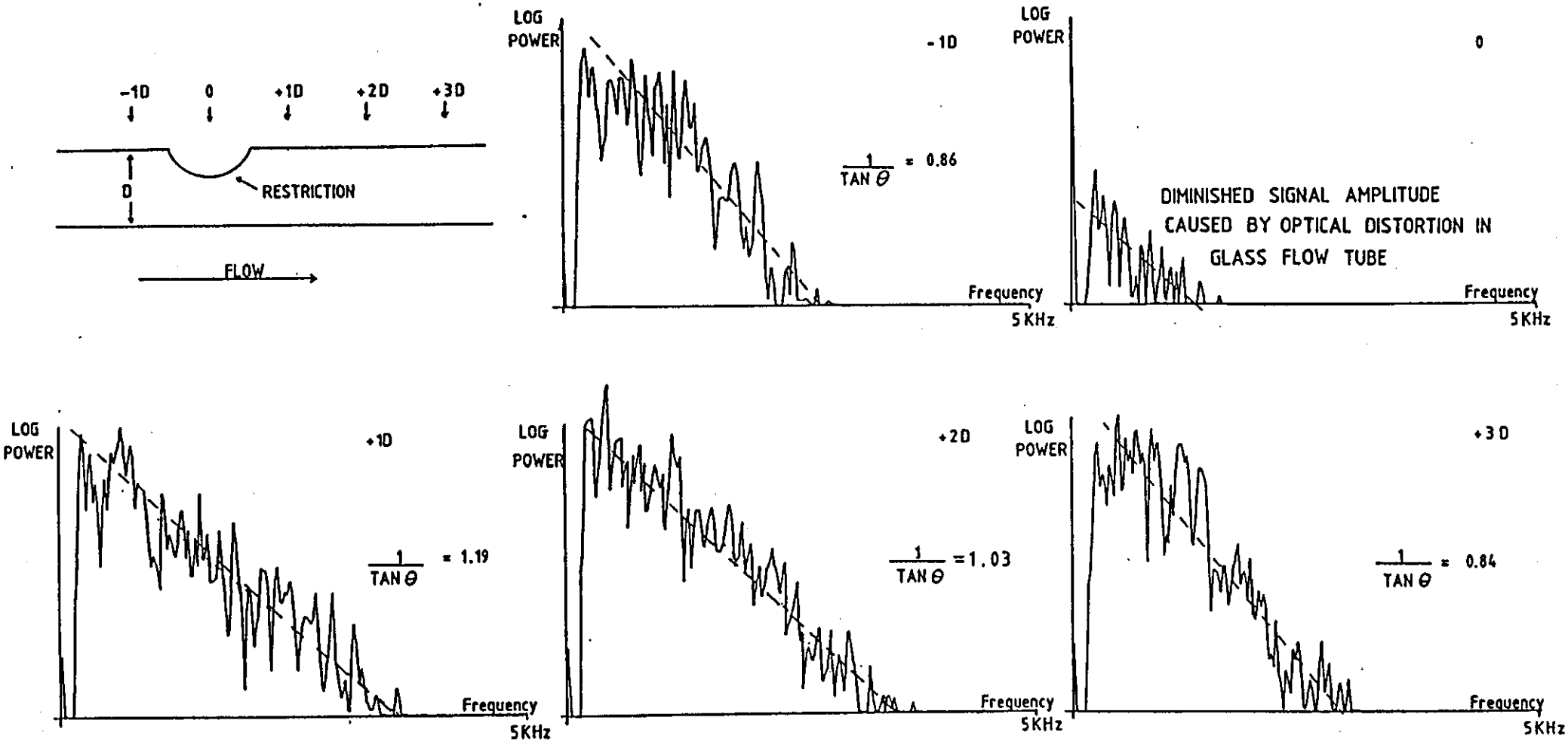

Figure 5.11: By applying the reciprocal log slope criterion,and despite limitations imposed by the first thrombus model (an indentation pressed into the glass flow tube),changes in velocity can be detected as the blood emerges through the restriction.Optical imperfections introduced into the glass are responsible for the anomolous results associated with the zero position.

CHAPTER 6

THEORETICAL JUSTIFICATIONS -AN ASSESSMENT

6.1 Introduction

Although the results obtained from the prototype system were encouraging,they lacked the merit of being anything other than empirical.Thus an idea had evolved,had been tried via a simple system and,within limitations,had worked.Accordingly it was next thought appropriate to consider the role of any possible theoretical justification for the results,with a view to then refining the method and effecting system design improvements.

Consequently,within the present chapter,it is the intention to examine more formally the anticipated contributions of factors which have hitherto been only briefly acknowledged.This new work concerns the role of multiple scattering,the possible quantification of some of the fluid jet parameters and the growth characteristics of developing thrombi.

6.2 Multiple Scattering and Laser Doppler Velocimetry

The propagation of light through a medium with the scattering and absorbtion characteristics of blood is highly complicated. An extrapolation of the theory developed for single particle models by Mie (1908) is not valid. The problem is that with a thick layer, or with an

increasing density of the scattering particles, light that is scattered once is very likely to be scattered repeatedly.All these multiple scatterings interfere with each other and it becomes extremely difficult to account for the contribution of each scattering particle.

According to Van de Hulst (1957), multiple scattering will be taking place in any turbid medium with an optical density that exceeds 0.1. Applying this criteria, bulk whole blood must be reckoned on as being a multiple scattering medium because the packed cell volume is virtually half of the total blood volume. Under these circumstances simple scattering may only be assumed for samples of less than about 50 um thickness.

Many of the Laser Doppler velocimeter systems associated with blood flow studies have been developed in a relatively empirical manner. A rigorous treatment, one which involves the statistics of multiple scattering, is of daunting complexity. In addition, experimental conditions are often such that they cannot conform to those presumed in the theory. This leads to approximations which re-introduce elements of empiricism.

Thus the apparently quite satisfactory treatment by Riva and Feke (1981) of the signal associated with retinal blood flow is based on a single scatter model. Their analysis is based on an extrapolation of the results obtained from tests performed using polystyrene spheres in distilled water as a flowing blood substitute.With such a fluid,flowing through a glass tube,the number of particles scattering light with a

frequency shift between f and f + df is equal to the number of particles with velocity V and V + dV. Therefore:

$$N(f)df = N(V)dV$$

Furthermore, since V is a function of the distance r from the tube centre to the particle, we can also write:

$$N(V)dV = N(r)dr$$

where N(r)dr is the number of particles between r and r + dr. Thus:

$$N(f) = N(r) \frac{dr}{dV} \frac{dV}{df}$$

For a circular tube of radius r and particles of uniform density ρ,

$$N(r) = 2\pi r\rho \qquad \text{for} \quad r < r_o$$
$$= 0 \qquad \text{for} \quad r > r_o$$

For a parabolic profile:

$$V(r) = V_o(1 - (r / r_o)^2)$$

Where V_o is the velocity at the centre of the tube. Therefore:

$$\frac{dr}{dV} = r_o^2 / 2V_o r$$

and, from the basic Doppler shift equation, we have:

$$\frac{dV}{df} = \frac{\lambda}{\sin\theta}$$

Therefore, the velocity distribution has the form:

$$N(f) = \frac{2\pi r \rho r_0^2 \lambda}{2 V_0 r \sin\theta} \qquad \text{for } f < f_{MAX}$$

$$\doteq \frac{\pi \rho r_0^2 \lambda}{V_0 \sin\theta}$$

$$= 0 \qquad \text{for } f > f_{MAX}$$

Therefore, if the light illuminates all the elements of the flowing liquid equally and if the velocity profile is parabolic, the power spectrum density of the scattered light will be flat between zero frequency shift and the maximum, $f_{MAX} = V_0 \sin\theta/\lambda$. This results from the fact that, for a parabolic velocity profile, there are equal numbers of particles flowing at each velocity up to the maximum velocity, V_0.

If instead of polystyrene spheres in water whole blood is used, the spectrum shape changes and the relatively well defined cut-off point is lost. One may regard the change as a progressive broadening of the tail of the spectral distribution and this is a manifestation of multiple scattering. Other than noting it's occurence, the authors make no attempt to build it into their model; they carry on to design a special purpose analyser which uses equations associated with their simplistic description as the basis for analogue computation.

Bonner et al (1981) have developed a general model of laser Doppler scattering within tissues perfused by small vessels.Here the situation is conducive to some simplification because the number of red cells in moderately perfused tissue is only in the order of 1 - 4% by volume of tissue. (In whole blood they account for 40% of the volume).Scattering of photons by tissue elements surrounding the blood vessels must however be taken into account.The theoretical treatment is therefore based on the following physical assumptions:

1. Visible photons diffuse through the tissue and are scattered many times by static centres of refraction such as somatic cells,connective tissue and blood vessel walls.This scatter imposes no Doppler shift.
2. The detected photons which diffuse back to the surface of the tissue have been scattered by moving red blood cells and have a distribution of angles determined by the highly anisotropic angular scattering cross section of those cells.
3. A photon diffusing between two points on the surface of a well perfused tissue will be scattered by one or more red blood cells.This scattering mechanism will give rise to a Doppler shift.
4. The mean number of red blood cells by which a single photon might be scattered increases linearly with local blood volume within the tissue. Multiple scattering from moving red blood cells increases the Doppler shift.

The model leads to predictions about the way in which photon

autocorrelations and photo current power spectra depend on moving particle variables such as angular scattering cross section, size, numerical density and speed distribution.The photon autocorrelation function is a method whereby the consequences of multiple scattering can be examined in the time domain,it describes the probability of a number of photon arrival events occuring at the detector within a time δt at a time t.The events occur at random but at any given time the probability of occurence is proportional to the light intensity.In general,the autocorrelation function (time domain) is related to the power spectrum (frequency domain) by the Wiener-Khinchine theorem.

In an extended treatment of the above work,Bonner and Nossal (1981) first define an intermediate scattering function:

$$I(\tau) = \sum_{m=1}^{\infty} P_m I_m(\tau) \Big/ (1 - P_0) \quad \text{------ 6.1}$$

where I_1 is the autocorrelation function for photons which experience one collision with a moving cell, I_2 is the autocorrelation function for photons which experience two collisions etc.and P_m is the probability that a photon will experience m collisions with moving red cells before leaving the tissue.

Sorenson et al (1976) have shown that $I_2(t)$,which is the autocorrelation of field components $I_2(\tau) = [E_2(t) E_2(t+\tau)]$,where E_2 (t) represents an electric field of unit amplitude which has been scattered two times,can be written as the product $I_2(\tau) = I_1^2(\tau)$ if there is no correlation between the positions of any two particles.This leads to the possibility of presenting equation 6.1 as:

$$I(\tau) = \sum_{m=1}^{\infty} P_m \left[I_1(\tau)^m \Big/ (1 - P_0) \right] \text{ ..... } 6.2$$

It is next noted that P_m can be written as:

$$\Sigma_r \, P(m|r) \cdot P(r)$$

where $P(m|r)$ is the probability that a photon makes m collisions with moving erythrocytes before emerging from the tissue, given that it makes r collisions in total - that is, (r-m) collisions with static elements. However, $P(m|r)$ is given by the binomial distribution - the probability of realizing m successes out of r tries. (In this context, collisions with moving cells out of total collisions).

The probability of success is proportional to the scattering cross section of the blood cell relative to the total scattering cross section of the tissue, $p = \sigma_{BLOOD} / (\sigma_{BLOOD} + \sigma_{TISSUE})$. If the blood volume is a small fraction of total tissue volume, p will simply be proportional to blood volume.

In the limit that r is large and p is much less than 1, the binomial distribution can be represented by the Poisson distribution $P(m|r) \rightarrow \exp(-\bar{m})(\bar{m}^j)/(j!)$, independant of r. Accordingly, if an incident photon experiences many collisions with static elements before leaving the tissue, equation 6.2 can be rewritten as:

$$I(\tau) = \sum_{m=1}^{\infty} \frac{\exp(-\bar{m})(\bar{m} I_1(\tau)^m}{m!} \Big/ 1 - \exp(-\bar{m})$$

$$= \left[\exp(\bar{m}(I_1(\tau) - 1)) - \exp(-\bar{m}) \right] / \left[1 - \exp(-\bar{m}) \right] \text{ ..... } 6.3$$

where $\bar{m}$ is the average number of collisions with a moving red cell; it is proportional to red blood cell number density.

A normalized autocorrelation function $g^{(2)}(\tau)$ can now be obtained and it will take the form:

$$g^{(2)}(\tau) = 1 + \beta(\exp(2\bar{m}(I_1(\tau)-1)(-\exp(-2\bar{m})) \quad \text{---------6.4}$$

β is a factor which depends primarily upon the optical coherence of the signal at the detector surface, it has a numerical value that lies between zero and unity. It is about 0.5 for a conventional LDV system and 0.2 for a fibre optic system.

As previously stated, the autocorrelation function is related to the power spectrum of the signal by the Wiener-Khinchine theorem. The use of this relationship yields:

$$P(\omega) = i_0^2\,\delta(\omega) + e\,i_0/\pi + i_0^2 S(\omega) + D(\omega) \quad \text{---------6.5}$$

where

$$S(\omega) = \frac{1}{\pi}\int_0^\infty \cos\omega t\left[g^{(2)}(\tau)-1\right]dt \quad \text{---------6.6}$$

and i_0 is the mean detected intensity, $\delta\omega$ is the detector shot noise and $D(\omega)$ is the amplifier noise.

Analysis of equations 6.4 and 6.6 reveals that the spectra associated with the first few individual scattering orders present in a complete flow spectrum have the form:

$$P_1(\omega) = \exp(-W) \quad \text{6.7}$$

$$P_2(\omega) = \frac{1}{4}(1+W)\exp(-W) \quad \text{6.8}$$

$$P_3(\omega) = \frac{1}{16}(W^2+3W+3)\exp(-W) \quad \text{6.9}$$

where W is inversely proportional to the blood cell's root mean square velocity ($W = \sqrt{1\cdot2}\,\omega_a / < \sqrt{\geq^2} >$).

The power spectrum curve changes from being essentially exponential to Gaussian shaped as m increases. This is in broad agreement with Bonner et al (1978), where it was found that for low orders of multiple scattering the power spectrum may be represented by:

$$P(\omega) = k i_0^2 (1+W) e^{-W} + i^2 \delta(\omega) + D(\omega) \quad \text{6.10}$$

The constant k decreases with decreasing spatial coherence of the detected signal.

With reference to the present thesis, it will be recalled that the power spectra obtained from those blood flow experiments associated with the previous chapter approximated to an inverse logarithmic function - the spectra were transposed to approximations to straight lines with velocity related slopes when using the logarithmic display capability of the FFT analyser. So, in the light of Bonner and Nossal's analysis, the interpretation to be made is that first order scattering is the

predominant signal and deviations from the straight line are accounted for by successively less intense multiple scattering contributions.

Of further interest in the context under discussion is the conclusion by Bonner and Nossal that once a certain degree of multiple scattering has been reached,the autocorrelation (thus the power spectrum) takes on a uniformity of shape.This indicates that laser Doppler velocimetry cannot then provide information concerning details of the velocity distribution but is sensitive only to the mean speed.There is good agreement between prediction from the theory and intensity autocorrelation functions obtained from tissue analogues.In the context of the proposed thrombus growth measurements,the conclusions drawn by Bonner and Nossal tend to support the decision to make measurements based on jet velocity since this parameter may be adequately described in terms of mean values.

Stern (1985) has approached the problem of multiple scattering as it applies specifically to fibre optic type LDV systems.Investigators such as Kilpatrick (1982) and Nishihara (1982),who have developed systems which measure heterodyne backscatter spectra from single optical fibres inserted into the blood stream,interpret their spectra in terms of a region of flow disturbance around the tip of the immersed fibre.The maximum frequency is presumed to arise from the light scattering at a greater distance in the undisturbed flow.

Stern suggests that the above interpretation, which pictures the backscattered light as a superimposition of near and far components,

must be an oversimplification and that very high orders of multiple scattering must be dominant and therefore accounted for. Stern also states that the theoretical models of Bonner and Nossal (1981) are not applicable to the intravascular case because the velocities and angles of scattering are highly correlated in bulk flow of whole blood. Inherent within the Bonner and Nossal treatment for microvessels was the premise that succeeding temporal phase shifts of the scatter vector would be totally independant of earlier ones.

Starting with Maxwell's equations for electromagnetic radiation combined with a Feynman diagram based technique, Stern develops a generalised transport equation for the Doppler shifted light. Making suitable approximations regarding the relation between the length scales of fluid structures and the photon mean free path,the generalised equation is converted into a local transport equation. This equation is seen to embrace the photon gas diffusion model used by some other authors. The frequency moments of the equation give the equation of radiative transport and the equations for the transport of Doppler fluxes which carry the mean Doppler shift and Doppler bandwidth. A Monte Carlo statistical sampling method is then employed for the numerical solution of the equations. The Monte Carlo transport algorithm calculates the detailed Doppler spectrum by accumulating the intensity for each range of frequencies separately.

Of great significance is the result that the shape of the spectrum is highly sensitive to the shape and depth of the hydrodynamic boundary layer around the fibre tip. Thus the difference between a rectangular

spectrum of the type found by Nishihara et al (1982) and a monotonically declining spectrum as found by Kilpatrick et al (1982) can be accounted for by a rather modest increase in the thickness of the boundary layer in the latter case.

The interpretation from the theory is that the backscattered light may be thought of as composed of light which has suffered a single large angle scattering, between being transported to and from the fibre, and many small angle scatterings which do not greatly diminish its directionality. Stern calls this phenomenon 'pseudo first order scattering' and it is seen as accounting for the success of naive models in explaining the spectra from single fibres.The Gaussian spectrum plus white noise model that emerges from Stern's treatment of the problem is in qualitative agreement with the findings of Bonner and co workers.

6.3 Fluid Jet Models

As indicated in Chapter 3,Forrester and Young (1970) have developed a mathematical model for flow through a mild stenosis and obtained approximate solutions to the equations that develop: velocity profiles have then been determined.The model is concerned only with the results associated with the steady flow of a Newtonian fluid acting on an axisymmetric stenosis but,within that limitation,gives results that are qualitatively correct.The derivations of the Forrester and Young equations for two dimensions are given in appendix B of this thesis.

Forrester and Young's work has been extended to cover a variety of

flow, vessel and fluid conditions but in most cases an axisymmetric stenosis has continued to be assumed.Young and Shih (1969) have investigated flow separation characteristics in non symmetric models but their work sheds little light on the problem of anticipated jet velocity values.

The assumption of axisymmetricity is a reasonable one in the context of atherosclerotic plaque formation but not so for thrombus formation.Indeed,a developing mural thrombus probably cannot be expected to rigorously conform to a specific shape and so hard fought for quantitative data from a geometric model is of only minimal practical value.In total therefore,fluid jet models contribute little information of any value to the proposed thrombus measurement rationale.

6.4.Thrombus Growth Characteristics

Begent and Born (1970) used dimensions obtained from a series of cine micrographs to plot the growth rate of thrombi in hamster cheek pouch venules; these vessels have diameters that range between 40-60 um. The thrombi were created by iontophoretic injection of ADP. The authors report that as long as the thrombus remains small relative to the diameter of the venule, the shape approximates to a segment of a sphere. Using this assumption the surface area of a thrombus was found to increase linearly with time, the volume increased logarithmically. Therefore a semi logarithmic plot of volume against time provided a rate constant of growth. This is shown in Fig.6.1.

In addition to morphological growth characteristics Begent and Born investigated the effects of blood flow on growth rate. Measurements were made of both mean blood flow velocity (calculated from the rate at which a detached platelet mass was swept along) and the growth rate constant.

The growth rate was found to increase with increasing mean blood flow velocity up to a sharp maximum at velocities of 300-400 micrometres per second. With higher velocities the growth rate decreased and remained approximately constant, at about half the maximum. As the mean flow velocities increased from about 600 to 2500 micrometres per second there was no platelet growth formation. These results are shown in Fig.6.2.

The authors suggests that the rate of platelet mass formation was determined by at least two opposing factors - the rate at which platelets were brought to the site and the rate of shear which would tend to prevent platelets from adhering: both factors depend on blood flow velocity. Thus with mean blood flow velocities of less than about 400 micrometres per second the increasing growth rate was a result of the increasing rate of supply of platelets and at higher velocities shear increased to such an extent that more platelets were prevented from adhering.

Arfors et al (1975) used measurements from thrombi caused by laser induced injury to rabbit arterioles to extend the work of Begent and Born. The arterioles ranged in diameter from 15-30 um and, here too,

thrombus dimensions were obtained from a series of cine micrographs. In most cases the platelet mass was found to resemble an ellipse with a circular cross section. The authors calculations contained a correction factor to minimise errors arising from volume encroachment with the vessel wall as the thrombus height increases. Broadly, all the results supported those of Begent and Born.

Subsequent and highly detailed studies by Baumgartner and co workers (Baumgartner, Turitto and Weiss 1980; Turitto and Baumgartner, 1979; Baumgartner and Muggli 1976) have revealed that platelet growth morphology results from the highly complex interaction of several factors. Thus shear rate is as important as flow rate, citrated blood gives radically different results from native blood and, additionally, time factors must be taken into consideration. By 40 minutes after exposure of a thrombus promoting subendothial surface, virtually all the thrombi have disappeared and only a thin monolayer of platelets is left: growth peaks at about 10 minutes after exposure.

6.5 Discussion

Whereas the shape of the power spectrum has been partially explained, the fluid jet parameters remain largely unquantified.The latter state of affairs stems from computational problems likely to be encountered when modelling the flow patterns associated with a thrombus, and a measure of uncertainty regarding the anticipated shape of that thrombus.Put another way,the work reviewed in the previous section gives insufficient spatial detail for meaningful thrombus related jet velocity

modelling and,even had that detail been available,it is doubtful that the necessary computational techniques could be called upon.

Unfortunately,therefore,the principles associated with the proposed measurement rationale remain largely conceptual and qualitative.Only a little corroborative information has been gained in the process of assessment, but,by the same token,the principles have not been demolished.Therefore,because the results from the prototype may still be interpreted as favourable and because of the advantages perceived to be attainable through success,further development may still be argued for.

Identifiable improvements, and thus the directions for development, now centre around the design of the laser Doppler velocimeter and the nature of the flow analyser.Desirable improvements to the velocimeter are that it should be built into a microscope style of presentation and that it should utilize the external reference beam implementation for maximum potential fidelity.

As previously indicated, the FFT analyser is limited to a sequential frame style of processing and display: this is inconvenient when following growth phenomena which exhibit a continuum of development.In addition there is the question of obtaining unequivocal velocity information from the power spectrum.A new velocimeter design and a special purpose frequency analyser are the subjects of the next chapter.

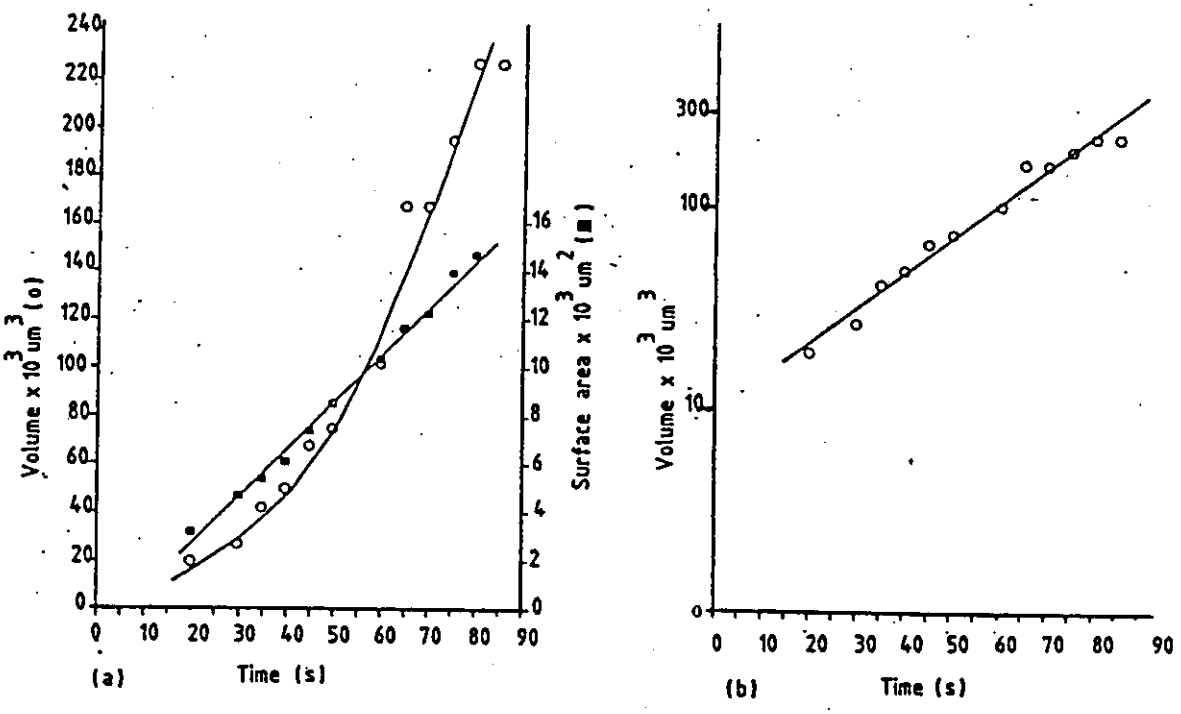

Figure 6.1: Increase in surface area (■) and volume (O) of a thrombus development with time.On the right,the increase in volume is plotted semi-logarithmically against time,showing the line of best fit.

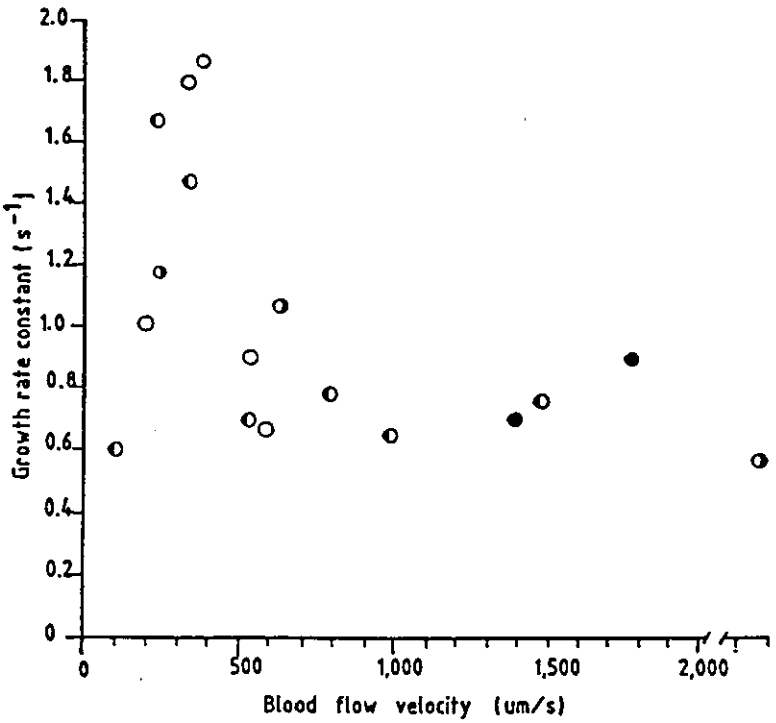

Figure 6.2: Effects of mean blood flow velocity in venules on the growth rate constant of thrombi.Diameters of the venules are: (O) 40-49 um; (◐) 50-59 um; (◑) 60-69 um; (●) >70 um.

CHAPTER 7

AN IMPROVED VELOCIMETER AND A SPECIAL PURPOSE ANALYSER

7.1 Introduction

This chapter describes the implementation of the improvements identified in the previous discussion. An external reference beam laser Doppler microscope and a special purpose analyser for extracting on-line velocity information from the ensuing output signal were therefore the declared objectives of this part of the study.

The design of the LDV microscope occured as a result of an increase in knowledge and practical experience. A measure of success had been achieved very rapidly with the double beam prototype device but,with use,some limitations became apparent.Of those limitations perhaps the most unsettling concerned the question of double beam LDV performance in an optically dense medium. Never-the-less, that experience gained with the arguably rather basic prototype did make a significant contribution to the design of the instrument about to be described.

The design for a special purpose analyser stemmed from the observation that,to a first order of approximation,the slope of the semi logarithmic plot of the Doppler shift power spectrum appeared to correspond to mean velocity.The observation could also be supported by

theory,if one postulated the predominance of the first order scattering contribution in the model developed by Bonner and Nossal (1981).

7.2 A Laser Doppler Microscope

This velocimeter,the second to be built as part of the rationale currently being described, is designed around the external reference beam configuration.This is the archetypal configuration employed in the pioneer work of Yeh and Cummins (1964) and subsequently used by many other investigators.The laser beam is split into a relatively intense incident beam and a relatively weak reference beam.The reference beam is directed onto a surface where it can beat with light from the incident beam that has been back scattered by moving particles and undergone a Doppler frequency shift.According to many authors, Cochrane and Earnshaw for example,the external reference beam configuration is the method of choice when dealing with a dense scattering medium such as blood.

In the particular implementation now under discussion a laser diode is used as the source of coherent radiation.The collimating optics are matched to the diode in a commercially available 'pen' assembly,the Mullard CQL13A. This device is shown schematically in figure 7.1a.The laser diode radiates at 820 nm and has a polarized beam output power of approximately 3 mW: the matched collimating optics give rise to a quoted beam coupling efficiency of around 50% and a usable width of 5.4 mm.

The general velocimeter configuration is shown schematically in figure 7.1b. The laser pen output beam first of all encounters the reflective face of a half silvered mirror,M1, inclined at an angle of 45°

to it.Half of the incident beam passes virtually straight through the mirror and is then turned back on itself by mirror M2.In addition to functioning in a reflex mode,this particular sub-assembly is also instrumental in providing a variable degree of beam attenuation, via a piece of polaroid filter attached to the front surface of M2. By rotating the mirror,and thus polarizer, a variable amount of polarized incident beam is reflected back and eventually becomes an intensity matched reference beam.It is steered 'up' through the microscope by a further reflection, at the rear surface of mirror M1.

The other half of the original incident beam is turned through 90° by the front surface of M1 and directed 'down' through a x10 microscope objective to the flow vessel.The objective is mounted in a precision focussing attachment, thereby obviating the need for all gross movement of the velocimeter body or flow vessel once the initial target location has been achieved.

Back scattered Doppler shifted light passes back through the objective and then virtually straight back through the half silvered mirror M1. Here, it and the reflexed reference beam from M2 share a common course and travel 'up' to the edge filter,M3. Often referred to as a heat control filter, this component is made up of multiple dielectric layers and allows the direct transmission of any light which lies in the wavelength range 750 to 1200 nm and the reflection of any lying in the range 400 to 700 nm.

The former wavelength range encompasses the laser diode wavelength and therefore allows both the reference beam and the Doppler shifted

beam to pass unhindered up to the detector stage.The latter wavelength range is in the visible region and steers a white light targeting beam down through the microscope objective and onto the flow cell.By utilizing a heat control mirror,rather than a simple half silvered mirror,one is able to maximize the intensity of the target beam without detriment to the signal and reference beams.

The visible target beam is a highly desirable adjunct in a system employing a coherent source with a near infrared wavelength output.There is now the expectation of laser diodes with output wavelengths in the visible red part of the spectrum,when such components become available it may be possible to dispense with the target beam of the LDV microscope.

The detector stage is similar to that already described in the context of the double beam velocimeter.It contains a receiving lens,a polaroid element,a pin hole aperture and a BPX65 photo diode.An 820 nm bandpass filter is included but much of it's function has already effectively been fulfilled by the edge filter.The photodiode is the detector element for the beat frequency produced by the oncoming reference and Doppler shifted beams.The detector output is converted from current to voltage,and it is also impedance buffered,by an amplifier incorporated within the main instrument construction.

7.3 Assesment of Data for the design of a special purpose analyser.

Initially the signal processing for the new device was the same as

that employed with the double beam velocimeter.That is, an audio monitor,a variable filter unit and a spectrum analyser.Once initial functional checks had been carried out with the aid of the vibrating crocus paper test rig,the next operation involved subjecting blood flow related FFT specra to analysis for further corroboration of the log line fit approximation.Then,if the fit was borne out,to utilize the principal in the design of a special purpose analyser.The construction of such an analyser would then facilitate further jet velocity investigations.

For the type of confirmation being sought there are three stages to an examination of the data, they are characterised by the following questions:

1. What model should be fitted to the data.

2. How should this model be fitted.

3. How well does the model describe the data.

There are two basic approaches to model selection. In the first,one has a theory about the process and this can be translated into the required mathematical model. In the second approach the procedure is entirely empirical; choose a model that fits the data. Despite the work of investigators such as Bonner and Nossal (1981),the history and context of the study as a whole suggested the adoption of the latter approach.

Thus if one is guided by the apparently logarithmic nature of the data, the general model to use is:

$$Y = ae^{-bx}\varepsilon$$

In the specific case under consideration Y is the power associated with some frequency X, a and b are constants and ε is the experimental error. An important assumption made here is that the experimental error, which is due to a variety of uncontrolled factors, is multiplicative. In other words, the larger the value of Y, the larger the effect of the error. This assumption does in fact seem to be borne out.

The easiest way of fitting the above model is to linearise by taking logs of both sides:

$$\ln(Y) = \ln(a) - bX + \ln(\varepsilon)$$

This may now be identified with the equation of a straight line, Y = mX + C. Specifically:

$$Y = a + bx + e$$

Due to problems encountered with spectrum data transfer via the IEEE data bus, analysis was performed by placing the hard copy outputs of spectra onto a digitizing tablet and creating files that could be analysed with a statistical package running on a mini-computer (Minitab running on a Prime 750). This technique was slow and discrete point picking inevitably led to some loss of resolution. However, this loss of resolution had little effect on the validity of the analysis and

the system as a whole was able to provide the sought after information.

In total, spectrum curves associated with some 30 different velocities were analysed, ranging from 0.1 cm/sec to 5 cm/sec. However, because of the rather laborious process involved in the data translation,many were derived from experiments in which other variables were also changed. For example,changes were made in laser intensity (to investigate penetration depth) and the angle of incidence of the measuring beam relative to the direction of flow during this phase of the work.Although many of the changes were relatively trivial the results they gave would require lengthy annotations.Therefore,in the interest of clarity of presentation only six will be used in the discourse that follows.The six are from experiments in which all variables other than flow have been held constant.The measurement angle is nominally 10° from the normal to the direction of flow.This angle was determined empirically,the criterion for acceptance being the best signal strength throughout the range of flow velocities.Figure 7.2 shows the six power spectrum curves presented for curve fitting: the curves shown are reconstructions from the digitized data files.

In a manner compatible with the philosophy previously explained,the first step in the curve fitting involves taking logarithms of both sides and fitting a straight line to each set of data.To facilitate this operation some shifting of the origin of each data set is necessary,to avoid problems associated with log zero.The lines produced by the log operation have the following characteristics:

TABLE 7.1

Curve	Velocity (CM/SEC)	Intercept (A)	Slope (B)	$\frac{1}{\lvert B \rvert} \times 10^{-2}$
1	0.70	6.5	-.0059	1.69
2	1.08	6.7	-.0037	2.70
3	1.26	6.9	-.0034	2.94
4	1.54	7.0	-.0027	3.70
5	1.61	6.8	-.0031	3.22
6	1.75	7.0	-.0028	3.57

The six log power curves and their fitted straight lines are shown in figure 7.3.

The properties of the curves can now be investigated more closely by trying to fit a model to all data sets simultaneously; so far each set of LDV data has been treated in isolation. Reverting once more to the use of log scales, where the exercise reduces to one of fitting straight lines, there are two ways in which these individual data set lines might be expected to differ.

a) They can have different intercepts.

and/or

b) They can have different slopes.

One can then examine the evidence for:

i) Given that each line has a different slope would a global model require each line to have a different intercept.

or

ii) Given that each line has a different intercept, does a global model also require that we fit a different slope to each line.

The evidence can be assessed by looking at how much of the total variation is explained by each of the alternatives. Using a sum of squares method of assessing the data, the alternatives yield the following breakdown:

TABLE 7.2

i)

Source of variation	Degrees of freedom	Sum of squares
Single slope	1	713 (82%)
Different slopes	5	104 (12%)
Extra for different intercepts	5	5 (0.6%)
Left Over	384	51
Total	395	873

ii)

Source of variation	Degrees of freedom	Sums of squares
Single slope	1	713 (82%)
Different intercepts	5	77 (9.0%)
Extra for different slopes	5	32 (4%)
Left Over	384	51
Total	395	873

The conclusion to be drawn from the above analysis is that the simpler model, where there is a common Y axis intercept but different slopes, is satisfactory and one loses very little information by employing it. The fitted curves, with one mean intercept value, are now:

TABLE 7.3

Curve	Velocity (CM/SEC)	Intercept (A)	Slope (B)	$\frac{1}{\lvert B \rvert} \times 10^{-2}$
1	0.70	6.8	-.0066	1.51
2	1.08	6.8	-.0037	2.70
3	1.26	6.8	-.0034	2.94
4	1.54	6.8	-.0029	3.44
5	1.61	6.8	-.0027	3.70
6	1.75	6.8	-.0026	3.84

These lines are shown in figure 7.4. and their suitably scaled reciprocal slope values are shown plotted against velocity in figure 7.5.

Two main points come out of the type of treatment just described.They are:

1. The suitability of the single intercept model is reassuring because an alternative conclusion would have implied a range in the scattering cell population densities at zero flow. (Witness,for example,the dilution results associated with figure 5.9).Such population changes would have been untenable.

2. There does appear to be a systematic departure from the model for most of the data sets. For example,upon examination of figure 7.3 it is noticeable that for the higher flow rates the data tends to be above the line in the middle and below at the end. There is therefore some curvature that has not been explained by the simple logarithmic model: it is a manifestation of multiple scattering and

qualitatively predictable from the equations developed by Bonner and Nossal (1981).

7.4.A Special Purpose Analyser

The simple logarithmic model is quite obviously an approximation, even when applied to situations which favour a low order of scattering. Never the-less, the model does still point to an apparently simple method of deriving a usable indicator of blood velocity. In essence, a circuit may be designed to detect root mean square (RMS) values of the Doppler shift spectrum at two separated frequencies, compute the logarithms of the two RMS values and then compute the reciprocal of the slope of the imaginary line joining the two selected frequency points.See figure 7.6. That reciprocal value should then be approximately proportional to the red cell velocity.

It is recognised that the dependence upon approximations might condemn such an instrument as inferior to, for example, the devices described by Riva and Feke (1981) and Bonner et al (1981). The former has derived equations to support an analogue computation of maximum red cell speed,the latter has supportive evidence for the design of an analogue processor for extracting mean blood flow. However, neither of the afore mentioned devices are without inherent approximations or multiple scattering imposed limitations. The perceived justification for the analyser about to be described is that it represents a pragmatic solution to the need for an instrument with which to assess the viability of the thrombus development measuring technique as a whole.

The circuit for the special purpose analyser is shown schematically in figure 7.7. The signal from the LDV detector amplifier is first passed through a high pass filter network, the cut-on frequency of which is selectable to either 100 Hz or 300 Hz and allows the removal of system noise without undue attenuation of signal components. The output from the filter then passes to an amplifier stage that has a gain which is variable between x100 and x1000. This brings the signal up to a typical amplitude of $\mp$ 1 volt. (Without the initial prefiltering the relatively large noise component would cause saturation of this amplifier stage.) The amplified output signal is split and goes into two parallel processing channels.

In one channel there is a bandpass filter with switch selectable centre frequencies of F1 = 1,2,4,8 and 16 KHz and in the other they are at F2 = 2,4,8,16 and 32 KHz. The Q value of each filter is 10. Analogue signals proportional to the selected frequencies, F1 and F2 , are available at the output of the two summing amplifiers,A2 and A3.

The output from each of the two filters goes into its own RMS converter stage. The output from this device is an analogue signal representing the mean power in the passband presented to it. The time constant for averaging time is selectable by capacitor value and in the application under discussion is fixed at 200ms. This was found to give optimum smoothing of the LDV signal, in a manner analogous to the x16 sweep averaging used in the FFT spectrum analyser. Functionally, the RMS converter output is then passed into the logarithmic response amplifier.

In practice the RMS converter, a type AD536, has a logarithmic output available and so both RMS and log computation are available from within one integrated circuit. Thus, in the circuit described so far, two frequency proportional voltages and two associated log power signals are available.

The next stage in implementing the slope algorithm is for differential amplifier A4 and its associated resistors to yield a voltage proportional to F2 - F1,the difference in pass band frequencies.The output from the difference amplifier then forms the numerator input of an analogue divider.The divider's denominator is P1 - P2,the difference in power associated with pass bands F1 and F2;this power difference is formed by differential amplifier A1 and it's associated resistors.The divider's output is the required velocity proportional signal.

7.5. Setting Up Procedure

The setting up of any analogue computer presents the potential for five main sources of error:

1.Cumulative errors introduced by errors in the computation of individual functions.
2.Offset errors insufficiently trimmed out of active component stages (operational amplifiers,multipliers,dividers etc)
3.Limitations in the accuracy of the dynamic ranges of some active components (multipliers and dividers in particular).

4.Component tolerances.

5.Thermally induced drifting of component values.

In the analogue computer just described,the errors were minimised at the passive component level by close attention to component type and a philosophy of 'select on test' for value matching. At the active component level all offset errors were carefully trimmed out and scaling factors arranged to ensure optimum compliance with guaranteed accuracy ranges. The absolute voltage requirements for the dividers are particularly stringent because numerator (N) and denominator (D) need to be kept within the range $.1v \leqslant Vin \leqslant 10v$ and,at all times $N \leqslant D$.

The above circuit was initially set up using the calibrator shown in figure 7.8. In this calibrator there are two Wien bridge configuration sine wave oscillators: one oscillator has an output frequency switchable to 1,2,4,8 and 16 KHz and the other switchable to 2,4,8,16 and 32 KHz. (It will be seen that these frequencies correspond to the bandpass frequencies associated with the main analyser circuit). Each oscillator output then goes into its own amplifier/ attenuator stage and, finally, these outputs are summed via a pair of resistors and an operational amplifier. Thus the output from the calibrator is a waveform made up of two sine wave frequency components, each of independantly adjustable amplitude.

Using any particular pair of calibration frequencies as the input to the computer it was found possible to get output values that were within 3% of the theoretical value. However, the accuracy was down to

being within only 10% of the theoretical value if different frequency combinations were used. This inter-range discrepancy could be attributed in part to the cumulative effects of the five error sources listed above and in part to inaccuracies in the filter characteristics. The parameter interactions that are introduced when any one is adjusted means that almost inevitably gain, Q value and centre frequency settings all depart from the ideal.It was therefore accepted as a further operational limitation that the two filter settings would have to be selected at the start of an experiment and maintained for it's duration.The lower frequency filter setting (F1) would be selected to avoid noise and the upper frequency (F2) selected to maximize linearity over the envisaged dynamic range.Figure 7.2 shows that at the upper frequency part of the spectrum there can be particularly gross departures from linearity.According to Riva and Feke the 'tail' to the spectrum is associated with multiple scattering.Therefore departure from the straight line approximation is likely to be most severe in the higher frequency region of the spectrum.

7.6 Functional Evaluation of the Analyser

Functional evaluation of the analyser involved appraising it's performance when making recordings of one cycle of a pulsatile signal. This was chosen as an efficient way of demonstrating the main advantages and disadvantages of the device.

Thus, refering to figure 7.9, a pulsatile blood flow signal has been produced by the asymmetric roller pump assembly previously

described in section 6 of chapter 5. (The characteristics of the generated pulse have been chosen to demonstrate the response limits of the analyser,not because they represent any particular physiological flow signal).Trace 7.9a shows the true flow signal,as recorded by an inline proximal electromagnetic flow probe.Trace 7.9b shows a recording from the same probe but with the associated electronics modified to give the meter a nominal 200 ms time constant.Trace 7.9c is the recording made by the special purpose analyser as the blood flows through a 1 mm I.D. glass flow tube.

The 200 ms time constants of the two RMS converters impose a severe frequency response limitation upon the analyser.Whereas a pulsatile flow signal is accepted,the output is effectively low pass filtered at nominally 0.5 Hz.Thus the pulse chosen for figure 7.9, devoid as it is of high frequency components by arterial pulse standards, is at about the limits of acceptability. However, if allowance is made for that frequency response limitation,then the results are in good agreement with those derived from an electromagnetic flow meter,albeit one with a similarly restricted frequency response imposed upon it.

Allowing for the additional fact that the two flow meters are probably measuring at slightly different flow profile positions (the electromagnetic probe's inter-electrode potential is proportional to the average velocity over the blood vessel cross section),the two damped signals do show a sufficient degree of similarity to support the credibility of the special purpose analyser.The conclusion to be drawn,therefore,is that the device will facilitate the continuous

recording of blood flow / velocity,but only sensibly with non pulsatile signals.From this it follows that the proposed thrombus growth measurements will need to be carried out in veins rather than arteries. However it is suggested that,during evaluation of the jet velocity concept as a whole,non pulsatile signals represent one less variable to contend with. Therefore the frequency response of the analyser is not regarded as being a particularly limiting feature at this stage.

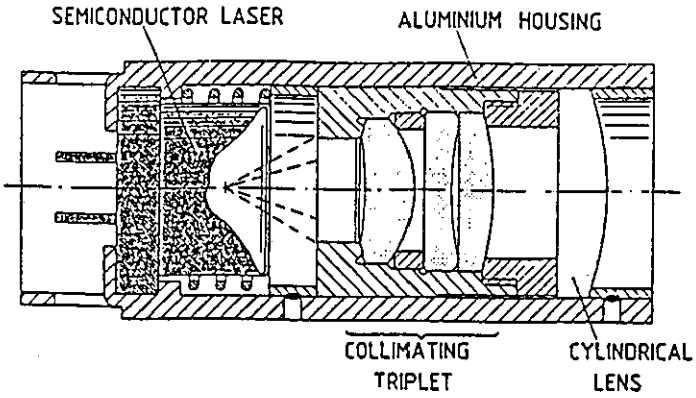

Figure 7.1a: The Mullard CQL13A laser diode 'pen' with built in collimating optics.

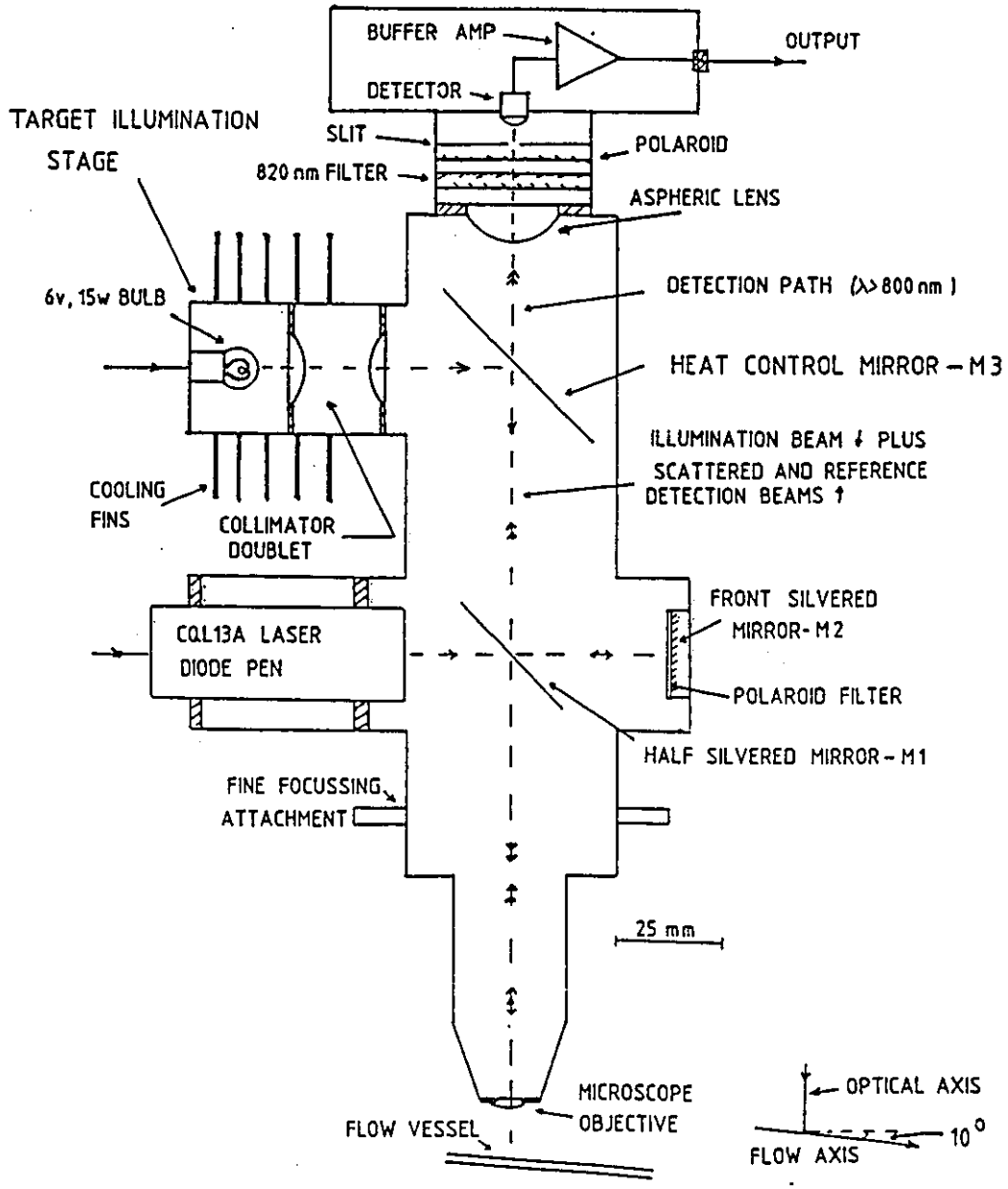

Figure 7.1b: Schematic diagram of the external reference beam system.

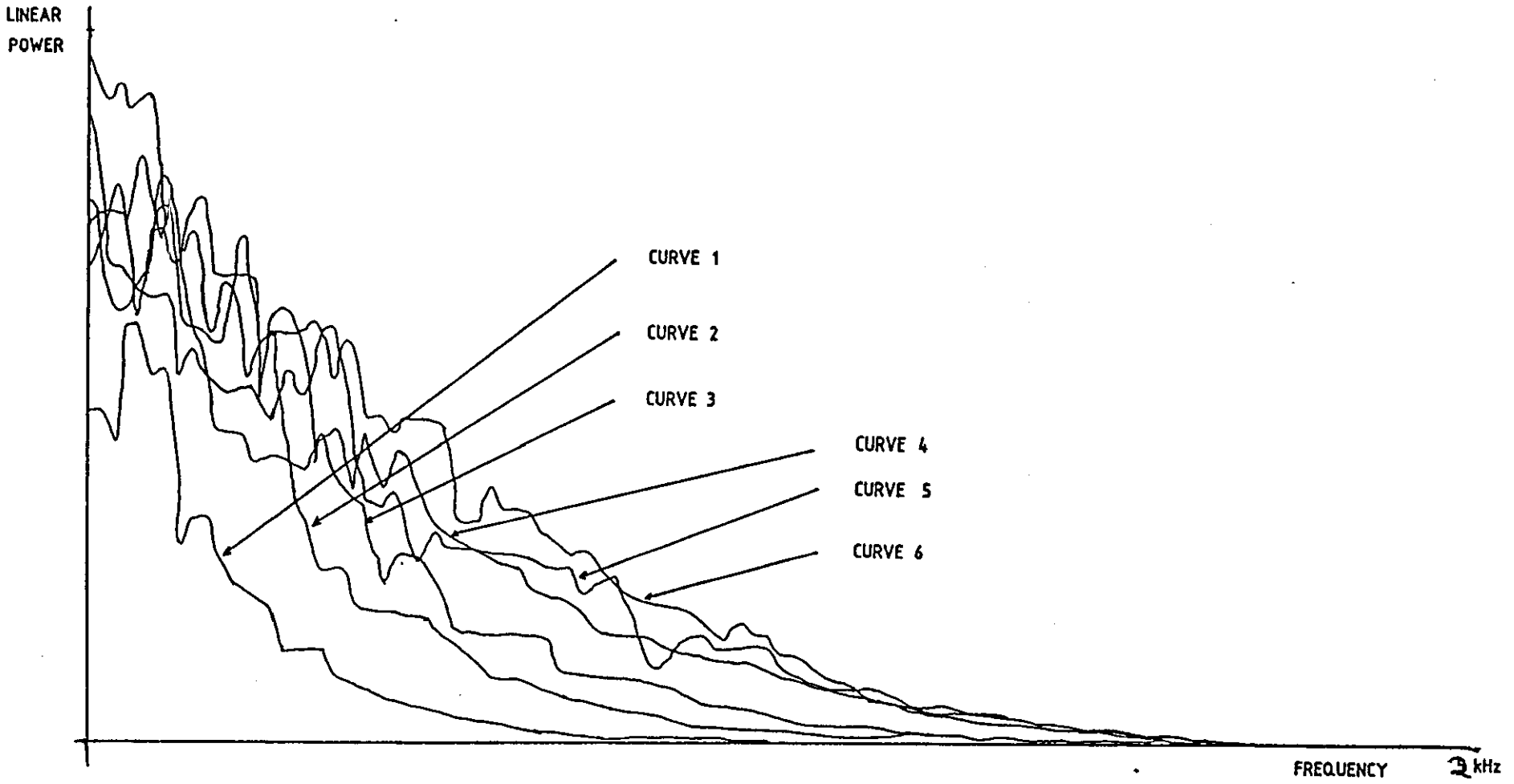

Figure 7.2: The six power spectrum curves used during the curve fitting.They have been reconstructed from digitized data files.

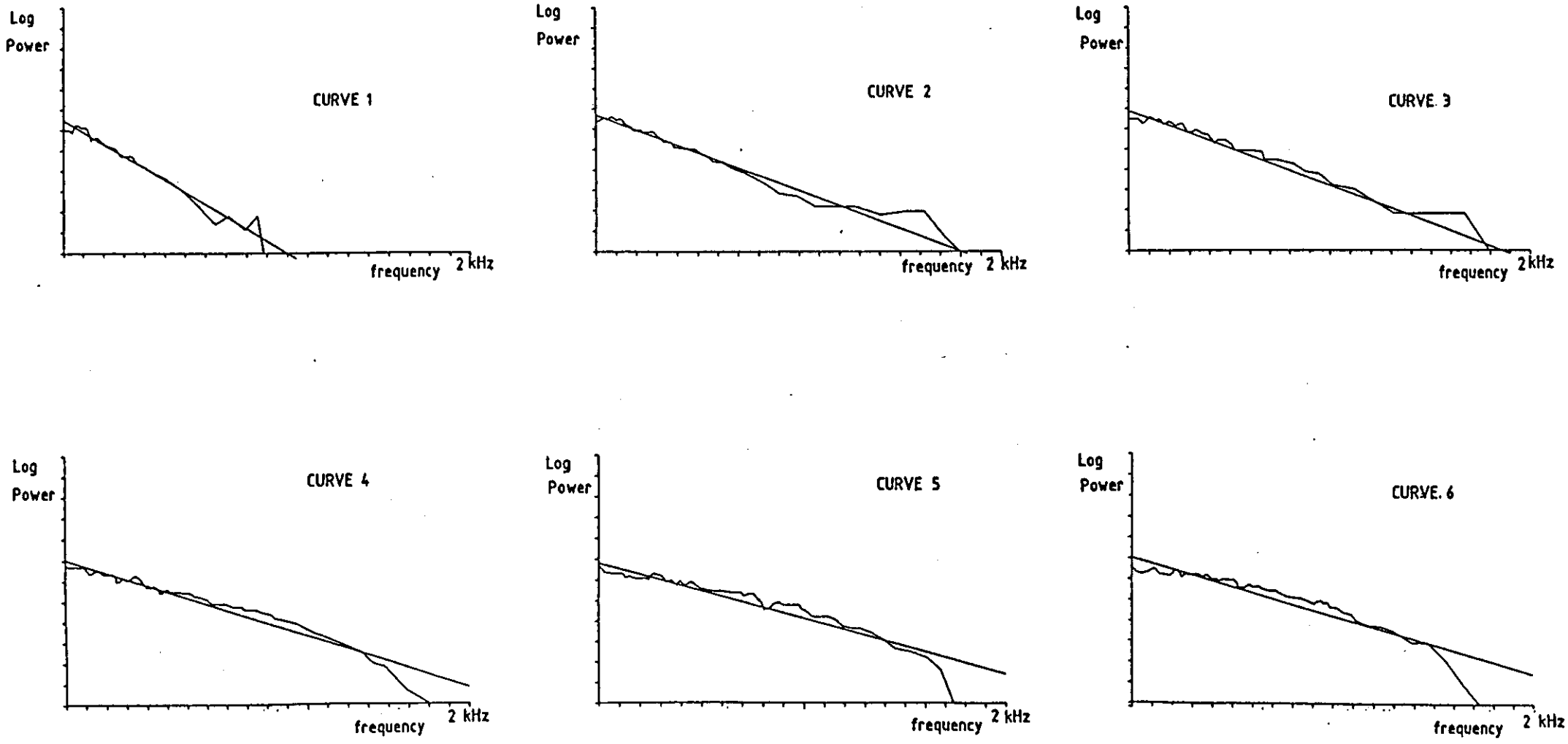

Figure 7.3: The six power curves plotted on a logarithmic scale and their fitted straight lines.

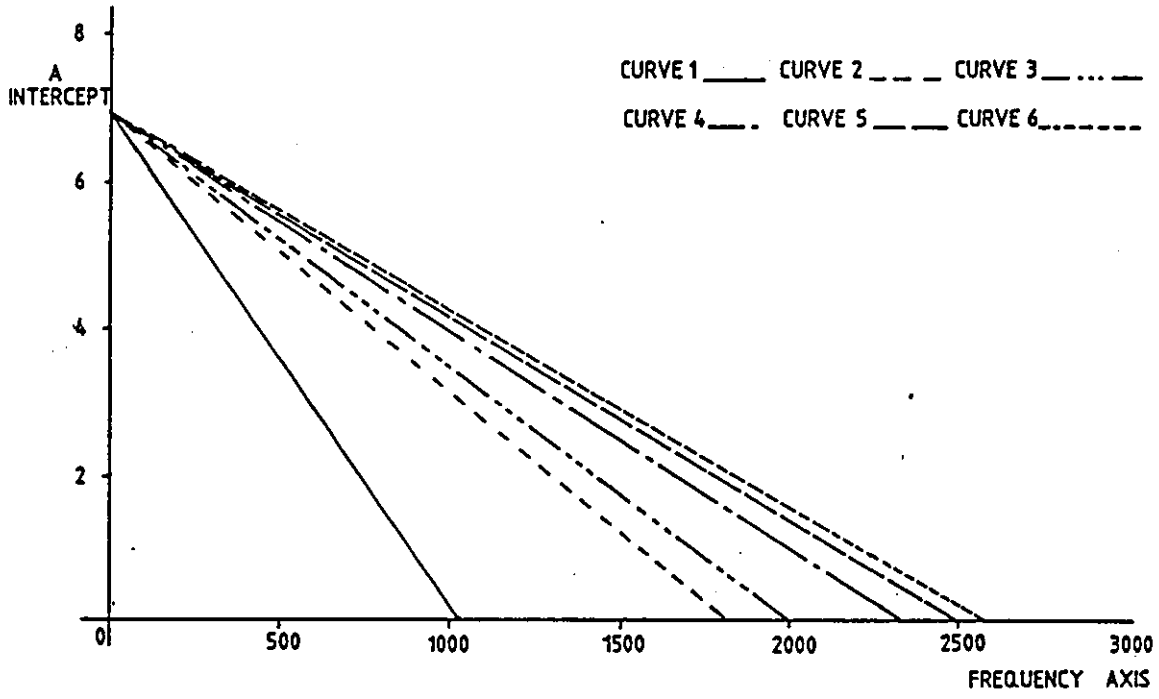

Figure 7.4: All six curves fitted to a common Y axis intercept.

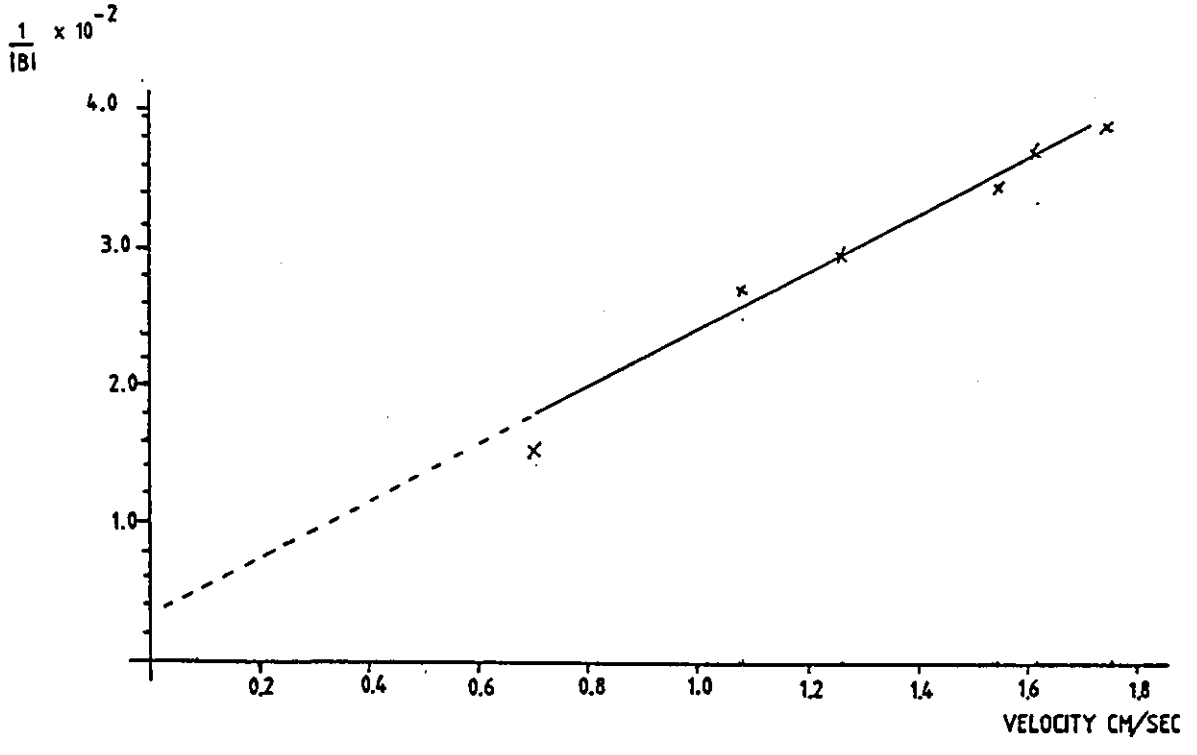

Figure 7.5: The reciprocals of the slopes of the previous diagram plotted against their associated velocity values.

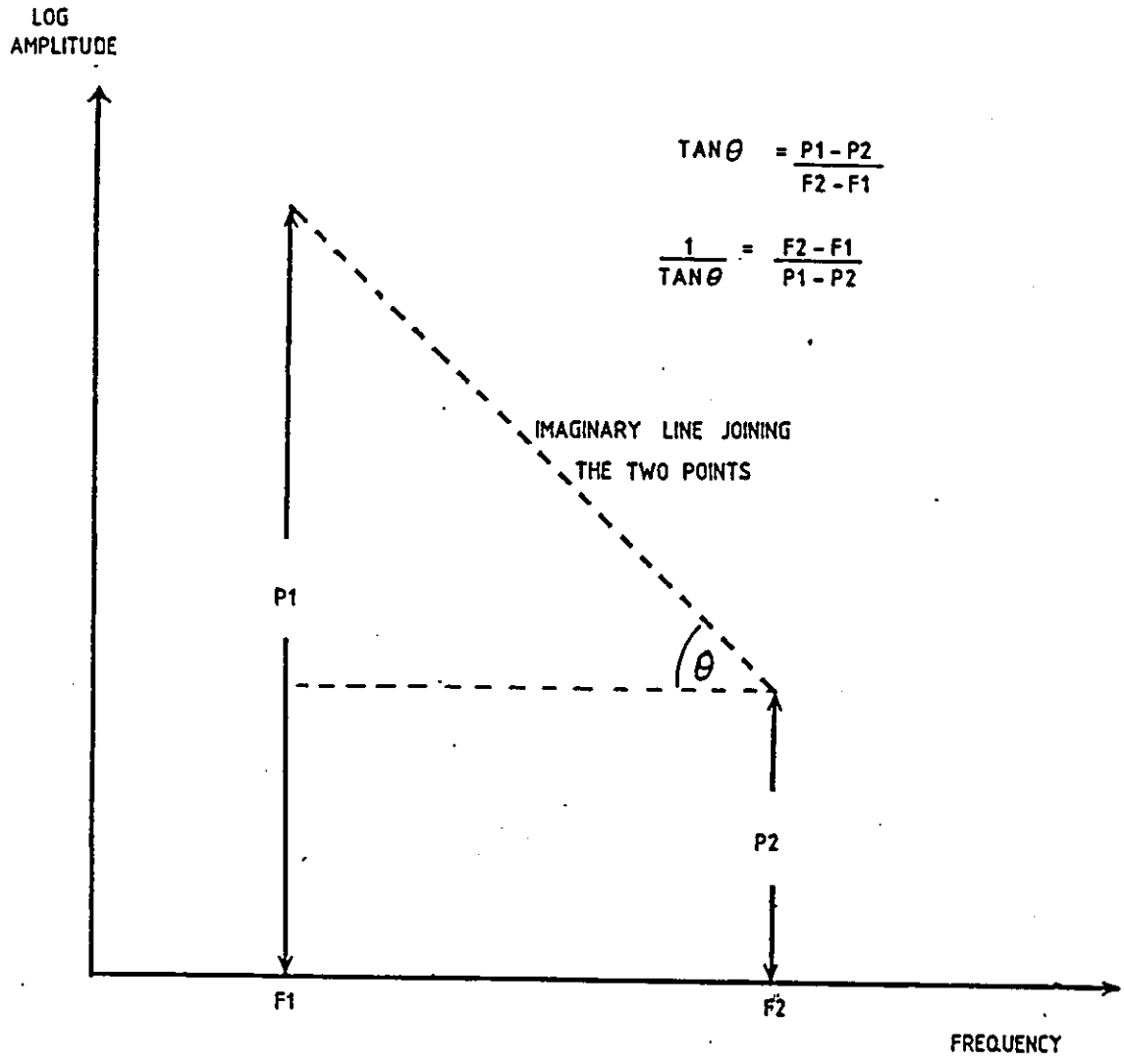

Figure 7.6: Showing how, in the special purpose analyser, the reciprocal of the slope is to be derived from two frequency points.

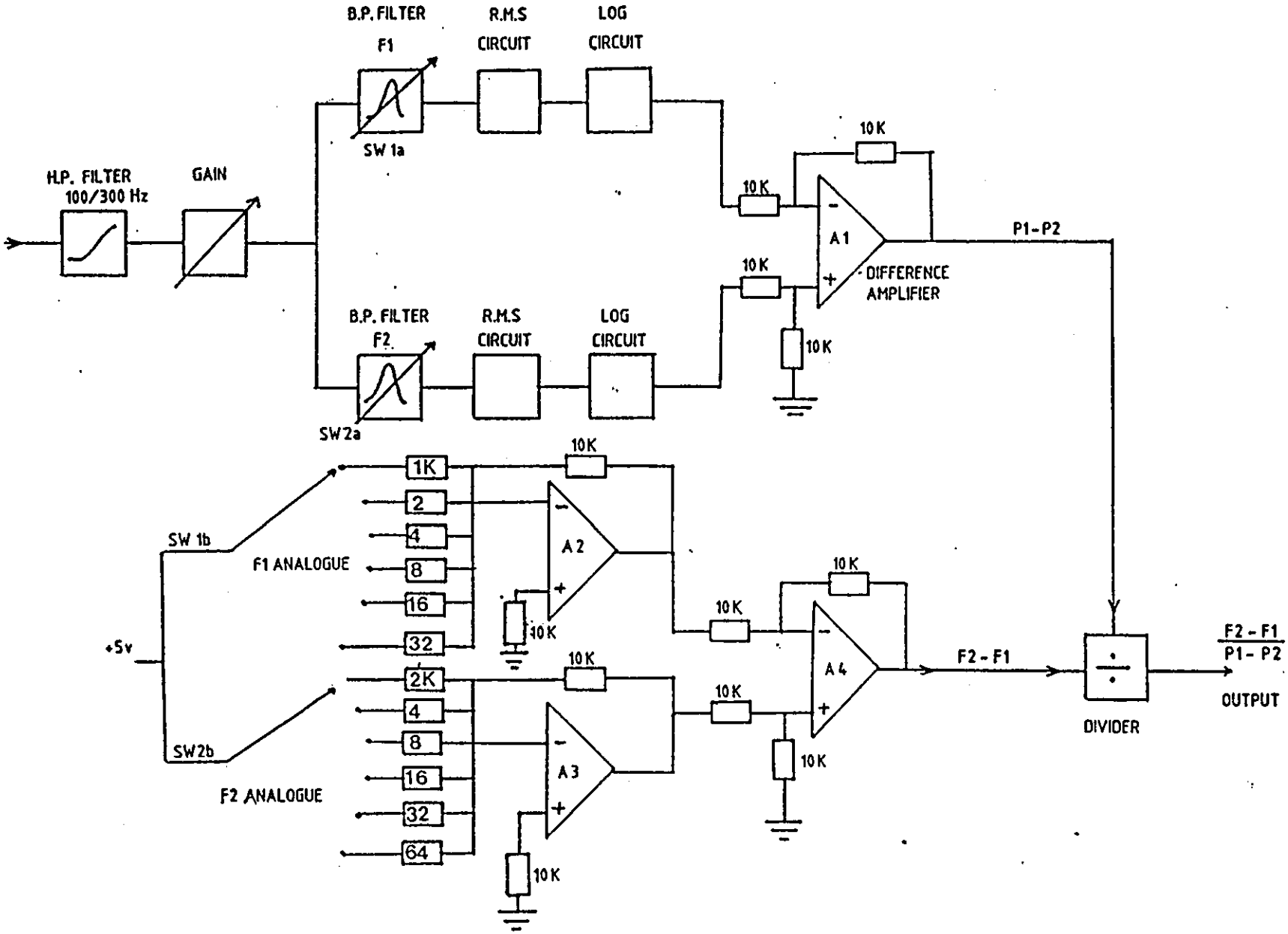

Figure 7.7: Circuit diagram of the special purpose analyser.The log function is in fact available within a type AD536 RMS converter.

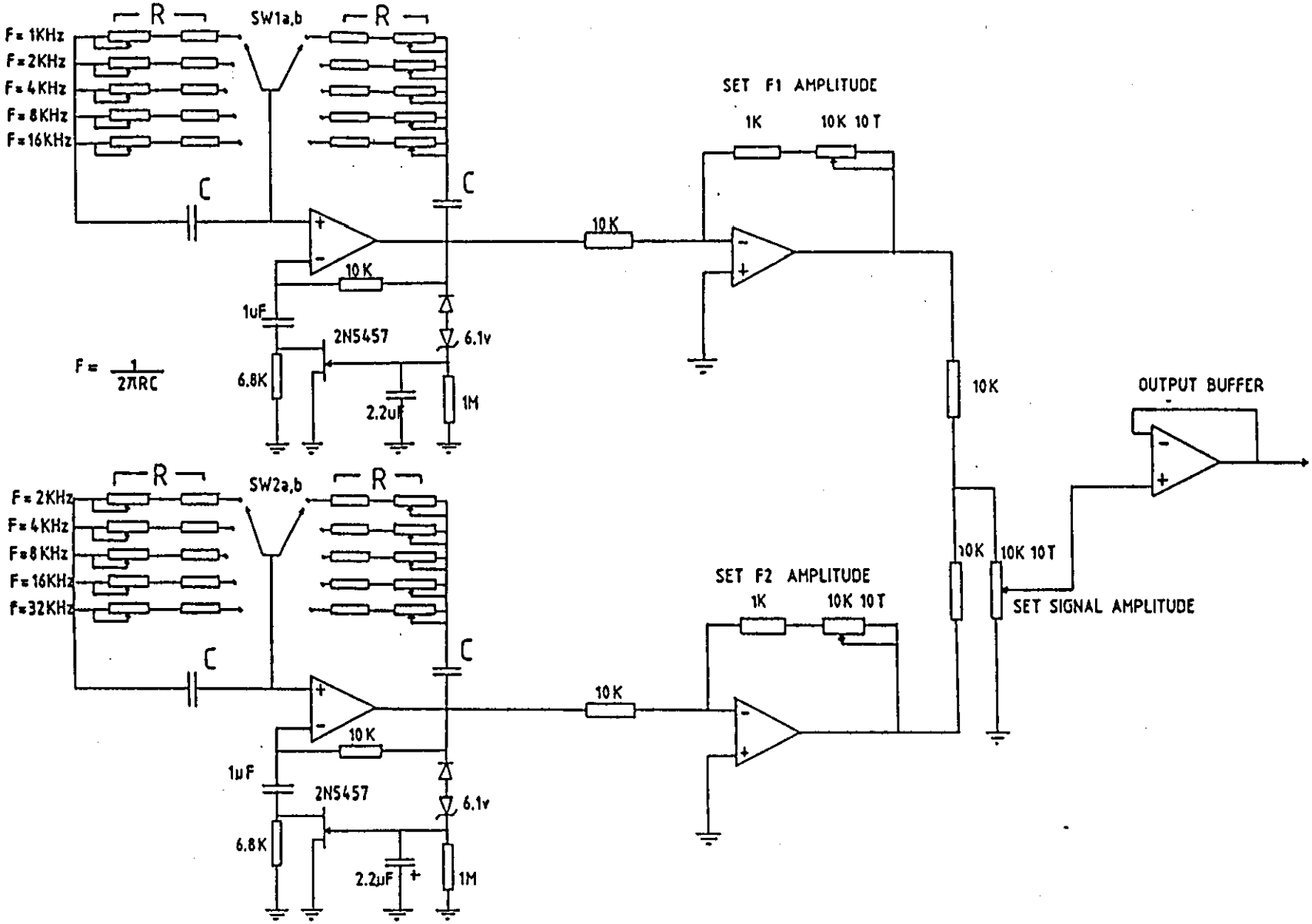

Figure 7.8: Circuit diagram of the calibrator built for setting up and validating the special purpose analyser.

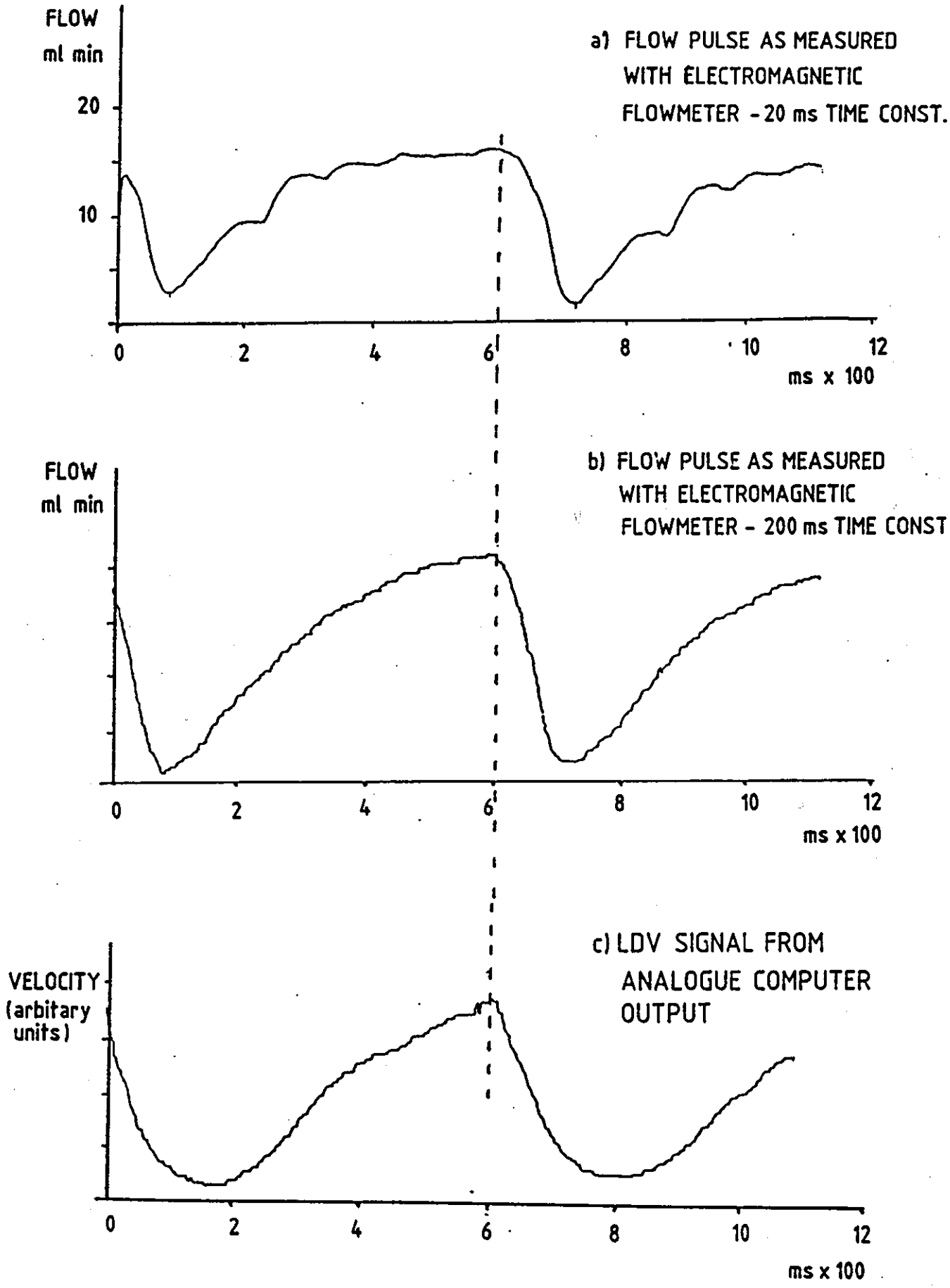

Figure 7.9: Showing that if allowances are made for frequency response limitations, the output of the special purpose analyser compares not unfavourably with that of an electromagnetic flowmeter. During the experiment associated with trace c the analyser's filters were set to F1 =1kHz and F2 =4kHz.

CHAPTER 8

EXPERIMENTS AND RESULTS

8.1 Introduction

Professionally, morally and logistically, it is highly desirable that a new instrument which is destined for use with animal preparations be first tested by simulation.This is in addition to any preliminary functional tests,of the type described in previous chapters.

Consequently the first sections of the present chapter describe a new series of flow vessel experiments,conducted with an improved thrombus model and employing the newly created velocimeter and analyser. There then follows a description of some in-vitro experiments which were attempted: unfortunately they were not successful and no results ensued.They too had been attempted by way of minimizing the dependence upon living animal tissue during the development stages of the instrumentation and methodology.

Finally there follows a description of two in-vivo experiments which were conducted and the results that were achieved.Although more work must be performed before any categorical judgements may be delivered,it is believed that the results from these in-vivo experiments do adequately demonstrate the viability of the underlying research objective.Unfortunately the results also represent the most that can

currently be achieved:operational restrictions arising from Home Office regulations and a dependance upon personnel from other disciplines are seen to become rate limiting factors within the framework of this thesis.

8.2 An Improved Thrombus Model

Experiments have previously been described,in chapter 5,in which a thrombus was modelled by a glass pip in the lumen of the flow tube.Although useful at that stage of the work,the model had the disadvantage of being difficult to control and was also prone to distortion associated uncertainties.Therefore,despite the fact that the laser Doppler based measuring technique gave encouraging results with the simple model,in reality such results were of only limited value.Consequently,an improved model was sought.

The idea evolved of fine magnetic particles being seeded into the test fluid (blood) and then held against a defined area of the test section's inside wall by the influence of an external magnet:the magnetic clump so captured should then approximate to a thrombus.The volume of that bore restricting 'thrombus' should be proportional to the number of magnetic seeding particles introduced and so dynamic studies could be conducted,without distortion of the flow vessel wall.

A fine iron powder was the first seeding agent to be used and further encouraging results were achieved.There was,however,a problem associated with controlling the number of particles introduced.The

design of the test rig dictated that the seeding particles be introduced by injection in suspension form;the iron dust was relatively dense and variable degrees of precipitation occured during the injection phase.In addition,even after relatively short periods,there was a tendancy to rust formation and obscuration of the vessel walls.

Fortuitously a magnetisable charcoal (Magsep,Serono Diagnostics Ltd) has been developed for immuno-assay studies (Dawes and Gardner,1978). Magsep consists of equal parts of charcoal and magnetisable iron oxide incorporated in a polyacrylamide gel.In the commercially available form it comes as a 25g/L aqueous suspension,with more than 80% of the particles lying within the size range of 1 to 10um.The density and size of the particles are such that the suspension settles only slowly and this,coupled with the freedom from rusting,makes Magsep the ideal replacement for iron dust in the present context.

The basic test rig and instrumentation used with the new occlusion model is,in many ways,similar to that already described in chapter 5.The addition of a self sealing rubber septum enables Magsep from a freshly charged syringe to be injected downstream of the peristaltic flow inducer.A small magnetically loaded scavenging sump downstream of the flow vessel prevents uncaptured Magsep from recirculating in an unpredictable manner or causing problems at the electromagnetic flow probe.

In order to evaluate the jet velocity measurement concept it is desirable that an independant measurement of the occlusion size be

made.This represents something of a paradox:if such a measurement could be made,would the laser technique be necessary in the first place? The redeeming difference is that the test rig is essentially non biological and accessibility is therefore not a great problem.After a great deal of experimentation a photo-electric technique was eventually decided upon, the operational principal being that the build up of the captured Magsep should attenuate the light passing from a photo emitter to an opposing detector.The monitor will therefore measure the effective area of the beam obscuring build up as it appears in profile across the transmission path.Figure 8.1 shows the new test rig with injection port and monitor.

The head of the monitor and it's relation to the flow tube and Magsep attracting magnet is shown in more detail in figure 8.2. Light from an 850 nm LED emitter is guided to the wall of the flow tube by a 1mm diameter plastic optical fibre. The diameter of the fibre is nominally the same as that of the flow tube so that occlusion size has the maximum and most linear effect on photon coupling. Light from the emitter that has passed through the flow tube and it's contents is then guided to a detector by a second length of plastic fibre. The emitter and detector fibres are directly opposite each other: the particle attracting magnet is at right angles to both the fibre coupling axis and that of the principal fluid flow.So that the consequence of different orientations of the occlusion relative to the measuring volume might be studied, the magnet and optical probe are fixed onto a head that is rotatable about the flow tube's radial axis. Therefore, rather than move the LDV assembly radially about the flow tube, the occlusion may be formed at different radial positions within the tube. The magnet is of

the rare earth variety and is 5 mm in length and 2.5 mm in diameter; at the end designated to attract the Magsep it is tapered to a diameter of 1mm by the addition of a suitably shaped 2 mm length of soft iron. The magnet and it's pole piece are mounted on a screw threaded linear adjuster, this in turn is mounted on the probe head and facilitates reproducible positioning.

The LED emitter is rated at 160 uW at 50 mA drive current.Under normal circumstances this would yield a perfectly adequate signal for detection.However because of the beam attenuation, brought about by the interposing blood,some additions have been made to maximize the signal and minimize the electrical noise.Instead of using a DC source to provide the drive current,a low duty cycle 100 mA pulse is applied to the photo emitter: a 1 ms pulse is applied every 10 ms.The pulse repetition frequency is in fact derived from the zero crossing points of the mains voltage,thereby ensuring that signal generation / detection occurs at periods of low electrical noise.The detector circuit then compromises a PIN photo diode,a detector amplifier and a sample and hold circuit linked to the emitter drive pulses.The sample and hold circuit therefore acts as a synchronous pulse amplitude demodulator for the occlusion modulated optical pulse.The output from the sample and hold circuit then passes to a low pass filter output stage to further remove mains noise and sampling artifacts.A switchable 10% change in the value of the emitter diode's current limiting resistor allows a measure of calibration of the probe.A schematic diagram of the circuit is shown in figure 8.3.

8.3 The Experiments and Results

From the outset it was appreciated that whereas the results obtained from this particular series of experiments might well yield semi quantitative results about the behaviour of magnetically attracted particles,the information to be gained about thrombus growth characteristics would,at best,be only semi qualitative.However,as a means of further validating the underlying concepts,a demonstrable measure of success with these experiments was considered to be a necessary precursor to any experiments involving animal tissue.

The experiments were all primarily orientated towards further demonstrating that an occlusion related velocity increase could be measured at some point distal to that occlusion.It was hoped that these experiments might have the added advantage of conclusively demonstrating the technique's ability to follow aspects of growth dynamics, this had not been possible with the simpler glass 'pip' model.In the experiments to be described the analyser filters were set and kept at F1 = 2kHz and F2 = 8 kHz.

Figure 8.4 shows the results associated with the injection of a 1 ml. suspension of 5% Magsep in saline.Based on experience gained with the glass pip model,the measurements have been made at a point 1 mm (1 diameter) distal to the centre of the developing occlusion.The resulting LDV trace quite clearly shows an increase in velocity that is related to the independant optical obscuration measurement.The former in fact continues to indicate particle build up after the latter has flattened

out through saturation of the sensing field.It will be noticed that the electromagnetic flow meter trace remains steady,indicating there to have been no overall change in system flow.These preliminary results do appear to suggest that an occlusion might be detected at a relatively early stage of it's development,almost certainly by the time of a 10% reduction in available lumen area.

That the 1 diameter measuring point was indeed the position of maximum velocity change is demonstrated in figure 8.5. Here an occlusion,produced under similar circumstances to the previous one,has been established in the flow tube.Velocity measurements have then been made along the tube length at four discrete diameter proportional positions.Quite clearly the choice of a 1 diameter distal measuring site is vindicated.Related experiments showed this position to not only yield the greatest velocity increase per se but also to be the most sensitive,as witnessed by the ability to respond to small changes.

Figure 8.6 shows the effect of measurement orientation.The magnet holding head has been rotated around from it's normal position at $+180^{\circ}$ to the LDV beam to $+135^{\circ}$,$+90^{\circ}$, and $+45^{\circ}$: there appears to be little effect.This lack of orientation sensitivity is another manifestation of photon diffusion. The tentative conclusion to be drawn from this is that when the LDV technique is applied to small vessels in an animal model,small changes in measurement orientation are unlikely to be critical.

Other experiments that were conducted, whilst revealing

characteristics of the magnetic material,did not yield results that were likely to be of significance in the true thrombus context.Never the-less it was reassuring that such characteristics could be identified by means of their associated jet velocity measurements. One of the most fundamental variables affecting the build up of the magnetic material at the intended occlusion site is the rate at which it is introduced.Thus figure 8.7a shows the results associated with the 1ml. of saline diluted material being injected over a 5 second time course.Figure 8.7b shows the trace associated with a 20 second injection period.The more rapid build up of magnetic material is seen to lead to an unstable occlusion and around 50% of it is rapidly swept away: even the cummulative effect of such bolus presentations is minimal.

Figure 8.8 shows a slightly anomalous occlusion dispersion being followed.The attracting magnet has been removed but for some reason the occlusion has not then fully dispersed,as indicated by both the optical density reading and the LDV measurement.However,using the peristaltic pump speed control to produce a rapid burst of increased fluid flow does disperse the previously stubbornly remaining occlusion: the sequence of events is collaborated by all three displayed parameters.

To make sure that the results associated with the 0.25 ml/sec flow through the 1 mm internal diameter flow vessel were not a fortuitous anomaly,the basic occlusion build up experiment was repeated in:

a) The 1 mm internal diameter tube with a 0.1 ml/sec blood flow rate

b) A 0.8 mm internal diameter tube with a 0.25 ml/sec blood flow rate

c) A 0.8 mm internal diameter tube with a 0.1 ml/sec blood flow rate.

The afore mentioned rates and sizes were chosen on account of their being representative of values that might reasonably be encountered in a range of small animal vasculature.Thus a maintained flow of 0.25 ml/sec through a 1mm I.D. tube corresponds to a velocity of approximately 32 cm/sec.and this is in accord with,for example,the velocity of 30 cm/sec in a dog saphenous vein of similar dimensions and quoted by McDonald (1960).The corresponding Reynolds number is 80.

The results are shown in figures 8.9 and 8.10. Maintaining the same flow rates in smaller diameter tubes gives rise to proportionally higher velocity gradients and this is reflected in the higher degree of occlusion instability associated with figure 8.10.Therefore,whereas when compared with the 1 mm I.D. tube qualitative differences do exist,they are all primarily attributable to the different rates of deposition of Magsep and it's concurrent partial removal by the altered velocity gradients.The results are therefore seen as being in accord with those obtained from the initial experiment associated with figure 8.4.

8.4 An Abandoned In-vitro Model

Originally the intention was to proceed to in-vivo work via the use of an in-vitro model - a piece of vein in place of the glass flow tube and a physiologically generated stenosis to replace the 'Magsep' analogue.It was envisaged that such a procedure should help in the determination of optimal thrombogenic stimulus parameters and thereby

minimise the future dependence upon the time and resources of other people.Thus veins could be removed from animals being sacrificed for other reasons,placed into iced saline and then used in the test rig at a convenient time. Stimulation parameter values could then be established without the need to set up in-vivo experiments and the associated legal requirements of having a Home Office licence holder in attendance.

The problem came in generating the occlusion.There are a variety of ways in which local thrombi can be artificially invoked but all depend upon the condition of the vessel and the blood.In removing the vessel and piping it into the flow circuit there is a high chance of damaging the inner surface,thereby exposing collagen and producing one large thrombogenic surface,rather than the desired localised one.The problem with the blood is just the opposite,it tends to become inactive through physical damage caused by stirring and pumping.Even a non recirculating pumping configuration that could be kept topped up with fresh blood failed to resolve the problem.After many attempts,the most successful of which was only marginally so,the intended in-vitro model was abandoned in favour of in-vivo experimentation.

8.5 Selection of an In-vivo Model

Logistic,physiological and pharmacological factors are all to be considered in the choice of a suitable animal model. Thus, for the intended operational context, the flow vessel should be accessible without major surgical intervention, should be of a size and flow status in keeping with the body of knowledge gained through previous

experiments and should be in a preparation exhibiting pharmacologically similar responses to man. The body of knowledge gained so far relates to non pulsatile flow in vessels with internal diameters in the range 0.8 to 1.0 mm. Therefore the use of veins of those diameters was decided upon: pharmacological considerations suggest that they be in a mammal.

The initial intention was to use the marginal vein of the rabbit ear: this vessel is superficial, is of the correct size and the animal is one commonly held for use in biological research. Unfortunately, within the restricted operational context,this model also proved too difficult to develop, on account of the rabbit being a very difficult animal to hold in a deep state of anaesthesia: either the animal is light and twitching or it is dead. Whereas up to 10 minutes of successful anaesthesia can be achieved with a combination of acetylpromazine, ketamine and xylazine (Ludders et al 1987),this is an inadequate length of time for the type of experimentation required in the present context.Thus this model also was eventually abandoned and an alternative one sought.

The superficial branch of the rat femoral vein proved to be much more satisfactory.A 25mm length of vessel could be exposed in the groin with only minimal surgery and the animal kept in a satisfactory state of anaesthesia with an intraperitoneal injection of 150mg/Kg of animal body weight of Inactin (Thiobutabarbitone).Although falling short of the ultimately non invasive potential of the rabbit ear vein,the rat femoral vein had the overwhelming advantages of reliability and repeatability; it falls within the diameter criterion of 0.8 to 1.0 mm.

8.6 Detection of Non-localised Velocity Increases

The first in-vivo experiment was designed to ascertain that blood velocity increases could indeed be recorded from an in-vivo preparation, despite all potential complications. The method chosen involved an affirmation of the dose response characteristics of Isoprenaline. This compound acts non selectively upon B receptors in the cardiovascular system to produce increases in blood flow. Although the femoral vein may in fact dilate in response to the compound, the cardiac output increases and a network of small feeder vessels also collectively dilates. The feeder vessels each have relatively small diameters but the summated response is of one large diameter conduit which allows the passage of more blood. The net result is an increase in the velocity of blood passing through the section of femoral vein under study (Rang and Dale,1987).

Adult white rats were anaesthetised by a licenced technician in the prescribed manner and placed ventral surface upper most in a suitably sized shallow perspex dish. One incision was made in the region of the left groin to expose the superficial branch of the femoral vein for the measurements and another in the right groin to expose the contralateral femoral vein as a site for drug injection via a suitably placed cannula. A third incision was made,in the region of the neck,to expose the carotid artery. This artery was also cannulated, with thin polythene tubing, and thereby connected to a blood pressure transducer and associated recording channel. The blood pressure signal is used as a method of monitoring both the physiological and pharmacological state of

the animal.

Once the small amount of surgery was complete the perspex dish was placed under the LDV microscope with the target vein nominally under the focussing objective. Exact location of the vein was achieved by movement of the microscope on a support which allowed 25 mm of adjustment in the x,y and z axes. Precision adjustment of the focussing objective allowed a further degree of fine control in the z axis. Course adjustment was undoubtedly aided by the use of the auxillary white light targeting beam but fine adjustment was invariably achieved by using the audio monitor as a guide to signal strength.

The experiment was conducted using dose concentrations of 5,10,15 and 20 ng of Isoprenaline per Kg. of animal body weight. The results are shown in figure 8.11. Three main observations can be made:

1) Although no independant flow/velocity system could be used to verify the results,they are qualitatively in good agreement with those associated with larger diameter vessels and the use of other measuring techniques. (Personal communications - Hunt A.A.E.,1988,referring specifically to results obtained from the femoral vein of the dog using an ultra sonic Doppler probe).

2) Although not particularly apparent from the traces, the signal was in fact cleaner than that associated with the glass flow tube model. This suggests that the LDV microscope and analyser were detecting levels of turbulence in the glass tube flow analogue which are absent in the

physiological counterpart. Therefore, if in the future arterial measurements are to be undertaken, the analyser time constant could probably be reduced and pulsatile signals recorded with a higher degree of fidelity than that associated with figure 7.9.

3) The system proved to be stable in use. Once set up for an experiment the apparatus required no further adjustment, unless there had been a gross movement of the animal. The latter event happened only infrequently.

Having established that the system could indeed follow in-vivo velocity changes it now appeared appropriate to consider making measurements on occlusion related increases. First of all however, it was necessary to consider ways in which that occlusion could be generated under controlled conditions.

8.7 The Thrombogenic Stimulus

Many techniques have been described whereby blood vessels are caused to be predisposed towards the growth of thrombi. Virtually all share the common feature of creating endothelial cell loss (denudation) so that exposed sub endothelial components (collagen in particular) promote platelet aggregation.

The work pioneered by Baumgartner and colleagues (1973,1976) used a physical scraping process to remove endothelial cells; a small inflated balloon is pulled through the vessel. Although elegantly simple the

technique is obviously highly invasive and produces a wide spread denudation.The jet velocity technique by its very nature requires a well defined and contained area for occlusion development.

Several other authors have used incident optical radiation to traumatize the vessel by creating burn induced lesions.Thus Kochen and Baez (1965) and Hovig et al (1974) have used pulsed ruby lasers to inflict injury to arterioles.Grant and Becker (1965) used 5ml pre-treatments of carbon loaded ink injected into the blood stream to enhance the energy transfer from the laser beam into the vessel.Kovacs and Gorog (1979) used a blue dye to enhance the effects of He-Ne radiation and produce similar intraluminal microburns.

Whilst still making use of optical radiation,but in a slightly different manner,Povlishock et al (1983) have described a technique based upon intravascular trauma created by photo generation of free radicals. A 2% solution of sodium fluoresin is injected into the blood vessel and filtered radiation (400 nm peak) from a mercury lamp is focussed down and allowed to interact with it to release free radicals at the desired position.

Electrical stimulation of a blood vessel represents another method of inducing vascular injury and consequent thrombus development.The predominant mechanism by which injury is induced may be expected to depend upon the magnitude of the current employed.Relatively low current,values of around 50 to 100 uA, will promote thrombus development.Piton et al (1978) ascribe this as being due to a change in

the 15 mV potential that normally exists between the inner and outer walls of a blood vessel and its effect thereafter on the charged blood cells. The normal state of affairs is for there to be a mild repulsion between blood cell and vessel wall; the thrombus formation is therefore a consequence of its removal or reversal. Higher stimulation current, those approaching 1000 uA, will also tend to produce a burning of the vessel wall and thus produce additional damage by a mechanism similar to that associated with incident high energy laser radiation.

Chemical stimulation represents another potent method of inducing thrombus development. As described in Chapter 1, mammalian platelets are aggregated by several agents which share the common feature of releasing adenosine diphosphate (ADP). The application of ADP to a vessel is therefore a potent thrombogenic stimulus. A small applied electric current will ensure permeation of ADP through the vessel wall and the desired platelet interaction. Such an iontophoretic application of ADP has been described by Begent and Born (1970) Micropipettes measuring 1-3 um across the tip were filled with a 1×10^{-2} M solution of the sodium salt of ADP in distilled water.With a negative potential applied to the micropipette and a current of 300 nA, ADP is expelled at the rate of about 1×10^{10} molecules per second. Thrombus development in hamster cheek pouch venules may be observed after only 5 seconds of such stimulation.

8.8 Detection of Velocity Changes Associated with Thrombus Development

Although the applied radiation and chemical stimulation methods

both had much to recommend them, electrical stimulation was the method chosen for the experiments about to be described. It was felt that the technique as a whole was simpler to implement and, additionally, some experience with the methodology was available elsewhere in the laboratory where the experiments were being accomodated and supervised.(Watts,1983)

A simple DC power supply,made up of a 9v PP3 battery with a 20K variable resistor, a 10K current limiting resistor and a 0 to 250 uA meter, was used as the source for stimulation. The negative side of the circuit was attached via a needle electrode to a convenient part of the rat body. The positive electrode was in the form of a 100u stainless steel wire and had to be introduced through the blood vessel wall at the intended trauma site. The wire was in fact introduced by first threading it through a 20g hypodermic syringe needle. Once so introduced the needle could be withdrawn over the wire,leaving about 0.1 mm of the tip of the wire in the vessel. This proved to be a delicate operation: too much wire sticking into the vessel creates an unintentional flow disturbance centre and,in extreme cases, may puncture the opposing wall.

The vein was often seen to contract down in diameter in response to the physical insult associated with introducing the wire. However if left for 10 minutes normal vessel function appeared to be re-established: it was only at this point that an LDV velocity base line value could sensibly be established. The results arising from two experimental runs are shown in figure 8.12.

The traces associated with runs 1 and 2 each represent the velocities measured one vessel diameter downstream of the centre of stimulation with delivered currents of 50,100, and 200uA.Because the two lower currents failed to produce enduring occlusions,each run represents the results from one animal.

In gross terms the results show grounds for subjectively graded comparison,the 200 uA current appears to produce an enduring occlusion,the 100 uA current appears to produce a pronounced but temporary occlusion,the 50 uA current does qualitatively the same thing but less so.The results don't otherwise readily stand upto more detailed comparison.

Because the best method of comparison appeared to be on the macroscopic scale,the traces associated with figure 8.12 were placed on a digitizing tablet and a computer program run which enabled a retrospective integration of the curve to be performed.Thus figure 8.13 shows what is effectively a cumulative platelet build up trace superimposed on the original velocity trace.Whereas for each run the slope of the 100 uA summation line is greater than that associated with 50 uA, the trend is not continued for 200 uA. Subjectively,the most appropriate guide appears to be the height of the summation line at a time corresponding to approximately 2 - 3 times the stimulus duration.This apparently adventitious method of arriving at an index is not without precedent.For example,an analogous degree of empiricism has been applied to evaluate bronchoactive agents in the guinea pig via an extrapolation of the respiratory rate integral (Ball et al.1987).

8.9 Discussion

Considerably more work is required to substantiate the generality of the observations associated with the previous section. Unfortunately, within the framework of this thesis, for both logistic and legal reasons, it is not currently possible to carry out the necessary amount of experimentation. Future work in this area must inevitably be designed and undertaken by those qualified in the more relevant disciplines of medicine and biology.

Never the less, it is suggested that the equipment and underlying techniques have been developed to a stage where their potentiality for assessing antithrombotic activity has been demonstrated. Through the sum of the information gained from in-vitro and in-vivo experiments it has been shown that blood velocity increases are detectable which reflect aspects of the growth rate of an induced thrombus. By extension, it is this that indicates the feasability of monitoring such growth as an index of efficacy of antithrombotic agencies. Observations made so far all indicate that the method should prove to be relatively free from environment artifacts and inexpensive to operate.

Although success is claimed for that which has been developed so far, almost inevitably there are already modifications / improvements which have been identified through use. Such changes, to the implementation rather than the underlying evolved rationale, represent one of the topics covered in the general assessment format of the next and final chapter.

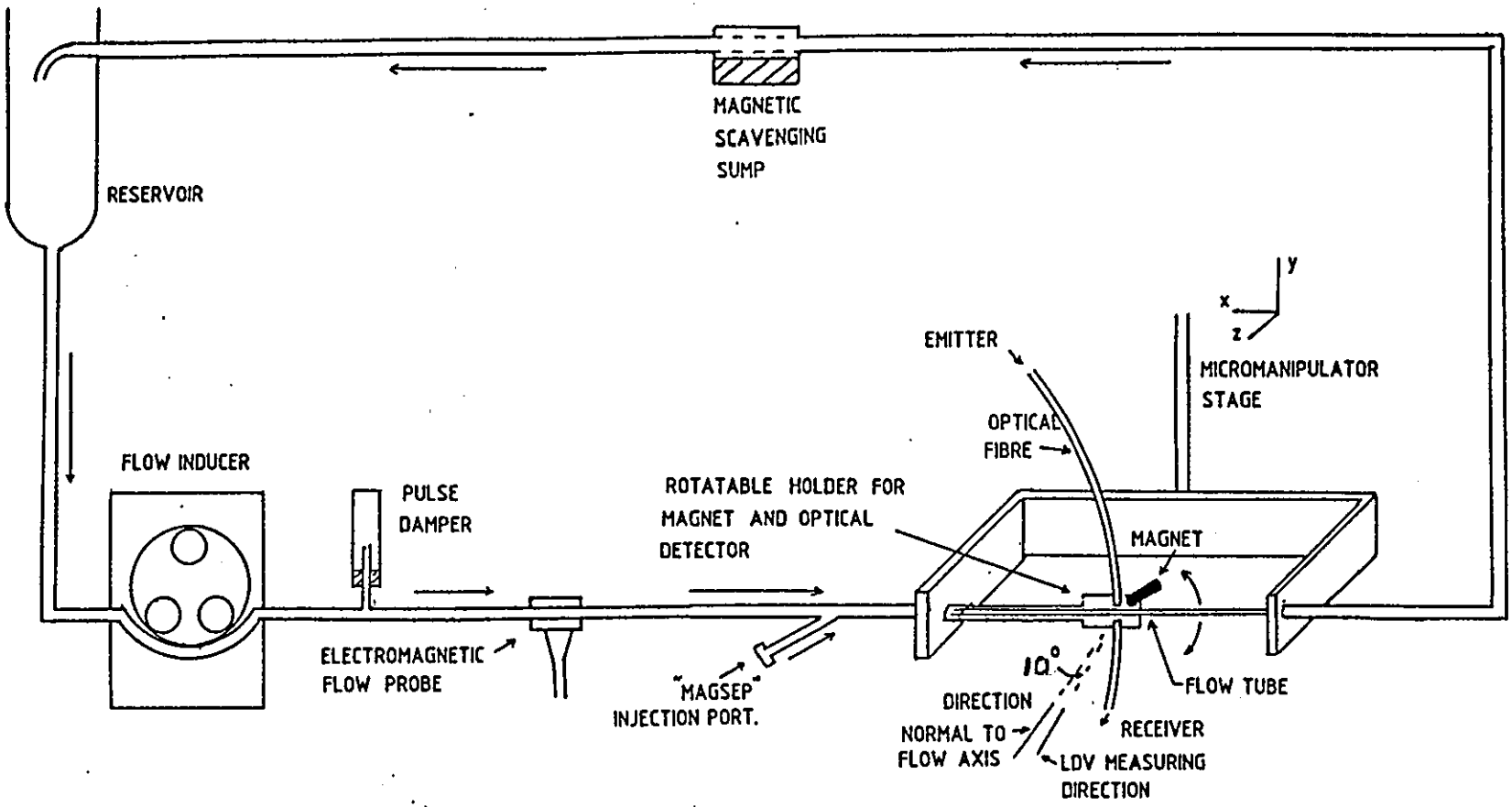

Figure 8.1: Diagram showing the test rig associated with the magnetic particle occlusion model.Optical fibre coupled photo emitters and detectors provide independent assessment of occlusion size.Velocity measurements are made at an angle of 6^{o} to the flow tube's main axis.

18696/1-2

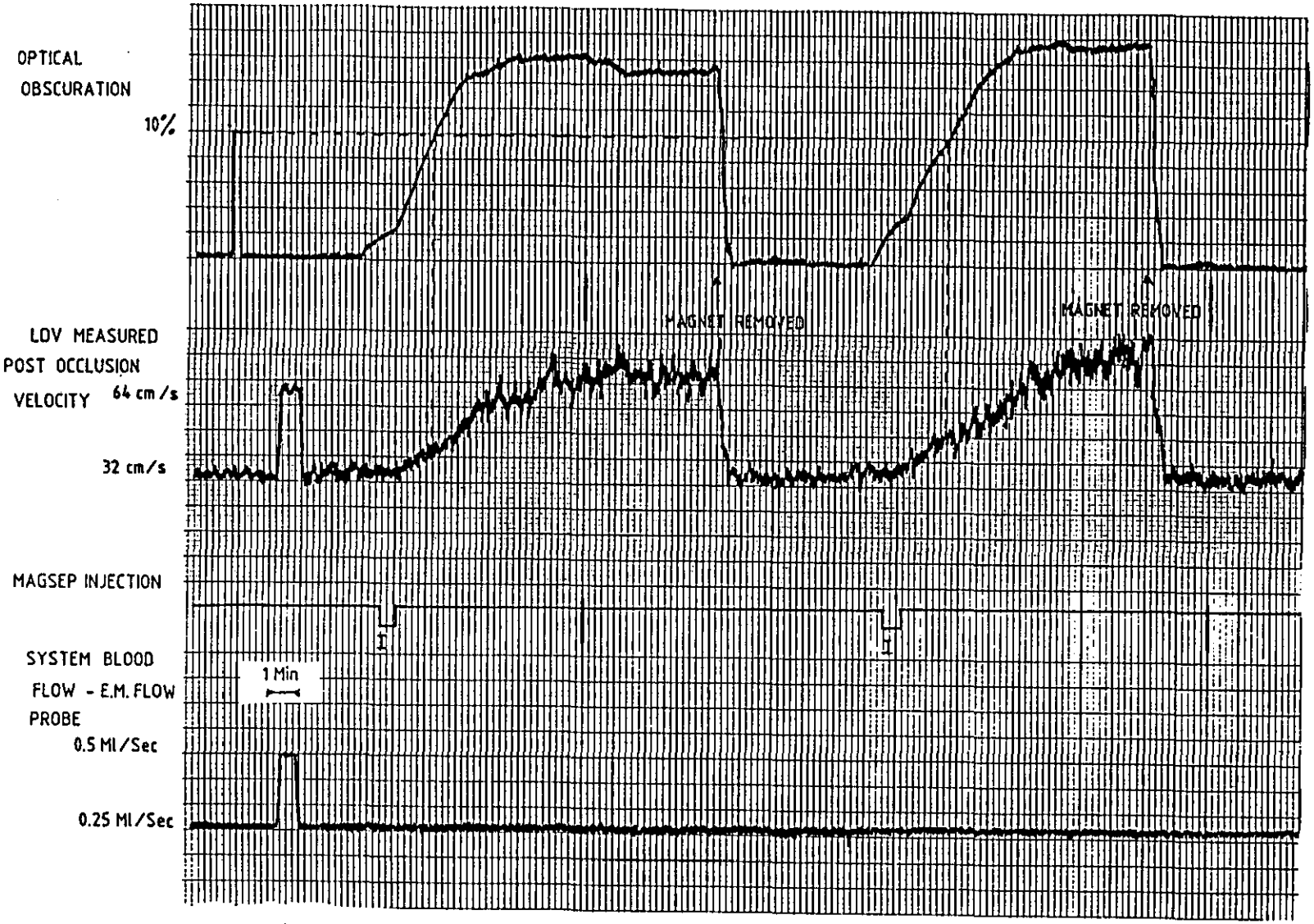

Figure 8.4: Results obtained from the injection of a 1ml. suspension of 5% of Magnetic material (Magsep) in saline.The velocity measurement was made at a distance equivalent to 1 diameter (1 mm) downstream of the occlusion centre.Projection of the optical obscuration calibration pulse onto the velocity signal is used to suggest that detection should be possible by 10% reduction in lumen size.

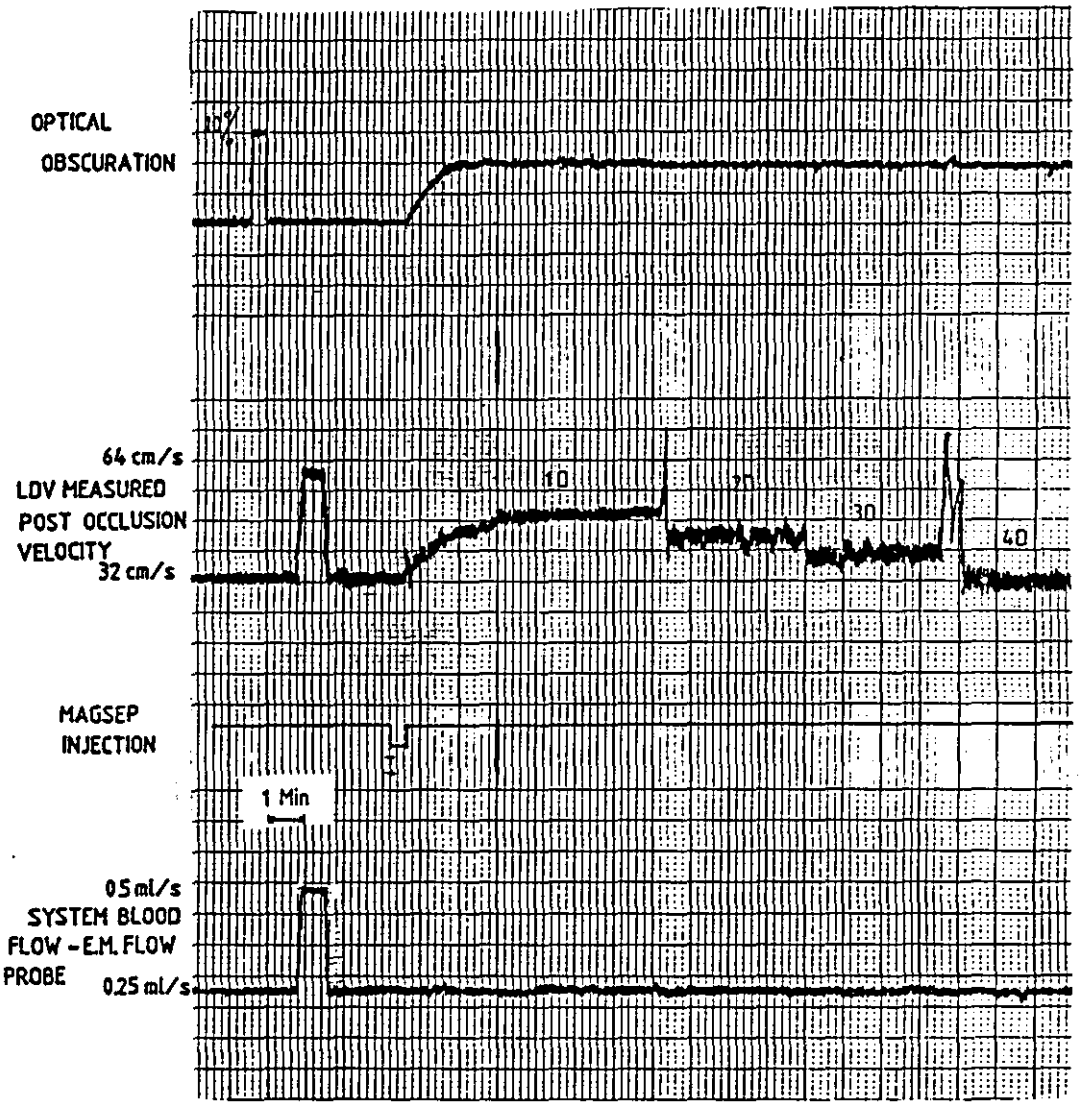

Figure 8.5: Result showing that maximum velocity increase is obtained at 1 diameter (1mm) post occlusion point. This is in agreement with the findings associated with the previously described glass pip model.

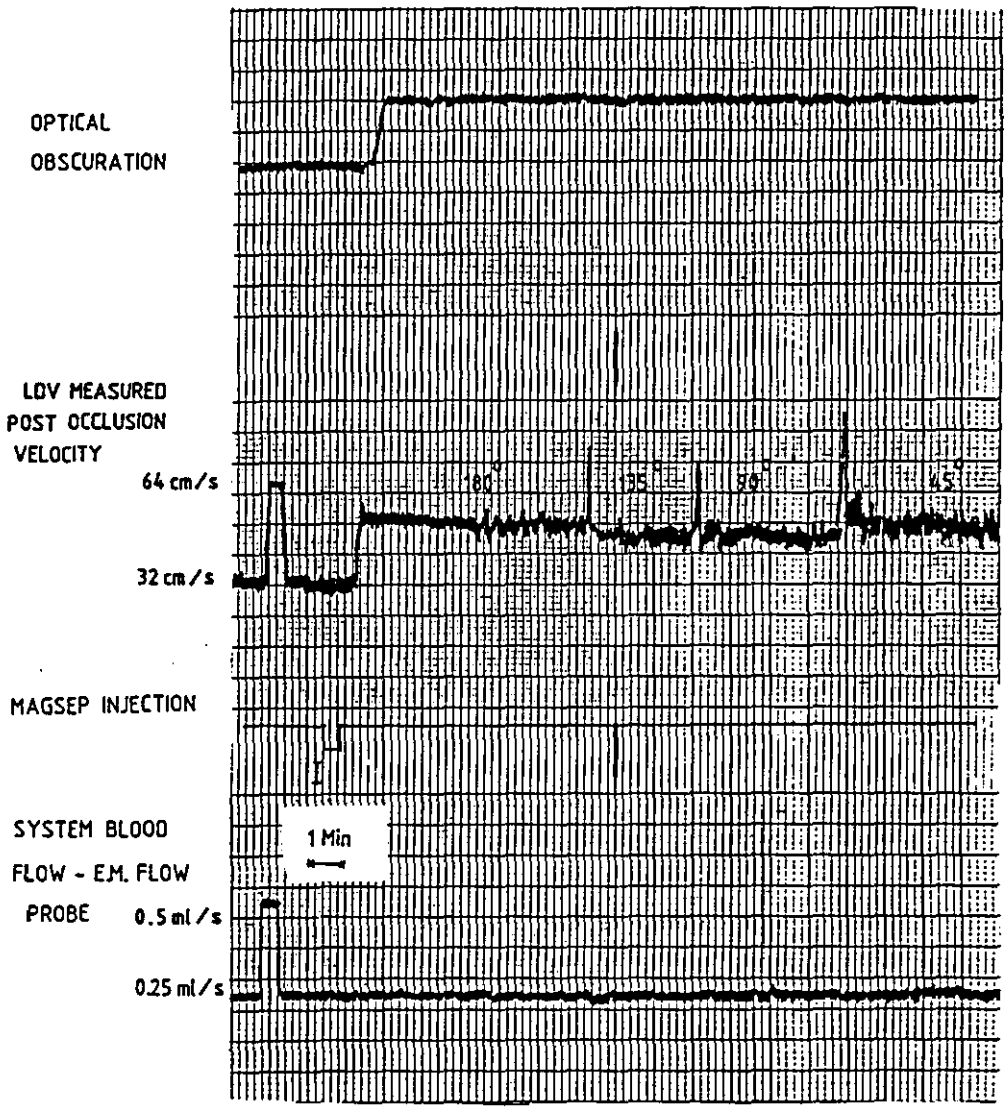

Figure 8.6: Result showing that changes in occlusion radial orientation relative to measuring position yield minimal changes in measured velocity increase.This is probably a manifestation of photon diffusion degrading the spatial resolution of the LDV system.

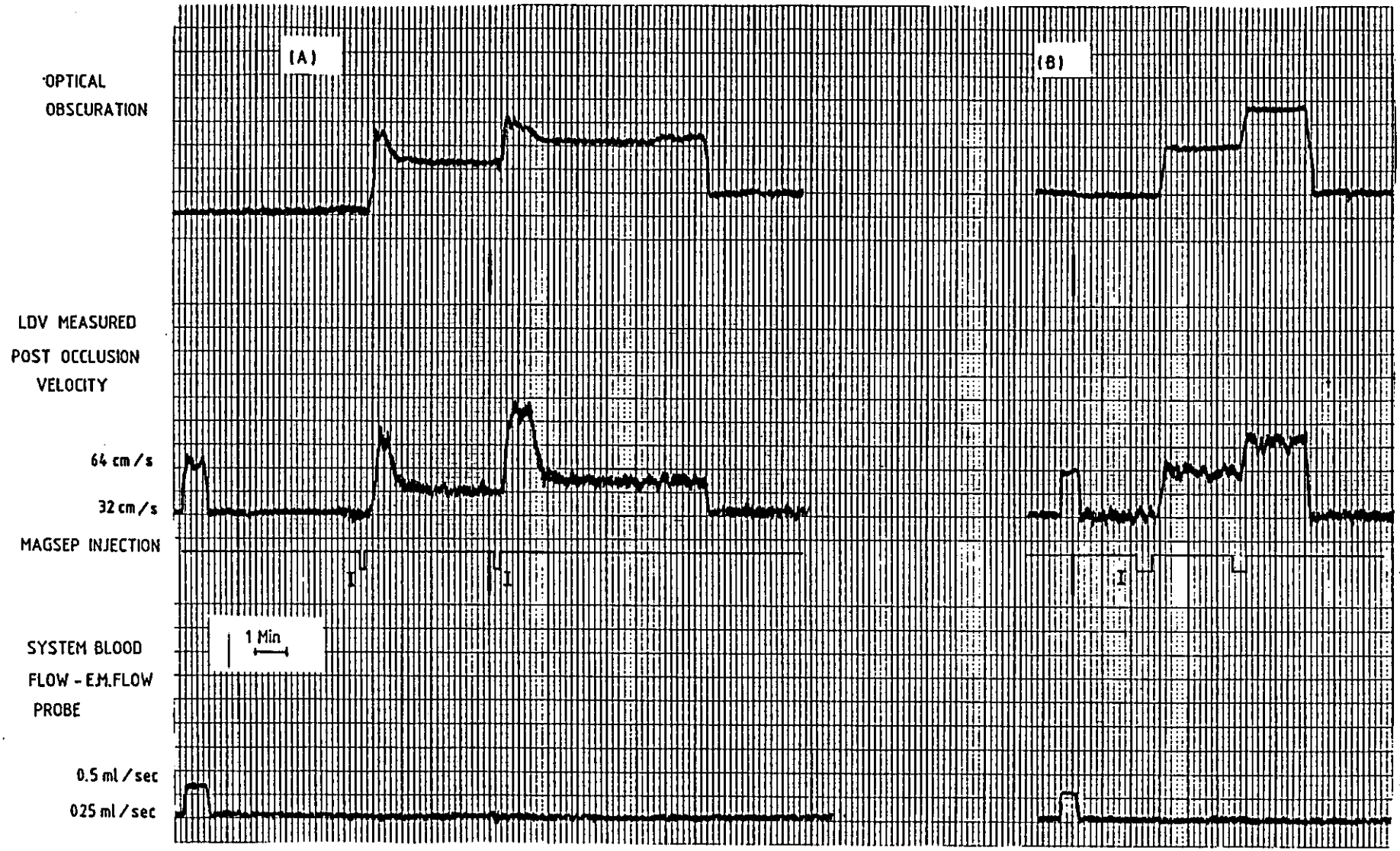

Figure 8.7: Showing the effects of Magsep injection time on occlusion stability. a) With a five second injection time around 50% of the material is swept away. Similar loss occurs following a second, compound, injection. b) With a twenty second injection time a stable occlusion is formed. A compound injection also then yields similarly stable results.

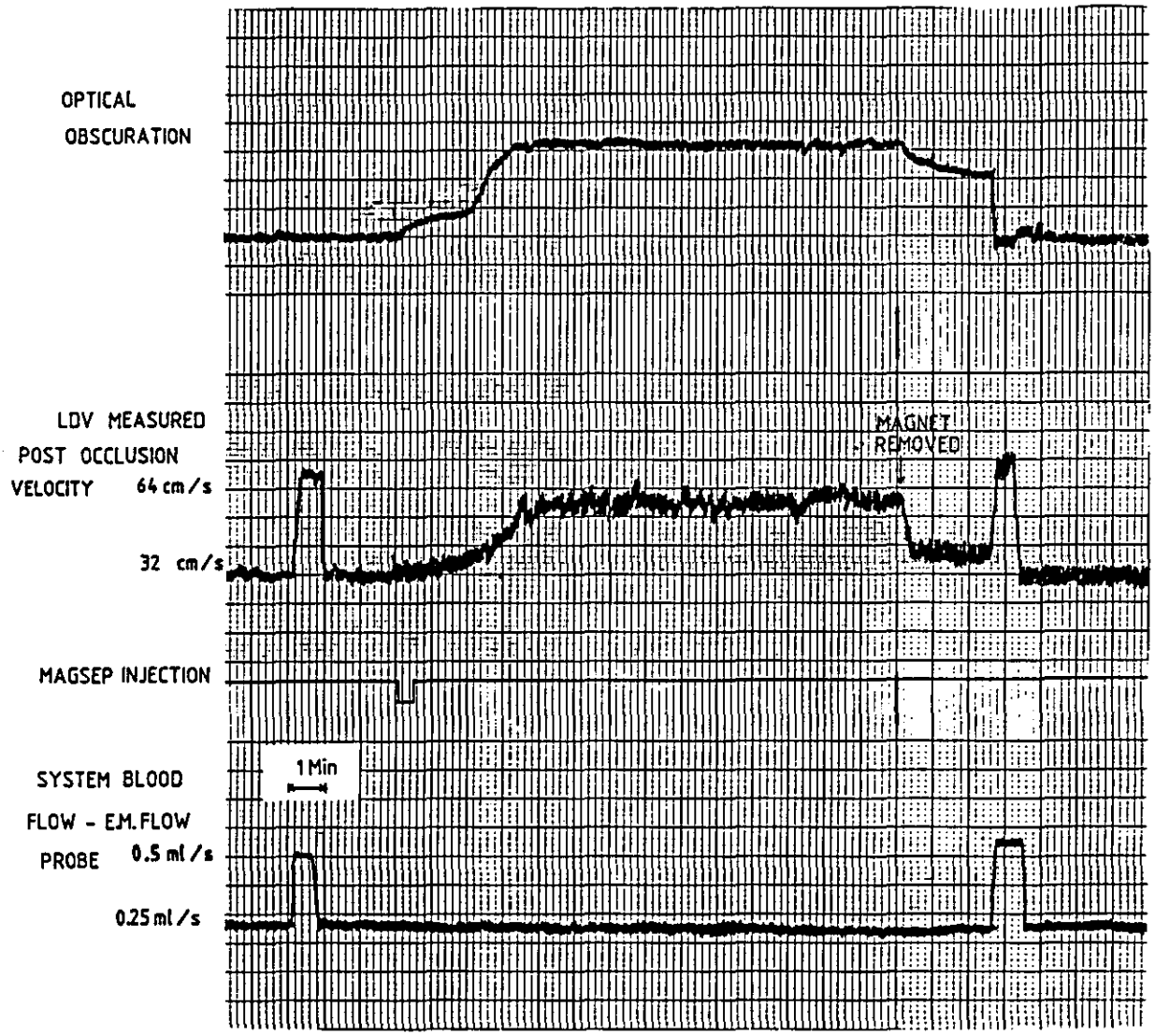

Figure 8.8: Response of the LDV measured post occlsion velocity to an anomalous occlusion dispersion. Following the removal of the attracting magnet Magsep remained: it was then dispersed by a short period of increased fluid flow.

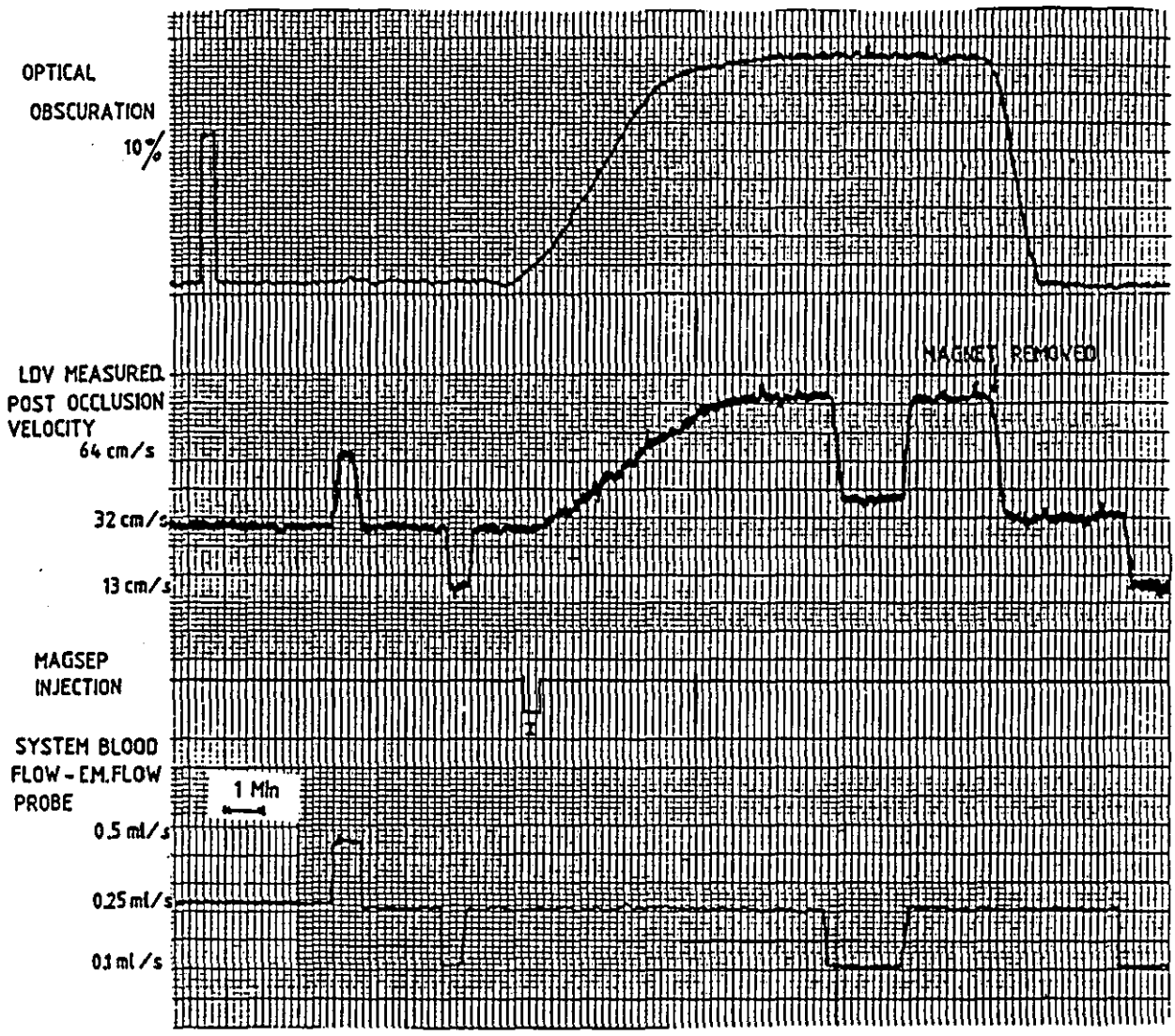

Figure 8.9: In a 1mm I.D. tube,with blood flow rates of 0.25 ml/sec and 0.1 ml/sec the results are similar.At 1 diameter downstream of the occlusion a jet is formed and it's velocity is approximately twice that of the bulk flow.

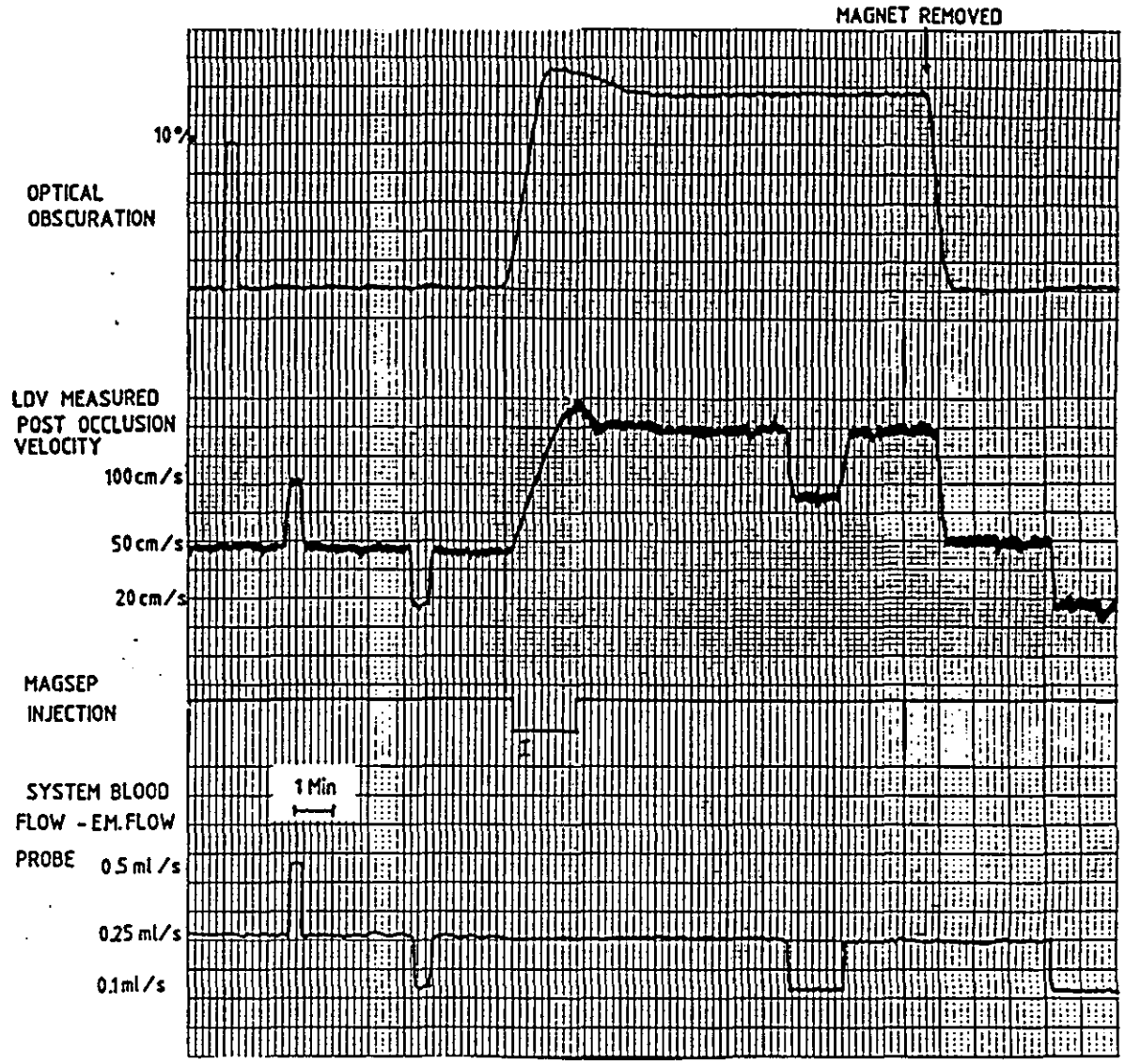

Figure 8.10: In an occluded 0.8mm I.D. tube, with blood flow rates of 0.25 ml/sec and 0.1 ml/sec, the results are qualitatively similar to those associated with the 1.0 mm I.D. tube. Higher velocity gradients and their effect on occlusion stability account for such differences as there are. In the narrow tube Magsep build up is more rapid and the velocity is higher: the velocity scaling factor has been adjusted accordingly.

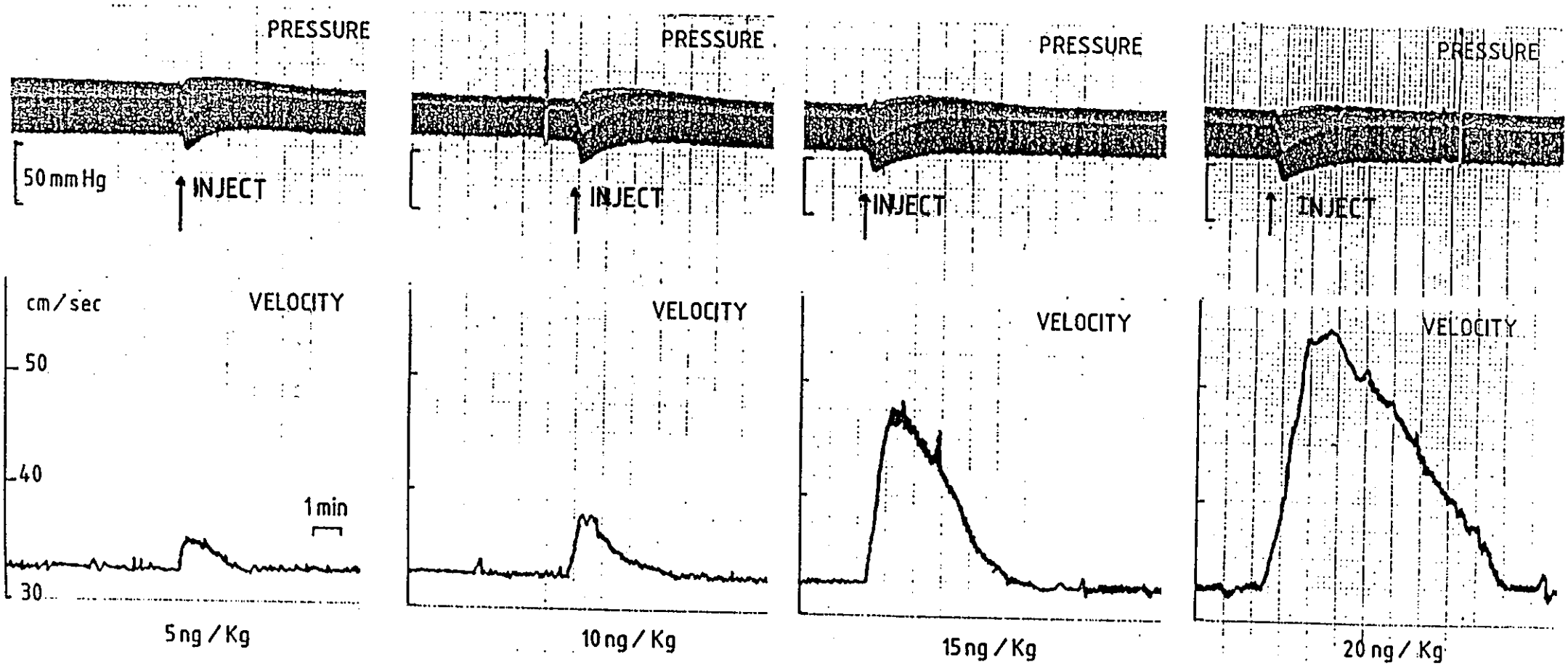

Figure 8.11: Isoprenaline induced velocity changes in a superficial branch of the rat femoral vein. Dose responses are in good qualitative agreement with those obtained from other preparations, using other measurement devices.

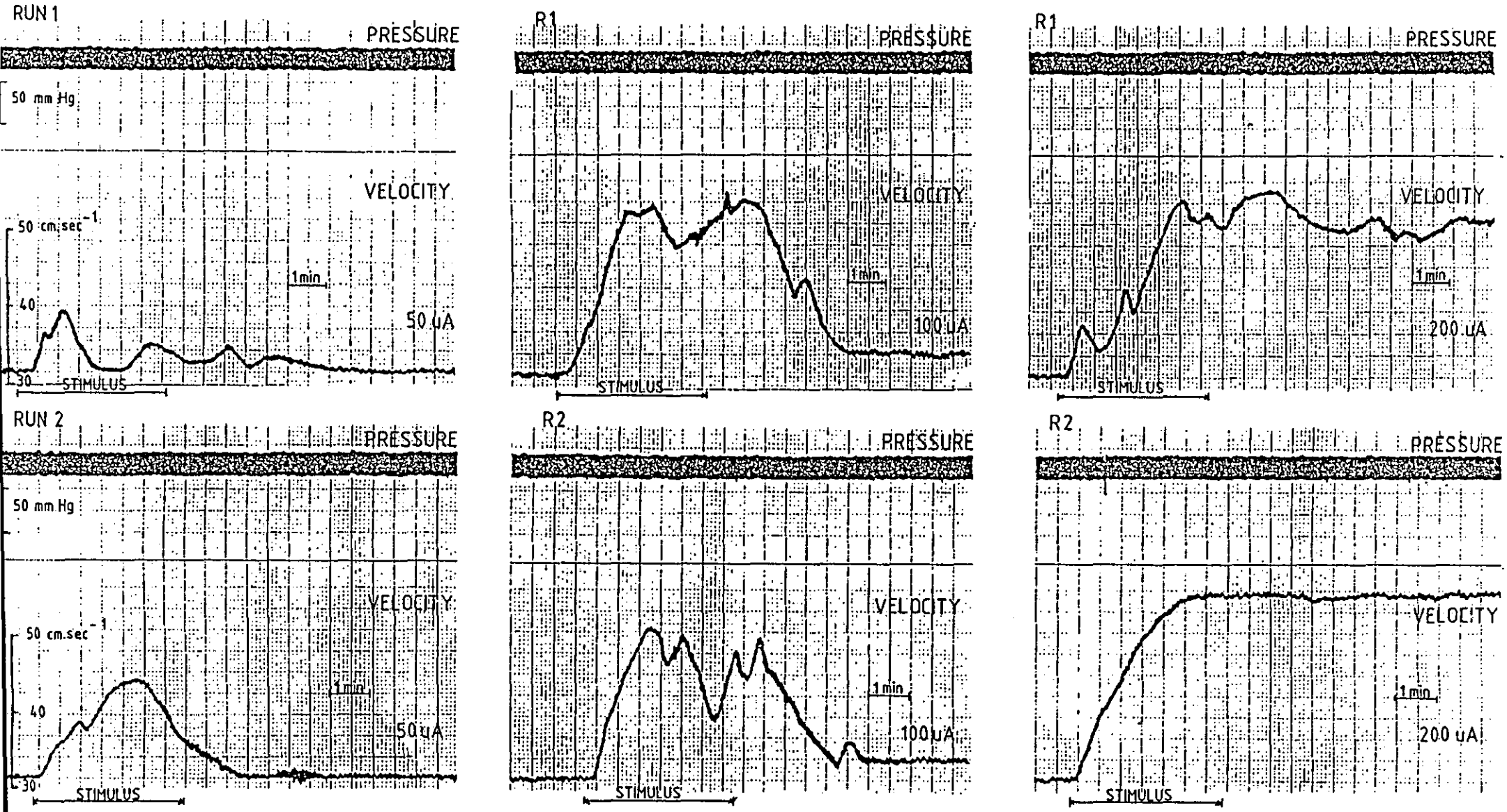

Figure 8.12: Occlusion related velocity changes induced in the superficial branch of the rat femoral vein by electrical stimulation. The measurement site is approximately 1 vessel diameter downstream of the centre of stimulation.

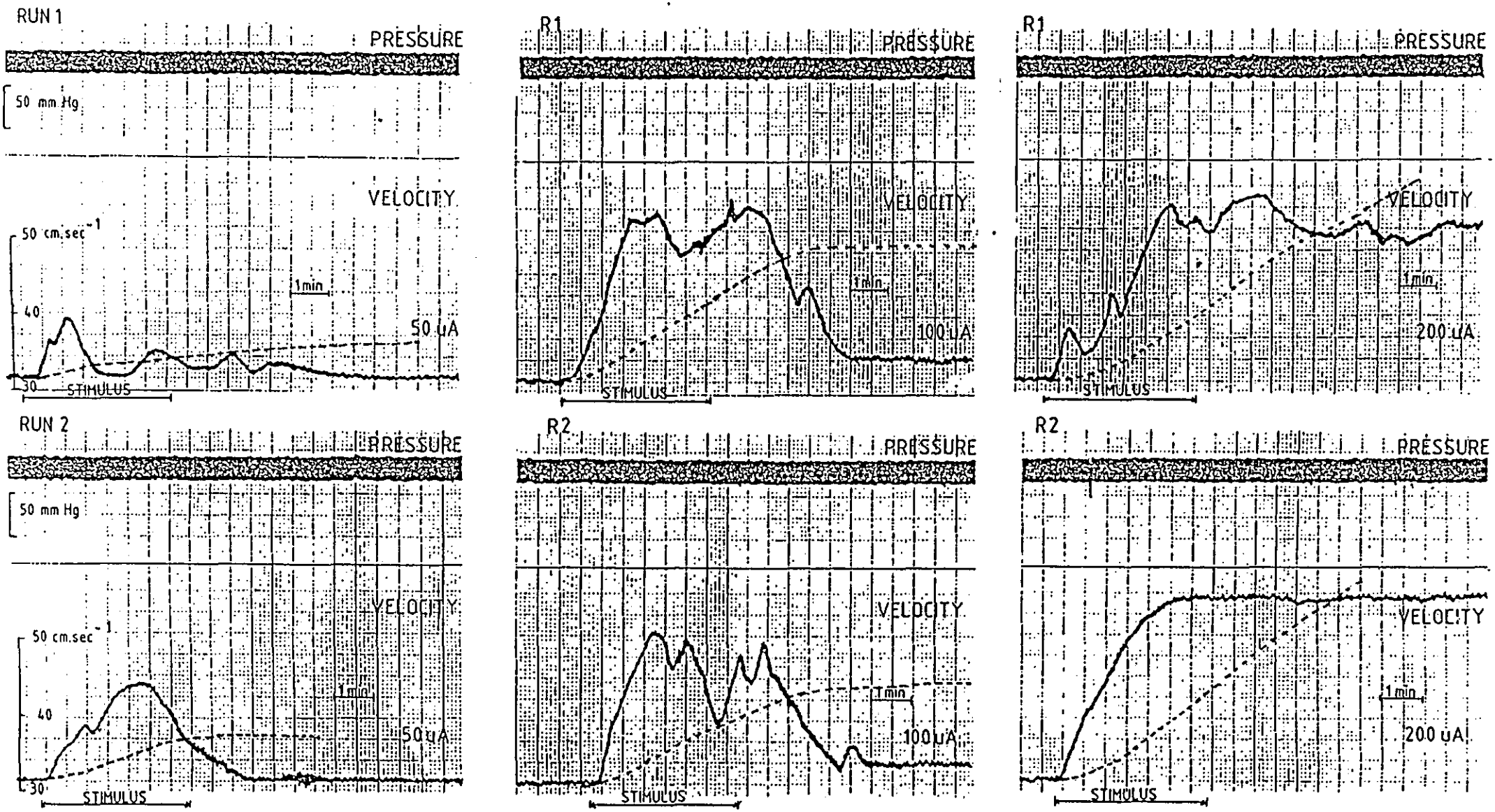

Figure 8.13: The same traces as were shown on the previous page with the addition of a curve representing the integrated function.Superficially at least,the integral appears to lead to a viable thrombus growth index.

CHAPTER 9

CONCLUSIONS

This thesis has set out to describe the work associated with the development of an in-vivo method for assessing the antithrombotic properties of pharmacological compounds. In order to carry out that work it was found necessary to understand the background to the problem and the current range of methodologies. This, and the underlying concepts associated with the new method, have been described. It is believed that the results contained within this thesis amply vindicate the course of research followed and the resultant practical implementations.

Never the less, whereas a method has been developed, it is recognised that only circumstantial evidence has been presented to suggest that it will in practice have any part to play in assessing the required properties of compounds. Fortunately or unfortunately, practical considerations and legislation combine together to dictate that such evidence will only be provided by those formally qualified in the disciplines associated with the biological sciences. A situation therefore exists which has many parallels in other areas of technology: acceptance of the method will depend upon it's use and, perversely, use will depend upon acceptance. Ultimately full acceptance may only be achieved when the method demonstrates itself, possibly even fortuitously, capable of providing some unique facet of information.

Acceptance of the technique may in fact be accelerated by parallel use of the instrumentation in other areas of drug research. Early indications are that in addition to the target antithrombogenic drug project, the laser Doppler microscope may be used to measure the flow of blood in the microvasculature of the brain, in the context of migraine research.

In any event, it must be recognised that even at best, the method will only be used to augment results derived from other experimental procedures. It is unlikely that any one method will ever prove to be the method of choice in antithrombotic drug research; several techniques provide complimentary information which, it is hoped, will lead to understanding and success.

Returning to the developed system as it now stands, one can identify that in addition to more basic pharmacological evaluation some histology should be performed, to correlate recordings with thrombus dimensions. Such lines of development are totally dependant upon the work of others and so have not been included within the main body of this thesis; they are however relatively simple to identify. More conjectural is the development of alternative configurations for the laser Doppler flow measuring system. An identifiable weakness of the present implementation is the assumption that the velocity of blood through the vessel is only influenced by the occlusion. In practice the bulk flow may change for other reasons or, as observed during the early stages of electrical stimulation, the vessel diameter may change and thereby influence the base line velocity. Such problems could be

overcome if pre and post occlusion velocity values were to be recorded simultaneously. Pre occlusion values would then act as the reference against which relative increases could be measured.

Future developments for the basic laser Doppler velocimeter thrombus measuring rationale might therefore include the construction of a dual channel device. Whereas for a single channel device the laser Doppler microscope described in Chapter 7 proved to be an excellent device for the intended operational context, its size would tend to preclude it from being the implementation of choice in a twin measurement head configuration. Conceivably a dual channel device could be built within one housing but individual beam alignment and focussing would be difficult. There exists, therefore, the possibility that a dual channel fibre optic device might prove to be more practicable implementation.

It is possible that the single channel device described by Dyott (1978) could be turned into a dual channel device by using a beam splitter cube to divert the laser beam to two virtually independant beam launching and detection stages. The twin velocimeter fibres could be terminated with GRIN rod lenses at their distal ends to provide focussing of the measurement beam into the blood flow. The lenses could be set some 3 - 4 mm apart in a holder which in turn could be held in intimate contact with the vein by ties of surgical cotton. An electrode, the source of the thrombogenic stimulus, could be set midway between the two sensing lenses. It is possible to envisage that ultimately such a system could be made both smaller and more robust by utilizing fibre

'pig tail' elements and splicers to form a quasi integrated velocimeter.

Still further work could include development of the signal processing system. Either a dual channel version of the special purpose analyser could be constructed or it may be opportune to investigate the role that could be played by cross correlation of a pre and post occlusion signal.

Cross correlation is the study of two variable quantities, one being shifted temporally or spatially relative to the other.In the present context this would refer to the post occlusion signal shifted by the transit time from the pre occlusion signal.In the time domain the flow velocity may be determined by introducing a calibrated delay into the correlation circuit and adjusting it to give a correlation maximum.The delay value then corresponds to the transit time,hence velocity.

If the correlation is performed in the frequency domain,the correlation function may be performed by utilizing properties inherent within the fast Fourier transform.The correlation coeficient will be at a maximum with the transit time compensated for by a delay but will fall as the Doppler shift spectrum contents of the post occlusion signal change with increasing post occlusion velocity.At this stage it is only possible to speculate that a reduced bit transform might give sufficient information in a sufficiently reduced processing time to allow an on-line processing capability,even for pulsatile signals.

In addition to providing a method for deriving velocity information,cross correlation is a powerful technique for extracting signals from noise. It is therefore possible that under some circumstances trans dermal recordings might be made,thereby realizing the potentially totally non invasive nature of optical measuring systems.Photon correlation spectroscopy (Pike,1969) is already a very powerful technique for dealing with weak LDA/LDV signals and is carried out using single bit processing. The concept currently being advanced would seek a signal to signal correlation rather than a source to signal correlation but might employ similar processing algorithms.

To conclude, it is believed that a system has been developed which will allow the antithrombogenic properties of pharmacological compounds to be assessed in-vivo; it is therefore in accord with the research objectives originally embarked upon. It is also recognised that more pharmacological evaluation is required before the true potential of the equipment and methodology can be assessed and unqualified success claimed. However, such evaluation must be performed by others, qualified in the relevant life science disciplines and possessing the appropriate skills. In the mean time several areas for fruitful and related instrumentation development have been identified and commented upon. Circumstances and acceptance of the basic measurement philosophy will dictate if they are to be acted upon.

APPENDIX A

THE FOURIER TRANSFORM

The Fourier transform and its application to frequency analysis stems from one facet of the work on 'An Analytical Theory of Heat' by the French mathematician Jean Joseph Fourier (1768 - 1830). He found that any periodic time function, even the most 'unruly' and 'irregular' could be broken down into an infinite sum of properly weighted sine and cosine functions, the resulting series being of the type:

$$y = \frac{a}{2} + a_1 \cos x + a_2 \cos 2x + \ldots . b_1 \mathrm{Sin}\, x\ b_2 \mathrm{Sin}\, 2x$$

$$= \frac{a_0}{2} + \sum_{r=1}^{\infty} (a_r \cos rx + b_r \mathrm{Sin}\, rx)$$

where $a_0 = \frac{1}{\pi} \int_{-\pi}^{+\pi} f(x)\, dx$

$$a_r = \frac{1}{\pi} \int_{-\pi}^{\pi} f(x) \cos rx\, dx \quad (r = 1,2,3\ldots.)$$

$$b_r = \frac{1}{\pi} \int_{-\pi}^{\pi} f(x) \sin rx\, dx \quad (r = 1,2,3\ldots.)$$

For a waveform x(t) of period T, that is x(t) = x(t+T), the Fourier series may be written:

$$x(t) = a_0 + \sum_{n=1}^{\infty} a_n \cos\left(\frac{2\pi nt}{T}\right) + b_n \sin\left(\frac{2\pi nt}{T}\right)$$

If the coefficients a_n and b_n are known, the magnitude of each frequency component in x(t) may be determined. The amplitude of the frequency $f_n = (n/T)$ is given by $\sqrt{a_n^2 + b_n^2}$.

The Fourier series, as such, requires a periodic time function and to overcome this limitation Fourier evaluated the series as the period of the waveform approached infinity. A transform pair may then be defined:

$$S_x(f) = \int_{-\infty}^{\infty} x(t)\, e^{-i2\pi ft}\, dt \quad \text{(forward transform)}$$

and $$x(t) = \int_{-\infty}^{\infty} S(f) e^{i2\pi ft}\, df \quad \text{(inverse transform)}$$

where $e^{\pm i2\pi ft} = \cos(2\pi ft) \pm i \sin(2\pi ft)$

$S_x(f)$, the Fourier transform of x(t), now contains the amplitude and phase information at every frequency present in x(t), without demanding

that x(t) be periodic.

If the Fourier transform is to be implemented using digital techniques the continuous input signal must be converted into a series of discrete data samples, separated by an interval Δt. Now evaluation of the transform integral requires that the samples be separated by an infinitesimal amount of time, i.e. $\Delta t \rightarrow dt$. With an analogue to digital converter, necessary to convert the time varying analogue input signal into digital data for processing, the afore mentioned conditions cannot be met and it is therefore necessary to calculate the function:

$$S'_x(f) = \Delta t \sum_{n=-\infty}^{n=\infty} x(n\Delta t) e^{-i2\pi f n \Delta t}$$

where $x(n\Delta t)$ are the measured values of the input function.

In order to calculate S'(f) from the transform as it now stands, it would be necessary to take an infinite number of samples of the input waveform and, since this would take an infinite amount of time, it is clearly impracticable. If the input is to sampled from some zero time for some finite time, T seconds, the transform must be further rewritten to include the finite sample number. The resulting transform is known as the discrete finite transform (D.F.T) and is given by:

$$S''(m\Delta f) = \Delta t \sum_{n=0}^{N-1} x(n\Delta t) e^{-i2\pi m \Delta f n \Delta t}$$

where m = the transform coefficient associated with the n th. data point in a series of N, $0 \leqslant m \leqslant N-1$.

Δf = frequency resolution
n = the n th. point in a series of N discrete data points, $0 \leqslant n \leqslant N-1$.
N = Number of discrete data points, equidistant in time.

This new equation assumes that the function observed between zero and T seconds repeats itself with period T for all time, whether or not x(t) is actually periodic.

The new transform no longer contains accurate magnitude and phase information about all the frequencies contained in $S_x(f)$. Instead $S''_x(f)$ describes the spectrum of x(t) upto some maximum frequency F_{max}, the value of which is dependent upon the sample spacing Δt. In 1948 Shannon demonstrated the degree of redundancy present in most communication channels and showed that in order to define a sinusoid uniquely it only requires slightly more than two samples per period. This sampling rate is often referred to as the Nyquist rate. Implicit in Shannons work is the condition that the value of Δf, the frequency resolution of the system, is a function of the sample length, T.

Calculation of the coefficients in the discrete Fourier transform has been made particularly efficient by the introduction of the Fast Fourier Transform (F.F.T) in 1965 by Cooley and Tukey. The F.F.T. can be used in place of the continuous Fourier transform only to the same

extent as the discrete Fourier transform, the difference being that there is a substantial reduction in computational steps. Previous methods required a number of computations proportional to N^2. By abolishing redundancy and exploiting symmetry within the calculation, the new method only requires a number proportional to $N \log_2 N$. The condition for the most efficient application of the F.F.T. is that the number of samples N, is equal to an integer power of 2, i.e. $N = 2^m$. A complete Fourier transform can be obtained quickly through simple addition and multiplication and, as such, is ideally suited to present day digital computer techniques.

APPENDIX B

THE FORRESTER AND YOUNG MODEL OF JET FORMATION

The shape of the axisymmetric stenosis used in the Forrester and Young model was specified as being bounded by a cosine curve. Its shape is therefore given by the equation:

$$R = R_0 - \frac{\delta}{2}\left(1 + \cos\frac{\pi z}{Z_0}\right) \quad \ldots\ldots\ldots \text{B.1}$$

$$-Z_0 \leq z \leq Z_0$$

where, referring to Fig.B.1:

Ro = the radius of the tube outside the stenotic region.
2Zo = the length over which the stenosis extends
δ = the maximum protrusion of the stenosis into the lumen.

The equations of motion for a viscous fluid are the Navier-Stokes equations. For two dimensional incompressible flow they may be written:

$$v\frac{\partial u}{\partial r} + u\frac{\partial u}{\partial z} + \frac{1}{\rho}\frac{\partial p}{\partial z} = \nu\left(\frac{\partial^2 u}{\partial r^2} + \frac{1}{r}\frac{\partial u}{\partial r} + \frac{\partial^2 u}{\partial z^2}\right) \quad \ldots\ldots \text{B.2}$$

$$v\frac{\partial v}{\partial r} + u\frac{\partial v}{\partial z} + \frac{1}{\rho}\frac{\partial p}{\partial r} = \nu\left(\frac{\partial^2 v}{\partial r^2} + \frac{1}{r}\frac{\partial v}{\partial r} - \frac{v}{r^2} + \frac{\partial^2 v}{\partial z^2}\right) \ldots \text{B.3}$$

The equation of conservation of fluid mass may be written:

$$\frac{\partial u}{\partial z} + \frac{1}{r}\frac{\partial}{\partial r}(r, v) \quad \ldots\ldots\ldots \text{B.4}$$

where p = fluid pressure
u = velocity component in the z direction
v = velocity component in the r direction
ρ = fluid density

In Forrester and Young's paper an exact analytical solution of the equations was deemed to be not feasible. Rather, approximations were sought that might allow a qualitative interpretation of the equations.

In previous work by Forrester (1968), it was found that if δ/Z_o is very much less than unity, then the axial normal stress gradient term in equation B.2 is negligible compared to the gradient of the shear component.

Additionally, if δ/Ro is small, the radial variation in pressure can be neglected. Thus for a 'mild' stenosis, one in which both δ/Zo and δ/Ro are small, equations B.2 and B.3 can be approximated as

$$u\frac{\partial u}{\partial z} + v\frac{\partial u}{\partial r} = \frac{1}{\rho}\frac{\partial p}{\partial z} + \nu\left(\frac{\partial^2 u}{\partial r^2} + \frac{1}{r}\frac{\partial u}{\partial r}\right) \quad \text{B.5}$$

and

$$\frac{\partial p}{\partial r} = 0 \quad \text{B.6}$$

Equation B.5 can now be intergated across the tube to obtain:

$$\frac{d}{dz}\int_0^R r u^2\, dr = -\frac{1}{\rho}\frac{dp}{dz}\frac{R^2}{2} + \nu R\left(\frac{\partial u}{\partial r}\right)_R \quad \text{B.7}$$

The boundary condition u=v=0 at r = R has been applied. The integrated form of equation B.4 is:

$$Q = \pi R^2 \bar{U} = \int_0^R 2\pi r u\, dv \quad \text{B.8}$$

$\bar{U}$ is the mean velocity at any given cross section with radius R, and Q is the volume rate of flow.

The assumption is then made that the radial dependence of the axial velocity can be expressed as a fourth order polynomial of the type:

$$\frac{u}{U} = Ak + Bk^2 + Ck^3 + Dk^4 + E \quad \text{B.9}$$

where k = (R - r)/R and U is the centre line velocity. A through E are coefficients and are evaluated from the following five conditions:

(a) at r = R, u = 0
(b) at r = 0, $\frac{\delta u}{\delta r} = 0$
(c) at r = 0, u = U
(d) at r = R, $\frac{dp}{dz} = u\left(\frac{\delta^2 u}{\delta r^2} + \frac{1}{r}\frac{du}{dr}\right)$
(e) at r = 0, $\frac{\delta^2 u}{\delta r^2} = -\frac{2U}{R^2}$

The boundary conditions of zero velocity at the wall and axisymmetric flow are given by (a) and (b). Condition (c) is simply a definition. Condition (d) is obtained from equation B.5. It has been assumed that at r = 0, the velocity profile is very nearly parabolic ($u = U[1 - (r/R)^2]$) so that the second derivative of u with respect to r can be approximated by (e). The assumption has therefore been made that it is only near the wall of the tube that the velocity profile will deviate significantly from the parabolic form.

Taking into account the coefficient evaluations, equation B.9 thus becomes:

$$\frac{u}{U} = \left(\frac{-g+10}{7}\right)k + \left(\frac{3g+5}{7}\right)k^2 + \left(\frac{-3g-12}{7}\right)k^3 + \left(\frac{g+4}{7}\right)k^4 \quad \text{B.10}$$

where

$$g = \frac{R^2}{uU}\frac{dp}{dz}$$

The velocity profiles are now seen to be functions of a single parameter, g, which in turn depends on the pressure gradient.

Equation B.10 can now be substituted into equation B.8 and integrated to give:

$$U = \frac{210}{97\pi}\frac{1}{R^2}\left(Q + \frac{\pi}{105u}R^4\frac{dp}{dz}\right) \quad \text{..... B.11}$$

The parameter g may be determined from equation B.7, an equation of momentum. However, rather than undertake the direct solution of the equation, Forrester and Young make the simplifying assumption of parabolic flow through the stenosis.

$$\text{i.e.} \qquad u = 2\bar{U}\left[1 - \left(\frac{r}{R}\right)^2\right] \quad \text{..... B.12}$$

Young (1968) had demonstrated that for low Reynolds numbers and for mild stenoses, the velocity profile approaches the parabolic distribution. Thus the validity of the assumption can be expected to increase as the Reynolds number is decreased.

Substitution of equation B.12 into the left hand side of equation B.7 and evaluation of the integral reduces the momentum equation to:

$$\frac{d}{dz}\left(\frac{2}{3}R^2\bar{U}^2\right) = \frac{1}{\rho}\frac{dp}{dz}\frac{R^2}{2} + \nu R\left(\frac{\partial u}{\partial r}\right)_R \quad \text{..... B.13}$$

Expressions for U and $(\partial u/\partial r)_R$ from equations B.8 and B.10 are now substituted into equation B.13 to give an equation which, when combined with equation B.11, yields for the pressure gradient:

$$\frac{dp}{dz} = \frac{5432}{1575\pi^2}\frac{Q^2}{R^5}\frac{dR}{dz} - \frac{8uQ}{\pi R^4} \quad \text{..... B.14}$$

Equations B.11 and B.14 can be substituted into equation B.10 to give the velocity, u, as a function of r and z

$$\frac{u}{U_o} = Re_o\left(\frac{R_o}{R}\right)^3\frac{dR}{dz}\left[-\frac{308k}{1575} + \frac{1204k^2}{1575} - \frac{4k^3}{5} + \frac{4k^4}{15}\right] + 2\left(\frac{R_o}{R}\right)^2(2k - k^2) \quad \text{..... B.15}$$

Re_o is the free flow Reynolds number

Two theoretical velocity profiles, as predicted from the above equation are shown plotted to scale in Fig.B.2. They are for tube geometry $z_o = 4R = 12\delta$, this having been the geometry used by Forrester and Young in some associated experiments.

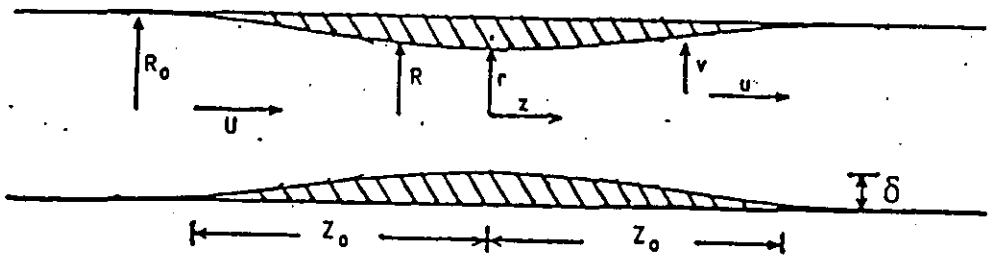

Figure B1: The shape of the axisymmetric stenosis model used in the work by Forrester and Young (1970). The legend key is contained within page 223

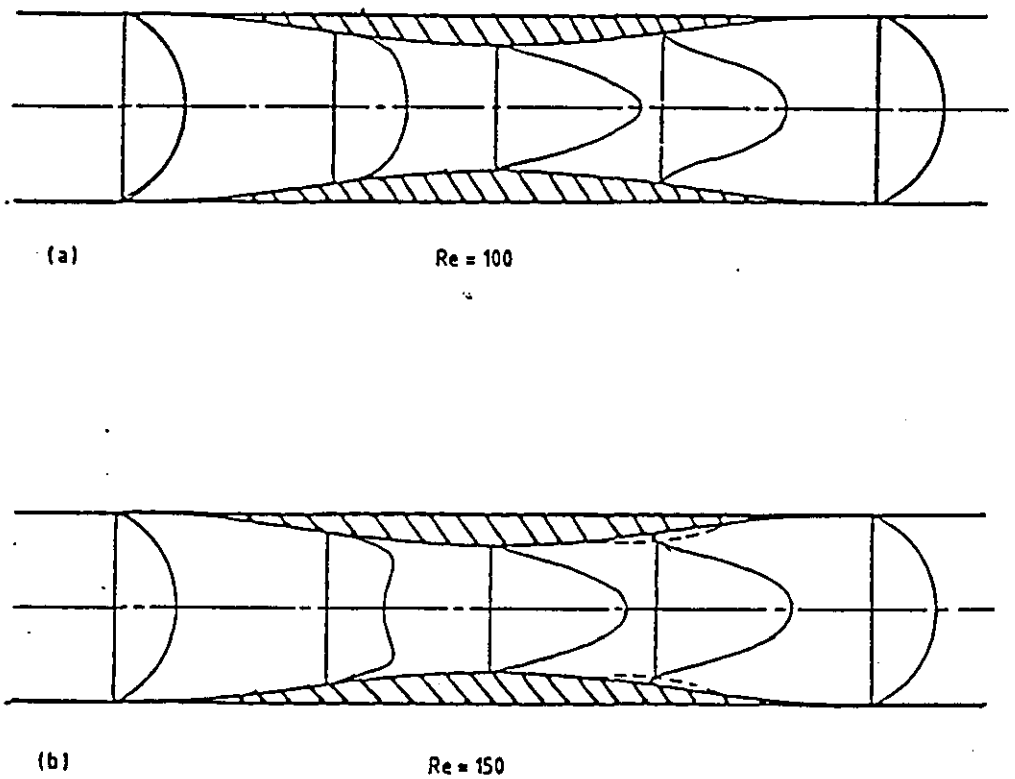

Figure B2: Two theoretical velocity profiles, for (a) Re = 100 and (b) Re = 150, resulting from the Forrester and Young model. In both cases afluid jet can be seen emerging from the restriction; fluid momentum effects are responsible for its propagation.The dotted lines at the exit of (b) represent the streamlines bounding the separation region.

REFERENCES

ARFORS, K.E., McKENZIE, F.N. and MATHESON, N.A. (1975) Measurement of the platelet response to laser induced microvascular injury, influence of haematological and haemodynamic variables. Thromb. Res., 21: 47 - 53.

AYYUB, G.E. and BIRKHAZI, A.B. (1978) Kinetics of aggregation of human platelets. J. Pharmaceut. Sci., 67: 939 - 945.

BADIMON, L., FUSTER, V., DEWANJEE, M.K. and ROMERO, J.C. (1982) A sensitive new method of 'ex vivo' platelet deposition. Thromb. Res., 28: 237 - 250.

BALL, D.I., COLEMAN, R.A., HARTLEY, R.W. and SHELDRICK, K.E. (1987) A novel method for the evaluation of bronchoactive agents in the conscious guinea pig. Brit. J. Pharmac., 90: 150P.

BAUMGARTNER, H.R. and MUGGLI, R. (1976) Adhesion and aggregation: morphological demonstration and quantitation in-vivo and in-vitro. Chapter 2 of 'Platelets in Biology and Pathology' (Ed. Gordon) Elsevier/North Holland Biomedical Press.

BAUMGARTNER, H.R. (1973) The role of blood flow in platelet adhesion,fibrin deposition and formation of mural thrombi. Microvasc. Res., 5: 167 - 179.

BAUMGARTNER, H.R., TURITTO, V.T. and WEISS, H.J. (1980). Effects of shear rate on platelet interaction with subendothelium in citrated and native blood. J. Lab. Clin. Med., 95: 2: 208 - 221.

BEGENT, N. and BORN, G.V.R. (1970) Growth rate in-vivo of platelet thrombi, produced by iontophoresis of ADP, as a function of mean blood flow. Nature, Lond., 227: 926 - 930.

BONNER, R.F. and NOSSAL, R. (1981) Model for laser Doppler measurements of blood flow in tissue. Appl. Opt., 20: No.12, 2097 - 2107.

BONNER, R.F., CLEM, T.R., BOWEN, P.D. and BOWMEN, R.L. (1981) Laser - Doppler continuous real time monitor of pulsatile and mean blood flow in tissue microcirculation. In 'Scattering techniques applied to supramolecular and nonequilibrium systems' Plenum Press ISBN 0-306-40828-7 (Ed. Chen,S,H., Chu,B. and Nossal,R.) Pages 685 - 701.

BONNER, R.F., BOWEN, P., BOWMAN, R.L. and NOSSAL, R. (1978) Real time monitoring of tissue blood flow by laser Doppler velocimetry. Proc.

Electrooptics and lasers conference '78. Pages 539 - 550.
Venue: Chicago

BORN, G.V.R. (1962) Aggregation of blood platelets by adenosine diphosphate and its reversal. Nature, Lond., 194: 927 - 929.

BORN, G.V.R. (1962) Quantitative investigations into the aggregation of blood platelets. J. Physiol. Lond., 162: Page 67P.

BORN, G.V.R. (1970) Observations on the change in shape of blood platelets brought about by adenosine diphosphate. J. Physiol. Lond., 209 : 487 - 511.

BORN, G.V.R. and HUME, M. (1967) Effects of the numbers and sizes of platelet aggregates on the optical density of plasma. Nature, Lond., 215 : 1027 - 1029.

BORN, G.V.R. and CROSS, M.J. (1964) Effects of inorganic ions and of plasma proteins on the aggregation of blood platelets by adenosine diphosphate. J. Physiol. Lond., 170: 397 - 414.

BORN, G.V.R., MELLING, A. and WHITELAW, J.H. (1978) Laser Doppler microscope for blood velocity measurements. Biorheology, 15 : 163 - 172.

BRECHER, G., SCHNEIDERMAN, M.A. and CRONKITE, E.P. (1953) The reproducibility and constancy of the platelet count. Am. J. Clin. Path., 23: 15 - 26.

BROWN, J.M., NAHORSKI, Z.T., WOODCOCK, J.P. and MORRIS, S.J. (1978) Transfer function modelling of arteries. Biol. Eng. Comput., 16: 161 - 164.

BULL, B.S., SCHNEIDERMAN, M.A. and BRECHER, G. (1965) Platelet counts with the Coulter counter. Am. J. Clin. Path., 44 : No 6, 678 - 688.

CARDINAL, P.C. and FLOWER, R.J. (1980) The electronic aggregometer, a novel device for assessing platelet behavior in blood. J. Pharmacol. Meth., 3: 135 - 158.

COCHRANE, T. and EARNSHAW, J.C. (1978) Practical laser Doppler microscopes. J. Phys. E. 11: 196 - 201.

COCHRANE, T., SHERIFF, S.B., BOULTON, A.J.M., WARD, J.D. and ATKINS,

R.M. (1986) Laser Doppler flowmetry in the assessment of peripheral vascular disorders: a preliminary evaluation. Clin. Phys. Physiol. Meas., 7: 1: 31 - 42.

COHEN, P., GARDNER, F.H. and BARNETT, G.O. (1961) Reclassification of thrombocytopenias by the CR-51 labelling method for measuring platelet life span. N. Eng. J. Med. 264: 1294 - 1306.

COULTER, W.H. (1953) Means for counting particles suspended in a fluid. U.S. Patent No. 2,656,508.

COX, R.T. and PONDER, E. (1941) A new form of diffractometer. J. Gen. Physiol. 24: 619.

CRONBERG, S. (1970) Evaluation of platelet aggregation. Coag., 3: 2: 139 - 151.

DAWES, C. and GARDNER, J. (1978) Radioimmunoassay of Digoxin employing charcoal entrapped in magnetic polyacrylamide particles. Clinica Chimica Acta 86: 353 -356.

DANDRIDGE, A. and GOLDBERG, L. (1982) Current induced frequency modulation in diode lasers. Electron. Lett., 18 : 302 - 304.

DAY, J.H., YOUNG, E. and HELFRICH, M. (1980) An evaluation of a whole blood platelet counter. Am. J. Clin. Path., 73: 4: 588 - 593.

de MULL, F.F.M., van SPIJKER, J., van der PLAS, D., GREVE, J., AARNOUDSE, J.G. and SMITS, T.M. (1984) Mini laser Doppler (blood) flow monitor with diode laser source and detection integrated into the probe. Appl. Optics, 23: 17: 2970 - 2972.

DEVANATHAN, R. and PARVATHAMMA, S. (1983) Flow of micropolar fluid through a tube with stenosis. Med. Biol. Eng. Comp., 21: 438 - 445.

DRAIN, L.E. (1972) Coherent and noncoherent methods in Doppler optical beat velocity measurement. J. Phys. part D, 5: 481 - 445.

DURST, F and WHITELAW, J.H. (1971) Optimization of optical anemometers. Proc. Royal Soc. 324: 157 - 181.

DYOTT, R.B. (1978). The fibre optic Doppler anamometer. IEEE J., 2: 13 - 19

EARNSHAW, J.C. and STEER, M.W. (1979) Laser Doppler Microscopy. Proc. R. Micr. Soc., 14 : 108 - 110.

FELTON, P.G. (1979). Measurements of particle/droplet size distribution by a laser diffraction technique. 2nd. European conference on particle size distribution, Nurenburg. Editor Letchomski, K. Published by NMA (Nurenberg). Pages 662 -680.

FEKE, G.T. and RIVA, C.E. (1978) Laser Doppler measurements of blood velocity in human retinal vessels. J. Opt. Soc. Am. 68: 526 - 531.

FORRESTER, J.H. and YOUNG, D.F. (1970). Flow through a converging - diverging tube and its implications in occlusive vascular disease. Int. J. Biomechanics, 3: 297 - 305.

FOX, J.A. and HUGO, A.E. (1966) Localization of atheroma: a theory based on boundary layer separation. Brit. Heart J. 28: 388 - 395

FRY, D.L. (1968) Acute vascular changes associated with increased blood velocity gradients. Circ. Res. 22: 165 - 197.

FUHR, P.L. (1985). Throughput comparison of microscope objectives and custom lenses for laser diode output beam collimation. Applied Optics, 24: 17: 2820 - 2822.

FUSTER, V., DEWANJEE, M.K., KAYE, M., JOSA, M., METKE, M.P. and CHESEBRO, J.M. (1979) Noninvasive radio isotope technique for detection of platelet deposition in coronary artery bypass grafts in dogs and its reduction with platelet inhibitors. Circulation, 60: 7: 1508- 1512.

GIDDENS, D.P., MABON, R.F. and CASSABIVA, R.A. (1976). Measurements of disordered flows distal to sub total vascular stenoses in the thorasic aortas of dogs. Circ. Res., 39: 112 - 119.

GRANT, L. and BECKER, F.F. (1965). Mechanisms of inflammation: (1) Laser induced thrombosis, a morphological analysis.Proc. Soc. Exp. Biol. Med., 119: 1123 - 1127.

GROVER, N.B., NAAMANN, J. and BEN-SASSON, S. (1969). Electrical sizing of particles in suspensions. Biophys. J., 10: 1418 - 1425.

GRYGLEWSKI, R.J., KORBUT, R., OCETKIEWICZ, A. and STACHURA, J. (1978). In-vivo method for quantitation of antiplatelet potency of drugs.

Naunyn. Schmiedebergs Arch. Pharmacol., 302: 25 - 30.

HAYNES, J.L. and SHOOR, B.A. (1978). Particle density measuring system. U.S. patent. 4, 110, 604.

HAYNES, J.L. (1980). High resolution particle analysis: the application to platelet counting and suggestions for further application in blood cell analysis. Blood Cells, 6 : 201 - 213

HORNSTRA, G. (1970). Method to determine the degree of ADP induced platelet aggregation in circulating rat blood. Brit. J. Haem., 19: 321 - 329.

HOVIG, T., McKENZIE, F.N. and ARFORS, K.E. (1974). Measurement of the platelet response to laser induced microvascular injury. Thromb. Diathes. Haem. (Stutt)., 32: 695 - 703.

JOHNSON, R.P.C. (1982) A laser Doppler microscope for biological studies. In 'Biomedical applications of laser light scattering' Ed. Ware, B.R., Lee, W.L. and Sattelle, D.B. Elsevier, North Holland. Pages 391 - 402.

JOHNSON, R.P.C. (1983). Laser Doppler Microscopy: especially as a method for studying Brownian motion and flow in the sieve tubes of plants. In 'Application of laser light scattering to the study of biological motion.' Ed. Earnshaw J.C and Steer M.W. Plenum Publishing. 147-63

JOHNSON, R.P.C. and ROSS, D.A. (1984). Laser Doppler microscopy and fibre optic Doppler anemometry. In 'The analysis of organic surfaces.' Ed. Echlin P. Published by Wiley.Chapter 20, pages 507 -28.

JURGENS, R. and BRAUNSTEINER, H. (1950). Zur pathogenese der thrombose. Schweiz. Med. Wschr., 80: 1388 - 1394.

KATCHEL, V. (1973). Eine electronische methode zur verbesserung der volumenauflosung des Coulter partikelvolumenmebbverfahrens. Blut, 27: 270 - 274.

KAYE, B.H. (1980). Unpublished lecture notes,referenced by KIRK, B, (1980) in 'An iris diaphragm based interface for use in eriometry' M.Sc. thesis, Laurentian University (Canada). Page 5.

KILPATRICK, D., TYBERG, J.V. and PARMLEY; W.W. (1982). Blood velocity

measurement by fibre optic laser Doppler anemometry. IEEE. transactions on biomedical engineering, Vol. BME 29, No. 2,

KOCHEN, J.A. and BAEZ, S. (1965). Laser induced microvascular thrombosis, embolization and recanalization in the rat. Ann. N.Y. Acad. Sci., 122: 728 - 737.

KOVACS, I.B. and GOROG, P. (1979). Laser induced thrombosis test suitable for pharmacology sceening studies. Microvasc. Res., 18: 403 - 412.

KUBAC, R.J., NEVRTAL, M., TOVAREK, L. and DOLEZAL, L. (1974). A method of analysis of the Doppler velocity meter signal for determination of haemodynamic parameters. Scr. Medica, 47: 61 - 75.

KUNTZ, D.W. (1984). Specifying laser diode optics. Laser Focus and Electro-optics 109: 44 - 50.

LING, S.C., ATABECK, H.B., FRY, D.L., PATEL, D.J. and JANICKI, J.S. (1968). Application of heated film velocity and sheer probes to haemodynamic studies. Circ. Res., 23: 789 - 801.

LUDDERS, J.W., THOMAS, C.B., SHARP, P. and SEDGWICK, C.J. (1987). An anesthetic technique for repeated collection of blood from New Zealand white rabbits. Lab. Animal Sci., 37: 6: 803 - 805.

LUMLEY, P. and HUMPHREY, P.P.A. (1981). A method for quantitating platelet aggregation and analysing drug - receptor interactions on platelets in whole blood in vitro.. J. Pharmacol. Meth., 6: 153 - 166.

LUMLEY, P. (1984) Personnal communications within Glaxo Group Reseach.*

MACHELLA, T.E. (1936). The velocity of blood flow in arteries in animals. Am. J. Physiol., 115: 632 - 644.

MARTIN, T.P, BARBER, D.C., SHERRIFF, S.B. and PRITCHARD, D.R. (1980). Objective feature extraction applied to the diagnosis of carotid artery disease using Doppler ultrasound techniques. Clin. Phys. Physiol. Meas., 1: 71 - 81.

McCABE, P.J. (1982). Assessment of AM23848B in a guinea-pig model of thrombosis. Glaxo Group Research,* report number WBC/82/007.

*Glaxo Group Research Ltd., Park Road, Ware, Herts., SG12 ODP.

McDONALD, A.D. (1960). Blood flow in arteries. Monog. Physiol. Soc. Lond. Published by Edward Arnold.

MIE, G. (1908) Beitrage zur Optik treiber Medien, speziell kollodialer Metallosungen. Ann. der Physik, Folge 4, Band 37: 881.

MISHINA, H. and ASAKURA, T. (1972). Laser Doppler flow measurements in medicine and biology. Opto-Electronics, 4: 399 - 405.

MISHINA, H., KOYAMA, T. and ASAKURA, T. (1976). Velocity measurements of blood flow in the capillary and vein using a laser Doppler microscope. Appl. Optics, 4: 10: 2326 - 7.

MISHINA, H., USHIZAKA, T. and ASAKURA, T. (1976). A laser Doppler microscope: its optical and signal analysing systems and some experimental results. Optics and Laser Technology, 121 - 127.

MORRIS, S.J., WOODCOCK, J.P. and WELLS, P.N.T. (1975). Impulse response of a segment of artery using transcutaneous ultrasonic flowmeters. Med. Biol. Eng., 13: 803 - 812.

MULLANEY, P.F. and CROWELL, J.M. (1976). Pulse height light scatter distributions using flow system instrumentation. J. Histochem and Cytochem., 23, 1, 298 - 304.

NEREM, R.M. and SEED, W.A. (1972). An in-vivo study of the nature of aortic flow disturbances. Cardiovasc. Res., 6: 1 - 14.

NEREM, R.M., RUMBERGER, J.A., GROSS, D.R., HAMLIN, R.L. and GEIGER, G.L. (1974) Hot-film anemometer velocity measurements of arterial blood flow in horses. Circ. Res., 34: 193 - 203.

NILSSON, G.E., TENLAND, T. and OBERG, P.A. (1980). A new instrument for continuous measurement of tissue blood flow by light beating spectroscopy. IEEE. Trans., BME-27, 12 - 19.

NILSSON, G.E. (1984). Signal processor for laser Doppler tissue flowmeters. Med. Biol. Eng. Comp., 22: 343 - 348.

NISHIHARA, H., KOYAMA, J., HOKI, N., KAJIYA, F., HIRONAGA, M. and KANO, M. (1982). Optical fibre laser Doppler velocimeter for high resolution measurement of pulsatile blood flows. Appl. Optics, 21: 10: 1785 - 1790.

OSTER, Z.H. and SRIVASTAVA, S.C. (1985) Thrombus radioimmunoscintigraphy: an approach using monoclonal antiplatelet antibody. Proc. Nat. Acad. Sci. USA., 82: 3465 - 8.

PADMANABHAN, N. (1980). Mathematical model of stenosis. Med. Biol. Eng. Comp., 18: 261 - 6.

PADMANABHAN, N. and DEVANATHAN, R. (1981). Mathematical model of an arterial stenosis, allowing for tethering. Med. Biol. Eng. Comp., 19: 385 - 389.

PIKE, E.R. (1969). Photon statistics. Proc. Florence Inaugral Conf., European Phys. Soc., Rivista del Nuovo Cimento, 1. Published by Compositori Viale (Bologna). p277 - 314.

PITON, J., BILLEREY, J., RENOU, A.M., CONSTANT, P. and CAILLE, J.M. (1978). Vascular thrombosis induced by direct electric current: a new technique for therapeutic embolisation. Neuropharmacol., 16: 385 - 388.

POVISHOCK, J.T., ROSENBLUM, W.I., SHOLLEY, M.M. and WEI, E.P. (1983). An ultrastructural analysis of endothelial change paralleling platelet aggregation in a light/dye model of microvascular insult. Am. J. Pathol., 10: 2: 148 - 160.

RANG, H. and DALE, H. (1987). 'Pharmacology', Churchill Livingstone Press, ISBN 0-443-03407-9.

RIVA, C.E., ROSS, B. and BENEDEK, G.B. (1972) Laser Doppler measurements of blood flow in capillary tubes and retinal arteries. Invest. Ophthalmol., 11: 936 - 944.

RIVA, C.E. and FEKE, G.T. (1981) Laser Doppler velocimetry in the measurment of retinal blood flow. In 'The biomedical laser'. Ed. Goldman, L. Springer Verlag.

ROBARD, S. (1966) Dynamics of blood flow in stenotic lessions. Am. Heart J., 72: 698 - 704.

RUDD, M.J. (1969). A new theoretical model for the laser dopplermeter. J. Sci. Inst. (J. Physics E) 2: 2: 55 - 58.

SATOMURA, S. (1957). Ultrasonic Doppler method for the inspection of cardiac functions. J. Acoust. Soc. Am., 29: 1181 - 1185.

SEED, W.A. and WOOD, N.B. (1970). Development and evaluation of a hot

film velocity probe for cardiovascular studies. Cardiovasc. Res., 4: 253 - 263.

SHERRIFF, SUSAN B., BARBER, D.C. MARTIN, T.P.R. and LAKEMAN, J.M. (1983). Mathematical feature extraction applied to the Doppler shifted signal obtained from the common carotid artery. Blood flow: theory and practice. Ed. Taylor, D.E.M. and Stevens, A.L. Academic Press.

SKIDMORE, R. (1979). The use of the transcutaneous ultrasonic flowmeter in the dynamic analysis of blood flow. Ph. D. thesis , University of Bristol.

SKIDMORE, R. and WOODCOCK, J.P. (1980). Physiological interpretation of Doppler shift waveforms - II Validation of the Laplace transform method for chacterisation of the common femoral blood velocity/time waveform. Ultrasound, Med. Biol., 6: 219 - 225.

SLINEY, D.H and FREASIER, B.C. (1973) Evaluation of optical radiation hazards. Appl. Opt., 12: 1 - 24.

SMITH, G.M. and FREULER, F. (1973). The measurement of intravascular aggregation by continuous platelet counting. Bibliotheca Anatomeca., 12: 229 - 234.

SPIELMAN, L. and GOREN, S.L. (1968). Improving resolution in Coulter counting by hydrodynamic focussing. J. Colloid Interface Sci., 26: 175 - 182.

STERN, M.D. (1975) In-vivo evaluation of the microcirculation by coherent light scattering. Nature, 254: 56 - 61.

STERN, M.D. (1985). Laser Doppler velocimetry in blood and multiple scattering fluids: theory. Appl. Optics., 24: 13: 1968 - 1986.

STRANDNESS, D.E., SCHULTZ, R.D., SUMNER, D.S. and RUSHMER, R.F. (1967). Ultrasonic flow detection, a useful technique in the evaluation of peripheral vascular disease. Am. J. Surg., 113: 311 - 319.

TALBOT, J.H. (1966). Fraunhoffer diffraction pattern of a random distribution of identical apertures in a plane screen. Proc. Phys. Soc., 89: 1043 - 1053.

TANAKA, T. and BENEDEK, G.B. (1975). Measurement of the velocity of blood flow (in-vivo) using a fibre optic catheter and optical mixing spectroscopy. Appl. Optics, 14: 1: 189 - 196.

THIELE, B.L., HUTCHINSON, K.J., GREEN, F.M. and STRANDNESS, D.E. (1983). Pulsed Doppler waveform patterns produced by smooth stenosis in the dog thoracic aorta. In 'Blood flow theory and practice', Ed. Taylor, D.E.M. and Stevens, A.L., Academic Press (London) Ltd.

THOM, R. (1972). Vergleichende Untersuchungen zur Electronischen Zellvolumenanalyse. AEG. Telefunken Publ. N1/EP/1698, Ulma Donan, W. Germany.

TURITTO, V.T. and BAUMGARTNER, H.R. (1979). Platelet interaction with subendothelium in flowing rabbit blood: effect of shear rate. Microvasc. Res., 17: 38 - 54.

van de HULST. (1957) Light scattering by small particles. Wiley, New York.

VELLA BRIFFA, D. and GREAVES, M.W. (1979). Inhibition of human blood platelet aggregation by photochemotherapy in-vitro and in-vivo. Brit. J. Dermatol., 101: 679 - 683.

WATTS, I.S. (1983). A pharmacological approach to the study of the vascular complications of diabetes mellitus in streptozolocin treated rats. Ph. D. thesis, University of London.

YAO, S.T. and NEEDHAM, T.N. (1970). Frequency analysis of Doppler shifted blood flow signals by a bandpass filter: preliminary report. Biomed. Engng., 5: 438 - 442.

YEH, Y. and CUMMINS, H.Z. (1964). Localised fluid flow measurements with a He-Ne laser spectrometer. Appl. Phys. Lett., 4: 176 - 178.

YOUNG, D.F. and SHIH, C.C. (1969. Some experiments on the effects of isolated protuberences on flow through tubed. Exp. Mechanics, 9: 225 - 229.

YOUNG, D.F. and TSAI, F.Y. (1973). Flow characteristics in models of arterial stenosis - 1 Steady flow. J. Biomechan., 6: 395 - 410.

YOUNG, T. (1813). An introduction to medical litetature. Published by Underwood and Black, (London).